Effector discovery and characterisation in the *Fusarium graminearum*-wheat floral interaction

Submitted by

Catherine Holly Walker

To the University of Nottingham as a thesis for the degree of Doctor of Philosophy in Biological Science, September 2019

I certify that all material in this thesis which is not my own work has been identified and that no material has been previously been submitted and approved for the award of a degree by this or any other University

Signature: …….

Abstract

Fusarium graminearum is the causal agent of Fusarium Head Blight (FHB) – a highly hazardous wheat disease which results in crop losses and mycotoxin contamination. A recent transcriptomic investigation of the *F. graminearum*-wheat interaction revealed an up-regulation in hundreds of genes encoding small secreted proteins (SSPs), or putative effectors, during infection which we hypothesise contribute towards pathogenicity. The aim of this study was therefore to bioinformatically identify and then functionally characterise effector candidates in wheat and *Nicotiana benthamiana* using a range of post-genomics techniques.

In this study, an effector discovery pipeline was established involving interrogation of the *in vitro* and *in planta* transcriptional profiles of genes belonging to the *F. graminearum* predicted secretome. This pipeline yielded twenty-four candidates for functional characterisation, seven of which were characterised using the *Barley Stripe Mosaic Virus*-mediated overexpression (BSMV-VOX) system. Transient expression of two FgSSPs, FgSSP32 and FgSSP33, in mature wheat ears led to a significant reduction in FHB disease symptoms. Single gene deletions of *FgSSP32* and *FgSSP33* were then generated using a split-marker transformation approach but found not to result in any changes in fungal pathogenicity on wheat.

Agrobacterium-mediated transient expression of FgSSP32 and FgSSP33 in the model species *N. benthamiana* led to the discovery that both proteins induce necrosis of the vascular tissue. Expression of proteins lacking a signal peptide did not result in necrosis suggesting that these proteins function apoplastically. Biochemical characterisation of *N. benthamiana*

leaves expressing FgSSP32 and FgSSP33 revealed that both proteins induce the production of a compound tentatively identified as 12-oxo-phytodienoic acid (12-OPDA) – a precursor to the phytohormone jasmonic acid (JA). In addition, apoplastic occlusions were observed in *N. benthamiana* leaves expressing FgSSP33 indicating a host defence response towards this protein.

Transcriptome data exploring *FgSSP32* and *FgSSP33* expression during the *F. graminearum*-wheat floral interaction, revealed that both genes are expressed during the symptomatic phase of infection – a phase characterised by penetration and colonisation of wheat cells by fungal hyphae. We therefore hypothesise that FgSSP32 and FgSSP33 contribute towards the symptomatic phase of *F. graminearum* infection by activating cell death responses leading to the release of nutrients for fungal sequestration. Further work is required to identify host interacting proteins which may lead to the identification of wheat genes involved in *F. graminearum* resistance or susceptibility.

Acknowledgements

Firstly, I would like to thank my supervisor Kim Hammond-Kosack for her constant support and guidance throughout this project. Her passion for science has been truly inspiring and I feel very lucky to have had a supervisor who strives for the best and has consistently pushed me to become better. I would also like to particularly thank Martin Urban, Ana Machado and Neil Brown as, without them, only a fraction of this work would have been possible. Thanks also go to the rest of the wheat pathogenomics group, particularly Kostya Kanyuka and Jason Rudd, whose discussions and ideas have pushed my work forward.

I would also like to thank all my friends and family starting with the Brum crew - Jodie, Lara and Tara - whose constant friendship has been one of the biggest sources of joy for me for all the years we've known each other. A huge thank you also has to go to Ryan - for all the hours he listened to me practice presentations, troubleshooted problems with me and, just generally, for all the encouragement he has given me over the past four years.

And finally, thank you to my family! Firstly, to my Nainy who has always inspired me with her curiosity and strength of mind. And, of course, to Mum, Dad, Lydia, Brian & Jesse for all their love and support throughout this whole process.

Contents

List of figures and tables

List of abbreviations

µg	Microgram
µl	Microlitre
µm	Micrometre
µM	Micromolar
12-OPDA	12-oxo-phytodienoic acid
15-ADON	15-acetyl-4-deoxynivalenol
3-ADON	3-acetyl-4-deoxynivalenol
3-D	Three-dimensional
aa	Amino acid
ADK	Adenosine kinase
ANCOVA	Analysis of covariance
ATMT	*Agrobacterium tumefaciens*-mediated transformation
Avr	Avirulence gene
AWF	Apoplastic washing fluid
BAK1	BRI1-associated receptor kinase
BIC	Biotrophic interfacial complex
BIFC	Bimolecular fluorescence complementation
birA	Biotin ligase
bp	Base pairs
BSMV	Barley Stripe Mosaic Virus
cDNA	Complementary DNA
CeBIP	Chitin elicitor binding protein
CM	Complete media
Co-IP	Co-immunoprecipitation
CP	Cerato-platanin
CPMV	Cowpea mosaic virus
cv	Cultivar
CYP51	Cytochrome P450 lanosterol C-14-α-demethylase
DMI	Demethylation inhibitor
DNA	Deoxyribonucleic acid

DON	Deoxynivalenol
dpi	Days post inoculation
ds	Double-stranded
ZEA	Zearalenone
EIHM	Extrainvasive hyphal membrane
ELISA	Enzyme-linked immunosorbent assay
ETI	Effector-triggered immunity
ETS	Effector-triggered susceptibility
EV	Empty vector
f. sp.	Forma specialis
FAO	Food and Agriculture Organisation
FCR	*Fusarium* crown rot
FEB	Fusarium Ear Blight
Fg	Fusarium graminearum
FGSC	Fusarium graminearum species complex
FgSSP	Fusarium graminearum small secreted protein
FHB	Fusarium Head Blight
Fol	Fusarium oxysporum f. sp. lycopersici
FoMV	Foxtail Mosaic Virus
FPKM	Fragments per kilobase of transcript per million mapped reads
g	Grams
g	Relative centrifugal force
gDNA	Genomic DNA
GFP	Green fluorescent protein
GLM	Generalised linear model
GLMM	Generalised linear mixed model
HIGS	Host-induced gene silencing
HPLC	High-performance liquid chromatography
HR	Hypersensitive response
hrs	Hours
HST	Host-selective toxin
HYG	Hygromycin

IH	Invasive hyphae
IN	Internode
JA	Jasmonic acid
kb	Kilobase pairs
L	Litre
LB	Lysogeny broth
LIC	Ligation-independent cloning
LRR	Leucine-rich repeat
LSD	Least significant difference
LysM	Lysin motif
m	Metre
M	Molar
MAPK	Mitogen-activated protein kinase
MAS	Marker-assisted selection
MCS	Multiple cloning site
mg	Milligram
min	Minutes
MIPS	Munich Information Services for Protein Sequences
ml	Millilitre
mM	Millimolar
mm	Millimetre
MPL	Maximum permitted level
MS	Mass-spectrometry
n	Number
NB	Nucleotide-binding
NCBI	National Center for Biotechnology Information
NEP1	Necrosis- and ethylene-inducing protein 1
NGS	Next-generation sequencing
NIV	Nivalenol
NLP	NEP1-like protein
NLR	NOD-like receptor
nm	Nanometre

NOD	Nucleotide oligomerisation domain
OA	Oxalic acid
OD	Optical density
ORF	Open reading frame
P	P-value
PAF	*Penicillium chrysogenum* antifungal protein
PAGE	Polyacrylamide gel electrophoresis
PAL	Phenylalanine ammonia-lyase
PAMP	Pathogen-associated molecular patterns
PCD	Programmed cell death
PCWDE	Plant cell wall-degrading enzymes
PDA	Potato dextrose agar
PDB	Potato dextrose broth
PHI-base	Pathogen-Host Interactions database
PLEXdb	Plant expression database
PR	Pathogenesis-related
PRR	Pattern recognition receptor
PTI	PAMP-triggered immunity
Ptr	*Pyrenophora tritici-repentis*
QTL	Quantitative trait loci
R	Resistance gene
RGD	Arginyl-glycyl-aspartic acid
RH	Relative humidity
RI	Rachis internode
RIP	Repeat-induced mutation
RNA	Ribonucleic acid
RNAi	RNA interference
RNA-seq	RNA sequencing
ROS	Reactive oxygen species
RPM	Revolutions per minute
RT-PCR	Reverse transcription-polymerase chain reaction
SA	Salicylic acid
SDS	Sodium Dodecyl Sulfate

SED	Standard error of difference
SEM	Standard error of the mean
SGT1	Suppressor of G2 allele of *skp1*
SIGS	Spray-induced gene silencing
SIX	Secreted-in-xylem
SNA	Synthetic nutrient agar
SNB	*Parastagonospora nodurum* blotch
SNP	Single nucleotide polymorphism
SOBIR1	Suppressor of BIR-1
SOC	Super-optimal broth
SP	Signal peptide
sRNA	small RNAs
ss	Single-stranded
Taq	Thermus aquaticus polymerase
TF	Transcription factor
TGB	Triple gene block
Ti	Tumour-inducing
TRI	Trichothecene
TRV	Tobacco rattle virus
UPS	Unconventional protein secretion
UTR	Untranslated region
UV	Ultraviolet
VIGS	Virus-induced gene silencing
VOX	Virus-mediated overexpression
WAK	Wall-associated kinase
Y2H	Yeast-two-hybrid
YPD	Yeast peptone dextrose
ZEA	Zearalenone
µmol	Micromole

Chapter 1 Introduction

1.1 Current threats to global food security and the influence of plant pathogens on agricultural ecosystem health

Since the advent of agriculture, human history has been both blighted and shaped by the devastating effects of plant disease. Perhaps the most notable illustration of the profound social and economic influence that plant disease can have on human populations is the infamous Irish potato blight – an epidemic which resulted in the death of over one million people and the immigration of a further two million more (O'Neill 2010). Almost two centuries later plant pathogens continue to hamper agricultural productivity and, despite advancements in our understanding of these pathogens, current agricultural practices only act to heighten the threat that plant pathogens pose to food safety and security (Oerke 2006; Bebber and Gurr 2015). An ever increasing-number of emerging infectious plant diseases have been reported in recent years, particularly those caused by fungal pathogens, which has come coupled with the worrying worldwide emergence of resistance to antifungal chemistries (Fisher 2012; Fisher et al. 2018). It is currently estimated that fungal and oomycete pathogens destroy a third of all food crops each year – a number liable to increase in the face of fungal resistance to chemical control and fluctuating climatic conditions (Hahn 2014; Garrett et al. 2006).

To meet the projected demand of the world's population, predicted to reach nine billion by 2050, food production must increase by a formidable 50% (Chakraborty and Newton 2011). Whilst the anthropological need for a secure food chain grows greater than ever, agricultural intensification poses

an existential threat to our ecosystems; with difficulty arising from the pressures on the availability of land and fresh water, rising fuel prices and climate change (Godfray and Garnett 2014)(FAO,2016). Climate change is just one of many manifestations of the Anthropocene era – a term which defines the profound impact that human activity has had on the environment, from land surface transformation to atmosphere composition (Lewis and Maslin 2015). Associated with increasing temperatures, higher concentrations of atmospheric carbon dioxide levels, and an increasing incidence of extreme climatic events, climate change acutely influences the biotic interactions between pathogens, pest, crops and weeds (Myers et al. 2017). While the true implications upon agricultural productivity are complex and far-reaching, climate change is already likely to have caused a global shift in the distribution of plant pathogens resulting in epidemics difficult to both predict and control (Bebber and Gurr 2015).

After maize (*Zea mays*), wheat (*Triticum aestivum* L. ssp. *aestivum*) is the most widely grown crop species across the globe with annual worldwide wheat production forecast to reach 769 million tonnes in 2019 (FAO, 2019). As a rich source of carbohydrate, protein, fibre and energy, wheat is a principal component of human nutrition in both developed and developing countries. Secure production of wheat is therefore imperative to the attainment of stable food systems. Nearly 200 diseases and pests of wheat have been documented so far, 50 of which are considered economically important, with yield losses estimated to amount to 13% despite implementation of disease control measures (Table 1.1; Figure 1.1)(Singh et al. 2016; Oerke 2006). Yield loss alone, however, is not an adequate metric

for capturing the multifaceted impact of crop disease which affects both food safety, quality, and nutritional value (Savary et al. 2012). To minimise the gap between actual and attainable crop yields, new and innovative disease control strategies must be exploited and development of these strategies requires greater knowledge of pathogen ecology, distribution, infection mechanism, and variability (Duveiller et al. 2012). With the stability of whole food systems under increasing risk due to the limited availability of resources necessary to sustain production, the securement of sufficient access to food and animal feed for peoples across the globe seems improbable (Wheeler and von Braun 2013). The advancement of methods to control fungal pathogens of crops must therefore undoubtedly play a leading role in the attainment of food security.

Table 1.1 Economically important fungal diseases of wheat across the globe.

Disease	Pathogen	Primary symptoms
Stem rust	*Puccinia graminis* f. sp. *tritici* Ericks and Henn	Red-brick urediniospores on the leaf, stem, glumes and awns of susceptible plants.
Stripe rust	*P. striiformis* Westend. f. sp. *tritici*	Pustules containing yellow urediniospores which usually form narrow stripes on the leaves.
Leaf rust	*Puccinia triticina* Eriks.	Pustules are circular and contain brown urediniospores. Found on the upper surfaces of leaves and leaf sheaths.
Septoria tritici blotch	*Zymoseptoria tritici*	Brown-coloured lesions which run parallel to leaf veins and can contain black pycnidia.
Septoria nodorum blotch	*Parastagonospora nodorum*	Dark brown lesions, sometimes with a halo of chlorosis on leaves and on glumes. Light brown pycnidia may also develop.
Tan spot	*Pyrenophora tritici-repentis*	Tan-to-brown flecks which expand to oval lesions with a chlorotic halo, differentiated from Septoria nodorum blotch by the absence of pycnidia.
Spot blotch	*Bipolaris sorokiniana*	Dark brown lesions on the leaf and infection of the spikelets leads to shrivelled grain.
Head (Ear) blight or scab	*Fusarium* spp.	Premature blighting of wheat ears and aggregation of light pink sporodochia.
Helminthosporium leaf blight	*Cochliobolus heterostrophus*	Tan, elongated lesions between veins with light brown to brown borders.
Wheat blast	*Magnaporthe oryzae Triticum* pathotype	Small elliptical lesions to entire blighting of the ear.
Take-all	*Gaeumannomyces graminis* var. *tritici*	Rotting of the roots and lower stems. Severely infected plants may appear stunted and fail to produce grain.

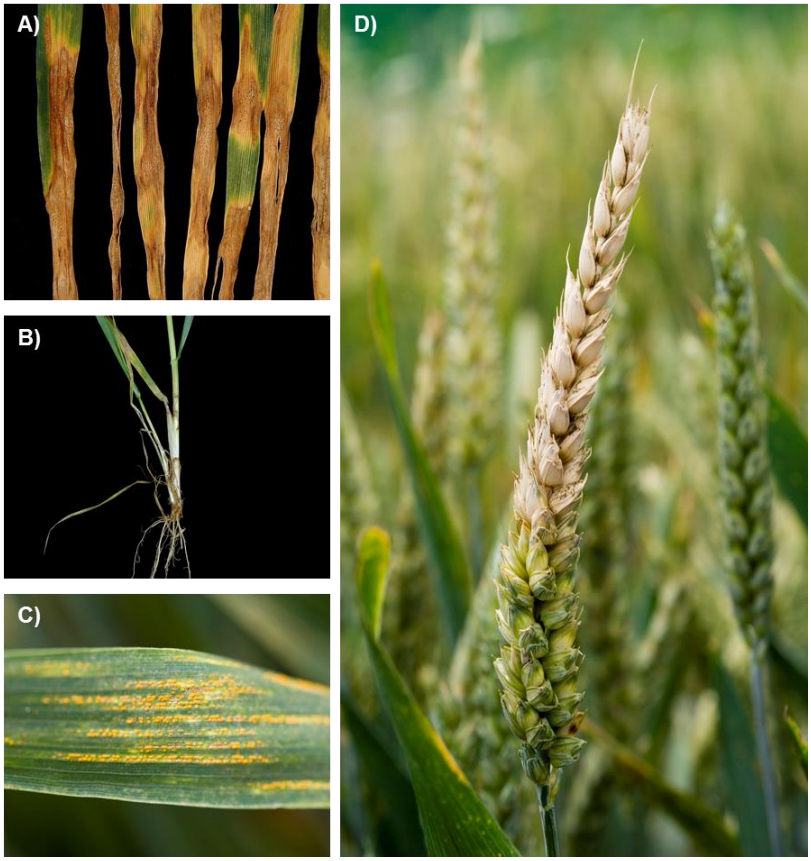

Figure 1.1 Economically important fungal disease of wheat. A) Symptoms of Septoria leaf blotch on wheat leaves. B) Symptoms of take-all infection in wheat roots and stems. C) Yellow rust pustules on wheat leaves. D) Fusarium head blight symptoms in wheat ears.

1.2 Dynamic interactions between pathogens and the plant immune system: the role of effectors

In natural ecosystems, successful colonisation of a plant host by a pathogen invader is rare despite continual bombardment from a diverse array of microbes aiming to take advantage of the nutrient-rich niches provided by plants. Pathogens that are successful in overcoming the many formidable preformed physical and chemical barriers afforded to the plant host must then encounter the host immune system - an innate system consisting of two interconnected tiers of receptors governing defence responses to microbes (Dangl, Horvath, and Staskawicz 2013). Defence responses are triggered by

the detection of pathogen-associated molecular patterns (PAMPs), such as chitin, by surface-localised pattern recognition receptors (PRRs) thus leading to the induction of a battery of defence responses (Boller and Felix 2009)(Zipfel and Felix 2005). These defence responses include the activation of ion channels and of intracellular signalling cascades to induce various antimicrobial responses including the production of reactive oxygen species (ROS), activation of transcriptional reprogramming of the host and the secondary re-enforcement of plant cell walls and surfaces (Boller and Felix 2009). This first layer of immunity is termed PAMP-triggered immunity (PTI) and, for the establishment of a compatible interaction with the host, successful pathogens must overcome PTI through the production of defence-manipulating molecules termed effectors. This interaction is known as effector-triggered susceptibility (ETS) and enables successful colonisation of the host.

In an evolutionary game of cat and mouse however, the plant surveillance system directly or indirectly recognises effectors through the recruitment of resistance (*R*) genes leading to effector-triggered immunity (ETI). The defence response launched in ETI is usually stronger than that induced during PTI and often culminates in the hypersensitive response (HR) - characterised by programmed cell death (PCD), limiting the access of pathogens to water and nutrients. A large class of *R* gene proteins are comprised of cytoplasmic receptors which share similarities with nucleotide oligomerisation domain (NOD) receptors and are therefore referred to as NOD-like receptors (NLRs) composed of nucleotide-binding (NB) and leucine-rich repeat (LRR) domains (Kanneganti, Lamkanfi, and Nunez 2007).

Activation of *R*-gene mediated resistance through effector recognition is associated with the activation of salicylic acid (SA)-mediated signalling pathways which trigger the expression of pathogenesis-related (*PR*) genes leading to increased resistance towards the pathogen (Glazebrook 2005). Co-evolutionary gain and loss of effector-encoding genes, also known as *Avr* genes, and *R* genes leads to an ever-changing battleground between pathogen and host. Identification of effectors is therefore crucial to gaining an understanding as to how to tip the balance in the favour of the plant host. This interaction between pathogen and host, known as the 'zig-zag-zig' model, relies upon the loss, acquisition, and modification of these effectors and the presence or absence of receptors that recognise them (Figure 1.2)(Jones and Dangl 2006).

Capitalisation of the knowledge gained from effector discovery has had wide-reaching implications for classical resistance breeders. Utilisation of effectors as germplasm probes for the detection of *R* genes has enabled the acceleration of *R* gene cloning and subsequent introgression of *R* genes into the host germplasm, and also allows the accurate detection of resistance in plant material (Jupe et al. 2012; Kim et al. 2012; Vleeshouwers and Oliver 2014). In the future, effector knowledge could be applied to the development of 'RNA fungicides' – an attractive emerging technology which exploits the ability of mobile RNAs to be trafficked between host and pathogen in a bidirectional manner (Nowara et al. 2010; Baum et al. 2007)(Machado et al. 2018). However, whilst many effectors have been identified in plant-infecting

filamentous pathogens, particularly in biotrophic fungi, few fungal effectors have been found to be essential to virulence.

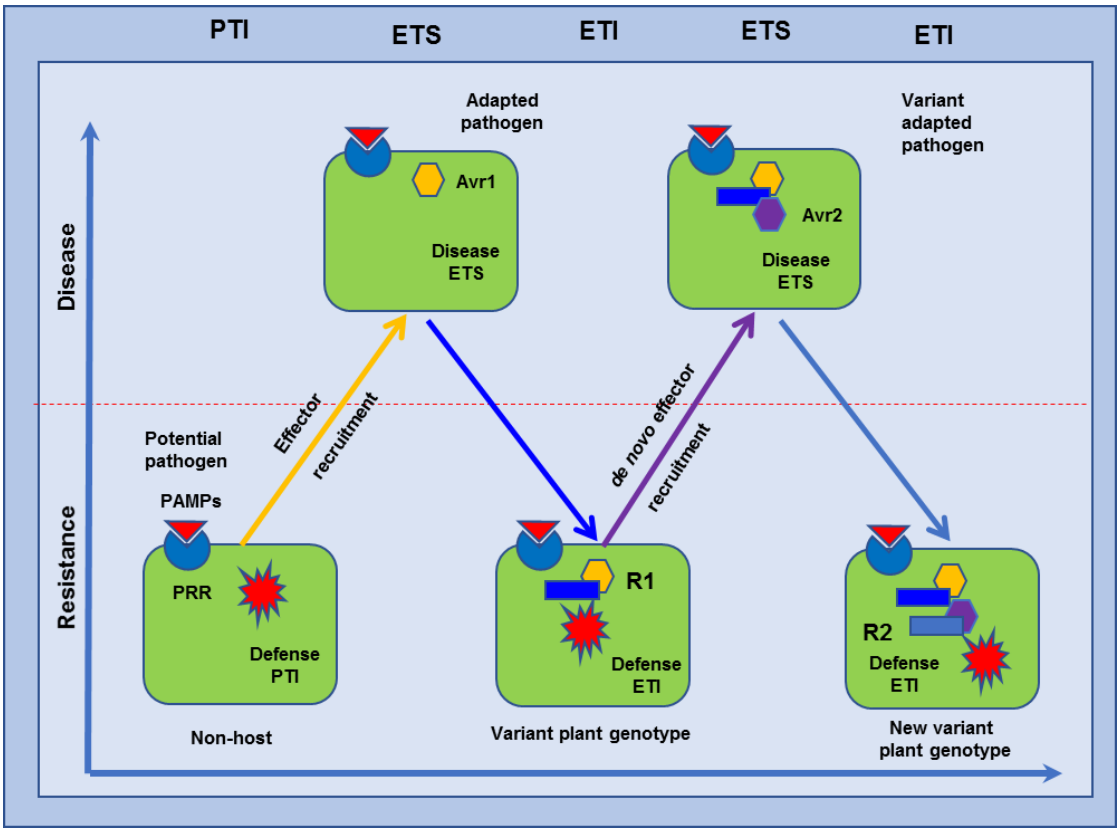

Figure 1.2 The zig-zag-zig model. Basal plant defence is initiated by the recognition of PAMPS by PRRs leading to PTI in which defence responses such as the production of reactive oxygen species (ROS), thickening of plant cell walls and activation of upstream defences. To overcome this first layer of defence, adapted pathogens acquire effectors that can circumvent PTI thus leading to effector-triggered susceptibility (ETS). Plants can acquire resistance proteins (R) that recognise effectors, which are then lost and gained in an ongoing battle between pathogen and host. Taken from Brown and Hammond-Kosack (2015) which was modified from Jones and Dangl (2006).

1.2.1 Characteristics of fungal effector proteins and effector identification

Effectors are broadly defined as small proteins or molecules, the main function of which is to facilitate host colonisation by manipulating host defences (Abramovitch et al. 2003; Rafiqi et al. 2012). Filamentous pathogen effector proteins are often defined as being small, secreted and cysteine-rich – the latter a characteristic thought to stabilise the protein from the harsh conditions of the apoplast (de Wit et al. 2009; Gan et al. 2013; Doehlemann et al. 2009). An N-terminal secretion signal targets effector proteins for secretion via the endoplasmic reticulum-Golgi apparatus pathway into the host apoplast. While some effector proteins are retained in the host apoplast, a sub-set of effectors are translocated back into the host cytoplasm where they target specific subcellular compartments (Petre, Lorrain, et al. 2016; Irieda, Ogawa, and Takano 2016; Djamei et al. 2011). The presence of this N-terminal signal peptide allows for bioinformatic identification of candidate effectors thus forming the basis of many well-established *in silico* effector discovery pipelines. Other characteristics frequently utilised in these pipelines include: lack of transmembrane domain, cysteine content, protein size (< 300 amino acids), presence or absence of known structural or functional domains, and lack of orthologue proteins outside the genus (Gibriel, Thomma, and Seidl 2016). While some of these characteristics are considered somewhat arbitrary, when used in conjunction with *in planta* expression data from host colonisation, they can be employed as a powerful tool for effector identification. As such, the advent of the genomic era has rapidly accelerated effector discovery.

1.2.2 Biotrophic fungal effector proteins

Biotrophic plant pathogens form an intimate relationship with their host throughout the infection process and the repertoire of effectors secreted during the establishment of this relationship are integral to pathogen virulence. One of the most extensively studied biotrophic plant pathogen-host interactions is between maize (*Zea mays*) and the corn smut pathogen, *Ustilago maydis,* which has resulted in the identification of numerous effectors acting to evade immune defences and modulate host metabolism. The *U. maydis* genome encodes for more than 450 secreted proteins; many of which are novel, clustered and differentially secreted throughout plant colonisation (Kamper et al. 2006; Schuster, Schweizer, and Kahmann 2018). One of the most strongly induced genes during the *U. maydis*-maize interaction is *Cmu1* and the encoded protein, Cmu1, is the most abundant protein in the host apoplast. Cmu1 is a chorismate mutase and is hypothesised to re-channel chorismate, a precursor to the plant defence hormone SA, from plastids to the cytosol – thus reducing the amount of chorismate available for SA biosynthesis. Cmu1 is a cytoplasmically functioning effector and is translocated into host cells from which it can then spread to neighbouring cells, metabolically priming plant cells for upcoming infection and minimising the PTI response (Djamei et al. 2011). Recently, Han et al. (2019) identified a maize kiwellin (ZmKWL1) which specifically blocks the active site of Cmu1 and phylogenetic analysis of the kiwellin family revealed that these proteins have a versatile scaffold that can counteract pathogen effectors with high specificity.

Another example of a *U. maydis* cytoplasmic effector is Tin2 which interacts with a phosphodegron-like motif of the cytoplasmic maize kinase ZmTTK1 thus preventing ubiquitination and proteasome-dependent degradation. The *tin2* mutant is attenuated in virulence and exhibits a striking phenotype whereby there is a complete lack of anthocyanin accumulation in infected tissue. Tin2 is thought to stabilise ZmTTK1 and promote anthocyanin biosynthesis thereby leading to an increase in anthocyanin accumulation. The increase in anthocyanin accumulation is hypothesised to negatively affect the lignin biosynthetic pathway by reducing the levels of the precursor *p*-coumaric acid thereby preventing lignification (Brefort et al. 2014; Tanaka et al. 2014). During maize colonisation, *U. maydis* secretes the apoplastic effector Pit2 which acts to inhibit at least four cysteine proteases – the activity of which actively promote SA-associated defences (Mueller et al. 2013). While *Pit2* mutants are still able to colonise maize plants, they are severely attenuated in tumour induction (Doehlemann et al. 2011). Pep1 also accumulates in the apoplast of maize during *U. maydis* infection and inhibits the maize peroxidase POX12 – a major producer of hydrogen peroxide in the apoplast (Hemetsberger et al. 2012). *Pep1* mutants, while able to form appressoria, are arrested during penetration and induce strong defence responses including a huge transcriptional upregulation of POX12 (Doehlemann et al. 2009).

The avirulence (Avr) effectors from the biotroph *Cladosporium fulvum,* causal pathogen of tomato leaf mold, are also some of the most extensively studied with at least ten having been functionally characterised (Thomma et al. 2005; Winnenburg et al. 2006). The interaction between *C. fulvum* and tomato

(*Solanum lycopersicum)* is typical of the gene-for-gene model whereby the perception of a protein encoded by an *Avr* gene by the matching resistance (R) protein results in ETI (Joosten and de Wit 1999). Numerous *Cf* resistance genes in tomato have been identified along with their corresponding *Avr* genes – for example the *Cf-9* gene which confers resistance against *Avr9* (van Kan, Van den Ackerveken, and De Wit 1991; Van den Ackerveken et al. 1993; Bolton et al. 2008). Avr9 was discovered when the 28-amino acid protein was purified from intercellular fluids of *C. fulvum*-infected tomato plants. Agroinfiltration of Avr9 into tomato carrying the corresponding *Cf-9* resistance gene results in the induction of the HR (De Wit and Spikman 1982b; Van der Hoorn et al. 2000). Like Avr9, the Avr4 effector was also isolated from apoplastic fluids and circumvents the ETI defence response mediated by the corresponding *Cf-4* gene product (Schottens-Toma, de Wit, and pathology 1988). Not only does Avr4 act to overcome ETI but it also acts as a virulence factor for *C. fulvum* by binding to chitin in the fungal cell wall protecting hyphae from plant chitinases thus preventing the initiation of PTI (van Esse et al. 2007; van den Burg et al. 2006). Avr2 is another *C. fulvum* effector initially discovered as an Avr protein that overcomes the *Cf-2* resistance gene but also acts as a virulence factor in susceptible plants. The Avr2 effector can overcome PTI in plants lacking the *Cf-2* gene by specifically targeting cysteine proteases which are required for the initiation of basal plant defence and virulence on susceptible plants is significantly reduced when this gene is silenced (Kruger et al. 2002; van Esse et al. 2008).

In addition to the Avr proteins, another six extracellular protein (Ecp) effectors have been identified from the *C. fulvum*-tomato interaction. The LysM domain-containing Ecp6 effector acts in a similar way to the Cf4 effector, sequestering chitin oligomers released by chitinases during infection and thereby suppressing PTI (de Jonge et al. 2010). Similarly, *Moniliophthora perniciosa*, a biotrophic fungal pathogen of cacao, expresses an inactive chitinase (MpChi) during infection. Despite the lack of chitinolytic activity, MpChi retains substrate binding activity and sequesters immunogenic chitin fragments thus preventing the elicitation of chitin-induced immune responses (Fiorin et al. 2018).

1.2.3 Hemibiotrophic fungal effector proteins

Traversing the continuum between biotrophy and necrotrophy, hemibiotrophs are required to produce defence-suppressing effectors prior to producing effectors that promote cell death thus facilitating both pathogenic lifestyles. One of the most well-studied hemibiotrophic pathogens is the ascomycete fungus *Magnaporthe oryzae*, the causal agent of rice blast disease, which is both an economic important pathogen as well as a model system for the study of genes involved in fungal pathogenesis (Ebbole 2007). Upon landing on the leaf surface, *M. oryzae* spores germinate and form specialised structures known as appressoria which facilitate turgor-driven penetration of the rice epidermis (Xu et al. 1997). After appressorial maturation, *M. oryzae* develops a penetration peg which differentiates into invasive hyphae (IH) and grows inside live host cells. In doing so, *M. oryzae* forms an intimate relationship with the host whereby intracellular IH are surrounded by a plant-derived extrainvasive hyphal membrane (EIHM) creating an enclosed

apoplastic compartment (Kankanala, Czymmek, and Valent 2007). In addition to the EIHM, *M. oryzae* develops another highly specialised infection structure known as the biotrophic interfacial complex (BIC). The BIC is a plant-derived, membrane-rich structure which develops at the tip of primary IH before repositioning to the side of a fully differentiated IH (Khang et al. 2010). The BIC and the EIHM represent two distinct pathways for effector secretion whereby cytoplasmic effectors have been shown to preferentially accumulate at the BIC prior to delivery into the plant cell (Giraldo et al. 2013). *M. oryzae* possesses a large repertoire of effector proteins secreted, not only into cells occupied by the fungus, but also into adjacent cells (Khang et al. 2010). Disease symptoms only become visible after this prolonged biotrophic period – a period facilitated by the secretion of defence-suppressing effectors (Zhang and Xu 2014).

In the *M. oryzae*-rice interaction, over 40 Avr proteins have been identified including the cytoplasmic AvrPiz-t and Avr-Pita effectors. AvrPiz-t suppresses PTI by inhibiting the ubiquitin ligase activity of the rice RING E3 ligase APIP6 and silencing of APIP6 leads to enhanced susceptibility of rice plants towards *M. oryzae* (Park et al. 2012). *Avr-Pita* encodes a putative neutral zinc metalloprotease predicted to bind directly to the cognate rice Pita protein to confer rice blast resistance (Jia et al. 2000). One of the most well characterised apoplastic *M. oryzae* effectors is a LysM-domain containing protein, Slp1, which is a functional orthologue of the *C. fulvum* effector Ecp6. Slp1 accumulates at the interface between the fungal cell wall and rice plasma membrane where it binds to chitin competing with the rice chitin elicitor binding protein (CeBIP) to prevent PTI initiation (Mentlak et al. 2012).

The LysM domain is widely conserved throughout the fungal kingdom and a LysM effector secreted in the early stages of infection in the hemibiotroph *Zymoseptoria tritici* has also been found to support the evasion of PTI through binding of fungal chitin (Lee et al. 2014).

Fusarium oxysporum f. sp. *lycopersici* (*Fol*) is the causal agent of vascular disease in tomato (Nirmaladevi et al. 2016). *Fol* secretes numerous effectors into the xylem – a class of proteins aptly named secreted-in-xylem (SIX) proteins. One of the first SIX proteins to be characterised was SIX1 which is required for full virulence on tomato and triggers disease resistance in plants carrying the *I-3* resistance gene (Rep 2005; Thatcher et al. 2012). Another SIX effector required for full virulence on tomato is SIX3, also known as Avr2, which activates resistance through interaction with the *I-2* resistance gene (Houterman et al. 2009). SIX3 shares an upstream promoter region with another SIX effector, SIX5, and both effectors are required to trigger *I-2* mediated immunity in tomato (Ma et al. 2015; Schmidt et al. 2013). While expression of SIX3 in heterologous systems is sufficient to trigger *I-2*-mediated necrosis, expression of SIX5 does not and, until recently, the role that SIX5 played in triggering *I-2* mediated immunity in tomato was unknown (Houterman et al. 2009). Recently however, using bimolecular fluorescence assays, Cao et al. (2018) demonstrated that SIX3 and SIX5 interact at the plasmodesmata, speculating that SIX5 mediates cell-to-cell movement of SIX3 which in susceptible plants leads to virulence and in plants containing *I-2* leads to resistance.

The necrosis- and ethylene-inducing protein 1 (NEP1)-like proteins (NLPs) are widely distributed across the bacterial and fungal kingdoms and were first

isolated from the culture filtrate of *Fusarium oxysporum* f. sp. *erythroxyli* (Bailey 1995; Gijzen and Nurnberger 2006). NLPs act as cytotoxic proteins in dicotyledonous plants, triggering leaf necrosis and plant-immunity defence responses (Qutob et al. 2006). The number of NLP family members varies significantly between microorganisms – for instance, *Z. tritici* has one NLP in the whole genome while 33 copies are found in the oomycete *Phytophthora sojae*.(Motteram et al. 2009; Dong et al. 2012). NLPs share a similar tertiary structure to actinopores, pore-forming toxins from sea anemones, leading to the hypothesis that NLPS destabilise plant plasma membranes resulting in cell death (Azmi et al. 2018). NLPs often exhibit dual function either as triggers of the immune response leading to resistance or as a toxin-like virulence factor (Azmi et al. 2018). The duality of the NLP superfamily is perhaps best demonstrated in the hemibiotroph *Colletrotichum higginsianum*. Six NLP homologs have been identified in *C. higginsianum* which exhibit contrasting expression profiles throughout infection. *ChNLP1*, for instance, is expressed specifically during the switch from biotrophy to necrotrophy and induces cell death in *N. benthamiana* when recombinantly expressed. In contrast, *ChNLP3* is specifically expressed in appressoria and is incapable of inducing cell necrosis (Kleemann et al. 2012).

1.2.4 Necrotrophic fungal effector proteins

The aim of many biotrophic and hemibiotrophic effectors is to suppress the host immune system in order for them to prevent the initiation of PCD, acting to limit the spread of an invading pathogen (de Wit et al. 2009). In contrast, induction of the HR is beneficial to pathogens which exhibit a necrotrophic lifestyle – providing dead tissue for the pathogen to feed from. The role that

necrotrophic effectors play therefore differs greatly from that of biotrophic pathogens and this class of effectors primarily includes toxins, secondary metabolites, cell death-inducing proteins and plant cell wall degrading enzymes (PCWDEs)(Lyu et al. 2016).

Many necrotrophic pathogens, such as the causal agent of wheat tan spot *Pyrenophora tritici-repentis* (*Ptr*), produce host-selective toxins (HST), such as Ptr ToxA, B and C – all of which are required for full virulence of the pathogen. These effectors are proposed to interact with wheat following an inverse gene-for-gene model, i.e. when recognised by the host, these toxins induce host susceptibility rather than resistance (Ciuffetti et al. 2010). Ptr ToxA was the first described necrotrophic proteinaceous effector and induces the formation of necrotic lesions on ToxA-sensitive wheat cultivars (Tuori, Wolpert, and Ciuffetti 2000). Resolution of the three-dimensional structure of Ptr ToxA revealed that this protein resembles the fibronectin type III domain which utilises an arginyl-glycyl-aspartic acid (RGD) motif to interact with plasma membrane proteins (Sarma et al. 2005; Manning et al. 2008). The presence of this RGD motif suggests that ToxA interacts with an extracellular receptor prior to internalisation into host cells and localisation to the chloroplasts, the predicted site of PtrToxA function (Pandelova et al. 2009; Manning and Ciuffetti 2005). The small, cysteine-rich ToxB and the non-proteinaceous and partially characterised ToxC both induce chlorosis in sensitive wheat lines (Strelkov et al. 2002; Effertz et al. 2002; Ciuffetti et al. 2010).

Parastagonospora nodorum, the causal agent of *Parastagonospora nodurum* blotch (SNB), is another necrotroph of global economic importance which

secretes proteinaceous effectors to induce ETS (Solomon et al. 2006). Several effector-host sensitivity gene interactions have been identified in this pathosystem including the effector *SnToxA*, identical to the *Ptr ToxA* gene, which induces necrosis on wheat lines carrying the host-sensitivity gene *Snn1* (Liu et al. 2012). While numerous necrotrophic effectors have been identified from *P. nodorum*, one of the most well characterised is the PCD-inducing SnTox1. SnTox1 is hypothesised to interact with an extracellular receptor to induce cell death and, due to the presence of chitin-binding domains, also functions to protect *P. nodorum* from wheat chitinases (Liu, Gao, et al. 2016).

Sclerotinia sclerotiorum is a host-non-specific necrotroph with a broad host range (Zhu et al. 2013). An important pathogenicity determinant of this fungus is oxalic acid (OA) - a metabolic effector which initially dampens the ROS burst before eliciting PCD once fungal infection is established (Kim, Min, and Dickman 2008; Williams et al. 2011). *S. sclerotiorum* mutants deficient in OA production are actively recognised by the host, eliciting the HR, and are unable to cause disease (Williams et al. 2011). OA also contributes towards pathogenicity by lowering the pH of host tissues, stimulating the production of pectinases, laccases and proteases (Fernandez-Acero et al. 2010; Manteau et al. 2003). Recently, Yang et al. (2018) characterised SsCP1 – a protein with a predicted effector function belonging to the cerato-platanin (CP) family (Derbyshire et al. 2017). CPs are known to play important roles in the pathogenicity of *Botrytis cinerea* and *Magnaporthe grisea* and elicit the HR in plant leaves following topical application (Jeong, Mitchell, and Dean 2007; Frias, Gonzalez, and Brito

2011; Pazzagli et al. 1999). Recombinant expression of SsCP1 in *N. benthamiana* was shown to induce cell death and SsCP1-deficient mutants are impaired in pathogenicity. Furthermore, SsCP1 was found to specifically interact with PR1 in the apoplast and possibly functions by interfering with the SA pathway (Yang et al. 2018).

B. cinerea, the causal agent of gray mould disease, is an aggressive necrotroph capable of infecting more than 200 host species (Williamson et al. 2007). Like *Sclerotinia,* the *B. cinerea* genome possesses a vastly expanded repertoire of carbohydrate-active enzyme-encoding genes which facilitate necrotrophic infection (Amselem et al. 2011). *B. cinerea* also secretes effectors and toxins which facilitate this necrotrophic lifestyle, several of which have been characterised, including: BcSlp1, a CP protein which contributes towards pathogenicity and elicits the HR (Frias, Gonzalez, and Brito 2011), BcXyg1, a secreted xyloglucanase which triggers BAK1 and SOBIR1-dependent PCD (Zhu et al. 2017), and BcNEP1 and BcNEP2, phytotoxic necrosis-inducing proteins which belong to the Nep1-like family (Schouten, van Baarlen, and van Kan 2008). While the majority of characterised effectors are proteinaceous, recent studies have shown that pathogen-derived small RNAs (sRNAs) can also function as effectors by hijacking host RNA-interference machinery to silence host immunity genes (Weiberg et al. 2013; Qiao et al. 2013). Over 70 sRNAs have been identified in *B. cinerea* with predicted effector function in *Arabidopsis* and tomato – several of which have been functionally validated (Weiberg et al. 2013; Wang, Weiberg, et al. 2017). The discovery that sRNA effectors function to suppress autophagic cell death, facilitating a short period of biotrophic

growth, suggests that the infection mechanisms utilised by *B. cinerea* are not as indiscriminate as once thought (Veloso and van Kan 2018).

1.2.5 Experimental methods employed for functional characterisation of fungal effectors

Whilst nomination of candidate fungal effector lists with ~10 to 500 entries is a relatively easy bioinformatics task, successful functional characterisation of effectors is challenging due to the huge diversity of effectors, lack of common functional signatures as well as widespread functional redundancy (Rafiqi et al. 2012). Despite these constraints, a great deal of progress has been made towards gaining an understanding of effector function using a variety of *in vitro* and *in planta* methods. Methods such as those described below can be used in synergy with genomics and high-throughput transcriptomic approaches to gain an accurate understanding of how effectors may function (Dong et al. 2016).

1.2.5.1 Experimental methods to deduce the contribution of effectors to fungal pathogenicity

Heterologous expression of proteins *in planta* is a widely used tool for the functional characterisation of fungal effectors. Stable or transient *in planta* expression can be achieved in a variety of ways and the methodologies employed can be dependent on the tractability of plant species to individual techniques. Stable transformation involves the generation of transgenic plants, the first step of which is to clone the effector of interest into an appropriate plasmid vector. This vector can then be delivered to the host by *Agrobacterium tumefaciens*-mediated transformation (ATMT) or by particle bombardment with DNA-coated microprojectiles. One of the first examples of this approach

was demonstrated by Hauck, Thilmony, and He (2003) who stably expressed the *Pseudomonas syringae* effector AvrPto in *Arabidopsis* to show that mutants were compromised in defence-related callose composition. A fluorescent or affinity tag may be added to the effector of interest enabling subcellular localisation and expression of the effector-encoding genes can be placed under the control of an inducible promoter (Dalio et al. 2018). ATMT has also been used to transform several plant pathogenic fungi including *F. oxysporum*, *B. cinerea, Verticillium dahliae* and *M. oryzae* amongst others (Khang et al. 2006; Rolland et al. 2003).

One of the primary drawbacks of stable transformation is the costly and low-throughput nature of this approach and, as such, the vast majority of effector characterisation is achieved by transient expression. Perhaps the most commonly used method of heterologous expression of effectors *in planta* is infiltration of transformed *Agrobacterium tumefaciens* T-DNA plasmid into *Nicotiana benthamiana* – a process known as agroinfiltration (Ma et al. 2012). Screening for the HR response in *N. benthamiana* leaves transiently expressing effector proteins provides a rapid screen for bacterial and filamentous pathogen effectors and has been utilised in numerous studies (Kettles et al. 2017). Furthermore, effectors with defence-suppressing activity can be screened in the assay by testing whether expression of effectors can reduce the symptoms induced by the cell death-elicitor INF1 of *P. infestans* (Kamoun et al. 1998). Evaluation of effector-induced phenotypes invariably relies upon the use of several stains to assess pathogenicity. Aniline blue, trypan blue and diaminobenzidine are used to stain callose, the deposition of

which is a hallmark of pathogen attack, dead tissue and ROS, respectively (Hood and Shew 1996).

The two main disadvantages of agroinfiltration are, firstly, that recombinant protein expression is limited to infiltrated tissues and, secondly, that monocotyledonous plants are recalcitrant to this technique. Both limitations can be overcome by using plant virus expression vectors, such as Potato Virus X and the Barley Stripe Mosaic Virus (BSMV), which can be manipulated to achieve long-lasting protein expression in a range of non-cereal and cereal hosts, respectively (Chapman, Kavanagh, and Baulcombe 1992; Haupt et al. 2001)(Hammond-Kosack et al. 1995).

While heterologous expression systems are often advantageous in terms of elucidating subtler phenotypes, one of the most widely used approaches for the validation of effector function is to knock-out or knock-down putative effector genes and assay for changes in pathogenicity. This can be achieved in several ways including by: gene deletion, the introduction of non-functional mutations and, finally, by gene silencing. In *U. maydis,* a highly efficient recombination system has enabled the generation of over a dozen effector mutants through gene replacement, including Pep1, Cmu1 and Pit2 (Doehlemann et al. 2009; Djamei et al. 2011; Mueller et al. 2013; Lanver et al. 2017). Similarly, a homologous gene recombination approach, known as split-marker deletion, is utilised for the generation of *F. graminearum* gene deletion mutants (Goswami 2012). Split-marker gene deletion is a PCR-based method which requires two rounds of PCR to amplify the 5’ and 3’ flanking regions (approximately 1kb in length) of the gene of interest which are subsequently fused to two-thirds of a selectable marker. Two resultant cassettes are then

used to simultaneously transform *F. graminearum* protoplasts leading to loss of function (Figure 1.3)(Maier et al. 2005).

Recent studies have shown that the expression of silencing constructs in plants can be used to target fungal transcripts – a tool known as host-induced gene silencing (HIGS). HIGS takes advantage of RNA silencing mechanisms in plant pathogenic fungi (Nunes & Dean, 2012) and the fact that RNA molecules are readily exchanged between pathogen and host (Tinoco *et al*., 2010). Pliego *et al* (2013) screened putative *Blumeria graminis* effectors by HIGS whereby hairpin RNAs which corresponded to *B. graminis* transcripts were delivered to barley epidermal cells via particle bombardment. Alternatively, RNA molecules involved in RNA silencing can be delivered via the BSMV vector which has been successfully used for the delivery of *Puccinia striiformis* gene fragments into wheat (Yin *et al*., 2011). Another method of characterisation garnering increasing interest is through the use of the bacterial and archaeal immune mechanism CRISPR/Cas-9, a powerful genome editing system that has recently been adapted for use in filamentous fungi and an effector in the oomycete *Phytophthora sojae* has been disrupted with this system (Nodvig et al. 2015; Fang and Tyler 2016).

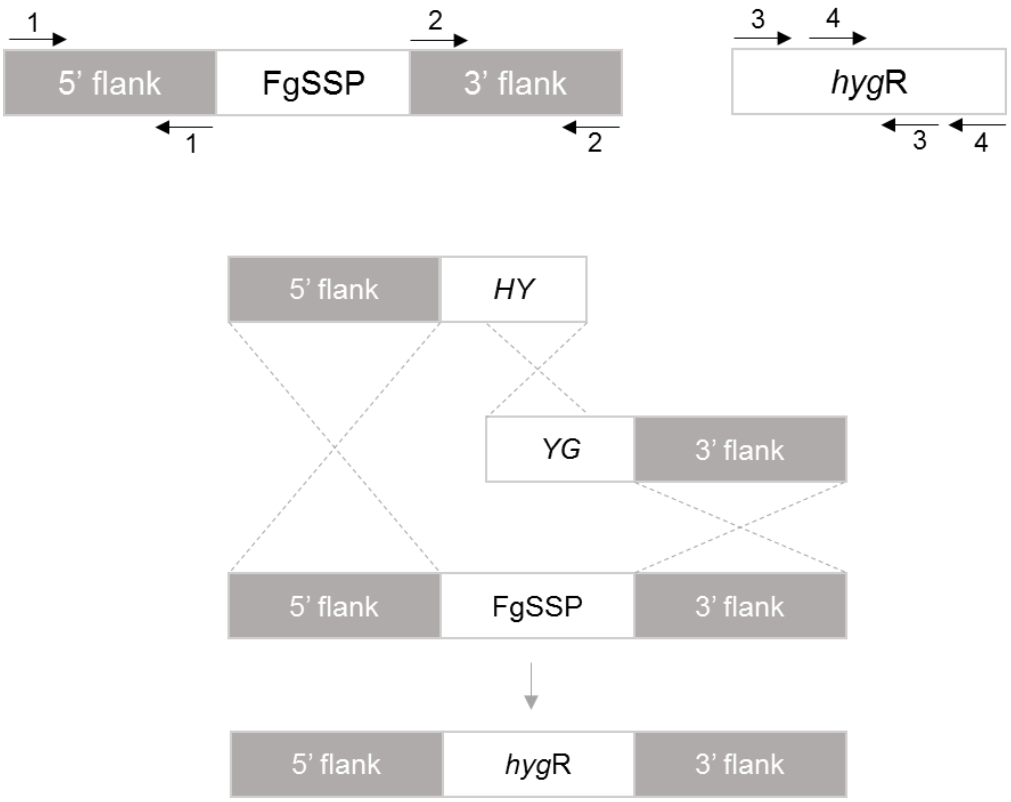

Figure 1.3 The split-marker transformation method for the generation of single gene deletions in *F. graminearum*. The regions flanking both the 5' and 3' end of the gene of interest are identified and primer pairs 1 and 2 are used to amplify these flanking regions. In addition, the first two thirds of a selectable marker, e.g. hygromycin (*hygR*), are amplified with primer pair 3 and the second two thirds of the selectable marker are amplified using primer pair 4. Primer pairs 1 and 3 are designed to contain homologous regions allowing fusion of the 5' flank to the first two thirds of *hygR* via Gibson assembly thereby forming cassette 1. Primer pairs 2 and 4 are also designed with homologous regions allowing fusion of the 3' flank of the GOI to the second two thirds of *hygR* thereby forming cassette 2. The two resultant plasmids from these reactions are then co-transformed into *F. graminearum* protoplasts. The *hygR* gene replaces the GOI as three rounds of homologous recombination occur; 1) between the 5' flanking region in cassette 1 and the *F. graminearum* genome, 2) between the two *hygR* regions in cassettes 1 and 2 and 3) between the 3' flanking region in cassette 2 and the *F. graminearum* genome.

1.2.5.1.1 Barley Stripe Mosaic Virus-mediated overexpression (BSMV-VOX)

As previously mentioned, viruses such as BSMV can be used for functional characterisation of genes in cereal host species. A number of BSMV-mediated tools exist that can contribute towards this goal which include: virus-induced gene silencing (VIGS), host induced gene silencing (HIGS) and virus-mediated over-expression (VOX) of proteins (Figure 1.4)(Lee, Hammond-Kosack, and Kanyuka 2012). BSMV has a tripartite genome comprising of RNAα, RNAβ and RNAγ, each RNA molecule being encapsulated in an individual rod-shaped virion, which can be engineered to serve as an expression vector in plants (Joshi, Joshi, and Ow 1990). As such, in recent years BSMV has become a popular vector for VIGS in wheat and barley (Lee, Hammond-Kosack, and Kanyuka 2012). Whilst VIGS is an effective tool for studying the effect of down-regulating target gene expression, there has been a paucity of studies that use the BSMV vector for overexpression of small heterologous proteins since VOX was first demonstrated *in planta* by Haupt et al. (2001). The authors of this study used BSMV to overexpress GFP to study the pathway of phloem unloading in barley revealing, however, one of the main caveats of the BSMV-VOX system. In this study, GFP expression in systemically infected barley tissue was patchy and, whilst Lawrence and Jackson (2001) initially hypothesised that this was due to BSMV exiting the vasculature, it is now generally acknowledged that this is due to the size of the fragment. This is because insert size is negatively correlated with vector stability in both BSMV and PVX (Bruun-Rasmussen et al. 2007). Virus genomes are generally compact

and insertion of genes larger than 500 base pairs that are not required for replication and propagation are often subject to deletion by homologous recombination (Avesani et al. 2007). Despite this constraint, due to the general consensus that effectors are small proteins, this system remains a useful tool for discovering effector function. Use of BSMV as an *in planta* expression vector for effector characterisation was first carried out by Manning et al. (2010) who overexpressed the host-selective toxin ToxA in wheat, barley and tobacco. Meng, Moscou, and Wise (2009) cloned the full-length barley 480 bp *Bln1* open reading frame (ORF) into a BSMV vector delivered into barley epidermal cells via bombardment to determine the role *Bln1,* a peptide induced by attack from *Blumeria graminis*, played in barley immunity towards this pathogen. Whilst this is a viable strategy for the study of transient protein expression in individually bombarded plant cells, this technique is not as useful for exploring fungal-plant interactions that involve multiple cells.

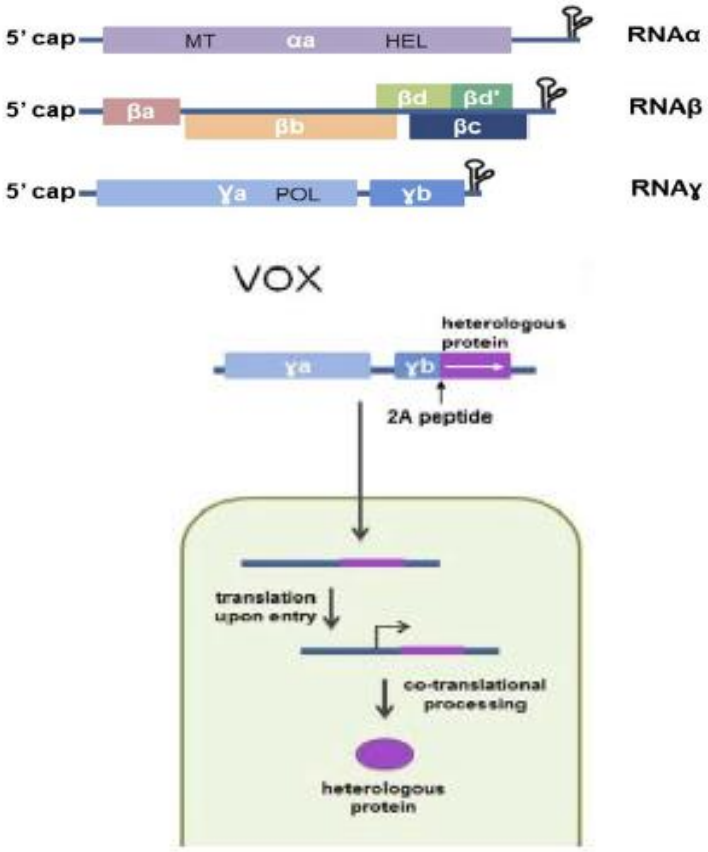

Figure 1.4 Mechanistic model for BSMV-VOX. The BSMV genome is comprised of three RNAs that are capped at the 5' end and form a tRNA-like hairpin structure at the 3' terminus. RNAα encodes the αa protein which contains the methytransferase and helicase domains. RNAβ encodes a coat protein and movement proteins and RNAγ encodes the polymerase component of replicase and a Cys-rich γb protein involved in viral pathogenicity. In BSMV-VOX the coding sequence for the protein of interest is inserted immediately upstream of the in-frame stop codon of the γb ORF. A small synthetic 2A gene which encodes an autoproteolytic peptide is inserted between the 3' terminus of the γb ORF and the gene sequence coding for the heterologous protein. This configuration enables self-processing of the γb fusion protein during translation of the virally encoded proteins thus releasing the free heterologous protein. Adapted from Lee *et al*. (2012).

1.2.5.2 Experimental methods to localise fungal effector proteins

While the above methods can be used to determine whether silencing or overexpression of effector genes can potentiate a change in the pathogen-host interaction, they provide little insight into the mechanisms by which the effector controls or alters the interaction outcome. As fungal effectors can be broadly classified into two types, apoplastic or cytoplasmic, determination of protein localisation is often the first step in exploring effector function (Petre, Saunders, et al. 2016; Irieda, Ogawa, and Takano 2016; Djamei et al. 2011). Effector localisation studies have classically relied upon *in situ* hybridisation of antibodies raised specifically against effectors or against an epitope tag – a technique which also facilitates immunodetection of effectors by electron microscopy (Szurek et al. 2002). This approach has several drawbacks; namely the expense of raising effector-specific antibodies and the laboriousness and time-consuming nature of immunodetection techniques. In the *M. oryzae*-rice pathosystem, live fluorescence microscopy of fluorescent protein-tagged Avr effectors is widely used for effector localisation studies. Live-cell imaging with fluorescence-tagged effectors enables the monitoring of the spatial and temporal location of effectors during infection and was used to identify the highly localised BIC in *Magnaporthe oryzae* at which effectors accumulate (Khang et al. 2010).

Fungal effectors exert their effects in a diverse number of ways and as such the plant compartments targeted are diverse. In order to determine the subcellular localisation of the rust fungus *Melampspora larici-populina* effectors, Petre et al. (2015) used confocal microscopy combined with co-immunoprecipitation methods and mass spectrometry in order to identify *N.*

benthamiana proteins which associated with the effectors in question. Using this method, the authors of this study were able to show that *M. larici-populina* effectors targeted multiple plant cell compartments and processes in plant cells. While a useful methodology for effector localisation in several fungal species, efforts to transfer this system to other genetically tractable fungi have failed and the addition of large fluorescent tags, such as GFP, may affect protein localisation and functionality (Khang et al. 2010; Rafiqi et al. 2012).

To overcome the limitations imposed by the described methods of localisation, Lo Presti et al. (2017) recently established an assay based on the biotinylation of cytoplasmic effectors that enables medium-throughput screening for effector uptake. This assay involves the generation of transgenic fungal strains expressing an effector-Avitag fusion and the generation of transgenic host plants cytoplasmically expressing a bacterial biotin ligase (*birA*). Uptake of the effector into the host cell leads to biotinylation of the Avitag – a modification readily detected by western blotting. Generation of transgenic fungal strains, however, is a time-consuming process and as such the development of a more high-throughput permutation of this assay is desirable.

1.2.5.2 Experimental methods to determine effector protein interactors and effector function

Identification of effector targets is perhaps the most important step in determining protein function. However, the lack of conserved motifs within effector protein sequences makes this task difficult, offering little clue as to molecular function (Dalio et al. 2018). Unbiased protein-protein interaction

studies can therefore provide a wealth of information as to effector function and often represent the first step in effector target identification. Target identification of the stripe rust effector, PEC6, was determined using two widely used techniques - a yeast-two-hybrid (Y2H) screen in conjunction with bimolecular fluorescence complementation (BiFC). Using PEC6 as bait, Liu, Pedersen, et al. (2016) screened a prey cDNA library generated from barley leaves infected with powdery mildew thus enabling the identification of the barley adenosine kinase (ADK)-PEC6 interaction. While a relatively rapid and easy way to screen for protein-protein interactions, Y2H screens yield high rates of false positives and negatives and, in addition, protein folding and expression in yeast systems may not mimic that seen in plant cells (Liu, Pedersen, et al. 2016). Validation of this interaction was thereby achieved using BiFC – a technique which enables direct visualisation of protein interactions in living cells and is facilitated by the fusion of two non-fluorescent fragments of a fluorescent protein (Kerppola 2006).

An alternative approach to Y2H is to overexpress a tagged effector of interest and use co-immunoprecipitation (CoIP) techniques to pull down interacting proteins and to identify these targets using mass-spectrometry (MS)(Fu et al. 2007). A more explorative approach could be to carry out a chemical analysis, using techniques such as MS and high-performance liquid chromatography (HPLC), of hosts recombinantly expressing effectors of interest to identify host compounds induced in response to effector presence.

Many of the methods outlined rely on prior knowledge of potential interactors. In cases where this is absent, one avenue for target identification is RNA-seq. RNA-seq analysis utilises deep-sequencing technologies to provide

high-resolution transcriptome profiling and forms the basis of many effector-discovery pipelines (Wang, Gerstein, and Snyder 2009). Application of an RNA-seq approach to resolve transcript abundance of hosts exposed to individual effectors can help identify up/downregulated genes, the products of which may interact with effectors of interest.

1.3 Fusarium head blight

Fusarium Head Blight (FHB), also known as Fusarium Ear Blight or Fusarium Head Scab, is currently recognised as one of the most damaging and hazardous diseases of wheat, and other small grain cereal crops, across the globe (ISPP, 2017). A disease that compromises grain yield, quality and food safety, in recent years FHB has re-emerged as a disease of significant economic importance resulting in direct crop losses of an estimated $2.7 billion in the US across a two-year period (Nganje et al. 2004).

First described in England in 1884, several years later FHB was reported in the US where, in the 1910's, five major FHB epidemics occurred (Parry, Jenkinson, and Mcleod 1995). Trends towards 1) reduced tillage, 2) expanding maize production thereby providing a source of inoculum and 3) changing climatic conditions have since seen the prevalence of FHB increase in Europe, China, USA and Brazil (Forrer et al. 2014). In China from 2000-2018, annual yield losses attributable to FHB amounted to 3.41 million tons and, in Argentina in 2012, a severe FHB epidemic resulted in yield losses of up to 70% (Palazzini et al. 2015). The occurrence of FHB wheat epidemics is primarily determined by weather conditions prior to the occurrence of anthesis – with warm and wet weather favouring the development of this disease (De Wolf, Madden, and Lipps 2003). These

meteorological factors also strongly determine the severity of epidemics and the accumulation of associated trichothecene mycotoxins. Alterations in climate patterns will therefore likely affect pathogen distribution and dynamics - with the distribution of several species from the *Fusarium* genus predicted to increase (Figure 1.5)(Backhouse 2014; Vaughan, Backhouse, and Del Ponte 2016).

While several species from the *Fusarium* genus are capable of causing FHB, the most aggressive and predominant causal agent of FHB is the ascomycete fungus *Fusarium graminearum* Schwabe (teleomorph *Gibberella zeae*)(Bottalico and Perrone 2002; O'Donnell et al. 2000). *F. graminearum* infection is characterised by bleaching of the wheat ear resulting in the production of withered, discoloured and light-weight wheat kernels (tombstone kernels) resulting in a reduction in both yield and quality due to selective loss of albumin and glutenin proteins in the wheat endosperm (Goswami and Kistler 2004; Boyacioglu and Hettiarachchy 1995). Whilst reduction in grain yield is highly undesirable, the main consequence of infection with *F. graminearum* is grain contamination with trichothecene mycotoxins, such as deoxynivalenol (DON), posing a food safety risk and health hazard to both humans and livestock (Pestka and Smolinski 2005). As resistance within wheat towards FHB is incomplete, control is primarily mediated by appropriate agronomic practices and chemical fungicide applications, to which *F. graminearum* is intrinsically insensitive (Buerstmayr, Ban, and Anderson 2009; Dill-Macky 2008). With this intrinsic insensitivity working in tandem with increasing fungicide resistance and an overall

increase in FHB incidence globally, an integrated control strategy must be successfully coordinated to attain adequate control of this disease.

Figure 1.5 Recorded distribution (black circles) and predicted distribution (grey areas) of *F. graminearum* based on nine climate-based parameters analysed by Backhouse (2014).

1.3.1 Mycotoxins in Fusarium Head Blight

Fusarium species produce a diverse array of metabolically active secondary metabolites, some of which are extremely damaging towards animals and thus termed mycotoxins (Desjardins and Proctor 2007). The mycotoxins most commonly associated with *F. graminearum* are zearalenone (ZEA) and the trichothecenes - a large family of sesquiterpenoid secondary metabolites, members of which inhibit eukaryotic protein synthesis and may cause toxicosis in humans and animals (Maresca 2013). Trichothecenes can be divided into four sub-types (A-B) with the type B trichothecenes particularly prevalent amongst the *Fusaria*. Type B trichothecenes, which include the nivalenol (NIV), deoxynivalenol (DON), and DON's acetylated derivatives 15-acetyl-4-deoxynivalenol (3-ADON) and 15-acetyl-4-deoxynivalenol (15-

ADON), are characterised by the presence of a C-8 keto group (Chen et al. 2019).

While type B trichothecene chemotypes only differ in terms of the position and pattern of acetylation and hydroxylation, there is great variation in regard to the toxicity of these compounds towards both plants and mammals (Kimora et al. 1998). NIV, for instance, is more toxic to mammals than DON and the limits to which NIV can accumulate in grain are therefore much more stringent (Chothorst & van Egmond, 2004). DON, however, is still one of the most significant and abundant contaminants of food and feed due to the frequent occurrence at which toxicologically relevant concentrations accumulate in grain (Lee and Ryu 2017). The chronic effects of consumption of mycotoxin-contaminated grain include anorexia, suppressed immune function, vomiting and reduced litter size in farmed animals (Pestka and Smolinski 2005). As such, regulatory organisations across the globe have established maximum permitted levels (MPLs) to which these toxins can accumulate in grain. For example, the European Commission has set MPLs for DON ranging from 200 µg/kg in processed cereal-based food for infants and up to 1,750 µg/kg in unprocessed durum wheat, maize and oats (Union 2007).

The prevalence of *F. graminearum* chemotypes varies between geographical regions. While NIV chemotypes are prevalent across Asia, DON chemotypes are more prescient in Europe and North America and, despite the diversity in trichothecene chemotypes, 15-ADON-producing strains account for the majority of FHB in North America (Boutigny et al. 2011). In the past decade however, genetically divergent *F. graminearum* populations have led to shifts

in the prevalence of chemotypes – exemplified by the displacement of the native 15-ADON chemotype in North America with 3-ADON (Ward et al. 2008; Burlakoti et al. 2008). Isolates with the 3-ADON chemotype produce higher amounts of DON and cause more severe FHB symptoms thus representing a concern for the North American grain industry (von der Ohe et al. 2010). In addition, a novel type A chemotype, characterised by the absence of a C-8 keto group, has emerged in North America. The NX-2 chemotype is believed to have recently evolved from a type B ancestor and exhibits similar toxicity to 3-ADON (Kelly et al. 2016). The causes for these population shifts are largely unknown but could be attributed to possible changes in agricultural practices or climatic conditions.

Several strategies can be implemented post-harvest to decontaminate grain including washing, dehulling, and chemical and thermal treatment (Fandohan et al. 2005; House, Nyachoti, and Abramson 2003; Park et al. 1996; Meister and Springer 2004). When all other lines of defence against mycotoxins have failed, mineral adsorbents, such as silicates or aluminosilicates, can be added to feedstuffs which can bind mycotoxins in the gastrointestinal tract, reducing adsorption and alleviating toxicity in certain instances (Awad et al. 2010).

1.3.2 Current strategies available for the control of Fusarium Head Blight

Some of the most common strategies utilised to minimise the FHB epidemic risk are based on inoculum reduction to prevent infection (Rojas et al. 2018). However, widespread adoption of reduced tillage practices for the preservation of vulnerable soils has had the unintended consequence of

increasing the prevalence of FHB epidemics (Dill-Macky 2008). As *Fusarium* species survive on crop residues from previous rotations, tillage strategies can greatly influence the level to which *Fusarium* inoculum builds-up prior to the next rotation, as well as DON accumulation in contaminated grains (Dill-Macky and Jones 2000; Schaafsma, Tamburic-Ilincic, and Hooker 2005). Stubble burning, while banned in the EU, is therefore an effective strategy for maintaining low inoculum levels – with the major caveat that reduction in FHB severity is not accompanied by yield gains due to the deleterious effect that burning has on soil quality (Burgess et al. 1996). Crop rotation with non-cereal species can also act to limit inoculum build-up (Pereyra, Dill-Macky, and Sims 2004; Qiu et al. 2016). A study by Dill-Macky and Jones (2000) found that FHB intensity was 25% lower in soybean-wheat rotations when compared to wheat-wheat rotations and 49% lower than corn-wheat rotations. Interestingly, while crop rotation strategies are known to influence both FHB severity and mycotoxin accumulation, long-term rotations do not affect *F. graminearum* species complex (FGSC) composition in *Fusarium* crown rot (FCR)-causing populations (Tillmann, von Tiedemann, and Winter 2017). Nitrogen fertiliser application may also affect disease development by increasing humidity in the canopy microclimate and precision application of fertiliser may therefore be integrated into control strategies (Heier et al. 2005). Other agronomic practices such as delayed sowing and irrigation management are also known to help reduce FHB inoculum (Gorczyca et al. 2018); for instance, excessive moisture in irrigated fields, particularly prior to anthesis, can exacerbate *Fusarium* infection (Cowger et al. 2009).

Deployment of disease-resistant cultivars is one of the most cost-effective and durable ways of controlling phytopathogenic fungi. Unfortunately, while over 250 quantitative trait loci (QTL) conferring resistance towards FHB have been described, the identification of single resistance genes within wheat and barley has remained elusive (Jia et al. 2018). These QTL, although from diverse germplasm resources, often contribute small amounts of resistance and are vulnerable to environmental effects (Ban and Suenaga 2000). The resistance conferred by these QTLs can be classified into five types: resistance to initial infection (type I), resistance to FHB spread within the host (type II), kernel size and number retention (type III), yield tolerance (type IV) and resistance to mycotoxin accumulation (type V).

A notable source of type II resistance lies within the Chinese wheat cultivar Sumai 3. The QTL *Fhb1* provides moderate broad-spectrum resistance against various isolates and species of *Fusarium* (Cuthbert et al. 2006). Transcriptomic analysis of Sumai 3 and two susceptible near-isogenic lines (NILs) revealed that genes encoding defence-related metabolites from the phenylalanine ammonia-lyase (PAL) pathway are upregulated in Sumai 3 (Golkari et al. 2009). More recently, map-based cloning of *Fhb1* led to the identification of a gene encoding a chimeric lectin with agglutinin and pore-forming toxin (PFT)-like domains on chromosome 3BS (Rawat et al. 2016). While the biochemical mechanism of PFT-mediated resistance in FHB is under debate, the authors of the study hypothesise that PFT arrests fungal growth by interacting with the fungal cell wall leading to increased membrane permeability in the pathogen. Prior to this study, the *Fhb1* QTL was thought to provide resistance through DON-detoxification (Niwa et al. 2014;

Lemmens et al. 2005). In contrast, Rawat et al. (2016) demonstrated that the DON-detoxification locus identified by Niwa et al. (2014) was independent of *PFT* although located in the same genetic block. Despite uncertainties about the mechanism of resistance, the recent development of diagnostic markers will facilitate marker-assisted selection (MAS) of *Fhb1* into elite wheat lines (Su et al. 2018).

The Sumai 3-derived QTL *Qfhs.ifa-5A* also provides effective resistance towards FHB. *Qfhs.ifa-5A* predominantly controls type I resistance, resistance towards initial infection, and to a lesser extent, type II resistance (Buerstmayr et al. 2002). Fine-mapping of *Qfhs.ifa-5A* across the pericentromic region of chromosome 5A led to the identification of two tightly-linked QTL related to anther extrusion (Steiner et al. 2019). QTLs for anther extrusion and QTLs for FHB resistance frequently coincide. Identification of anther extrusion as a major component of *Qfhs.ifa-5A* resistance therefore enables fast and reliable phenotypic selection in the absence of disease (Lu et al. 2013). Another proposed mechanism through which *Qfhs.ifa-5A* confers resistance is via the production of a type I non-specific lipid transfer protein (LTP) which is constitutively expressed in *Qfhs.ifa-5A*-carrying wheat lines (Schweiger et al. 2013). While LTPs have been implicated in plant defence against multiple pathogens, the role the LTP expressed in *Qfhs.ifa-5A* lines plays has yet to be determined.

A major FHB resistance QTL has also been identified on the short-arm of chromosome 6BS – the *Fhb2* QTL which was shown to reduce FHB in greenhouse tests by 56% when compared to lines carrying the susceptible allele (Cuthbert, Somers, and Brule-Babel 2007). Comparative metabolomic

profiling revealed that metabolites belonging to the phenylpropanoid, lignin, glycerophospholipid, flavonoid, fatty acid and terpenoid biosynthetic pathways accumulate to greater levels in wheat lines carrying the *Fhb2* QTL. Transcriptomic analysis from the same study also revealed that there was a significant induction in genes encoding several receptor kinases, transcription factors and mycotoxin detoxification factors (Dhokane et al. 2016). *Fhb2* is therefore currently thought to function through DON detoxification and via cell wall reinforcement acting to restrict the pathogen spread within the spikelet (Kazan and Gardiner 2018).

The most widely applied fungicides for FHB control are those belonging to the sterol demethylation inhibitor (DMI) class, including the triazoles (McMullen et al. 2012). Triazoles function by inhibiting ergosterol synthesis by binding to the fungal cytochrome P450 lanosterol C-14-α-demethylase (CYP51) – an essential enzyme which mediates membrane permeability (Lepesheva and Waterman 2007). To maximise benefits of DMI control, spraying must occur at anthesis when wheat is most vulnerable to FHB infection. Flowering times within the crop canopy typically occur within a fourteen-day period thus making it difficult to protect the crop with a single fungicide application. Even when DMIs are applied within this window, complete control of FHB is rarely achieved due, in part, to the high level of intrinsic resistance *F. graminearum* displays towards these fungicides due to the presence of an additional *CYP51* gene (Fan et al. 2013).

Due to concerns over the environmental impact of pesticides and increasing rates of resistance observed towards these compounds, biological control agents (BCA) have garnered increasing attention over recent years as an

environmentally-friendly alternative (Alabouvette, Olivain, and Steinberg 2006). Several bacterial BCAs, including *Bacillus* spp., *Penicillium* spp., and *Streptomyces* spp., have been shown to have an antagonistic effect on *F. graminearum* growth *in vitro*, in glasshouse and in field conditions (Schisler, Khan, and Boehm 2002; Schisler et al. 2006; Palazzini et al. 2007). Despite years of research, however, only one BCA is currently commercially available to control FHB – Polyversum®, a commercialised formulation of *Pythium oligandrum* strain ATCC 38472 (Meszka and Bielenin 2010).

In recent years, technologies which exploit RNA interference (RNAi) silencing mechanisms have emerged as an attractive alternative to traditional chemical fungicides (Machado et al. 2018). Delivery of RNAi signals which trigger gene silencing can be achieved by the generation of transgenic plants expressing these signals and the subsequent transfer to the pathogen, known as host-induced gene silencing (HIGS), or external spray application known as spray-induced gene silencing (SIGS). Delivery of dsRNA targeting the *CYP51* ergosterol biosynthesis genes by both HIGS and SIGS was shown to result in increased resistance towards *F. graminearum* infection in both *Arabidopsis* and barley under glasshouse conditions (Koch et al. 2013; Koch et al. 2016). One of the main advantages of SIGS is that, unlike HIGS, it does not raise public concerns over the widespread growth of genetically modified material. However, effective implementation of SIGS technologies in the field imposes a number of challenges including the durability of dsRNAs and the cost associated with generating these RNA fungicides (Machado et al. 2018).

The individual disease control strategies outlined above, while alone provide incomplete disease control, can be used in conjunction with one another as part of an integrated disease management programme. Such programmes should also consider the genetic structure and diversity of *F. graminearum* populations as different chemotypes are known to response differentially to disease control strategies (Gale et al. 2002; Fernando et al. 2006; Zeller, Bowden, and Leslie 2004). Application of these methods alongside climate-based forecasting models and air-sampling technologies could offer substantial reductions in FHB incidence severity (West et al. 2017; Shah et al. 2019).

1.4 *F. graminearum* infection process in susceptible wheat varieties

1.4.1 Infection cycle

FHB is initiated when airborne sexual ascospores or asexual conidia are deposited on the flowering spikelets of susceptible wheat genotypes (Parry, Jenkinson, and Mcleod 1995). Choline acetate and glycine betaine present in wheat anthers act as stimulants towards *F. graminearum* growth, specifically inducing an increased rate of hyphal branching, and when anthesis coincides with warm and wet weather infection is particularly severe (Pearce, Strange, and Smith 1976). Upon landing on the outer glumes or external anthers, *F. graminearum* infection cushions are formed from runner hyphae leading to penetration of the wheat floral tissue (PUGH, Johann, and Dickson 1933; Brown et al. 2010; Boenisch and Schafer 2011). Spores may also enter the plant through natural openings such as the base of the palea and lemma and degenerating anther tissues (Bushnell et al. 2003). Symptoms of infection first appear as dark-brown spots on the glumes of infected florets and, within

time, the inflorescence may progressively bleach while the grain within shrinks (Goswami and Kistler 2004). These symptoms may often be accompanied by the appearance of pink asexual sporodochia or black perithecia on wheat ears – although the latter is only observed in regions with conducive climatic conditions, for example in mid-west USA (Osborne and Stein 2007). As the primary source of inoculum in the field, the development of perithecia is critical to *Fusarium*'s life cycle. Sexual development begins, as with all ascomycetes, with the formation of binucleate hyphae which develop into asci-filled perithecia from which ascospores are forcibly discharged (Trail 2009). Both perithecia and sporodochia are overwinter on crop residues and constitute the primary sources of inoculum in the field (Figure 1.6)(Shaner 2003).

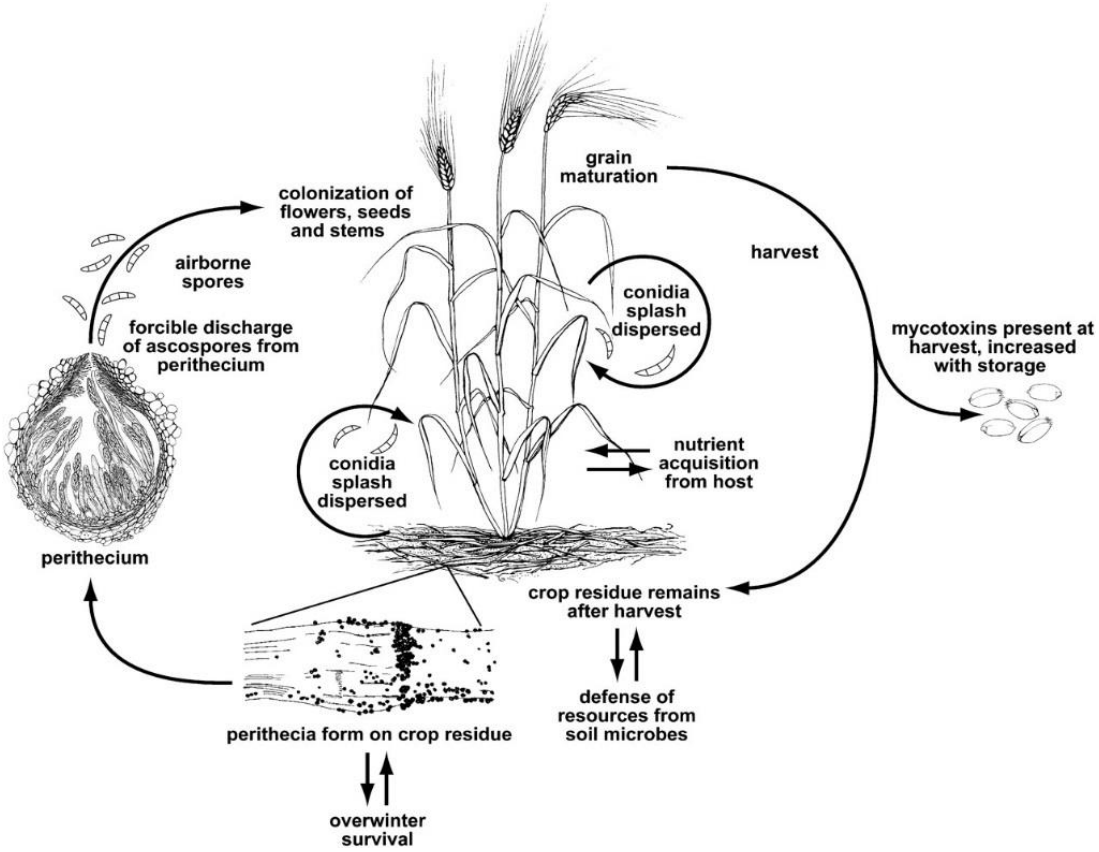

Figure 1.6 The life cycle of *F. graminearum* (sexual phase *G. zeae*). Taken from Trail (2009).

1.4.2 The symptomless and symptomatic phases of *F. graminearum* infection

Prior to 2010, while the mode of action in which *F. graminearum* establishes infection in a single spikelet was well known, the mechanisms the fungus utilises to spread from spikelet to spikelet remained unclear. In addition, controversy over the mode of nutrition utilised by *Fusarium* existed and was disputed amongst researchers. A detailed microscopic investigation of the *F. graminearum* infection pathway in the wheat ear revealed that *F. graminearum* establishment begins asymptomatically – in a manner reminiscent of an apoplastic biotroph (Figure 1.7)(Brown et al. 2010; Brown et al. 2017). The advancing infection front in the rachis was found to localise solely to the apoplast of the cortex where parenchyma cells, although in close contact with intercellular hyphae, remained intact. Behind the advancing infection front, disease symptoms were shown to develop coincidently with intracellular colonisation and plasmolysis of host cells. The pathways through which cell death is initiated during this phase of infection remain unknown. At this later stage of infection, inter- and intracellular hyphae become abundant and hyphal diameters are considerably enlarged compared to the leading infection front. Once the ear is completely colonised, the pathogen accumulates below the surface of the rachis and this hyphal mass ruptures the epidermis giving rise to aerial mycelium. Exhibiting both biotrophic and necrotrophic modes of nutrition, *F. graminearum* infection of wheat can therefore be considered to exist along a continuum – from symptomless to symptomatic infection – the extremities of which are phenotypically distinct (Figure 1.7)(Brown et al. 2011; Brown et al. 2010).

Figure 1.7 Top row shows the disease progression of a wheat ear infected with the PH-1 strain of *F. graminearum* over a period of 3 to 12 days post inoculation (dpi) where black dots on the wheat spikelets indicate initial point of inoculation. The second row of images shows an inoculated wheat head 3dpi (A). Images C & D show spikelets exhibiting no macroscopic symptoms despite hyphae in contact with host cell walls. Image B shows the macroscopic symptoms of *F. graminearum* infection on a wheat spikelet and how this coincides with the penetration of host cells. Taken from Brown *et al*. (2010).

1.5 Molecular strategies employed by *F. graminearum* during infection

1.5.1 The role of mycotoxins in *F. graminearum* virulence

The particularly destructive nature of *F. graminearum* is in part due to the ability of the fungus to produce type-B trichothecene mycotoxins which, in addition to being highly toxigenic, play an important role in fungal virulence (Harris et al. 1999). As such, mycotoxin levels are well known to correlate with FHB severity and incidence (Neilsen et al. 2011). These mycotoxins, which include DON and NIV, are sesquiterpenoids - potent inhibitors of eukaryotic protein synthesis differentially interfering with the initiation, elongation and the termination stages of synthesis (Goswami and Kistler 2005; Cundliffe, Cannon, and Davies 1974).

Fifteen enzymes are required for trichothecene biosynthesis, twelve of which reside in the core-*TRI* gene cluster (Figure 1.8)(Alexander, Proctor, and McCormick 2009). DON accumulation correlates closely with *TRI* gene transcription and, in trichothecene biosynthesis induction media, production of DON coincides with a dramatic alteration of hyphal morphology which form bulbous sub-apical structures (Jonkers et al. 2012; Chen, Kistler, and Ma 2019). Tri1 and Tri4, both cytochrome P450 oxygenases, co-localise to highly remodelled organised smooth endoplasmic reticulum (OSER) structures which are referred to as toxisomes – the presumed sites of DON biosynthesis (Menke et al. 2013; Boenisch et al. 2017). *Tri6* and *Tri10* lie within the core-*TRI* cluster, acting as positive regulatory genes for trichothecene biosynthesis. In addition to these pathway-specific regulators, trichothecene biosynthesis is also regulated by global regulators which

control responses to carbon, nitrogen, light and pH (Hou et al. 2015; Merhej, Richard-Forget, and Barreau 2011).

Genetic disruption of *Tri5*, the first enzyme in the DON biosynthetic pathway which encodes a trichodiene synthase, produces a fungal mutant unable to spread beyond an inoculated wheat spikelet and across the rachis (Bai et al. 2001). The aggressiveness of both *F. graminearum* and *F. culmorum* therefor correlates closely with DON production and is required for full virulence of *F. graminearum* on wheat spikes (Mesterhazy 2002; Proctor, Hohn, and Mccormick 1995). Infection with the *ΔTri5* mutant mounts an enhanced plant defence response characterised by cell wall thickening impeding rachis colonisation (Jansen et al. 2005). A recent study comparing the metabolic profiles of wildtype and Δ*Tri5*-infected wheat rachis tissues revealed that extensive metabolic rearrangements occur. While the wildtype PH-1 initiates an oxidative burst and PCD, spread of the DON-deficient Δ*Tri5* mutant beyond the rachis is blocked by defence responses produced by the JA pathway including cell wall enforcement (Bonnighausen et al. 2019). A transcriptomic study exploring gene expression during the different phases of the *F. graminearum*-wheat floral infection also revealed that the expression of *TRI* genes were dramatically induced, particularly during the symptomless phase of infection (Brown et al. 2017). DON treatment of wheat leaves has been shown to induce hydrogen peroxide production and DNA laddering, hallmarks of PCD, and to rapidly induce the transcription of defence-related genes in a concentration-dependent manner (Desmond et al. 2008). At lower concentrations, DON in fact inhibits PCD in *Arabidopsis* cells leading researchers to hypothesise that, during the symptomless phase of infection,

DON functions to suppress host defences until accumulation of DON at higher concentrations induces PCD (Diamond et al. 2013; Brown et al. 2017). Interestingly, while DON is integral to wheat ear infection processes, DON is not required for full virulence on barley, maize and Arabidopsis floral tissue raising important questions about the role of DON in tissue specificity (Jansen et al. 2005; Harris et al. 1999; Cuzick, Urban, and Hammond-Kosack 2008).

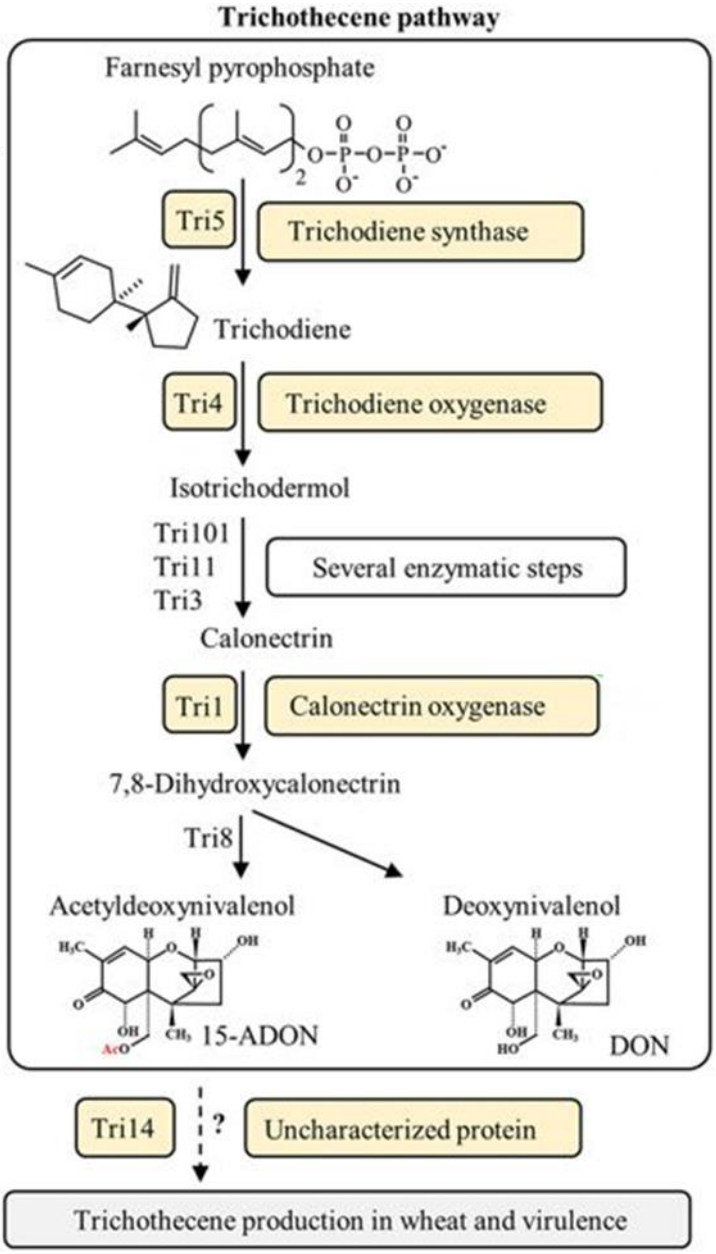

Figure 1.8 Trichothecene biosynthetic pathway adapted from Boenisch et al (2017).

1.5.2 The role of other *F. graminearum* genes experimentally proven to contribute towards fungal virulence

While the importance of the DON to *F. graminearum* virulence has been well established, several other virulence factors have been identified upon which the integrity of *F. graminearum* infection relies. The repression of the activity of Fgl1, a secreted lipase, severely impairs the virulence of *F. graminearum*, although the exact mechanism through which Fgl1 lipase does so remains unclear (Voigt, Schafer, and Salomon 2005; Walter, Nicholson, and Doohan 2010; Blumke et al. 2014). Another integral component to *F. graminearum* virulence is the siderophore triacetyl fusarinine C (TAFC), a secreted virulence factor (Oide et al. 2006). TAFC is a cyclic peptide which binds iron to a very high affinity and is required for iron import into *Fusarium* cells where it is proposed to protect hyphae from hydrogen peroxide damage (Urban and Hammond-Kosack 2013; Oide et al. 2014). In the Pathogen-Host Interaction database (PHI-base)(http://www.phi-base.org/), 21 other genes have been deposited whereby gene deletion mutants exhibit a loss of pathogenicity on wheat ears (Table 1.2)(Cuzick et al. 2019).

Table 1.2 List of *F. graminearum* virulence genes curated into PHI-base (Version 4.7). Deletion of these genes is reported to lead to loss of pathogenicity on wheat tissues.

Gene name	PHI-base ID	Protein	Function	Mutant phenotype	Reference
FgGT2	PHI:7559	Glycosyltransferase	Catalyses the formation of the glycosidic linkage to form a glycoside	Severely impaired in hyphal growth and non-pathogenic in wheat ears	King et al. (2017)
Fgrab51	PHI:4999	RabGTPase	Involved in endocytosis	Reduction in vegetative growth, differential hyphal branching and loss of pathogenicity and DON production	Zheng et al. (2015)
Fgrab52	PHI:5000	RabGTPase	Involved in endocytosis	Reduction in vegetative growth, differential hyphal branching and loss of pathogenicity and DON production	Zheng et al. (2015)
Fgrab6	PHI:5001	RabGTPase	Regulatory role in transport through the Golgi apparatus	Reduction in vegetative growth, differential hyphal branching and loss of pathogenicity and DON production	Zheng et al. (2015)
Fgrab7	PHI:5002	RabGTPase	Localises to the vacuolar membrane and regulates vacuoles and autophagosomes	Reduction in vegetative growth, differential hyphal branching and loss of pathogenicity and DON production	Zheng et al. (2015)
Fgrab8	PHI:5003	RabGTPase	Important for polarised growth and endocytosis	Reduction in vegetative growth, differential hyphal branching and loss of	Zheng et al. (2015)

				pathogenicity and DON production	
MAP1	PHI:3517	Mitogen-activated protein kinase	Regulation of various cellular processes	Non-pathogenic on wheat ears and only able to grow superficially on spikelet tissues and extruded anthers	Cuzick, Urban, and Hammond-Kosack (2008)
CPK1	PHI:3087	Catalytic subunit of cyclic AMP (cAMP)-dependent protein kinase A	Component of major signalling transduction pathways	Reduction in vegetative growth, conidiation, and DON production	Hu et al. (2014)
CPK2	PHI:3088	Catalytic subunit of cyclic AMP (cAMP)-dependent protein kinase A	Component of major signalling transduction pathways	Total loss of pathogenicity when knocked down alongside *CPK1*	Hu et al. (2014)
FgSte50	PHI:3375	Mitogen-activated protein kinase	Regulation of various cellular processes	Defective in conidiation, DON biosynthesis and pathogenicity	Gu et al. (2015)
Fgk3	PHI:4587	Glycogen synthase kinase	Inhibits activity of glycogen synthase	Defective in growth, conidiation, germination and exhibit significant reduction in pathogenicity and DON production	Qin et al. (2015)
cdc2A	PHI:4941	Cyclin-dependent kinase	Involved in cell cycle progression	Perithecia fail to form ascospore cirrhi and defective in infectious growth	Liu et al. (2015)
ScOrtholog_YVH1	PHI:5768	Phosphatase	Negative regulator which inactivates phosphorylated elements in MAPK cascades	Penetration-deficient and unable to infect an inoculated spikelet	Yun et al. (2015)
MGV1	PHI:266	Mitogen-activated protein kinase	Regulation of various cellular processes,	Hypersensitive to MsDEF1 and highly compromised in pathogenicity	Ramamoorthy et al. (2007)

			regulates sensitivity to the plant defensin MsDEF1		
STE7	PHI:1004	Mitogen-activated protein kinase kinase	Regulation of various cellular processes, regulates sensitivity to the plant defensin MsDEF1	Hypersensitive to MsDEF1 and highly compromised in pathogenicity	Ramamoorthy et al. (2007)
STE11	PHI:1016	Mitogen-activated protein kinase kinase kinase	Regulation of various cellular processes, regulates sensitivity to the plant defensin MsDEF1	Hypersensitive to MsDEF1 and highly compromised in pathogenicity	Ramamoorthy et al. (2007)
FgVam7	PHI:4865	Soluble *N*-ethylmaleimide-sensitive factor attachment protein receptor (SNARE) proteins	Regulatory role in cellular differentiation and virulence	Reduction in vegetative growth, conidiation and conidial germination, sexual reproduction and virulence	Zhang et al. (2016)

1.6 *Fusarium graminearum* omics

1.6.1 Genomics

Over twenty years ago the full genome of the model yeast organism, *Saccharomyces cerevisiae,* was the first eukaryotic genome to be sequenced in a collaborative effort that drew on the expertise of over 600 scientists across the world (Goffeau et al. 1996). Since this first breakthrough, many fungal human and plant pathogens have been sequenced leading to a vastly improved understanding of these organisms and, consequently, improved methods of control.

The first fungal plant pathogen genome to be sequenced was of *Magnaporthe grisea*, the causal agent of rice blast disease, using a whole-genome shotgun approach (Dean et al. 2005). A few years later, the first isolate of *F. graminearum*, PH-1, was sequenced, assembled and annotated by the BROAD institute also using a whole-genome shotgun approach (Cuomo et al. 2007). PH-1 (NRRL 3184), a highly virulent strain isolated in North America, was selected for sequencing by the International *Gibberella zeae* Genomics Consortium (IGGC) due to PH-1 being highly fertile, a trichothecene-producer, an abundant sporulater in culture, and readily transformable (Trail and Common 2000). The initial assembly of PH-1 possessed a 36.1Mb genome aligned to four chromosomes and was predicted to encode 11,640 genes. This initial assembly was later improved by BROAD and refined by the Munich Information Services for Protein Sequences (MIPS)(Wong et al. 2011; Guldener, Mannhaupt, et al. 2006). This refined gene set was used to develop an *F. graminearum* species-

specific Affymetrix array which has subsequently been used in many *in vitro* and *in planta* experiments (Guldener, Seong, et al. 2006a).

Despite this refinement, genomic closure remained particularly poor in the telomeric and centromeric regions of the genome. King *et al* (2015) therefore recently re-sequenced and reassembled the *F. graminearum* genome using a whole shotgun sequencing approach, revealing that the *F. graminearum* genome consists of 38Mb distributed across four scaffolds and predicted to contain 14,164 nuclear protein-encoding genes (Table 1.3). This version of the *F. graminearum* genome, RRES v4.0, is now almost fully assembled with only twelve 'N' bases and was deposited onto the European Nucleotide Archive (ENA; Project number PRJB5475). Over 30 *Fusarium* genomes are now sequenced and publicly available in EnsemblFungi enabling in-depth comparative analysis.

Annotation of the RRES v4.0 gene call revealed that a total of 12,691 genes had BLAST2GO annotation or had blast hits mapping to over a thousand-gene ontology (GO) terms (King et al. 2015a). The most highly represented GO terms were those involved in metabolic and cellular processes, localisation, singular-organism processes and biological regulation. Hydrolytic enzymes are also well-represented in the *F. graminearum* genome in comparison to other fungal plant pathogens (Cuomo et al. 2007). Using the MIPS v3.2 2011 assembly and annotation, Brown, Antoniw, and Hammond-Kosack (2012) refined the *F. graminearum* secretome which was predicted to contain 574 genes – 119 of which are hydrolytic enzymes involved in breaking down plant cell walls. Secretome prediction using the new RRes v4.0 gene call revealed that *F. graminearum* secretome instead

contains 616 genes – the identification of which forms the first step in many bioinformatic effector discovery pipelines (King et al. 2015a). Of the current predicted secretome, 497 proteins lack any functional annotation.

Table 1.3 A comparison of features of the *F. graminearum* BROAD FG3.0 and RRESv4.0 genome annotations

Feature of *F. graminearum* genome	**BROAD FG3.0 Cuomo et al. (2007)**	**RRES v4.0 King et al. (2015)**
Length (bp)	36,073,610	36,563,796
Gene number	11,640 genes	14,164
Chromosome number	4	4
Mitochondrial genome length (bp)	95,676	95,638
Unknown base pairs	210,520	12
Scaffolds	31	5
GC content (%)	48.3	48.2
Repetitive (%)	0.24	0.24
Transposable elements (%)	0.029	0.060

In comparison to other *Fusarium* spp. genomes, the *F. graminearum* genome is considerably smaller; with *F. oxysporum* and *F. verticillioides*, for instance, possessing 59.9 and 41.7 Mb genomes mapping to 15 and 11 chromosomes, respectively (Ma et al. 2010). This reduction in genome size is, in part, due to the lack of high-identity duplicated sequences in comparison to other filamentous fungi – a reduction that can be partly accounted for by the homothallic nature of *F. graminearum*, which rarely outcrosses, thereby limiting repeat acquisition (Goswami, Xu, and Kistler 2004). The lack of repetitive sequences is also attributable to the presence of an active repeat-induced (RIP) mutation system - a fungi-specific system which selectively mutates duplicated sequences, believed to provide defence against the spread of transposable elements at the expense of gene family expansion (Cuomo et al. 2007; Galagan and Selker 2004; Rep and Kistler 2010).

In the original genome sequencing project, a second strain of *F. graminearum* was sequenced alongside PH-1 – GZ3639, also of US origin. Cuomo et al. (2007) identified 10,495 SNPs between these two strains - the majority of which localised to sub-telomeric, discrete AT-rich regions and a few ‘mid-chromosome’ regions. Genes located in these high-density SNP regions were found to be specifically expressed during *in planta* infection and enriched for genes required for pathogenicity/virulence, genes coding for secreted proteins and discrete gene clusters involved in the biosynthesis of specific secondary metabolism. These ‘mid-chromosome’ regions, which house a large number of SNPs, are thought to be the demarcation lines of an ancient chromosome fusion event which accounts for the relatively small

chromosome number of *F. graminearum* and the high degree of polymorphism between strains (Cuomo et al. 2007). In contrast, highly conserved genes and many of the experimentally verified *F. graminearum* virulence factors were under-represented in SNP-dense regions, instead localising to regions of low recombination frequency thought to protect them from gene loss (Brown, Antoniw, and Hammond-Kosack 2012). Instead of these islands of elevated genomic diversity, *F. oxysporum* and *F. solani* possess small, supernumerary chromosomes which house lineage-specific sequences and highly repetitive regions enriched in effectors, transcription factors and proteins involved in signal transduction (Ma et al. 2010). Comparative genomics of *Fusarium* spp. has therefore revealed that genomes can be divided into two categories, core and accessory, with over 9000 genes considered core (King et al. 2015a; Ma et al. 2010).

To capture the full gene repertoire of a fungal species, multiple complete genomes of different strains must be sequenced – a process referred to as pangenome analysis. To date, the diversity in *F. graminearum* isolates sequenced remains low – with sequences isolated primarily restricted to the Americas. Walkowiak et al. (2016) recently sequenced nine *F. graminearum* isolates, along with several other species from the FGSC, enabling the identification of the genes core to *F. graminearum* biology (n=13,470). The non-core genes, termed accessory genes, were hypothesised to be involved in niche specialisation within and between species. In addition, Kelly and Ward (2018) sequenced 60 more *F. graminearum* isolates and assembled the pangenome enabling clarification of population level differences in gene content. Interestingly, the vast majority of the accessory genome (98%)

displayed some degree of conservation between the sequenced isolates indicating that accessory genes are often passed between *F. graminearum* isolates.

1.6.2 Transcriptomics

While genome sequencing and annotation provides a global view of genes present in an organism, it provides little clue as to the transcriptional and post-transcriptional regulation of these genes. Transcriptomic profiling can be achieved by using the next-generation sequencing technology (NGS) RNA-seq, which has become a powerful tool used to investigate gene expression in a vast array of model and non-model organisms (Wang, Gerstein, and Snyder 2009). The application of these technologies to plant pathology has greatly accelerated the rate of discovery of pathogen genes involved in virulence mechanisms and provides information about the regulation mechanisms and networks to which these genes belong.

Transcriptomic analysis of the *F. graminearum*-wheat interaction has been extensively studied in recent years – in no small part due to the development of a species-specific Affymetrix GeneChip microarray (Guldener, Seong, et al. 2006a). To maximise the likelihood of representing all putative genes, the automatic gene calls from the BROAD and MIPS assemblies were used to generate the custom microarray. To validate the performance of the GeneChip, Guldener, Seong, et al. (2006a) used the array to detect differential transcript accumulation between *in vitro* cultures subject to differing nutritional regimes (complete media (CM), CM minus carbon and CM minus nitrogen) alongside an *F. graminearum*-barley infection experiment. Since this initial study, the Affymetrix microarray has been

utilised in ~17 studies, the majority of which are now deposited on the EMBL-EBI Array Express (https://www.ebi.ac.uk/arrayexpress/)(Brazma et al. 2003).

Some of the first experiments utilising the array focused on interrogating fungal gene expression during conidial and perithecial development. Hallen et al. (2007) carried out a developmental time course experiment in culture where timepoints represented the development of the major cell types comprising perithecial development, finding that 12% of expressed genes appeared to be specific to perithecial development. Later, Seong et al. (2008) performed a similar experiment looking at gene expression during conidial germination aiding identification of genes specifically expressed during the distinct milestones of spore development.

Several other groups have used the microarray to explore the gene expression profile of *F. graminearum* during infection of varying cereal hosts and tissue types. Lysoe, Seong, and Kistler (2011) explored *F. graminearum* gene expression patterns during wheat ear infection across a period of 0-192 hours. This study revealed that the number of genes expressed increased considerably at 92h, over 8000 genes, before declining at later time points. More recently, Brown et al. (2017) used the Affymetrix GeneChip to interrogate fungal gene expression during the symptomless and symptomatic phase of *F. graminearum*-infection of wheat ears - revealing that these two phases are both phenotypically and transcriptionally distinct. While transcripts for the genes involved in mycotoxin biosynthesis were abundant in the symptomless tissues, transcripts encoding distinct groups of putative effectors were found in both symptomless and symptomatic tissue

suggesting that *F. graminearum* uses effectors to facilitate both biotrophic and necrotrophic lifestyles. To better understand *F. graminearum* infection processes of different host species, Harris et al. (2016a) carried out a transcriptome comparative analysis of *F. graminearum* during infection of wheat, barley and maize. While the expression profiles of *F. graminearum* during wheat and barley infection were strikingly similar, a considerable number of host-specific genes were identified for each cereal species. Another transcriptomic experiment investigating gene expression on living and dead wheat ears revealed that only a limited number of *in planta* expressed genes are required for infection of living tissues (Boedi et al. 2016)

Transcriptome profiling of *F. graminearum* mutants can also help to elucidate the networks involved in gene expression. Gene expression analysis of the *Tri6* and *Tri10* transcription factor mutants, both of which exhibit reductions in pathogenicity and mycotoxin production, revealed that the transcript levels for over 200 genes were altered *in planta* compared to the wild-type (Seong et al. 2009b). A similar study was conducted to explore gene expression of the *Fgp1* mutant, a *WOR1*-like protein involved in pathogenicity and toxin production, under *in vitro* and *in planta* conditions (Jonkers et al. 2012). Like *Tri6* and *Tri10* mutants, transcripts of many of the genes involved in mycotoxin biosynthesis were not detected which may alone explain the reduction in pathogenicity exhibited by the *Fgp1* mutant.

1.6.3 Proteomics

With the increasing availability of fungal genomes, transcriptomes and sophisticated bioinformatic tools, proteomic capabilities have vastly

increased in recent years. The development of powerful techniques, such as tandem liquid chromatography-mass spectrometry (LCMS), has propelled proteomic analysis to an indispensable status in regards to the study of plant-microbe interactions; enabling determination of protein abundance, location, interaction, and function (Wright et al. 2012). While full characterisation of the total proteome is challenging, integration of ~omics data could enable significant progress in our understanding of *F. graminearum* pathogenicity, virulence and host resistance (Yang et al. 2013).

In the past, proteomic studies of *F. graminearum* have mainly focused on characterisation of the *in vitro* secretome. Using both one-dimensional electrophoresis (1-DE) and two-dimensional electrophoresis (2-DE) followed by mass-spectrometry (MS) analysis, Phalip et al. (2005) identified unique proteins involved in cell wall degradation in the first example of an *in vitro* gel-based secretome study. The results of this study were particularly helpful in verifying the predicted *F. graminearum* secretome defined by Brown, Antoniw, and Hammond-Kosack (2012). Subsequent studies have also used gel-based proteomics approach to characterise the *F. graminearum* secretome across a range of conditions. For instance, Yang et al. (2012) characterised the secretome of *F. graminearum* grown in liquid culture containing either wheat or barley extracts in order to mimic the host-pathogen interaction leading to the identification of proteins primarily involved in fungal cell wall remodelling and degradation of plant cell walls.

Several studies have focused on the impact of DON on the *F. graminearum* secretome. Rampitsch et al. (2013) used standard proteomic extraction techniques and LCMS to characterise the secretome of PH-1 and the *ΔTri6*

and *ΔTri10* deletion strains under *in vitro* conditions. Using this approach, the authors identified 29 proteins which exhibited differential abundance between the comparative secretomes thus representing potential virulence factors. To analyse the effect of DON production during the host infection process, Taylor et al. (2008) carried out proteomic analysis of *F. graminearum* cultures grown under trichothecene-inducing conditions using quantitative protein MS using isobaric tags for relative and absolute quantification (iTRAQ). iTRAQ is a non-gel-based technology which, in this instance, enabled the identification of 130 differentially expressed proteins which were therefore hypothesised to contribute towards fungal virulence.

1.7 Projects aims and objectives

As the prevalence of FHB continues to increase worldwide, the need for effective, durable and sustainable methods of disease control heightens (Backhouse 2014). A greater understanding of the mechanisms employed by *F. graminearum* to facilitate infection is integral to the development of these control measures. Recent transcriptomic analysis of *F. graminearum* during the wheat-floral interaction revealed that, during both the symptomless and symptomatic phases of infection, unique sub-sets of genes encoding small, secreted proteins are upregulated (Brown et al. 2017). In this study, we hypothesise that these putative effectors contribute towards *F. graminearum* pathogenicity to facilitate either 1) a biotrophic lifestyle during the symptomless phase of infection, or 2) a necrotrophic lifestyle during the symptomatic phase of infection. Prior to this study, no classical, small, secreted effectors had been identified in *F. graminearum* despite the numerous efforts to identify putative effectors *in silico* (Lu and Edwards

2016). The main aim of this PhD has therefore been to identify bioinformatically and then functionally characterise *F. graminearum* small secreted proteins (FgSSPs) predicted to contribute towards fungal pathogenicity. The primary method of characterisation utilised in this study was the previously described BSMV-VOX system which, despite widespread use of the VIGS system, is not routinely used for functional characterisation of fungal proteins in cereal hosts (Lee, Hammond-Kosack, and Kanyuka 2012).

The primary hypothesis tested in this study was that *F. graminearum* effectors contribute towards fungal virulence. Furthermore, we hypothesised that the *F. graminearum* infection phase during which an effector is produced influences the mode of action of said effector.

To test these hypotheses, the following experiments/studies were undertaken:

1. Bioinformatic selection of FgSSPs for functional characterisation.
2. Screening of FgSSPs for ability to contribute towards the establishment of FHB in wheat using the BSMV-VOX system.
3. Further characterisation of proteins with disease-facilitating capabilities via the generation of single gene deletion mutants and by recombinant protein expression in *N. benthamiana*.
4. Determination of the importance of secretion to disease-contributing effectors.
5. Definition of the mechanism of action of putative effectors through immunodetection and chemical analysis of host plants.

Chapter 2 General materials and methods

2.1 Plant material and growth conditions

Nicotiana benthamiana plants were grown in controlled environment chambers for the preparation of BSMV sap inoculum, screening recombinant effector proteins for cell death-inducing activity and for virus-induced gene silencing experiments (VIGS). *N. benthamiana* seeds were germinated in Levingtons F2+S compost (Everris Ltd, Ipswich, UK) in a 7cm x 7cm x 9cm plastic pot and kept in a humid chamber under the following conditions: day/night temperatures of 23°C/20°C at 60% relative humidity (RH) and a 16-h photoperiod with approximately 130µmol m^{-2} s^{-1} light. Seedlings were then transplanted into individual 5 cm × 5 cm × 8 cm plastic pots when two weeks old and returned to the same growth conditions. For gene silencing experiments, plants were grown for three weeks while all other experiments used four-week old plants.

The *F. graminearum*-susceptible wheat (*Triticum aestivum*) cv. Bobwhite was used as the host plant throughout this investigation for BSMV-VOX experiments and testing the pathogenicity of *F. graminearum* single gene deletion mutants. Seeds were pre-germinated overnight by soaking in water and then sown in Rothamsted soil mix and grown in a controlled environment chamber under the following conditions: day/night temperatures of 22°C/18°C at 60% relative RH and a 16-h photoperiod with approximately 140µmol m^{-2} s^{-1} light. During stem elongation, approximately four to five weeks after sowing, approximately 1L of phosphate fertiliser (5g/L)(Phostrogen All Purpose Plant Food, Solabiol) was applied to each tray of wheat plants.

2.2 Fungal strains, plate cultures and conidial suspension preparations

The global reference American wildtype strain of *F. graminearum* PH-1 was used throughout this study for fungal transformation and BSMV-VOX experiments (Cuomo et al. 2007). The PH-1 strain is a DON/15-ADON producer and is fully pathogenic on the wheat cv. Bobwhite (Urban et al. 2003). Wild-type and gene deletion fungal strains were maintained as 20% glycerol stocks at -80°C and cultured on synthetic nutrient deficient agar (SNA) plates (1g KH_2PO_4, 1g KNO_3, 0.5g $MgSO_4x7\ H_2O$, 0.5g KCl, 0.2g glucose, 0.2g sucrose, 0.6ml NaOH (1M), 20g agar/L sterile distilled water). Plates containing *F. graminearum* cultures were incubated at room temperature under constant illumination from one near-UV tube (Phillips TLD 36W/08) and one white light tube (Phillips TLD 36W/830HF). To remove old conidia and induce fresh conidia formation, eight-day old SNA plates were washed with an overlay of sterile TB3 (0.3% yeast extract, 0.3% Bacto Peptone and 20% sucrose) and incubated for a further two days. After two days, conidial suspensions were harvested in sterile water, filtered through miracloth (Calbiochem) and adjusted to a conidial concentration of 1×10^5/ml in sterile water for point inoculation of wheat. Conidial spore suspensions were stored at -80°C. Liquid cultures of fungal strains were grown in 10ml of yeast peptone dextrose (YPD) or potato dextrose broth (PDB) in 50ml falcon tubes for RNA and gDNA extractions. Cultures were incubated for three days in the dark at 25°C with shaking (100RPM) before vacuum-filtering through Miracloth and snap-freezing in liquid nitrogen. For antibiotic selection of *F. graminearum* gene deletion strains generated using the split-marker

transformation method, strains were grown on SNA containing 50µg/ml of hygromycin.

2.3 *Fusarium graminearum* wheat inoculation

At anthesis, approximately 52-55 days after seed sowing, 5µl of a 1 x 10^5/ml conidial suspension was pipetted into the floral cavity between the palea and lemma of the first two florets of the 13th and 14th spikelets from the base of the wheat ear. Inoculated plants were then placed in a humid chamber for 48h. For the first 24h, the humid chamber was covered to place the plants in darkness. In the BSMV-VOX experiments, a minimum of ten inoculations per experimental treatment were sampled per study. In gene deletion pathogenicity assays, a minimum of five ears per treatment were sampled. Control plants were inoculated with sterile water and are referred to as mock inoculations. Disease progress was recorded by counting the number of visibly diseased spikelets below, but not including, the points of inoculation. Macroscopic symptoms were recorded every three days up until the whole wheat ear showed signs of visible disease symptoms.

2.4 Photography

Plants were photographed using a Nikon D80 digital camera with a Sigma DC MACRO HSM 17-70mm objective. Images were photographed on black velvet background under white and UV light conditions. For fluorescence photography, plants were illuminated with blue light (440–460 nm excitation) using a Dual Fluorescent Protein flashlight (NightseaA). Long-pass (510 nm) or band-pass (500–555 nm) filters (Midwest Optical Systems) were mounted onto the camera objectives to block blue or blue plus red light, respectively, reflected from the excitation source (Bouton et al. 2018).

2.5 Molecular cloning methods

2.5.1 Genomic DNA extraction

Genomic DNA (gDNA) was isolated from *F. graminearum* mycelia grown in liquid cultures. Mycelia was harvested from cultures by vacuum-filtration and ground in liquid nitrogen using a pestle and mortar. Samples were then incubated in DNA extraction buffer (Ten 2X (Trizma Hydrochloride [pH8.0)), SDS (2%), Polyvinylpyrrolidone, β-mercaptoethanol (1%)) and precipitated using ammonium acetate (2.5M) and isopropanol. Pellets were washed with 70% ethanol and then resuspended in sterile water before quantification with a NanoDrop 2000c spectrophotometer (Thermo Fisher Scientific, Waltham, MA, USA).

2.5.2 RNA extraction

F. graminearum infected-Bobwhite rachis internodes and *N. benthamiana* samples were harvested, snap frozen in liquid nitrogen and homogenised using a pestle and mortar. Total RNA was extracted using Trizol® (Invitrogen, USA) as per the manufacturer's instructions. Total RNA was resuspended in deionised water and stored at -80°C. Purified RNA was quantified using a NanoDrop 2000c spectrophotometer (Thermo Fisher Scientific, Waltham, MA, USA) by absorbance at 260nm and the purity was evaluated by determining the 260 / 280 nm absorbance ratio. RNA was visualised on an agarose gel to inspect RNA quality. Purified RNA was then used in reverse-transcription PCR (RT-PCR) experiments for further downstream applications.

2.5.3 Reverse-transcription PCR (RT-PCR)

An aliquot of 1µg of total RNA was treated with 1 unit of RQ1 RNAse-free DNase I (Promega, Madison, WI, USA) to remove gDNA contamination. The DNase-treated RNA was then used for cDNA synthesis using the High Capacity cDNA reverse transcription kit (Applied Biosystems, Foster City, CA, USA) according to the manufacturer's instructions. Resultant cDNA was used for subsequent PCR analyses.

2.5.4 Primer design

All primers were designed using the Primer3 software within the Geneious software and synthesised by Eurofins Genomics (Ebersberg, Germany). The primers used in this study are listed in the appendices.

2.5.5 Polymerase chain reaction (PCRs) analyses

For colony and diagnostic PCRs, RedTaq Ready Mix PCR reaction mix (Merck, NJ, USA) was used and, for molecular cloning experiments, Phusion High Fidelity PCR Master with HF buffer (New England Biolabs, MA, USA). All PCR reactions were run on a Bio-Rad T100 Thermal Cycler (Bio-Rad, CA, USA).

2.5.6 Gel electrophoresis

Gel electrophoresis was used to confirm nucleic acid integrity and to confirm the size of amplicons generated by PCR. RNA, gDNA and cDNA were visualised on 1% agarose gels (Fisher Scientific, UK) made using 1xTBE (Tris-borate EDTA). Ethidium bromide (10mg/ml) was added to TBE to a final concentration of 0.5µg/ml. Nucleic acids were mixed with loading buffer (ThermoFisher, Scientific Waltham, MA, USA) at a 5:1 ratio prior to well

loading and run alongside either a 100bp or 1kb ladder (ThermoFisher, Scientific Waltham, MA, USA) according to the predicted size of nucleic acids. Agarose gels were then run in horizontal tank apparatus – typically for 1h at 80V. Gels were then visualised and photographed in a UV transilluminator (Syngene, USA). If PCR products were to be used for downstream applications, gels were visualised on a transilluminator and gel bands were excised using the QIAquick gel extraction kit (Qiagen, Venlo, Netherlands).

2.2.7 *Escherichia coli* transformation and culture

Several plasmids were generated in this study using methods described in chapters 4, 5 and 6 and plasmid maps are found in the appendices. Plasmids were introduced into competent *E. coli* cells by heat-shock transformation. An aliquot of 30µl of competent *E. coli* was mixed with 1-50ng of plasmid and incubated on ice for 25 min. Samples were then heat-shocked at 42°C for 30-45s and placed immediately on ice. Cold super-optimal broth with catabolite repression (SOC) medium was then added to each tube and incubated at 37°C for 60 min with shaking (250RPM). Transformed *E. coli* cultures were then diluted and plated onto LB Miller agar containing the appropriate antibiotic and incubated overnight with no shaking. To verify transformation, individual colonies were picked for colony PCR. Positive colonies were cultured in liquid LB Miller overnight, and plasmids were isolated using the QIAPrep Spin Miniprep Kit (Qiagen, Venlo, Netherlands). Isolated plasmids were then sequence-verified using Eurofins Genomics sequencing service. The following *E. coli* competent cells were used in this study: JM109 (Promega, Madison, WI, USA) and NEB-5α (New

England Biolabs, MA, USA) competent cells. Transformed *E. coli* strains were maintained as glycerol stocks and kept at -80°C.

2.2.8 *Agrobacterium* transformation and storage

Sequence-verified plasmids were used to transform the electrocompetent *Agrobacterium tumefaciens* strain GV3101. Electrocompetent cells were generated by inoculating 5ml of LB Lennox broth (10g/L tryptone, 5g/L yeast extract and 5g/L NaCl) containing 25µg/ml of gentamycin with the GV3101 strain which carries the virulence helper plasmid pMP90. Following incubation at 28°C for 30-36h in a shaking incubator, the 5ml culture was added to 250ml of LB Lennox broth in a 2L flask containing 25µg/ml of gentamycin. Cultures were shaken overnight at 28°C at 250RPM until the OD_{600} of the culture reached 1.2-1.5. The cells were then spun down in a 500ml sterile bottle at 4°C for 15 min at 4,000x*g*. The supernatant was then removed, and the cell pellet was washed seven times with 250ml of cold sterile distilled water. Cells were then resuspended in 25-50ml of cold sterile 10% glycerol and spun down at 4°C for 10 min at 3000x*g* and resuspended for a second time in 2ml of 10% glycerol. Approximately 10ng of plasmid DNA was added to 20µl of electrocompetent *Agrobacterium* cells and incubated on ice for 5 mins. *Agrobacterium* was then electroporated using a Bio-Rad Micropulser. Cells were then diluted in LB Lennox broth and cultured at 37°C for 60 min. Cultures were further diluted (1:10) in LB Lennox broth and plated onto LB Lennox plates containing the appropriate antibiotics. Plates were incubated at 28°C for three days. Positive colonies were maintained as glycerol stocks kept at -80°C.

2.6 Agroinfiltration

Modified *Agrobacterium* strains were streaked onto LB Lennox plates containing the appropriate selectable markers. After two days, *Agrobacterium* strains were picked from these plates and cultured in LB Lennox broth overnight at 28°C with constant shaking (250RPM). Bacterial cells were pelleted at 4000x*g* for 15 min at 4°C and then resuspended in agroinfiltration buffer (10mM $MgCl_2$, 10mM 2-(*N*-morpholino) ethanesulfonic acid (MES) pH5.6, and 0.1mM acetosyringone) to various optical densities (600nm) ranging from 1.0-1.5. Agroinoculum was then incubated for 3hrs at room temperature before infiltration into *N. benthamiana* leaves. The majority of plants infiltrated in this study were four weeks old. Leaves were punctured with a sterile 10µl pipette tip and *Agrobacteria* were infiltrated into the abaxial side of the leaf using a needleless 1ml syringe until completely infiltrated.

Chapter 3 Bioinformatic analysis and selection of candidate small secreted genes for functional characterisation

3.1 Introduction

Effector proteins greatly influence the degree of host specialisation achieved by a pathogenic fungal species and, as such, identification of effectors is integral to a fully integrated disease prevention strategy. Prior to the advent of the '-omics' era, effector discovery relied heavily upon laborious and time-consuming proteomic and biochemical techniques. However, with over a thousand fungal genomes either fully or partially sequenced, effector research has been greatly stimulated by the advancement in genomic and transcriptomic techniques (De Wit and Spikman 1982a; Rampitsch et al. 2013). As effectors are broadly defined as secreted molecules that modulate the host-pathogen interaction, identification of the fungal secretome represents the first step of many effector discovery bioinformatic pipelines. A large proportion of fungal secretomes are often comprised of plant cell wall degrading enzymes (PCWDEs), employed by necrotrophic pathogens for nutrient acquisition. PCWDE sequences are easily identified by the presence of conserved enzymatic structures and sequence domains which are deposited into the online CAZy database (Sperschneider et al. 2018)(Cantarel et al. 2009).

The identification of several conserved amino acid motifs in oomycetes has greatly aided effector discovery in *Phytophthora* species. The most common oomycete effector motif is RxLR, posited to mediate effector translocation into host cells, which has led to the identification of over 700 putative effectors in *P. sojae* and *P. infestans* (Whisson et al. 2007; Jiang et al. 2008;

Kale et al. 2010; Wawra et al. 2013). In contrast, no common effector motifs have yet been identified across fungal species and this lack of sequence-based commonalities between fungal effectors has impeded effector discovery (Sperschneider et al. 2015). Most effector discovery pipelines therefore rely upon the presence of characteristics commonly observed to unify effectors such as high cysteine-content, small protein size, and presence within genomic regions which undergo high levels of recombination and / or are enriched in repeats and transposons (Gibriel, Thomma, and Seidl 2016). Numerous effectors are known, however, to deviate from the manually applied thresholds that researchers impose upon protein size and cysteine content and effectors with enzymatic activity have also been characterised (Gout et al. 2006; Bohnert et al. 2004; Djamei et al. 2011). When used in conjunction with *in planta* transcriptome data, these pipelines can still represent a powerful tool for effector discovery despite criticism that application of these criteria narrow our view on effector biology and, consequently, our view of host-pathogen communication strategies.

Over a decade ago, the genome of the first isolate of *Fusarium graminearum* (PH-1) was sequenced, assembled and annotated by the Broad institute – representing a huge leap forward in our understanding of this fungal pathogen (Cuomo et al. 2007). Since then, various '-omics' approaches have been utilised in conjunction with forward and reverse genetics to investigate the function of genes predicted to play a role in the fungal infection strategy. Despite this, to date, very few effectors have been identified in *F. graminearum* (Oide et al. 2006; Blumke et al. 2014) – even with the availability of the refined fungal secretome (Brown, Antoniw, and Hammond-

Kosack 2012). The most well characterised of these effectors is the secreted lipase Fgl1 – a protein with enzymatic function which does not conform to the aforementioned effector characteristics observed in other well characterised effectors (Voigt, Schafer, and Salomon 2005).

In 2006, a species-specific Affymetrix microarray was developed by Guldener, Seong, et al. (2006a) followed by numerous studies exploiting this microarray for the interrogation of the *F. graminearum* transcriptome in both *in vitro* and *in planta* conditions (Table 3.1)(Lysoe, Seong, and Kistler 2011; Seong et al. 2008; Hallen et al. 2007; Stephens et al. 2008; Zhang et al. 2012b). As many of these studies were undertaken prior to the discovery of the symptomless phase of *F. graminearum,* Brown et al. (2017) recently undertook a spatial and temporal transcriptomic investigation of *F. graminearum* characterising the fungal metabolic state and the secretome during both the symptomless and symptomatic phases of early FHB establishment and infection. This study revealed an upregulation in distinct groups of putative effectors within the symptomless and symptomatic phases hypothesised to facilitate infection by either 1) suppressing host defences to enable stealthy colonisation of the host, or, 2) by locally activating host cell death thereby releasing nutrients for fungal sequestration.

The first part of this chapter aims, via a suite of computational analyses, to identify *F. graminearum* small secreted proteins (FgSSPs), or putative effectors, from the refined *F. graminearum* secretome for functional characterisation using the BSMV-VOX system (Chapter 4). Identification of *F. graminearum* effectors that contribute towards fungal pathogenesis may help identify targets for chemical and RNA fungicides or identify susceptibility

targets in host organisms which could be targets for gene editing. The studies in the second half of this chapter focuses on the validation of the Affymetrix microarray data generated by Brown et al. (2017) by quantitative-reverse transcription PCR (RT-qPCR).

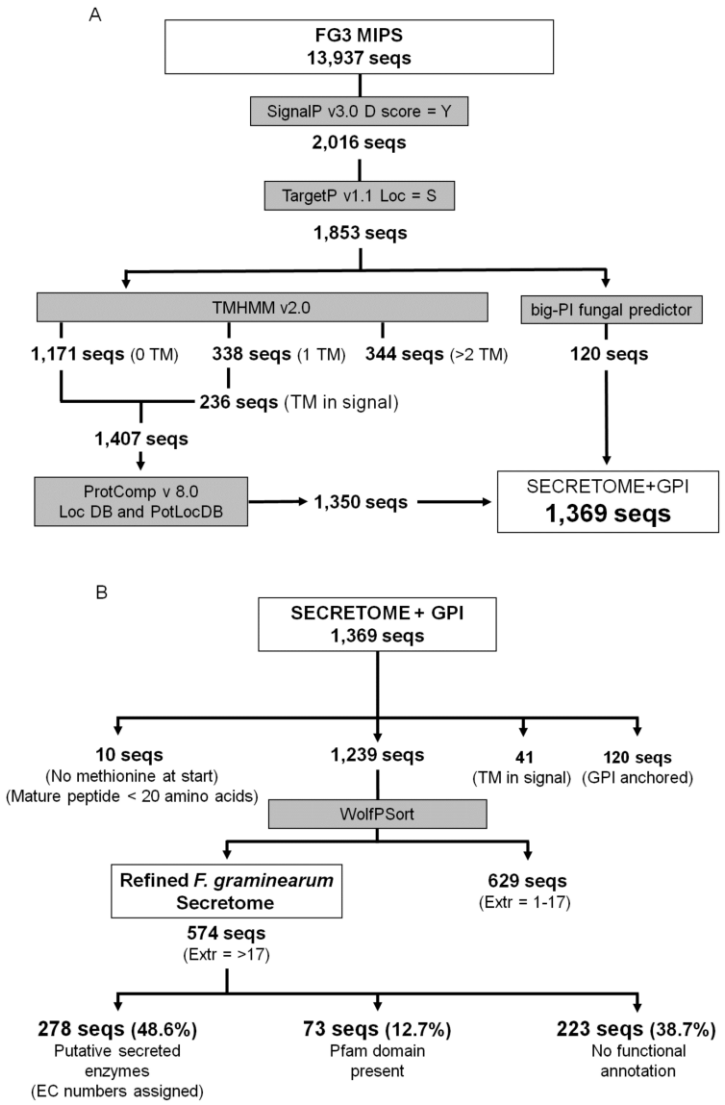

Figure 3.1 Bioinformatic pipelines used to predict the *F. graminearum* A) total and B) refined secretomes taken from Brown, Antoniw, and Hammond-Kosack (2012).

3.2 Materials and methods

3.2.1 Identification or putative effectors

Putative effectors were identified from the predicted refined secretome of *F. graminearum* through the application of bioinformatic approaches in conjunction with the exploration of transcriptome data investigating early *F. graminearum* infection (Figure 3.1)(Brown, Antoniw, and Hammond-Kosack 2012). The primary transcriptome dataset utilised explored *F. graminearum* gene expression within the symptomless and symptomatic phases of FHB within the wheat rachis tissue (Brown et al. 2017); data which was supplemented with the *in vitro* profiles of the fungal transcriptome in complete growth medium (CM) and nutrient-poor media (Guldener, Seong, et al. 2006a)(Table 3.1). *F. graminearum* genes 1) at least 2x more expressed *in planta* than *in vitro*, 2) exhibiting expression levels greater than 400 MAS5 normalised expression, 3) with a predicted protein size of less than 180 amino acids, 4) with a cysteine content of greater than 2%, 5) that did not exhibit redundancy in protein family domain e.g. multiple proteins with a glycosyl hydrolase Pfam domain, 6) that did not contain cell-wall degrading enzyme (CWDE) motifs were selected for functional characterisation and further in-depth bioinformatic analysis (Figure 3.2). Throughout this analysis, two previously characterised FgSSPs, FgSSP6 and FgSSP7, were included along with Tri4 and Tri5. FgSSP6 and FgSSP7 are two cerato-platanin proteins previously characterised and found to contribute towards fungal pathogenicity (Machado, A, thesis). Tri4 and Tri5 both belong to the DON biosynthetic cluster are therefore important to virulence (Alexander, Proctor, and McCormick 2009). These proteins were included throughout the analysis

to make comparisons between the characteristics of FgSSP candidates against previously characterised proteins known to contribute towards pathogenicity.

Table 3.1 List of datasets used for exploration of *in planta* and *in vitro* expression profiles of putative effectors

Host	Isolate	Experimental design	Time points	Reference
Barley	Butte86-AD	*In planta* time-course experiment in barley ears and *in vitro* nitrogen and carbon starvation conditions	24,48, 72, 96 & 144 hpi	Guldener, Seong, et al. (2006a)
-	PH-1	24-hour time course experiment during conidial germination	2, 8, & 24hpi	Seong et al. (2008)
Wheat	Wild-type PH-1 / *ΔTri6*[1] / *ΔTri10*[2]	Mutant and wild-type isolates inoculated onto wheat heads and harvested at 4 days	4dpi	Seong et al. (2009b)
Wheat	CS3005	Wheat seedling time-course	2, 14, & 35dpi	Stephens et al. (2008)
Wheat	PH-1	Wheat ear time-course	24,48, 72, 96, 144 & 192hpi	Lysoe, Seong, and Kistler (2011)
Wheat	PH-1	Wheat stem experiment up to perithecial development	24, 28 & 96 hpi	Guenther et al. (2009)
-	PH-1 / *ΔFgp1*[3]	Isolates grown *in vitro* in trichothecene induction media	5dpi	Jonkers et al. (2012)
Wheat	PH-1	Wheat coleoptile time-course	16, 40 & 64 hpi	Zhang et al. (2012b)
Wheat	PH-1 / *ΔFgp1*	Wheat ear experiment	72hpi	Jonkers et al. (2012)
Wheat	PH-1	Dead and alive wheat ears	3 & 5dpi	Boedi et al. (2016)

[1] *ΔTri6*: Gene ID = FGSG_03536, [2] *ΔTri10:* Gene ID = FGSG_03538, [3] *ΔFgp1:* Gene ID = FGSG_12164, Dpi = days post inoculation; Hpi = hours post inoculation

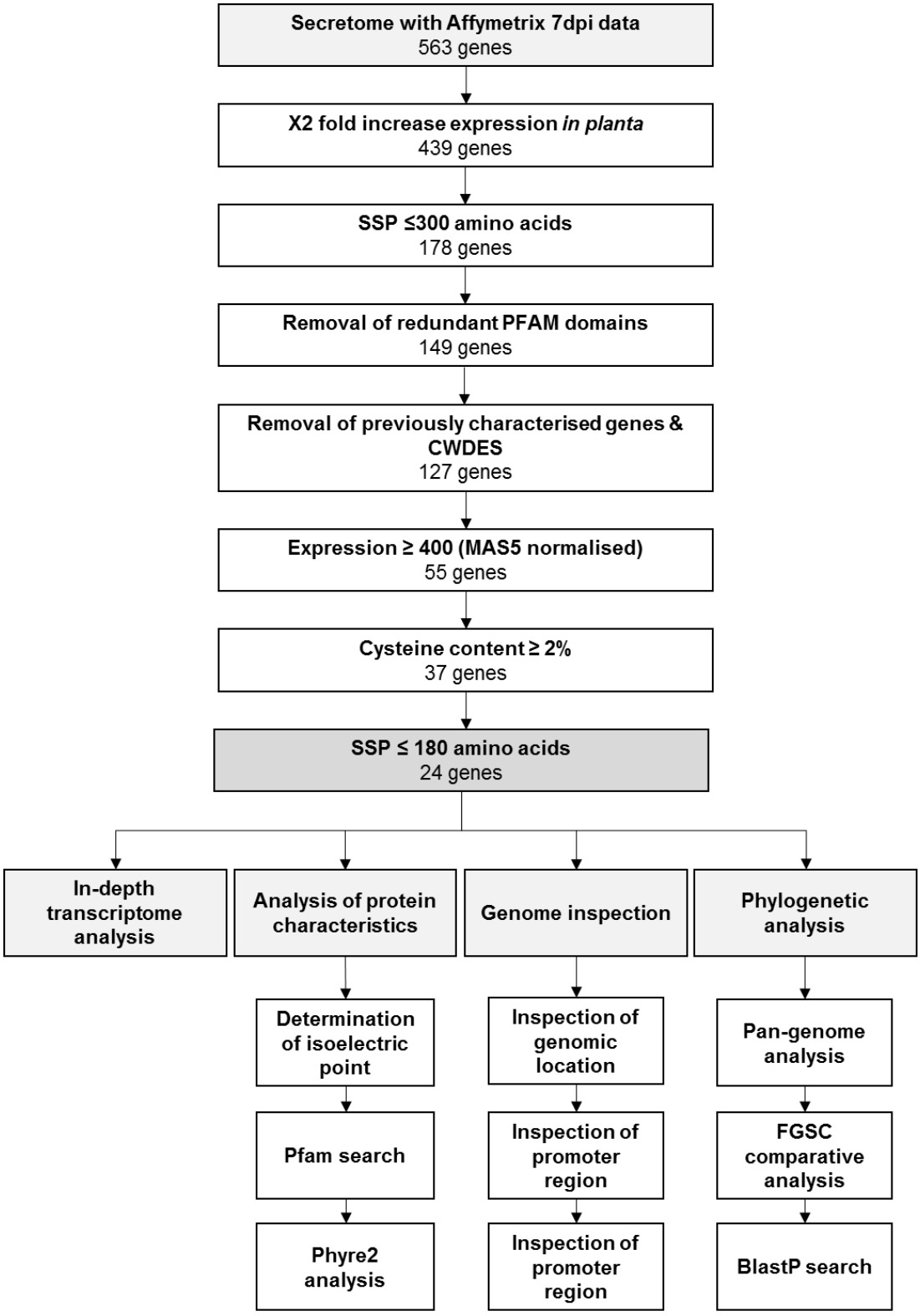

Figure 3.2 Bioinformatic pipeline for identification of putative effectors in *F. graminearum* and techniques used for in-depth analysis of candidates.

3.2.1.1 Determination of protein characteristics of putative effectors

Protein sequences of putative effectors were retrieved from EnsemblFungi (Version 86, July 2016) using the Biomart tool (http://jul2016.archive.ensembl.org/index.html)(Zerbino et al. 2018) from which the cysteine content of proteins was manually calculated and cysteine connectivity predicted using DiANNA software (http://clavius.bc.edu/~clotelab/DiANNA/)(Ferre and Clote 2006). The isoelectric point (http://isoelectric.ovh.org/) and molecular weight of proteins (https://www.bioinformatics.org/sms/prot_mw.html) were determined using predictive online software. The remote homology recognition software Phyre2 (http://www.sbg.bio.ic.ac.uk/~phyre2) was used to make predictions of the 3D protein structure of putative effectors using confidence and identity thresholds of 70% and 13%, respectively (Soding, Biegert, and Lupas 2005). The presence of intergenic repeats within the protein sequence was computed using the RADAR software (http://www.ebi.ac.uk/Tools/pfa/radar/).

3.2.1.2 Inspection of the genomic location of putative effectors

To inspect the genomic location of individual genes, the Fgra3Map tool was used to determine chromosome location and whether genes lay within regions subject to high levels of recombination frequency (Antoniw et al. 2011). EnsemblFungi was used to inspect proximity of putative effectors to neighbouring genes curated in the pathogen-Host interactions database PHI-base (http://www.phi-base.org/)(Urban et al. 2015). To determine whether putative effectors existed within secreted clusters, SignalP was used to determine whether neighbouring genes were also secreted (http://www.cbs.dtu.dk/services/SignalP/)(Petersen et al. 2011). Upstream

regions of the putative effectors were inspected to identify the promoter regions.

3.2.1.3 Phylogenetic analysis of putative effectors

The pangenome of *F. graminearum*, consisting of 18 different isolates, was examined for gene presence/absence and for single nucleotide polymorphisms in the coding sequences of putative effectors (Table 3.2) Pangenome strains were isolated from the two southern states in Brazil where FHB epidemics are most frequent and severe (Machado, Rothamsted, unpublished). Homologs were identified in other species found in the *F. graminearum species complex* (FGSC) in Geneious (Table 3.2)(Walkowiak et al. 2016). Multiple sequence alignments of protein sequences were carried out with the ClustalW program available in Geneious v8.1.3 using the BLOSUM cost matrix where gap penalties were set at the default values. BlastP was used for protein comparative analysis using an e-value threshold of 10^{-6} (https://blast.ncbi.nlm.nih.gov/Blast.cgi) and the phylogenies of protein homologs were explored in EnsemblFungi. BlastCD analysis was also carried out in order to identify any conserved domains within the protein sequences (http://www.ncbi.nlm.nih.gov/Structure/cdd/wrpsb.cgi)(Marchler-Bauer et al. 2015). EffectorP v2.0 software was utilised in order to ascertain whether candidate FgSSPs had a predicted effector function (http://effectorp.csiro.au/)(Sperschneider et al. 2018).

3.2.1.4 Transcriptomic analysis of putative effectors

The transcriptional profiles of putative effectors were further explored in the published datasets listed in table 3.1. Comparisons between datasets were

made to determine whether any of the selected candidates exhibited unusual or differential expression profiles.

Table 3.2 List of *F. graminearum* strains isolated from Brazil used in pangenome analysis and FGSC species.

Code	Species	Trichothecene genotype	Geographic origin	Year of isolation	Aggressiveness	Genome Sequencing
CML 3064	*F. graminearum*	15-ADON	Rio Grande do Sul	2007	+++	Illumina Hi-Seq
CML 3065	*F. graminearum*	15-ADON	Rio Grande do Sul	2009	+++	Illumina Hi-Seq
CML 3066	*F. graminearum*	15-ADON	Rio Grande do Sul	2009	+++	Illumina Hi-Seq / PacBio
CML 3067	*F. graminearum*	15-ADON	Rio Grande do Sul	2010	+	Illumina Hi-Seq
CML 3068	*F. graminearum*	15-ADON	Rio Grande do Sul	2007	++	Illumina Hi-Seq
CML 3069	*F. graminearum*	15-ADON	Rio Grande do Sul	2010	+	Illumina Hi-Seq
CML 3070	*F. graminearum*	15-ADON	Rio Grande do Sul	2011	++	Illumina Hi-Seq
CML 3071	*F. graminearum*	15-ADON	Rio Grande do Sul	2010	++	Illumina Hi-Seq
CML 3402	*F. graminearum*	15-ADON	Parana	2011	+++	Illumina Hi-Seq
CML 3403	*F. graminearum*	15-ADON	Parana	2011	+++	Illumina Hi-Seq
CML 3404	*F. graminearum*	15-ADON	Parana	2011	+	Illumina Hi-Seq
CML 3405	*F. graminearum*	15-ADON	Parana	2011	+++	Illumina Hi-Seq
CML 3406	*F. graminearum*	15-ADON	Parana	2011	+++	Illumina Hi-Seq
CML 3407	*F. graminearum*	15-ADON	Parana	2011	++	Illumina Hi-Seq
CML 3409	*F. graminearum*	15-ADON	Parana	2011	+++	Illumina Hi-Seq
DAOM180378	*F. graminearum*	15-ADON	Canada	1981	+++	Illumina-GAII

Code	Species	Trichothecene genotype	Geographic origin	Year of isolation	Aggressiveness	Genome Sequencing
NRRL28336	*F. graminearum*	3-ADON	USA	ND	++	Illumina-GAII
DAOM24116	*F. graminearum*	3-ADON	Canada	ND	+++	Illumina-GAII
CML 3074	*F. asiaticum*	NIV	Rio Grande do Sul	2011	ND	No
CML 3378	*F. cortaderiae*	NIV	Rio Grande do Sul	2010	ND	No
CML 3379	*F. cortaderiae*	3-ADON	Rio Grande do Sul	2010	ND	No
CML 3382	*F. austroamericanum*	3-ADON	Rio Grande do Sul	2010	ND	No
CML 3384	*F. austroamericanum*	3-ADON	Rio Grande do Sul	2010	ND	No
CML 3374	*F. meridionale*	NIV	Rio Grande do Sul	2007	ND	No
CML 3381	*F. meridionale*	NIV	Rio Grande do Sul	2010	ND	No
-	*F. culmorum*		UK		ND	
-	*F. venenatum*		UK		ND	

Aggressiveness determined by wheat ear pathogenicity assays carried out by A. Machado (thesis) whereby isolates were categorised as causing either mild (+), moderate (++) or severe (+++) symptoms.

3.2.2 Validation of Affymetrix microarray data by quantitative reverse transcription PCR (RT-qPCR)

At anthesis, wheat (cv. Bobwhite) was point inoculated with 5µl of a 5 x 10^5/ml PH-1 conidial suspension pipetted into the floral cavity between the palea and lemma of the first two florets of the 13th and 14th spikelets from the base of the wheat ear. Seven days later, six rachis internodes (RI) below the initial point of inoculation from 15 wheat ears were individually excised, as well as the inoculated spikelet. Rachis internodes exhibiting the same level of macroscopic disease symptoms were combined: RI1+2 (symptomatic), RI3+4 (onset), and RI5+6 (symptomless)(Figure 3.3). Samples were flash-frozen and rachis internodes were pooled together for grinding in a pestle and mortar. To replicate *in vitro* conditions, PH-1 conidia were cultured in yeast extract peptone dextrose (YPD) for three days. Total RNA was extracted using the Trizol method and 1µg of RNA was DNase treated with RQ1 DNase (Promega) and cDNA was subsequently synthesised using MultiScribe Reverse Transcriptase® (ThermoFisher Scientific). Primers that amplified across the *F. graminearum* actin (*FgActin*) gene were used to test cDNA quality and primers that amplified across an intergenic region (*Tri4/Tri5*) were used to test for the presence of gDNA contamination. Gene expression analysis was performed by RT-qPCR and standard curves of gDNA of known concentrations were generated for each primer pair tested. cDNA was diluted to 10ng/µl with dH_2O. A 2µl aliquot of cDNA was used in each reaction with SYBR Green JumpStart Taq ReadyMix (Sigma Aldrich). Triplicate reactions were performed for each sample primer-pair combination and reactions were carried out using the following thermocycle: 2 mins at

95°C followed by 35 cycles of 15s at 95°C, 30s at 60°C and 45s at 72°C. All RT-qPCR experiments were performed on a Real-Time PCR system 7500 (Applied Biosystems, UK). The absolute expression of putative effectors was determined using the standard curve method and normalised to *F. graminearum* actin expression (Larionov, Krause, and Miller 2005). Expression data was statistically analysed using a student's t-test with a p-value of 0.05.

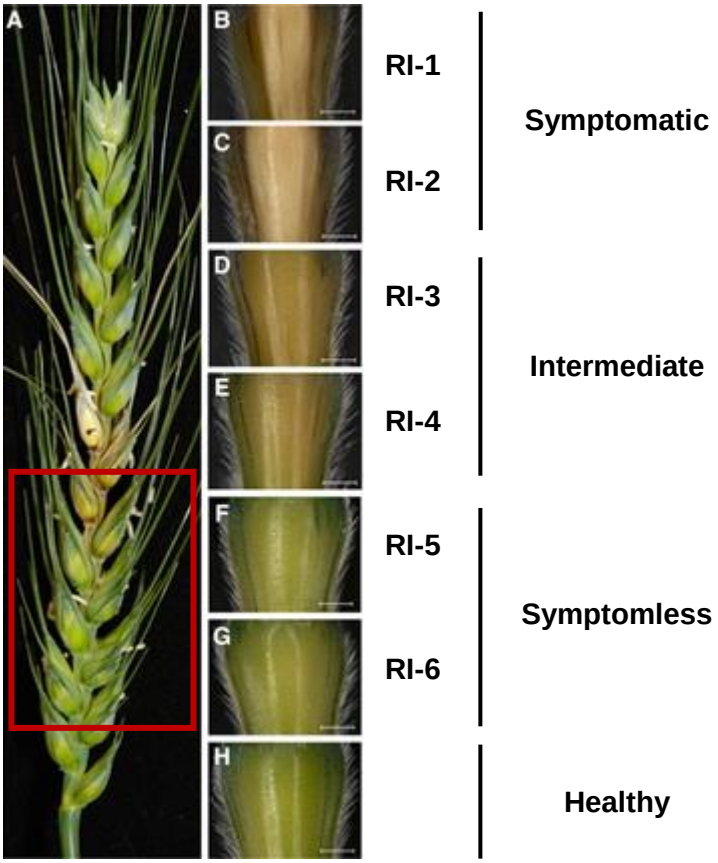

Figure 3.3 Experimental set-up for validation of the Affymetrix microarray transcriptome exploring the symptomless and symptomatic phases of *F. graminearum* infection. Red box indicates the six rachis internodes isolated from point-inoculated wheat ears. Ears were inoculated with *F. graminearum* conidial spore suspensions ($5x10^5$spores/ml). RI = rachis internode.

3.3 Results

3.3.1 Selection of putative effector proteins predicted to play an active role in the *F. graminearum*-wheat interaction

Putative effectors were selected on the basis of *in planta* expression profiles during FHB infection and the presence of characteristics associated with known fungal effectors (Figure 3.2). This bioinformatic pipeline yielded twenty-four putative effectors predicted to play a role in fungal pathogenicity and candidates were then prioritised for characterisation based on further in-depth bioinformatic analysis. The final twenty-four candidates chosen for functional characterisation using the BSMV-VOX system were subsequently grouped based on which phase of *F. graminearum* infection individual *FgSSP* transcripts were most abundant, grouped as: symptomless, onset or symptomatic FgSSPs (Table 3.3)(Brown et al. 2017). Of the putative effectors selected, FgSSP22, FgSSP23, FgSSP24, FgSSP26, FgSS30, FgSSP32 and FgSSP33 were tested in BSMV-VOX experiments.

3.3.1.1 Putative effectors most highly expressed during the symptomless phase of F. graminearum infection

During the symptomless phase of the *F. graminearum*-wheat floral interaction, a prolonged period whereby the advancing hyphal infection front extends 1cm beyond visible symptoms, 2671 genes are differentially regulated (Brown et al. 2017). Within this subset of differentially regulated genes were eleven of the twenty-four selected putative effectors: *FgSSP13, FgSSP14, FgSSP17, FgSSP23, FgSSP24, FgSSP26, FgSSP27, FgSSP31, FgSSP34* and *FgSSP35*. The characteristics of selected candidates are described in tables 3.3-3.5.

Table 3.3 Gene IDs and protein characteristics of putative effectors identified through detailed bioinformatics analyses.

FgSSP[1]	BROAD ID	RRES v5.0 ID	Chromosome number	Exon number	Full-length (aa)[3]	Mature length (aa)	Cys no.[2]	RADAR[4]	Isoelectric point
FgSSP13	FGSG_00230	FgramPH1_01t00613	1	1	127	108	6	-	7.68
FgSSP14	FGSG_00847	FgramPH1_01t02121	1	2	64	48	4	-	4.74
FgSSP15	FGSG_01239	FgramPH1_01t03065	1	2	165	149	6	-	4.7
FgSSP16	FGSG_01831	FgramPH1_01t03065	1	3	98	81	8	2	4.1
FgSSP17	FGSG_02378	FgramPH1_01t05709	1	4	117	99	8	-	4.83
FgSSP18	FGSG_02685	FgramPH1_01t06433	1	3	147	128	8	2	6.45
FgSSP19	FGSG_03600	FgramPH1_01t13257	2	2	182	166	8	2	4.64
FgSSP20	FGSG_03911	FgramPH1_01t14013	2	2	183	167	4	2	5.1
FgSSP21	FGSG_04074	FgramPH1_01t14407	2	1	190	171	6	-	6.88
FgSSP22	FGSG_04745	FgramPH1_01t16217	3	2	92	74	6	2	8.11
FgSSP23	FGSG_05341	FgramPH1_01t17671	3	1	189	173	5	2	4.75
FgSSP24	FGSG_07988	FgramPH1_01t08839	2	1	179	161	4	-	8.31
FgSSP25	FGSG_08238	FgramPH1_01t09441	2	1	195	127	4	-	8.46
FgSSP26	FGSG_08987	FgramPH1_01t28189	4	2	119	103	6	-	6.61
FgSSP27	FGSG_09127	FgramPH1_01t27865	4	3	115	97	8	-	5.78

Table 3.2 continued

FgSSP[1]	BROAD ID	RRES v5.0 ID	Chromosome number	Exon number	Full-length (aa)[3]	Mature length (aa)	Cys no.[2]	RADAR[4]	Isoelectric point
FgSSP28	FGSG_10206	FgramPH1_01t07541	1	1	162	146	8	2	7.57
FgSSP29	FGSG_11033	FgramPH1_01t21071	3	3	108	90	2	2	6.6
FgSSP30	FGSG_11225	FgramPH1_01t21531	3	2	113	94	8	2	4.83
FgSSP31	FGSG_12514	FgramPH1_01t12011	2	2	118	101	5	-	5.7
FgSSP32	FGSG_15251	FgramPH1_01t15675	2	1	67	47	6	-	7.24
FgSSP33	FGSG_15437	FgramPH1_01t25187	4	2	70	53	8	-	5.73
FgSSP34	FGSG_15448	FgramPH1_01t25477	4	2	90	71	8	-	7.72
FgSSP35	FGSG_15469	FgramPH1_01t09349	2	2	92	74	6	2	4.93
FgSSP36	FGSG_15661	FgramPH1_01t15975	2	1		77	10	-	7.36
FgSSP6	FGSG_10212	FgramPH1_01t07553	1	2	139	121	4	-	8.33
FgSSP7	FGSG_11205	FgramPH1_01t21471	3	2	140	122	4	2	8.18
TRI4	FGSG_03535	FgramPH1_01t13107	2	4	520	520	6	-	8
TRI5	FGSG_03537	FgramPH1_01t13111	2	2	375	375	8	-	5

[1] FgSSP = *F. graminearum* small secreted proteins, [2] Cys = cysteine, [3] aa = amino acids; [4] RADAR = Rapid automatic detection and alignment of repeats score.

Table 3.4 Phylogenetic distribution of candidate FgSSPs and protein family analysis.

FgSSP	Pfam no.	Pfam domain	Phyre hits	BLAST2GO	Recombination region[1]	Paralogue no. [2]	Orthologue no.[2]	*Fusarium* specific?[3]	Secreted cluster?[4]
FgSSP13	-	-	-	-	Mid	0	11	No	-
FgSSP14	-	-	-	-	Low	0	24	No	-
FgSSP15	-	-	-	-	Low	0	75	No	-
FgSSP16	PF06766	Hydrophobin	Class II Hydrophobin	Hydrophobin precursor	High	0	75	No	-
FgSSP17	-	-	-	-	High	1	86	No	-
FgSSP18	-	-	-	-	Low	0	138	No	-
FgSSP19	-	-	-	-	Low	2	26	No	2
FgSSP20	PF09056	Phospholipase	Phospholipase	Phospholipase	-	0	147	No	-
FgSSP21	-	-	-	Cell wall protein	Low	2	178	No	-
FgSSP22	PF11402	Antifungal	PAF protein	Antifungal protein	High	0	33	No	VII
FgSSP23	PF14856	Necrosis-inducing factor	-	-	Low	0	35	No	-
FgSSP24	-	-	-	Cell wall protein	Low	2	178	No	-
FgSSP25	-	-	-	-	Mid	2	168	No	-
FgSSP26	-	-	-	Long chronological lifespan protein	High	0	226	No	-

FgSSP27	-	-	-	-	Low	1	99	No	-
FgSSP28	-	-	-	-	Low	0	31	No	-
FgSSP29	-	-	-	-	Low	0	10	No	-
FgSSP30	-	-	-	-	Low	0	12	No	9
FgSSP31	-	-	-	-	High	0	6	Yes	-
FgSSP32	-	-	-	-	High	0	0	Yes	-
FgSSP33	-	-	-	-	Mid	0	7	Yes	-
FgSSP34	-	-	-	-	High	1	19	No	-
FgSSP35	-	-	-	-	Low	0	17	No	-
FgSSP36	-	-	-	-	Mid	4	28	No	-
FgSSP6	PF07249	Cerato-platanin	Polysaccharide binding	Cerato-platanin	Low	1	423	No	-
FgSSP7	PF07249	Cerato-platanin	Polysaccharide binding	Cerato-platanin	Low	1	370	No	8
TRI4	PF00067	P450		Cytochrome P450	Mid	1	142	No	-
TRI5				Trichodiene synthase	Mid	0	45	No	-

[1] Signifies location of *FgSSPs* within genomic regions subject to low, mid, or high levels of recombination (Antoniw et al. 2011), [2] Paralogue and orthologue number determined using phylogenetic data from EnsemblFungi in 2018, [3] *Fusarium* species specificity determined by examining the phylogenetic data from EnsemblFungi in 2018.[4] Signifies presence of *FgSSPs* within the secreted gene clusters identified by Brown, Antoniw, and Hammond-Kosack (2012).

Table 3.5 Expression profiles of candidate *FgSSPs* in the *F. graminearum*-wheat interaction.

FgSSP	Phase[1]	CM[2]	MM-C[3]	MM-N[4]	Spikelet[5]	Symptomatic[6]	Onset[7]	Symptomless[8]	Rank[9]	Fold change[10]
FgSSP13	Symptomless	23.43	22.39	10.11	69.87	70.22	175.33	436.19	23	18.61
FgSSP14	Symptomless	280.74	869.15	406.72	508.92	611.25	1166.39	1984.51	13	7.07
FgSSP15	Symptomless	22.24	35.39	44.35	1449.36	337.13	253.97	601.32	14	27.04
FgSSP16	Symptomatic	38.46	42.01	19.77	10953.55	2674.13	330.49	457.84	3	69.53
FgSSP17	Symptomless	2.24	13.05	28.31	708.88	160.76	194.6532	752.28	21	335.58
FgSSP18	Symptomatic	32.59	23.68	46.75	1902.59	4434.39	2968.98	2180.06	6	136.06
FgSSP19	Symptomatic	9.80	39.07	30.90	974.39	1106.86	726.24	732.49	18	112.93
FgSSP20	Symptomatic	97.44	3239.64	77.89	4538.26	4481.23	2235.83	325.17	5	45.99
FgSSP21	Symptomatic	1253.98	71.40	174.83	8781.04	10047.87	9474.20	8656.80	4	8.01
FgSSP22	Onset	21.56	21.37	24.52	9855.47	25910.10	32541.72	6281.38	1	1509.21
FgSSP23	Symptomless	33.17	30.13	35.00	117.30	484.39	631.96	1196.32	17	36.06
FgSSP24	Symptomless	56.34	102.78	197.90	10495.28	10109.54	10283.39	20817.93	2	369.53
FgSSP25	Symptomatic	1038.63	16091.61	14129.72	183.91	2083.96	1480.59	320.06	11	2.01
FgSSP26	Symptomless	293.22	830.49	926.56	817.57	799.01	1045.27	1277.58	16	4.36
FgSSP27	Symptomless	47.82	36.16	13.84	78.00	188.85	291.32	518.33	22	10.84
FgSSP28	Onset	405.23	626.34	235.27	1329.68	1064.14	1132.82	830.00	15	2.63

Table 3.5 continued

FgSSP	Phase[1]	CM[2]	MM-C[3]	MM-N[4]	Spikelet[5]	Symptomatic[6]	Onset[7]	Symptomless[8]	Rank[9]	Fold change[10]
FgSSP29	Symptomatic	25.21	9.78	13.10	2803.35	1618.20	1031.75	149.94	9	64.18
FgSSP30	Onset	25.33	9.91	24.75	581.75	3339.58	3576.78	633.32	8	141.20
FgSSP31	Symptomless	11.96	15.94	13.90	236.97	1431.46	1114.66	2195.08	10	183.48
FgSSP32	Symptomatic	5.26	4.35	12.36	151.31	973.26	275.036	166.90	20	184.98
FgSSP33	Symptomatic	52.48	19.76	71.92	546.39	2076.70	2025.59	700.95	12	39.57
FgSSP34	Symptomless	51.27	41.37	73.63	198.37	657.02	1684.92	3983.74	7	77.70
FgSSP35	Symptomless	39.12	61.54	25.79	49.55	56.18	153.845	433.27	24	11.08
FgSSP36	Symptomless	96.64	158.01	127.26	601.19	933.55	913.89	976.67	19	10.11
FgSSP6	Symptomatic	14719.57	12743.76	8795.15	3793.09	7469.71	6379.59	4616.81	-	0.51
FgSSP7	Symptomatic	148.88	13829.56	11365.11	1130.27	10733.24	8747.26	2088.75	-	72.09
TRI4	Symptomless	34.15	10.37	64.99	3619.87	17955.39	35477.72	57722.30	-	1690.07
TRI5	Symptomless	7.38	3.92	14.09	1169.26	6803.84	11634.39	27078.83	-	3669.20

[1] Phase during which expression of *FgSSP* peaks in the Affymetrix microarray dataset (Brown et al. 2017), [2] Expression in complete media (CM) taken from Guldener, Seong, et al. (2006b),[3] Expression in minimal media supplemented with carbon, [4] Expression in minimal media supplemented with nitrogen, [5] Expression in spikelet tissue from the Brown et al. (2017) dataset, [6] Expression in symptomatic tissue from the Brown et al. (2017) dataset, [7] Expression in onset tissue from the Brown et al. (2017) dataset, [8] Expression in symptomless tissue from the Brown et al. (2017) dataset,[9] Ranking of candidate FgSSPs in terms of peak expression across all tissue types from the Brown et al. (2017) dataset, [10] Fold-change in gene expression observed between the peak of gene expression and *in vitro* conditions.

The first candidate, FgSSP13, was selected due to the high number of cysteine residues present within the protein sequence. Orthologues of FgSSP13 are widespread within the *Fusarium* genus. However, as expression of *FgSSP13* is lower than other candidates, this candidate was not given high priority status for functional characterisation. Like FgSSP13, FgSSP14 orthologues are also widespread within *Fusarium* and other ascomycetes such as the *Trichoderma* species. *FgSSP14* was shown by Brown et al. (2017) to be upregulated during the symptomless phase of the *F. graminearum*-wheat interaction. Interestingly however, in a transcriptome experiment exploring gene expression during fruiting body formation *in vitro*, *FgSSP14* was the only up-regulated candidate effector (Figure 3.4)(Sikhakolli et al. 2012). *F. graminearum* is capable of both asexual and sexual reproduction with the former resulting in the production of conidia and the latter with the production of fruiting bodies, known as perithecia, which initiate FHB via the forcible discharge of ascospores (Hallen et al. 2007). Perithecia are known to form later in the *F. graminearum*-wheat interaction – the upregulation of *FgSSP14* during the symptomless phase and during perithecial development is therefore counterintuitive. This made *FgSSP14* an interesting candidate for functional characterisation. In a study undertaken to explore *F. graminearum* adaptation to different hosts, including wheat, barley and maize, *FgSSP14* was one of two *FgSSPs* specifically up-regulated during wheat infection (Appendix 2)(Harris et al. 2016b).

FgSSP17 was selected based on the high cysteine content of this protein, with the full-length peptide containing eight cysteine residues, and as the encoding gene resides in a genomic location subject to high levels of

recombination. In many pathogenic species, effectors are predicted to evolve at an accelerated rate relative to the core genome. The residence of genes within genomic regions exhibiting high levels of plasticity is therefore believed to be a signpost for effector identification (Gout et al. 2006; Hogenhout et al. 2009). FgSSP17 is also highly up-regulated during the symptomless phase when compared to *in vitro* conditions, exhibiting a fold-change of more than x300 (Table 3.5).

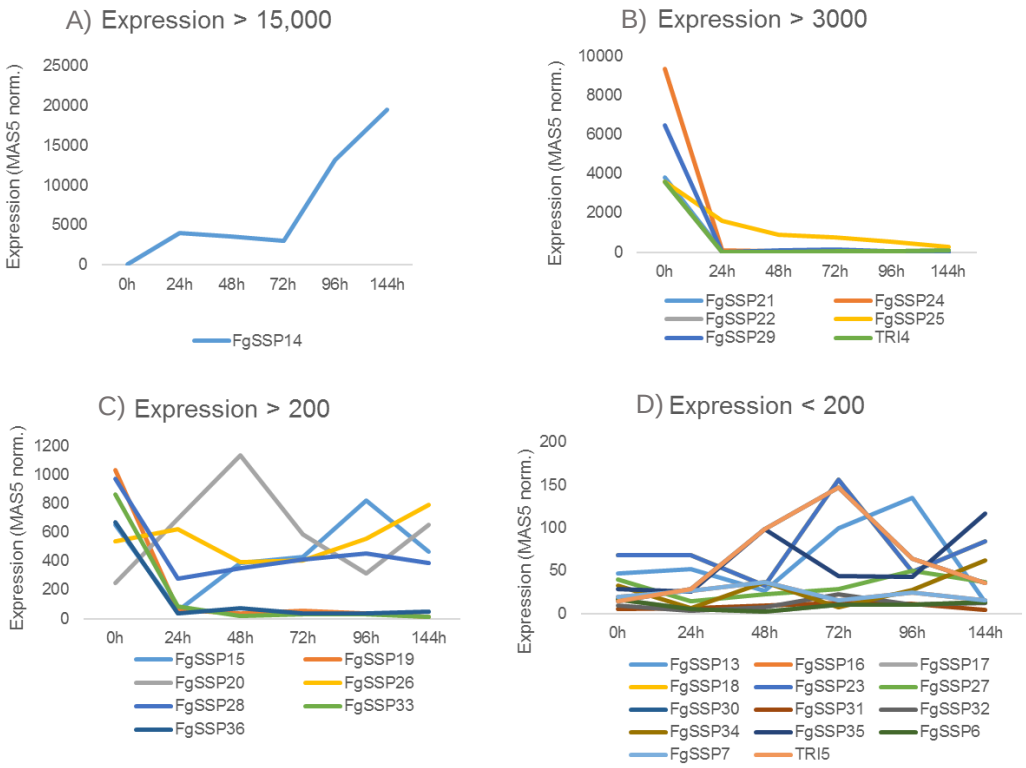

Figure 3.4 Transcriptional profile of the highly expressed *FgSSP14* gene relative to other *FgSSPs* in the vegetative phase of *F. graminearum*. Graph A shows the expression pattern of FgSSP14 which peaks at ~20,000 (MAS5 normalised). Graph B shows the expression pattern of FgSSPs with a peak expression value of more than 3000 (MAS5 normalised). Graph C shows the expression pattern of FgSSPs with a peak expression value between 200-3000 (MAS5 normalised). Graph D shows the expression pattern of FgSSPs with a peak expression value of less than 200 (MAS5 normalised). Data taken from Sikhakolli et al. (2012).

FgSSP23 contains the Pfam domain PF14856 first identified in the *Cladosporium fulvum* effector Ecp2; consequently, designated as the homologue of *C. fulvum* Ecp2 effector (Hce) domain. This domain corresponds to the mature part of the Ecp2 effector and is widespread among the homologues of Ecp2. Whilst the exact function of Ecp2 is unknown, this protein is postulated to function as a necrosis-inducing factor thus suggesting that *FgSSP23* may play a similar role in *F. graminearum* (Stergiopoulos et al. 2010). Ecp2 is hypothesised to be a core effector recognised by single cognate Cf-proteins regardless of pathogen species. For example, the ability of Ecp2 homologues from the black sigatoka pathogen of banana, *Mycosphaerella fijiensis*, to trigger necrosis has been demonstrated (Stergiopoulos et al. 2010). However, expression of *FgSSP23* peaks during the symptomless phase of infection, during which time *F. graminearum* is unlikely to deploy necrosis-inducing virulence factors and is therefore likely to play a different role in the fungal-wheat interaction.

One of the most highly expressed genes during the symptomless phase of infection is *FgSSP24* – a homologue of *PhiA*, first characterised in *Aspergillus nidulans* (Melin, Schnurer, and Wagner 2003). *PhiA* encodes a secreted cell wall protein and, in *A. nidulans,* deletion of this gene results in abnormal conidiophore development due to the altered morphology of phialides in mutants. Whilst the importance of *PhiA* in asexual reproduction is evident, PhiA is also hypothesised to play a secondary protective role against toxic metabolites (Melin, Schnurer, and Wagner 2003). Efforts to identify candidate effectors in *C. fulvum* led to an attempt to characterise the *CfPhiC* homologue, predicted to be contribute towards pathogenicity.

Deletion of the *CfPhiC* gene, however, led to a lethal phenotype and, as this gene was shown to be upregulated throughout infection, was considered unlikely to function as an effector (Bolton et al. 2008). The *F. graminearum* homologue of *PhiA* however, is extremely highly expressed during the symptomless phase of infection – during which time asexual reproduction of *F. graminearum* would not have begun (Figure 3.6). The curious expression of this gene in relation to its predicted function makes *FgSSP24* an interesting gene for characterisation. *FgSSP24* has three paralogues, also located on chromosome 2, all of which are secreted. Paralogues are genes that have shared ancestry as a result of a duplication event whereas orthologues are genes that have common ancestry as a result of speciation (Koonin 2005). The shared nucleotide sequence identity of the genes encoding these paralogues is 57% and the shared amino acid sequences identity of these proteins is 40%. In all the paralogues a ‘SGMGQG’ motif, which is also conserved within other PhiA homologues, is present (Figure 3.5). One of the *FgSSP24* paralogues (*FgSSP21*) is also one of the final twenty-four candidates for characterisation; however, unlike *FgSSP24*, the expression of *FgSSP21* peaks during the onset phase of infection. The remaining two paralogues, *FGSG_08122* and *FGSG_03662*, are most highly expressed *in vitro,* in-keeping with the hypothetical role that these genes play in conidial germination (Figure 3.6).

Figure 3.5 Multiple sequence alignment of FgSSP24 and FgSSP21 and the two other PhiA paralogues (FGSG_03662; FGSG_08122). The shared amino acid sequence identity of these proteins is 40%. * denotes amino acid sequence conserved between paralogues.

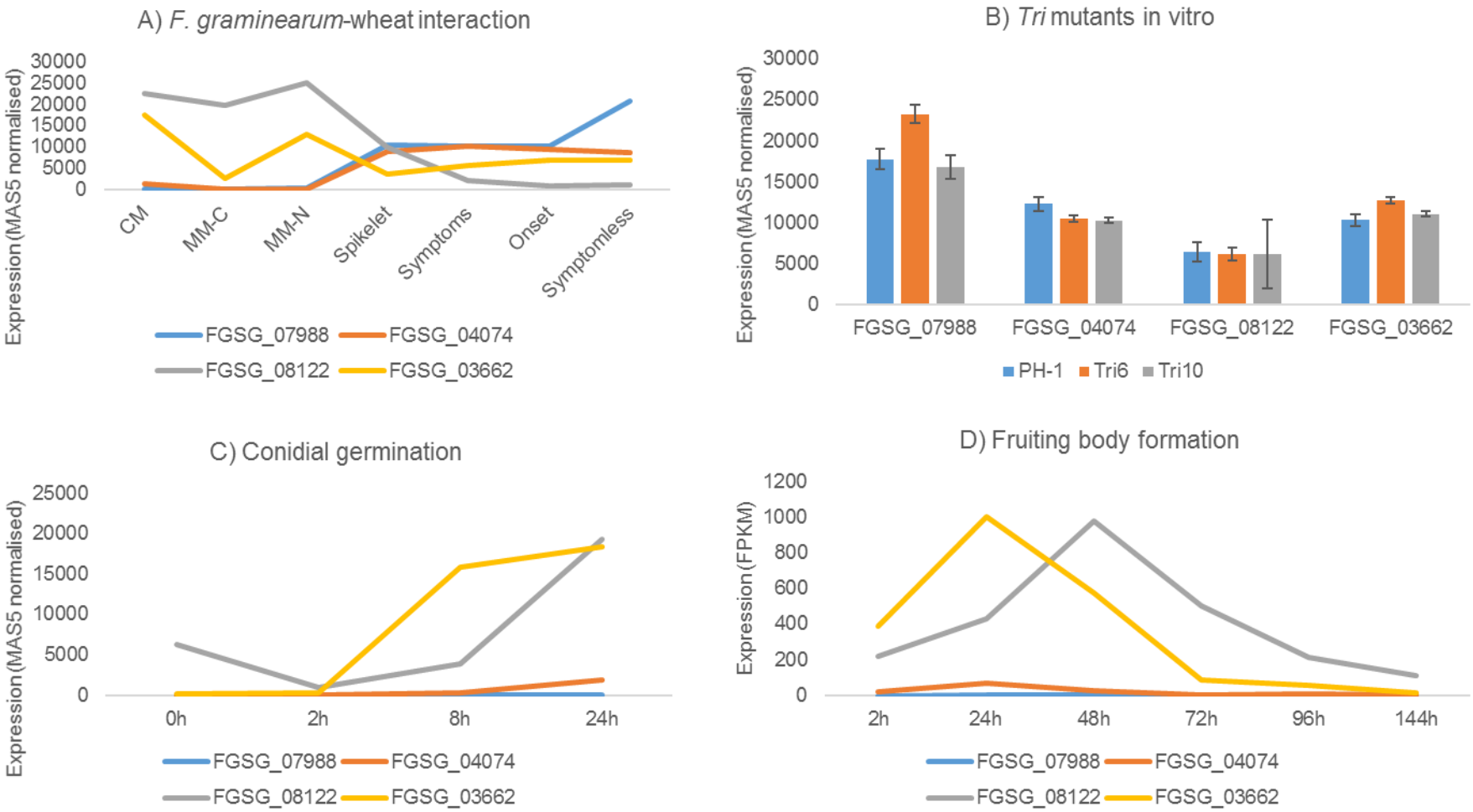

Figure 3.6 Expression profiles of the four *FgPhiA* paralogues. A) Affymetrix expression data of *F. graminearum*-infected wheat (Brown et al. 2017); B) Expression in the Δ*Tri6* and Δ*Tri10* mutants in *vitro* (Seong et al. 2009a); C) Expression during conidial germination (Seong et al. 2008); D) expression during fruiting body formation (Sikhakolli et al. 2012).

FgSSP26 exhibits a high cysteine content and relatively high level of expression, compared to other candidate effector genes, and resides in an area of high recombination frequency. FgSSP26 has a Blast2GO annotation of long chronological lifespan protein which have been linked to apoptosis in yeast and a conserved triosephosphate isomerase (TIM) phosphate binding motif (Herker et al. 2004). There is no literature that implicates long chronological lifespan proteins in fungal pathogenicity. Both FgSSP27 and FgSSP31 were selected, again, due to the presence of effector-associated characteristics. FgSSP31 is of interest due to its expression profile – exhibiting a fold change between *in vitro* conditions and the symptomless phase of more than x180. FgSSP31 homologues are also restricted to the *Fusarium* genus – with thirty-two known homologues identified within the genus.

The differences in structural and genomic variation between isolates within fungal species can be captured through pangenome analysis. By capturing the full gene repertoire, the genome of a species can be subcategorised into genes that are ‘core’ to lifestyle and survival or genes that are dispensable or ‘accessory’ (Hurgobin and Edwards 2017). All selected FgSSPs are present in each isolate of the *F. graminearum* pangenome and therefore belong to the core genome. SNP calling of isolates revealed that *FgSSP34* exhibits the highest mutation rate of all the selected *FgSSPs (*Appendix 2) – perhaps not surprising in light of the residence of this gene within a region subject to high levels of genomic recombination. *FgSSP34* is a promising effector candidate, strongly expressed during the symptomless phase of infection.

Despite the relatively low expression of *FgSSP3*5 as compared to the other candidate effectors, the unusual distribution of the genes' orthologues makes FgSSP35 an interesting choice for characterisation. FgSSP35 has six homologues within the *Fusarium* genus, five more from the *Magnaporthales* genus and two in *Gaeumannomyces tritici* (Figure 3.7).This gene is one of two *FgSSPs* specifically expressed on wheat in a comparison of gene expression against barley and maize (Harris et al. 2016b). FgSSP35 is a cysteine-rich candidate with a high number of intergenic repeats. Regions of high genome diversity have been shown to house many genes which influence the host-pathogen interaction which are specifically expressed during this interaction (Cuomo et al. 2007). In *U. maydis,* 18% of secreted proteins are dispersed in regions with large regions of repetitive DNA despite the low overall presence of repetitive DNA in the genome as a whole (Kamper et al. 2006). The presence of intergenic repeats, which increase phenotypic plasticity, is therefore a signpost for effector function and may suggest a rapidly evolving genomic environment thus promoting sequence diversification - something that is essential for the survival of effectors in the evolutionary battle between host and pathogen (Rouxel et al. 2011; Levdansky et al. 2007; Ma and Guttman 2008).

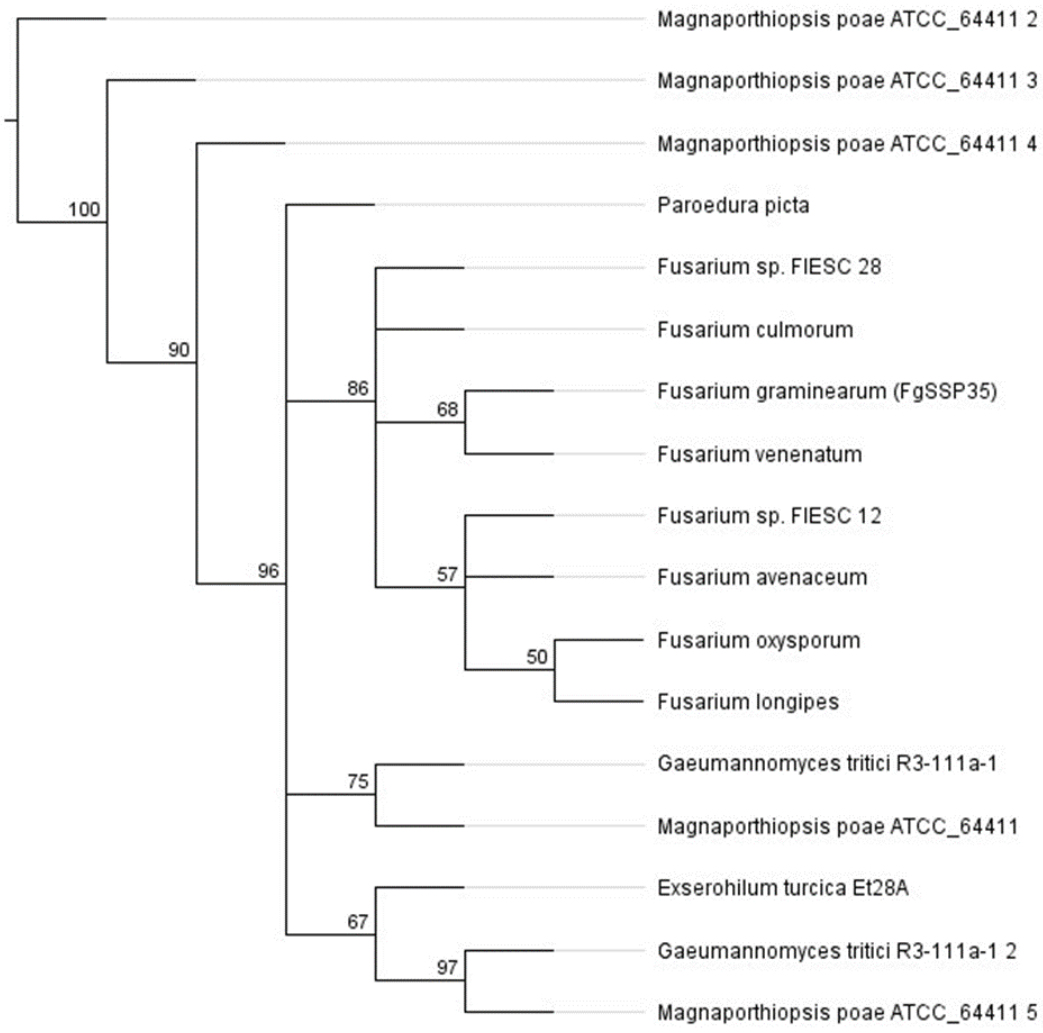

Figure 3.7 A rooted phylogenetic tree of the protein sequences of FgSSP35 homologues identified from a BlastP search. A neighbour-joining analysis with Jukes-Cantor correction and bootstrap support was performed on protein sequences. Branch length and bootstrap values were obtained from 500 replicates and branch labels indicate bootstrap values. The *Magnaporthiopsis poae ATCC_64111 2* sequence was used as the outgroup.

3.3.1.2 Putative effectors most highly expressed during the symptomatic phase of F. graminearum infection

The remaining thirteen putative effectors were most highly expressed during the symptomatic phase or the bridge between the symptomless and symptomatic phases, known here as the 'onset' phase: *FgSSP15, FgSSP16, FgSSP18, FgSSP19, FgSSP20, FgSSP21, FgSSP22, FgSSP25, FgSSP28, FgSSP29, FgSSP30, FgSSP32, FgSSP33* and *FgSSP36.* The ranking of these *FgSSPs* in terms of peak expression is found in table 3.5.

FgSSP15 was identified as a putative effector due its small size and high cysteine content. FgSSP16 was selected as an effector candidate as it contains a fungal hydrophobin Pfam domain (PF06766). Hydrophobins are small, cysteine-rich proteins, secreted only by filamentous fungi, and have the ability to form a water-repellent coating on the surface of an object (Sunde et al. 2008). FgSSP16 has 100% protein sequence similarity to a class II hydrophobin precursor in *F. culmorum,* FcHyd5p, and is associated with the gushing phenomena in beer (Stubner et al. 2010; Sarlin et al. 2012). A pairwise alignment between FgSSP16 and the *M. grisea* protein Mhp1 revealed a high level of sequence similarity (62.7%). Mhp1 is also a hydrophobin and has been found to be required for fungal development and plant colonisation (Kim et al. 2005). However, gene deletion mutants of *FgSSP16* previously generated at Rothamsted were inconclusive in terms of their contribution towards pathogenicity (Martin Urban, personal communication). Despite this, due to the number of effector-associated characteristics, FgSSP16 remains a candidate for functional characterisation.

FgSSP18 and FgSSP19 were identified as putative effectors due to the high cysteine content of each protein as well as exhibiting a RADAR score of 2. Interestingly, like other putative FgSSP effectors, *FgSSP18* was found to be downregulated in an *Fgp1* mutant when explored under either in *in vitro* or *in planta* conditions (Jonkers et al. 2012). Fgp1 is a homologue of the WOR1 protein from *Candida albicans* which functions as a key regulatory component controlling the dimorphic switch (Huang et al. 2006). Deletion of *Fgp1* in *F. graminearum* results in severely reduced virulence, as well as a loss of trichothecene accumulation in infected wheat floral tissue (Jonkers et al. 2012). In contrast, *FgSSP18* is found to be upregulated in strains lacking the transcription factors Tri6 and Tri10 – key regulators in trichothecene biosynthesis (Seong et al. 2009b). Differential expression of effectors in DON-deficient *F. graminearum* strains poses an interesting question as to how other fungal mechanisms could potentially compensate for the lack of the DON production.

FgSSP20 contains a phospholipase A Pfam domain (PF09056) and is one of the more highly expressed candidates, peaking at 4481.23 (MAS5) and exhibiting a x45 fold change expression increase *in planta* (Table 3.5). Phospholipases released by fungi play important roles in nutrient acquisition, tissue invasion and modulation of the host immune response (Kohler et al. 2006). In *F. graminearum*, deletion of the gene encoding a phospholipase C results in reduced pathogenicity, conidium germination and DON accumulation (Zhu et al. 2016)

FgSSP21 is a paralogue of the previously described FgSSP24. Both proteins are homologues of the *A. nidulans* PhiA protein and FgSSP21 and FgSSP24

share an amino acid identity of 45.3% (Figure 3.5). The expression profiles of these two paralogues are, however, quite different. Unlike *FgSSP24*, the expression of *FgSSP21* peaks during the symptomatic phase of infection (Figure 3.6). Both *FgSSP21* and *FgSSP24*¸ although predicted to function during asexual development, are not up-regulated during conidial germination or fruiting body formation, suggesting that both genes may function differently to the *PhiA* homologue in other species (Sikhakolli et al. 2012). *FgSSP21* also lies within 20kb of *FGSG_04068*, a Rho GTPase, the deletion of which results in reduced virulence. *F. graminearum* Rho GTPases have been found to contribute towards growth, conidia formation, sexual reproduction, DON production and pathogenicity in *F. graminearum* (Zhang et al. 2013).

The most highly expressed of all off the putative effectors is *FgSSP22* and is one of the few candidates to have a Pfam domain (PF11402). FgSSP22 contains an antifungal domain, first isolated and identified from *Penicillium chrysogenum,* known as PAF (Binder et al. 2010). PAF is one of the most well studied secreted antifungal proteins and has been shown to disrupt Ca^{2+} signalling and homeostasis. The continued disturbance of these two Ca^{2+} mediated events can trigger programmed cell death (PCD)(Galgoczy et al. 2013). These small, basic and cysteine-rich PAF proteins have been shown to be widespread among the *Fusaria* and an uncharacterised PAF protein in *F. boothii* has 100% protein sequence similarity to FgSSP22 (Figure 3.8)(Galgoczy et al. 2013). The biological role of these proteins however remains unclear, although speculated to play a role in defending the ecological niche against other microorganisms (Marx 2004). Whatever the

function, *FgSSP22* is potentially important to pathogenicity due to high level to which this gene is expressed during the transitionary period between the symptomless and symptomatic phases of *F. graminearum* infection. Expression of *FgSSP22* is 1550 times more expressed *in planta* than *in vitro* exhibiting similar expression levels to the *Tri5* and *Tri6* genes. In addition, this gene is located within one of the high recombination gene clusters of secreted genes which resides in a region of the genome where a high recombination frequency has been identified in the *F. graminearum* secretome analyses published by Brown, Antoniw, and Hammond-Kosack (2012)(Figure 3.9).

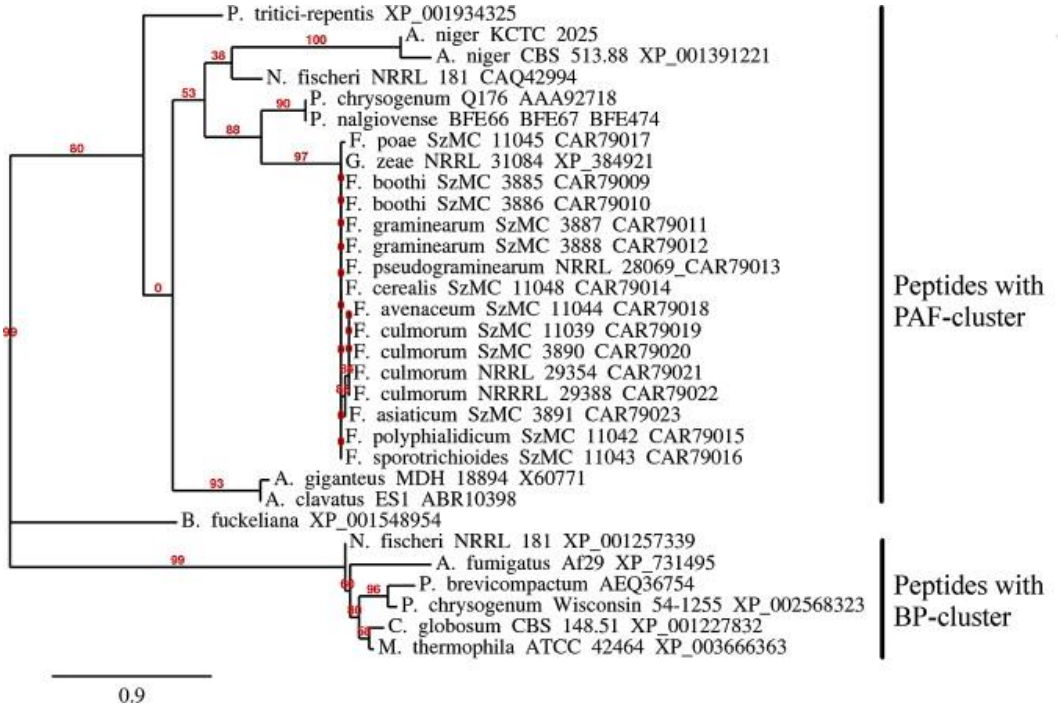

Figure 3.8 Phylogenetic tree of *Penicillium* antifungal protein (PAF) homologues in ascomycete fungi. The codes after the species names indicate 1) the culture collection of the secreting isolates an 2) the account number of the peptide. BP indicates 'Bubble protein' cluster – another protein produced by ascomycetes which inhibits the growth of yeasts. Figure taken from Galgoczy et al. (2013).

FgSSP25 belongs to large uncharacterised gene family with homologues found in the *Hypocreales, Nectriaceae* and the *Leotiomyceta*. FgSSP28, FgSSP29 and FgSSP30 orthologues are also widespread amongst the *Fusaria.* Like *FgSSP22***,** *FgSSP30* belongs to the gene cluster 9 enriched for genes coding for predicted small secreted proteins identified by Brown, Antoniw, and Hammond-Kosack (2012)(Figure 3.9).

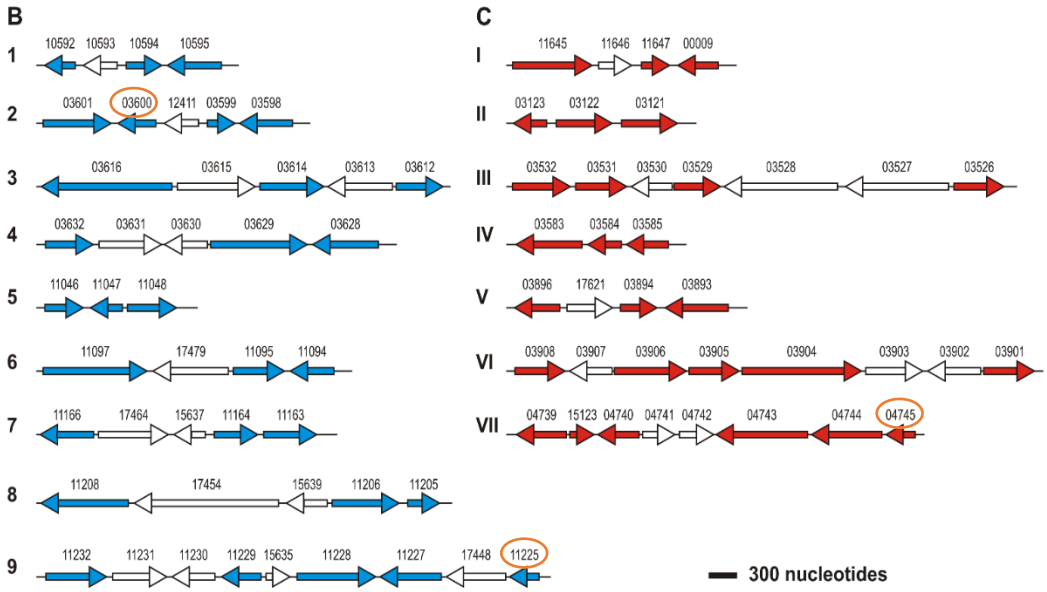

Figure 3.9 Gene clusters of secreted *F. graminearum* proteins. Blue represents genes that reside in areas of low recombination and red in high. Coloured arrows are secreted proteins and non-coloured are non-secreted. Arrow length is proportional to gene length to scale with the bar representing 300 nucleotides. Red circles around genes represent effector candidates. Taken from Brown *et al.* (2012).

The gene encoding FgSSP32 lies within a region of the *F. graminearum* genome subject to high levels of recombination. Interestingly, no FgSSP32 orthologues are recorded in the NCBI database (Accessed April 2019). Orthologues of FgSSP32 do however exist in a number of sequenced *Fusarium* isolates and species obtained from Brazil and North America – including *F. austroamericanum, F. meridionale* and *F. cortidariae* which belong to the FGSC (Rothamsted-EMBRAPA bilateral project data unpublished)(Table 3.2). The pairwise alignment between FgSSP32 protein orthologues from the FGSC is 88% and all cysteine residues within the sequences are conserved. The orthologue which exhibits the lowest level of similarity at the protein level is from *F. venenatum* which shares 62.7% sequence identity with FgSSP32 (Figure 3.10). Despite residence in a genomic region of high recombination, FgSSP32 is well-conserved in the *F. graminearum* pangenome with no mutations reported.

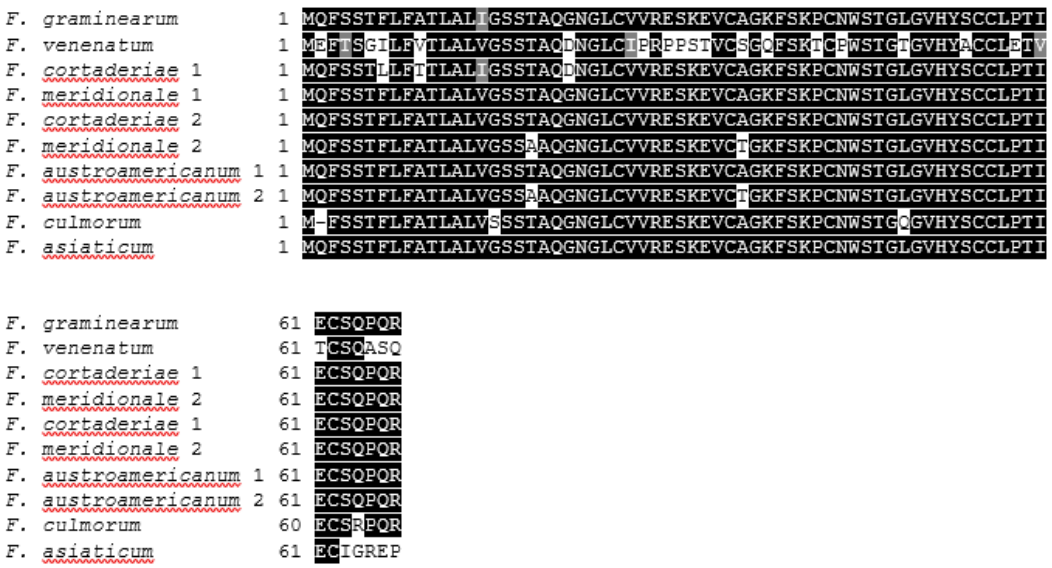

Figure 3.10 Protein alignment of FgSSP32 homologues found in the FGSC. Multiple sequence alignments were carried out in Geneious and visualised using the T-coffee software (Tommaso et al. 2011).

FgSSP33 is specific to the *Fusarium* genus with 21 homologues identified in BlastP and is present in all of *F. graminearum* Brazilian strains (Figure 3.11). Within the pangenome, the coding sequence of *FgSSP33* is well conserved – with just one synonymous mutation found in strains CML3049 and CML3404 and two synonymous mutations of G45S and A55T. The A55T mutation was found in the North American isolates Fg233423 and DAOM180378 and the G45S mutation was found in the Brazilian strains CML3070 and CML3066. Whether or not the amino acid substitution in this sequence correlates to a change in pathogenicity within these isolates is not known. In contrast to FgSSP32, the protein sequence of FgSSP33 is 100% conserved in the *Fusarium* isolates listed in table 3.2.

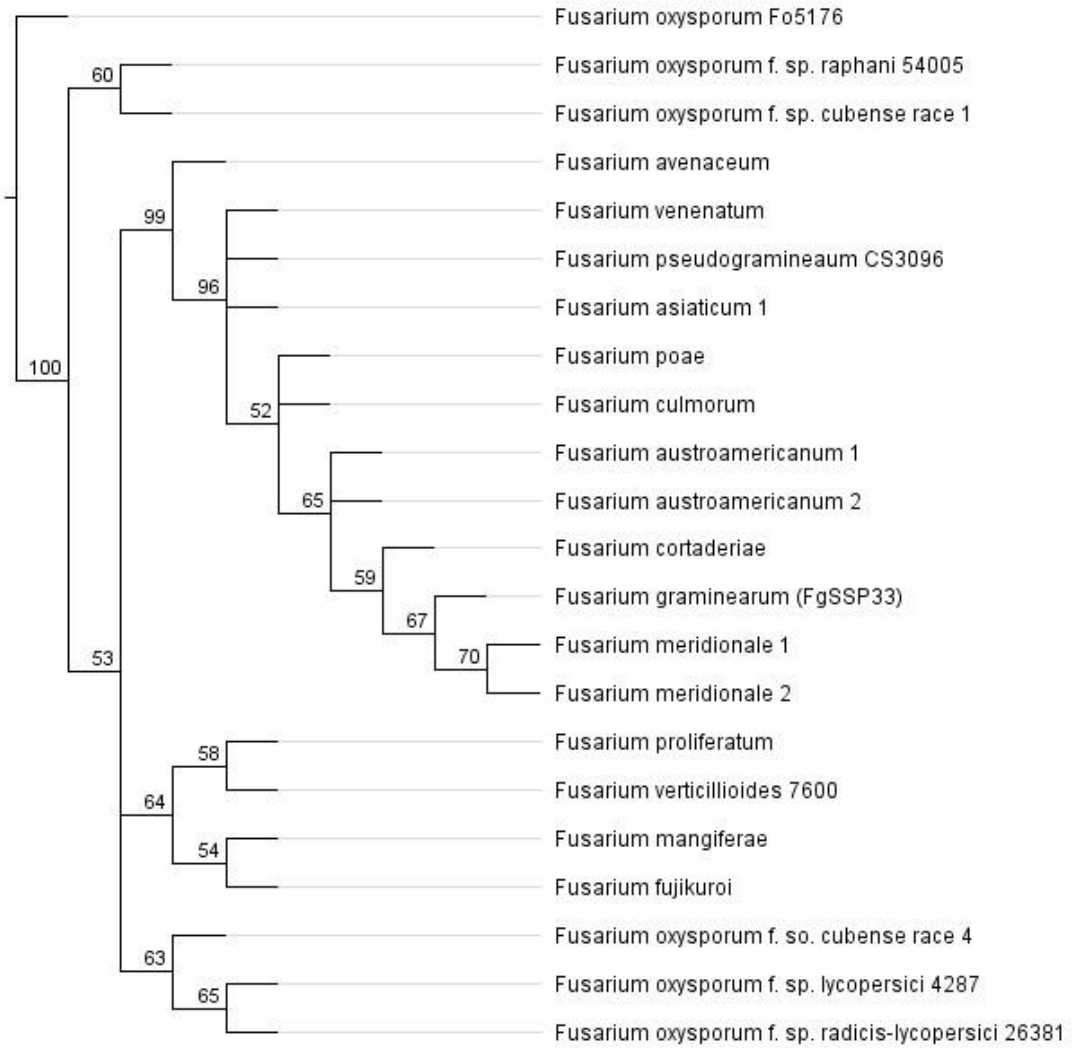

Figure 3.11 A rooted phylogenetic tree of the protein sequences of FgSSP33 homologues identified from a BlastP search. A neighbour-joining analysis with Jukes-Cantor correction and bootstrap support was performed on protein sequences. Branch length and bootstrap values were obtained from 500 replicates and branch labels indicate bootstrap values. The *Fusarium oxysporum Fo5176* sequence was used as the outgroup.

3.3.1 Validation of Affymetrix microarray expression profiles of putative effectors by quantitative reverse-transcription polymerase chain reaction (RT-qPCR)

Real-time qPCR (RT-qPCR) is routinely used to verify global gene expression Affymetrix microarray results due to the high sensitivity and wide dynamic range of this technology (Ujvari et al. 2014). The Affymetrix microarray gene expression data, which formed the foundation of the bioinformatic pipeline described in figure 3.2, was an amalgamation of several experiments: 1) studies which documented the transcriptional profile of *F. graminearum* during barley head, wheat head and wheat crown infection, as well as *in vitro* nutrient rich and poor comparisons (Guldener, Seong, et al. 2006b; Lysoe, Seong, and Kistler 2011) and 2) an experiment which explored the transcriptional profile of *F. graminearum* during the symptomless, onset and symptomatic phases during the wheat floral interaction (Brown et al. 2017). The following experiments aimed to determine whether the gene expression profiles from the Affymetrix microarray were comparable to those obtained by RT-qPCR.

In order to replicate and validate the Affymetrix microarray data generated by Brown et al. (2017), wheat ears were point-inoculated with *F. graminearum* and the gene expression profiles of candidate *FgSSPs* were explored during the symptomless, onset and symptomatic phases of infection. These distinct phases were isolated by harvesting rachis internodes sequentially below the initial point of inoculation – whereby internodes closest to the point of inoculation represented the symptomatic phase and internodes further away represented the symptomless phase (Figure 3.3). At the time of harvesting,

quantitative disease assessments were made to track *F. graminearum* disease progression in individual wheat plants. Disease progress, as determined by the number of visibly diseased spikelets below the point of inoculation, showed variability with the number of spikelets showing symptoms ranging from 0-3 spikelets (Figure 3.12). This variability was particularly seen in the plants used for RNA extractions in biological replicates one and two. This variability in symptoms was reflected in *FgActin* expression – the expression of which provides a marker for fungal biomass (Brown et al. 2011). Previous studies have shown fungal biomass is low in symptomless tissues and increases after intracellular colonisation during the symptomatic phase of infection (Brown et al. 2017). Two of the biological replicates in this study followed the same pattern previously observed, however, *FgActin* expression in biological replicate 2 was more variable than expected and as such was removed from the following analyses (Figure 3.12). To explore gene expression *in vitro, F. graminearum* was cultured in YPD rather than complete media (CM) as done by Guldener, Seong, et al. (2006b). Efforts to culture *F. graminearum* in CM led to the unexpected upregulation of *FgSSPs,* the reason which could not be accounted for. YPD was therefore selected as an alternative for *in vitro* culture as this broth is more routinely used in our laboratory.

The expression profiles of eight *FgSSPs* (*FgSSP14, FgSSP17, FgSSP23, FgSSP24, FgSSP26, FgSSP30, FgSSP32* and *FgSSP33*) were validated by RT-qPCR with expression of *FgSSPs* normalised to the expression of *FgActin* to account for differences in fungal biomass between tissue samples. The RT-qPCR expression profiles of *FgSSP14, FgSSP17,*

FgSSP24, FgSSP26, FgSSP32, and *FgSSP33* all showed a high level of similarity to the expression profiles of these genes in the Affymetrix microarray dataset (Figure 3.13a, b). Attempts were made to determine the expression profile of *FgSSP22* but efforts to find primers that could efficiently amplify this transcript were unsuccessful. Despite the differences in *FgSSP* expression between the phases of *F. graminearum* infection, none of the *FgSSPs* were significantly differentially expressed between phases – perhaps a result of removing the second biological replicate from the analyses. In the Affymetrix expression profile, *FgSSP30* was found to be upregulated during the symptomatic and onset phases of infection and lowly expressed during the symptomless phase – however, RT-qPCR analysis revealed that expression of this gene peaked in the symptomless phase of infection with expression remaining low in the other phases (Figure 3.13b). In the Affymetrix microarray, the expression of *FgSSP23* was shown to peak during the symptomless phase, whilst in the RT-qPCR analysis, expression was found to peak during the symptomatic phase of infection (Figure 3.13a).

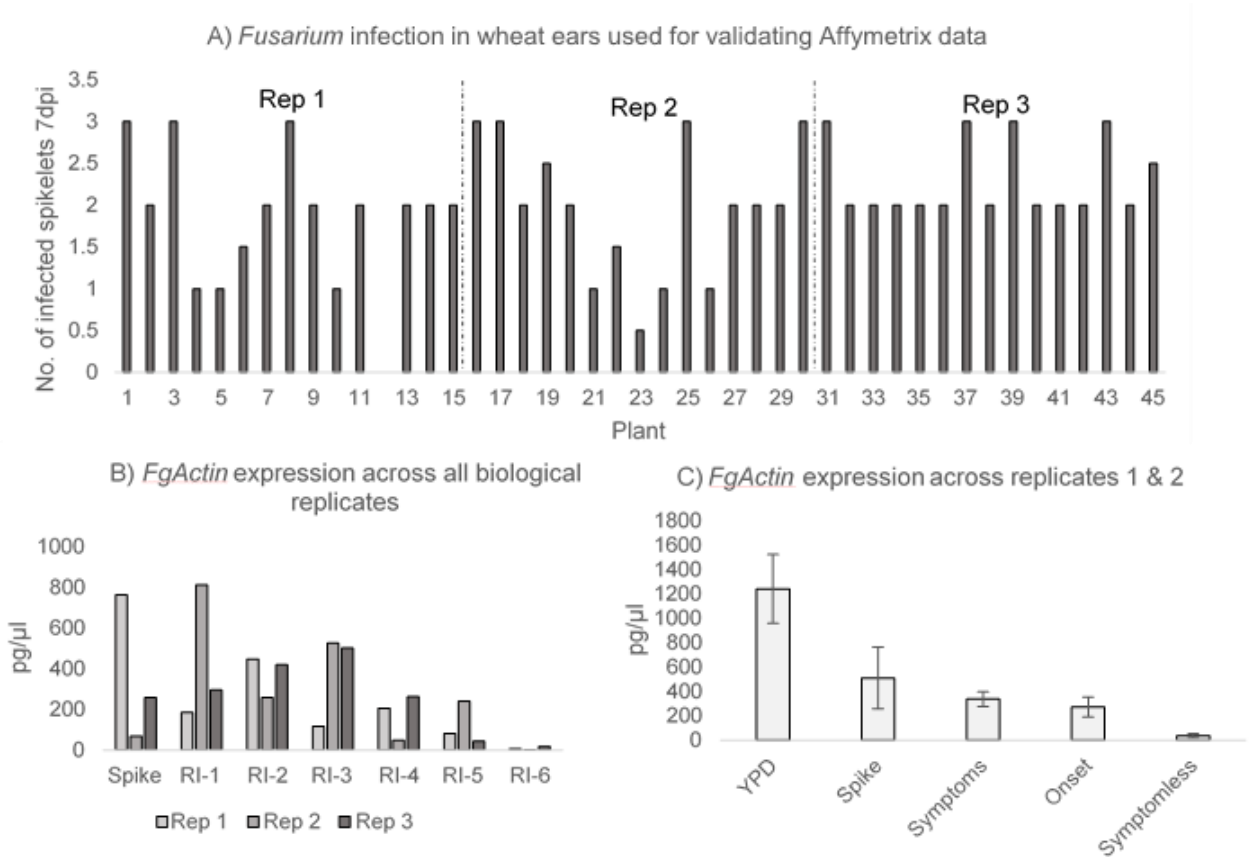

Figure 3.12 A) The number of visibly diseased spikelets of *F. graminearum*-infected wheat 7dpi. Biological replicate 1) plants 1-15, 2) 16-30, and 3) 31-45. B) Absolute quantitative *FgActin* expression determined by RT-qPCR. C) Absolute quantitative *FgActin* across biological replicates one and three where samples are pooled on the basis of symptoms. Error bars represent S.E.M.

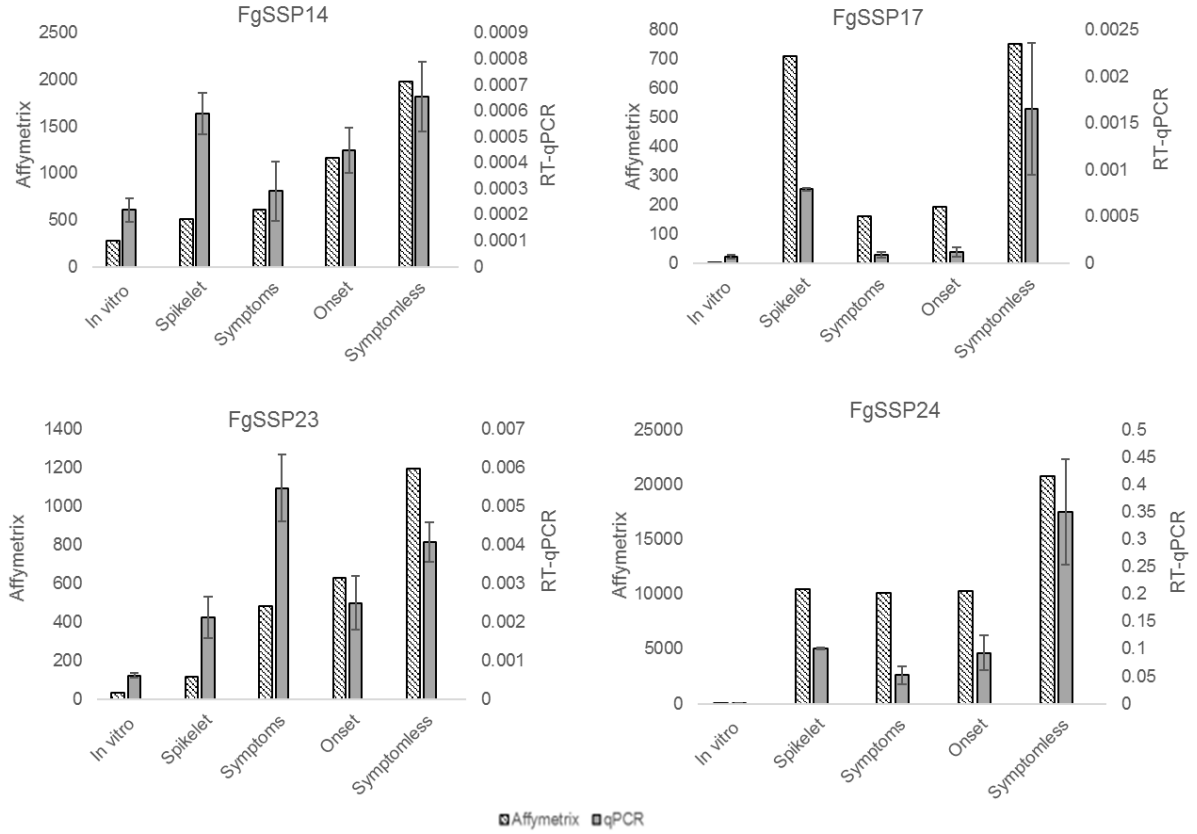

Figure 3.13a Comparison of Affymetrix vs RT-qPCR gene expression profiles *FgSSPs.* The primary vertical axis displays Affymetrix expression (MAS5 normalised) and the secondary vertical axis displays expression determined via RT-qPCR method using the standard curve method and data normalised to *FgActin* expression.

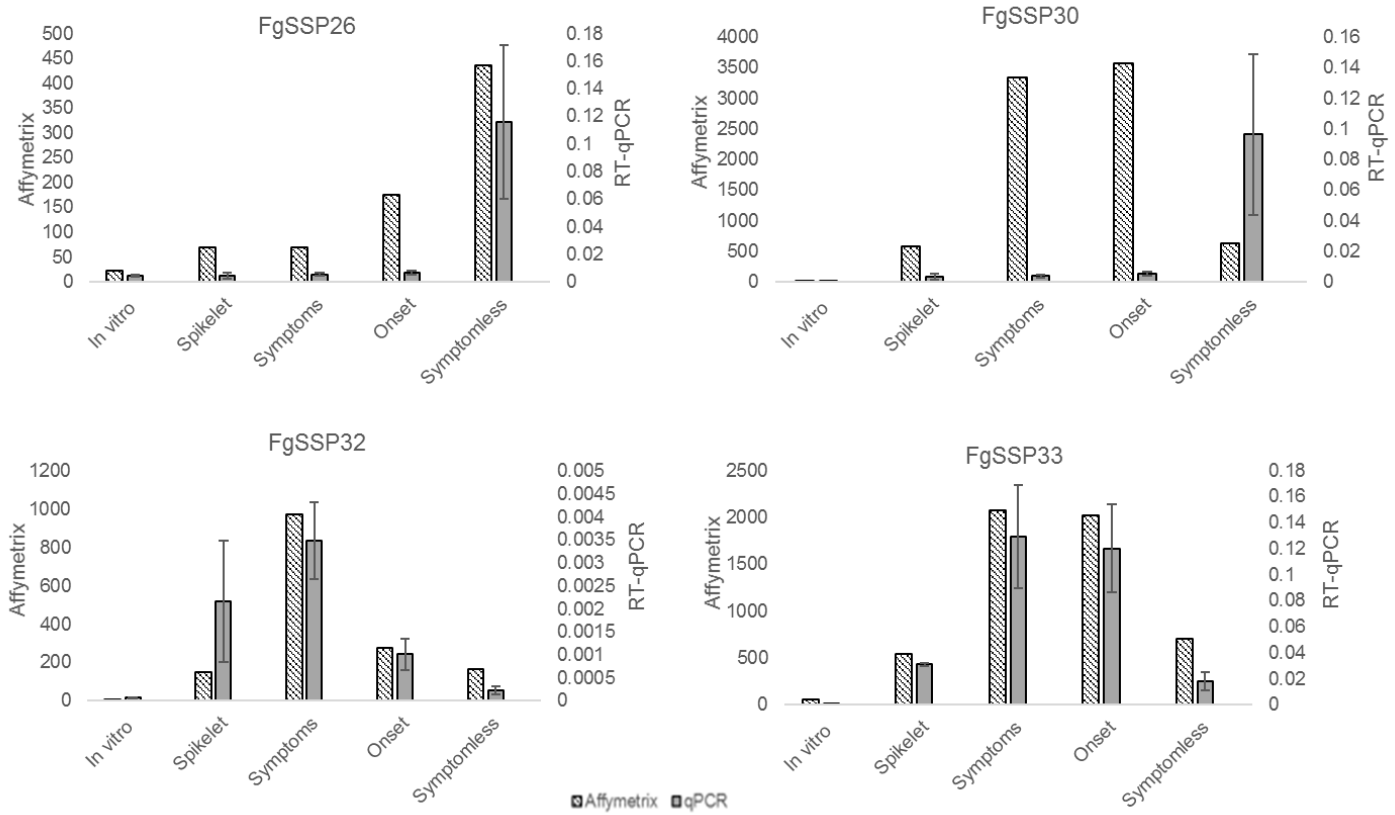

Figure 3.12b Comparison of Affymetrix vs RT-qPCR gene expression profiles *FgSSPs.* The primary vertical axis displays Affymetrix expression (MAS5 normalised) and the secondary vertical axis displays expression determined via RT-qPCR method using the standard curve method and data normalised to *FgActin* expression.

3.4 Discussion

Bioinformatic prediction of fungal effectors has been hindered by the lack of sequence conservation in protein sequences, a feature attributable to the inherent plasticity of fungal genomes (Jones et al. 2018). Identification of fungal effectors thereby entails a composite approach encompassing transcriptomics, comparative genomics, and inspection of the genomic landscape of putative effectors. While efforts to predict the *F. graminearum* effector repertoire have previously led to the identification of ~40 SSPs, these efforts have mainly relied upon interrogation of the transcriptional profiles of small genes within the predicted secretome, rather than a comprehensive bioinformatic analysis (Lu and Edwards 2016). For this study, I carried out and report upon an in-depth bioinformatic analysis of the predicted *F. graminearum* secretome enabling the identification of putative effectors for functional characterisation using the BSMV-VOX system (Chapter 4). The bioinformatic pipeline applied in this study yielded twenty-four putative effectors which were further prioritised for characterisation by exploring proteomic, genomic and transcriptomic attributes of each candidate sequence. The main criteria applied in this pipeline were small protein size, high cysteine content and *in planta* expression. Of the twenty-four identified putative effectors, only four contained Pfam domains and the rest were unannotated. The absence of functional annotation within putative effectors is in-keeping with the observation that many fungal effectors lack recognisable homology (Sperschneider et al. 2015).

A transcriptomic investigation of *F. graminearum* during wheat infection revealed that the fungal secretome was distinct during the symptomless and symptomatic phases of infection (Brown et al. 2017). In these two phases, *F. graminearum* differentially coordinates the spatial and temporal induction of effectors to facilitate either a

biotrophic or necrotrophic lifestyle. Twelve of the twenty-four candidates were predicted to be secreted during the symptomless phase of infection, during which time these proteins are hypothesised to function as defence-suppressors enabling stealthy colonisation of the host. In contrast, the remaining *FgSSPs* were upregulated during the symptomatic phase of infection and are predicted to function as defence-activators – inducing localised cell death to provide nutrients for fungal sequestration.

A wide range of transcriptomic datasets were used to globally interrogate the expression profiles of individual *FgSSPs*. While the primary dataset used in this analysis was the Brown et al. (2017) dataset, analysis of other datasets enabled comparisons between gene expression of *FgSSPs* during infection of different hosts and tissue types. The degree to which these datasets aligned was variable. For example, the genes encoding FgSSP20, FgSSP21 and FgSSP22 are all upregulated in the latter phases of each time-course experiment (Table 3.6). This supports the observation that each of these genes are upregulated during the symptomatic phase of the Brown et al. (2017) transcriptome dataset. While the degree to which the other datasets overlap, the majority of *FgSSPs* fit a consistent trend of either being expressed early on in infection or later. An RNA-seq dataset was also used to support the bioinformatic analysis in this study. This dataset explored gene expression during *in planta* infection using *F. graminearum*-infected wheat rachis tissues harvested at 5dpi (Table 3.6). *FgSSPs* were ranked in terms of how highly expressed these genes were within the whole of this RNA-seq transcriptome dataset. Overall, the majority of *FgSSPs* were lowly ranked in terms of expression compared to other *F. graminearum* genes. A notable exception is *FgSSP22* which ranked as the 18th most highly expressed gene in one of the samples.

A recent study by Harris et al. (2016b) exploring host-specific expression of genes revealed that only two of the selected gene candidates, *FgSSP14* and *FgSSP35*, were specifically expressed during the *F. graminearum*-wheat interaction. The majority of *FgSSPs* selected were specifically expressed either on wheat and barley or on all three hosts tested (wheat, barley and maize). As a pathogen of a diverse range of hosts, exploitation of the flexibility of the *F. graminearum* genome enables the fungus to adapt in accordance to host or substrate. Identification of genes that are solely expressed during wheat infection, as opposed to during infection of other host species, could be an interesting future strategy in terms of prioritising effectors for characterisation.

Pangenome analysis of *F. graminearum* identified a total of 161 core putative effectors among all 16 genomes, while a remaining 35 are predicted to reside within the variable portion of the genome (Machado et al., Rothamsted-EMBRABA unpublished). All *FgSSPs* identified in this analysis reside within the core *F. graminearum* genome perhaps indicating the importance of the contribution of these genes to pathogenicity (Table 3.8). Furthermore, an inspection of the SNPs present revealed a high level of conservation within *FgSSPs* found in all the pangenome isolates. The coding sequences of nine of the *FgSSPs* did not contain any non-synonymous mutations and thereby exhibited 100% protein sequence conservation between isolates. This conservation of gene sequence is interesting as many of these genes reside within regions of the genome subject to high levels of genetic recombination. For instance, *FgSSP32* was identified by King et al. (2015b) as a potential effector, noting the presence of this gene within a putative ‘virulence hot-spot’ housing species-specific secretory genes subject to rapid rates of evolution. The coding sequence of *FgSSP32* across the pangenome contains neither

synonymous (point mutations that do not result in a codon change) nor non-synonymous mutations (point mutations or base pair insertions or deletions that result in a codon change).This may suggest that *FgSSP32* has either 1) recently evolved or 2) that this gene plays an important role in fungal virulence and can therefore not be lost from the fungal genome. In contrast, the coding sequence for *FgSSP21* and *FgSSP34* exhibits a high number of SNPs. The majority of SNPs found in *FgSSP21* localise to the central region of the coding sequence from 0.5kb-1kb while SNPs in *FgSSP34* are found throughout. FgSSP21 is a paralogue of another FgSSP candidate, FgSSP24. FgSSP24, however, is 100% conserved within the pangenome. Like FgSSP21 and FgSSP24, several other FgSSP candidates have paralogues. This is an interesting observation considering that the *F. graminearum* genome has a repeated-induced mutation (RIP) mechanism which serves to remove duplicated sequences (Cuomo et al. 2007). As a result, there is very little evidence of gene duplication within the *F. graminearum* genome. The observation that such a large proportion of candidate FgSSPs have paralogues may indicate that 1) the RIP mechanism is less effective on smaller sequences 2) these FgSSPs have recently evolved and the RIP mechanism has not yet eliminated the paralogues.

Of the twenty-four selected FgSSPs, just three can be considered specific to the *Fusarium* genus – FgSSP31, FgSSP32 and FgSSP33 (Table 3.4). FgSSP32 has no homologues outside of the FGSC and there are no homologues in the closely related *F. venenatum*. Species-specificity of effectors is thought to indicate late evolutionary origin and to facilitate disease on specific hosts (Stergiopoulos et al. 2010). FgSSP31, FgSSP32 and FgSSP33 are therefore particularly promising candidates for characterisation. Another interesting observation is that just two of the selected

FgSSPs belong to the secreted gene clusters identified by Brown, Antoniw, and Hammond-Kosack (2012). These clusters were not found to demonstrate any clear conservation in function and did not represent any gene duplication events. The contribution of these clusters to pathogenicity therefore remains unclear.

In the bioinformatic analysis described in figure 3.2, a large proportion of *FgSSPs* were found to be differentially expressed in *ΔTri6* and *ΔTri10* mutants *in planta* when compared to the wildtype PH-1 (Table 3.5)(Seong et al. 2009a). *Tri6* and *Tri10* are both transcription factors that regulate the *Tri5* biosynthetic cluster and deletion of these genes leads to both severe impairment in pathogenicity and DON production (Seong et al. 2009b). The entire repertoire of genes in the regulatory remit of these transcription factors is unknown, however, both are known to regulate genes outside of the *Tri5* cluster that are related to housekeeping functions, secondary metabolism and pathogenesis (Seong et al. 2009a). The observation that *FgSSPs* are differentially expressed in these mutants during the *F. graminearum*-wheat interaction leads us to question two points: 1) are these *FgSSPs* under the regulatory control of these transcription factors and 2) when DON is removed from the pathosystem, does the fungus compensate for the loss of this virulence factor by up-regulating the genes controlling other virulence mechanisms? Metabolic profiling of rachis internodes from wheat ears inoculated with PH-1 and *ΔTri5* revealed extensive metabolic rearrangements mainly affecting metabolites for general stress perception and signalling (Bonnighausen et al. 2019). Transcriptomic analysis of wheat subject to the same experimental set-up could help to reveal how *F. graminearum* effectors respond to the loss of DON to the pathosystem.

In the second part of this chapter, I aimed to validate the Affymetrix microarray expression profiles of bioinformatically-selected *FgSSPs* by RT-qPCR. As the

second biological replicate of the experiment showed a large amount of variability in terms of both FHB disease symptoms, and consequently *FgActin* expression, this replicate was removed from the analyses. *FgActin* expression in the other two replicates used in this study followed the same profile as found in previous studies whereby expression decreased in rachis tissue sequentially excised below the point of inoculation. As generation of the material for this study was extremely time-consuming, this experiment was not repeated and the RT-qPCR analyses relied on two biological replicates alone. For the most part, the RT-qPCR analysis validated the gene expression data obtained from the Affymetrix microarray data – however, due to the low number of replicates, *FgSSP* expression did not significantly differ between the phases of *Fusarium* infection. Overall, the RT-qPCR data confirms the appropriateness of using Affymetrix microarray transcriptome data as a basis for bioinformatic selection of candidate effectors.

In summary, interrogation of various transcriptomic datasets and further in-depth bioinformatic analysis of putative effectors enabled the identification of several promising FgSSP candidates. Efforts to prioritise candidates enabled targeted identification of proteins most likely to influence the *F. graminearum*-wheat interaction which will be subsequently characterised using the BSMV-VOX functional genomics system. Discovery of effectors that contribute towards pathogenicity can help to control FHB in a number of ways, namely through the development of novel chemistries that could target these required effectors or through the identification of wheat germplasm which recognises these effectors and triggers defensive responses.

Chapter 4 Analysis of the contribution of *F. graminearum* putative effectors to *F. graminearum* floral wheat infection using the Barley Stripe Mosaic Virus-mediated overexpression system

4.1 Introduction

Recent advances in transcriptomic and genomic sequencing technologies have facilitated the identification of vast numbers of genes predicted to contribute towards virulence in plant-infecting organisms – many of which are yet to be characterised. Functional characterisation of these genes requires *in planta* expression which can be achieved either by the generation of stable transformants or by transient expression of recombinant proteins. While stable transformation has the advantages of reproducibility and potential large-scale production, this technique requires great investments in terms of both time and money and is therefore unsuitable for high-throughput functional studies (Kusnadi, Nikolov, and Howard 1997). As such, the demand for transient *in planta* expression has increased; offering, in addition to flexibility and speed, the ability to express recombinant proteins in a range of host genetic backgrounds and control over timing of said expression (Scholthof, Scholthof, and Jackson 1996). Transient expression therefore proffers an appealing and cost-effective alternative to stable transformation and, as a result, has emerged as an attractive platform for *in planta* biopharmaceutical production (Komarova et al. 2010).

Transient expression can be achieved in several ways, including by the biolistic delivery of nucleic acids, by infiltration with modified *Agrobacteria* (agroinfection) and by infection with modified plant virus vectors ((Wang et al. 1988; Komori et al. 2007; Baulcombe, Chapman, and Cruz 1995). While biolistic bombardment delivers nucleic acids directly into live cells, expression is restricted to the cells that receive the

nucleic acid-coated particles. Bombardment can also lead to tissue damage rendering this technique unsuitable for effector characterisation (Canto 2016). Agroinfection, a widely used technique in dicotyledonous species, exploits the natural gene transfer mechanism utilised by *A. tumefaciens* to pass on bacterial T-DNA to plant cells from its tumour-inducing (Ti) plasmid (Barton et al. 1983). A series of 'disarmed' binary vector systems have been developed whereby T-DNA-containing vectors are readily modified to carry heterologous sequences of interest (Bevan 1984). Delivery of vectors into the host is typically achieved by flooding the intercellular space of a leaf with modified *Agrobacterium*, a process known as agroinfiltration, leading to active transference of T-DNA harbouring the gene of interest into the plant nucleus (Schob, Kunc, and Meins 1997; Kapila et al. 1997).There are, however, several drawbacks to agroinfiltration – namely that recombinant protein expression is limited to infiltrated tissues and that most monocotyledonous species are recalcitrant to the technique (Cheng et al. 2004). Both drawbacks can be overcome by the use of modified plant virus vectors – a technique which exploits the rapid replication cycles of viruses and their ability to reprogram infected cells to produce virally-encoded proteins (Siegel 1983).

In the early eighties, several discoveries and technical advances in the field of virology precipitated an explosion of research into the possibility that plant viruses could serve as expression vectors - firstly, the observation that cloned copies of viral *Cauliflower Mosaic Virus* (CaMV) DNA retain infection-capability when mechanically inoculated onto plants (Howell, Walker, and Dudley 1980). Attempts to develop an expression vector based on CaMV (*Caulimovirus* genus) were, however, hampered by the complex replication mechanism of this double-stranded (ds) DNA virus that ultimately led to the rapid loss of heterologous sequence insertions (Pfeiffer and

Hohn 1983). As a result, attention quickly turned to the development of single-stranded (ss) + RNA virus vectors, such as Brome Mosaic Virus (BMV) from the *Bromovirus* genus – developments facilitated by *in vitro* transcription systems enabling the synthesis of infectious cDNA clones from RNA viruses (Ahlquist et al. 1984). Delivery of viral DNA was initially achieved by rub-inoculating infectious transcripts onto host plants – an inefficient process restricting the development of vectors to those that were mechanically transmissible (Peyret and Lomonossoff 2015). This method was superseded by the delivery of viral genome sequences by agroinfection, whereby infection of the host with *Agrobacteria* enabled systemic spread of the virus vector (Grimsley et al. 1986).

The majority of work on plant virus vectors has focused on ssRNA viruses, such as *Potato Virus X* (PVX; Genus *Potexvirus*) and *Tobacco Mosaic Virus* (TMV; Genus*Tobamovirus*), many of which can be manipulated to allow both virus-mediated over expression (VOX) and virus-induced gene silencing (VIGS) in dicotyledonous species (Chapman, Kavanagh, and Baulcombe 1992; Donson et al. 1991; Palmer and Rybicki 2001). In contrast to the developments seen in dicotyledonous-infecting virus vectors, there was a paucity of research focusing on the development of virus-based expression vectors for monocotyledonous species prior to 2001.

The most widely used virus for both VIGS and VOX studies in monocots is the *Barley Stripe Mosaic Virus (*BSMV*)* – a member of the *Hordeivirus* genus which infects many agriculturally important crops including wheat, barley and oats, reviewed by Lee, Hammond-Kosack, and Kanyuka (2012). BSMV has a tripartite (+) sense RNA genome comprised of RNA α, β and γ strands as shown in figure 1.4.The first successful demonstrations of the BSMV-VOX system involved

expression of green fluorescent protein (GFP)(~700bp) as either a fusion to the N-terminus of a βb triple gene block protein (TGB_1) or as a C-terminal fusion of the γb coat protein – the latter driving higher levels of protein expression (Lawrence and Jackson 2001). These first experiments utilised BSMV to explore cell-to-cell movement and phloem unloading in barley but also revealed, however, the major caveat of the BSMV-VOX system. In initial BSMV-VOX studies, GFP expression was reported to be patchy in systemically-infected tissues (Lawrence and Jackson 2001; Haupt et al. 2001). Whilst initially hypothesised that this was due to BSMV exiting the vasculature, fragment size is now generally acknowledged to be correlated with vector instability, with inserts greater than 160 amino acids (aa) known to impair stability of the BSMV genome (Lawrence and Jackson 2001; Bruun-Rasmussen et al. 2007).

Since these initial studies, the BSMV vector system has been further refined, firstly through the insertion of a synthetic autoproteolytic 2A peptide sequence from picornaviruses at the 3' terminus of the γb protein (El Amrani et al. 2004; Pogue and Holzberg 2012). As direct heterologous protein fusions to γb are expected to compromise functionality and localisation, this system allows co-translational self-processing resulting in release of the free heterologous protein (Lee, Hammond-Kosack, and Kanyuka 2012). Cleavage of the 2A peptide, however, is rarely complete (Bouton et al. 2018). Recently, a new four-component BSMV vector was developed which overcomes, not only this, but also the limitation of low cargo capacity exhibited by the three-component BSMV system (Cheuk and Houde 2018). In this vector, the γ genome was modified to produce γ_1 and γ_2 genomes with insertion sites placed downstream of γa and upstream of γb, respectively. Both insertion sites lie downstream of the sub-genomic promoters thereby obviating the

need for the self-cleaving 2A peptide as heterologous proteins are not expressed as fusions in this system. This new vector has been used to express proteins as large as 700 amino acids, allowing for coexpression of two different fluorescent marker proteins.

While the majority of attention has focused on BSMV as a protein expression tool for cereals, the *Wheat Streak Mosaic Virus* (WSMV), *Triticum Mosaic Virus* (TriMV) and, more recently, the *Foxtail Mosaic Virus* (FoMV) have all been developed for use as monocotyledonous expression vectors over the past ten years (Table 4.1)(Tatineni et al. 2011; Tatineni et al. 2015; Bouton et al. 2018). While WSMV and TriMV-based vectors have both been used to stably express GFP, wider uptake of these VOX viruses has been hampered by the low-throughput transcript inoculation method and by the severity of symptoms induced by both viruses. Similarly, BSMV induces moderate chlorotic symptoms in wheat and barley which can obscure the evaluation of fungal genes in disease studies (Buhrow, Clark, and Loewen 2016). FoMV, on the other hand, induces much milder systems than the aforementioned viruses and, as a monopartite virus, viral inoculations are more high-throughput. Recent improvements to the FoMV vector have enabled systemic expression of proteins as large as 600 amino acids in wheat and maize tissues, establishing this virus as a promising new tool for monocotyledonous functional genomics (Bouton et al. 2018).

The typical inoculation method for both BSMV and FoMV is the leaf abrasion method – whereby agroinfiltrated *N. benthamiana* sap is used as a source of viral inoculum and rub-inoculated onto host leaves. Recently, a new seed imbibition protocol for BSMV inoculation of cereals was developed which is reported to result in improved expression stability in different tissue types, with expression being transmissible to the next generation (Cheuk and Houde 2017). While the BSMV-VOX system has

been used to functionally characterise several fungal effector proteins, such as the *Pyrenophora tritici-repentis* effector ToxA effector, improvements in both the inoculation methods and vector could now result in increased uptake of the BSMV-VOX system (Tai et al. 2007; Xu et al. 2015; Franco-Orozco et al. 2017).

The aim of this chapter was to use the BSMV-VOX system to express putative *F. graminearum* small secreted effectors in wheat to assess the contribution of said proteins towards fungal virulence. In previous studies, BSMV-VOX has proven to be a useful screening tool for effector function – particularly for the identification of proteins which, while not being essential to virulence, contribute towards pathogenicity and severity of infection.

Table 4.1 Comparison of VOX vectors for expression in monocotyledonous species.

Virus Spp.	***Barley Stripe Mosaic Virus* (BSMV)**	***Foxtail Mosaic Virus* (FoMV)**	***Wheat Streak Mosaic Virus* (WSMV)**	***Triticum Mosaic Virus* (TriMV)**
Genus	Hordeivirus	Potexvirus	Poaecevirus	Tritimovirus
Genome	Tripartite ss (+) RNA	Tripartite ss (+) RNA	Monopartite ss (+) RNA	Monopartite ss (+) RNA
Cereal hosts for VOX	Wheat Barley Maize Oat Brachypodium	Wheat Maize Switchgrass Barley Oat Foxtail grass	Wheat Oat Maize Barley Rye	Wheat
Tissue type/ Seed transmission	Floral Leaf Root (Seed with the 4-component system)	Leaf	Leaf Stem Floral Roots	Leaf Stem Crown
Maximum insert size (aa)	Typically 160 with the 3-component system and up to 700 with the new 4-component system	600	700	700
Symptom severity	Moderate	Mild	Moderate to severe	Moderate
Resistance to the virus within host cultivars?	*Bsr1 R* gene in *B. distachyon.* Modjo *R gene* in *Barley.* *Rsm1* recessive *R* gene in Barley. *Rsm1Mx R* gene in barley.	None characterised.	*Wsm1 in Thinopyrum intermedium,* wheat and maize. *Wsm2* dominant *R* gene in wheat and maize. *Wsm3* in maize and *T. intermedium.*	*Wsm1* in *Thinopyrum intermedium.*
Expressed as a fusion protein?	Yes in 3-component system / No in 4-component system	No	Yes	Yes
Inoculation method	Leaf abrasion method with virus-infected *N. benthamiana* sap	Leaf abrasion method with virus-infected *N. benthamiana* sap	Rub inoculation with in vitro transcripts	Rub inoculation with in vitro transcripts
References	1,2,3,4,& 5	6 & 7	8, 9, 10 & 11	9 & 13

[1] Cheuk and Houde (2018); [2] Cui et al. (2012); [3] Sisler and Timian (1956); [4] Timian and Franckowiak (1987); [5] Edwards and Steffenson (1996); [6] Liu, Xie, et al. (2016); [7] Bouton et al. (2018); [8] Tatineni, Kovacs, and French (2014); [9] Friebe et al. (2009); [10] Haley et al. (2002);[11] Mcmullen et al. (1994); [12] Tatineni et al. (2015).

4.2 Materials and methods

4.2.1 Plant growth conditions

N. benthamiana plants were grown for the preparation of BSMV-VOX sap inoculum. Plants were grown for four weeks in a controlled environment chamber at 23°C (light) and 18°C (dark) with a 16h photoperiod at 60% RH. The susceptible wheat (*Triticum aestivum*) cv. Bobwhite was used as the host plant throughout BSMV-VOX experiments. Seeds were pre-germinated overnight by soaking in water and sown in Rothamsted soil mix and grown in a controlled environment chamber at 22°C (light) and 18°C (dark) with a 16h photoperiod (approximately 140µmol m^{-2} per second of light) at 60% relative humidity. During stem elongation, approximately four weeks after sowing, phosphate fertiliser was applied to wheat plants.

4.2.2 Preparation of BSMV-VOX constructs

The BSMV-VOX system is comprised of three T-DNA binary plasmids: pCaBS-α, pCaBS-β and pCassRZ-γb-2A-LIC (Figure S1). cDNA was generated via RT-PCR from *F. graminearum*-infected wheat (cv. Bobwhite) ear tissue seven-days post inoculation. cDNA clones of the selected *FgSSPs* of interest were cloned from cDNA by PCR using the primers listed in table 2.1 (Chapter 2). Adaptor sequences were incorporated at the 5' and 3' ends of the effector gene sequences for subsequent cloning into the pCassRZ-γb-2A-LIC vector via ligation-independent cloning (LIC). The BSMV plasmid derivatives, pCaBS-α, pCaBS-β and pCassRZ-γb-2A-LIC, were separately transformed into the *A. tumefaciens* strain GV3101 via electroporation. A control sequence was transformed into the pCassRZ-γb-2A-LIC plasmid derived from a multiple cloning site, MCS4D, from the plasmid pBlueScriptK. After electroporation, transformed cells were grown in 3ml of LB Lennox at 28°C for two hours and then plated onto LB Lennox agar plates containing 50µg/ml of kanamycin and 25µg/ml of gentamycin. Single colonies of transformed *Agrobacterium* were then selected and stored as glycerol stocks at -80°C.

4.2.3 Viral inoculation of *Nicotiana benthamiana*

Modified *Agrobacterium* strains were grown in LB Lennox broth containing 50µg/ml of kanamycin and 25µg/ml of gentamycin for two days at 28°C with constant shaking (250RPM). Bacterial cells were pelleted at 4000x*g* for 15 minutes at 4°C and then resuspended in agroinfiltration buffer to an optical density (600nm) of 1.5. *Agrobacteria* containing the pCaBS-α, pCaBS-β and the appropriate pCassRZ-γb-2A-LIC derivative were mixed to a 1:1:1 ratio

and incubated for 3h at room temperature. *Agrobacteria* with then infiltrated into the abaxial side of the leaves of four-week old *N. benthamiana* leaves with a 1ml needleless syringe. Infiltrated leaves were harvested and snap-frozen in liquid nitrogen four days post agroinfiltration and stored for up to 3 months at -80°C.

4.2.4 Viral inoculation of wheat

Agroinfiltrated *N. benthamiana* leaves, harvested four days post inoculation, were ground in a pestle and mortar with sodium phosphate buffer (0.5mM Na_2HPO_4, 0.5mM NaH_2PO_4, pH 6.8) to obtain sap as a source of viral inoculum for wheat. A 1.5ml aliquot of sodium phosphate buffer was added to 1g of *N. benthamiana* tissue and approximately 3g of *N. benthamiana* tissue was used to inoculate 15 wheat plants. Viral inoculation was carried out at flag leaf emergence approximately 42-days post sowing. The flag leaf and second fully expanded leaves were dusted with carborundum to mechanically wound leaves for viral inoculation. The virus-containing sap was then rub inoculated onto the flag leaf of the primary tiller and the second fully expanded leaf. After inoculation, plants were placed away from light to recover overnight. Viral symptoms, namely pale wheat ear and leaf stripes, appear approximately 7-8 days after viral inoculation. A total of seven BSMV-VOX experiments were carried out between the years of 2016-2019.

4.2.5 Inoculation of wheat ears with *F. graminearum*

At anthesis, approximately 52-55 days after sowing, wheat ears were infected with *F. graminearum* PH-1 as described in chapter 2.3. Disease progress was recorded every three days until the total ear was infected. As BSMV infection can obscure FHB symptoms, bent awns (as shown in figure

4.3) was used as an additional metric to identify *F. graminearum*-infected spikelets.

4.2.7 Detection of viral transcripts in virally infected wheat ears

Prior to *F. graminearum* infection, the top two spikelets of virus-infected wheat ears were snap frozen in liquid nitrogen and stored at -80°C. Spikelet tissue was ground in a pestle and mortar and RNA was extracted with Trizol (Invitrogen) as per the manufacturer's instructions. A 1µg aliquot of RNA was DNase treated with RQ1 DNase (Promega) and cDNA was subsequently synthesised using MultiScribe Reverse Transcriptase® (ThermoFisher Scientific). The primers used to generate the modified pCassRZ-γb-2A-LIC constructs were used to amplify *FgSSP* gene transcripts by PCR (Table 4.2).

4.2.8 Double Antibody Sandwich Enzyme-Linked Immunosorbent Assay (DAS-ELISA) for determining BSMV titre in virus-infected wheat

The viral titre of BSMV in wheat ears was determined using DAS-ELISA. The IgG capture antibody (DSMZ) was diluted (1:1000) in coating buffer (4mM Na_2CO_3, 9mM $NaHCO_3$, 0.75 NaN_3, pH9.6) and coated onto 96-well immunosorbent plates (Merck) for two hours at 37°C. Plates were than washed with PBS-Tween (PBST) buffer three times before wheat sap samples were added to each well. Plates were then incubated overnight at 4°C before another round of washing with PBST. The conjugate IgG-AP antibody was diluted in conjugation buffer (1:1000) and added to the test wells and incubated for two hours at 37°C. Plates were again washed with PBST before the addition of pNitrophenyl phosphate substrate (Merck) and subsequent incubation at room temperature for a maximum of one hour. Thereaction was stopped by the addition of sodium hydroxide (0.75M) to test

wells and plates were analysed using the Varioskan Flash spectral scanning reader (ThermoScientific). The results of the DAS-ELISA were statistically analysed using a student's t-test whereby results were deemed significant at $P<0.05$.

4.2.9 Statistical analysis of BSMV-VOX experiments

The statistical software GenStat (17.1.0.13780, VSN International Ltd, Hemel Hempstead) was used for the statistical analysis of quantitative disease assessments from the BSMV-VOX experiments. For individual experiments, the proportion of spikelets showing macroscopic *F. graminearum* disease symptoms was analysed using generalised linear modelling (GLM) assuming a binomial distribution with a logit link function (Lee et al. 2014). The variate modelled was the number of diseased spikelets as a proportion of total diseased spikelets below the point of *F. graminearum* inoculation. Individual batches of plants, where batch means groups of plants inoculated at the same time, were termed as blocks in the model. Significance of the model was assessed using an approximate chi-squared test deemed significant at $P\leq0.05$. For the statistical analysis of all experimental replicates, a generalised linear mixed model (GLMM) was applied assuming a binomial distribution with logit link function (Lee et al. 2014). The random factors of the model were described by batches nested within experimental replicates. The treatment, e.g. FgSSP expressed, was designated as the fixed effect and the response variate was the proportion of diseased spikelets. To determine whether treatments were significantly different from one another, the least significant difference (LSD) was calculated.

4.3 Results

4.3.1 Overexpression of *F. graminearum* small secreted proteins in wheat using the BSMV-VOX system

Twenty-four small secreted proteins (SSPs) from the *F. graminearum* secretome were identified as putative effectors using the bioinformatic pipeline described in chapter 3. Of these twenty-four SSPs, seven were selected for functional characterisation in wheat using the BSMV-VOX system to determine whether overexpression of these fungal proteins would influence FHB symptoms. The following FgSSPs, *FgSSP22*, *FgSSP23, FgSSP24, FgSSP26, FgSSP30, FgSSP32* and *FgSSP33*, were cloned into the BSMV-VOX vector and subsequently transformed into *Agrobacterium*. Attempts were also made to clone several other FgSSPs into the BSMV-VOX vector, however, these attempts were hampered by the inability to amplify transcripts from cDNA of *F. graminearum*-infected wheat ears. To overcome this in future studies, a direct gene synthesis approach should be taken as many of these FgSSPs were promising effector candidates (Table 4.2).

Transformed *Agrobacterium* isolates, each carrying a different viral construct, were individually agroinfiltrated into well-spaced *N. benthamiana* to allow virus and virion accumulation in the host leaves, whilst at the same time preventing cross-contamination. All experiments included a no virus and a viral control (BSMV:MCS4D), the latter of which contains a non-coding multiple cloning site from the plasmid pBluescript K. Wheat ears were sampled in experiments and *FgSSP* transcripts were detected through RT-PCR as proxy for confirmation of protein production (Figure 4.4). Throughout

experiments, statistical comparisons between treatments were made against the viral control as BSMV, which induces symptoms of chlorosis in the wheat ear, is known to exacerbate *F. graminearum* infection (Buhrow, Clark, and Loewen 2016). On average 12 days post fungal inoculation (dpi), 83% of spikelets from ears expressing the viral control exhibited fungal symptoms in contrast to the no virus control ears which exhibited 55% fungal infection (Figure 4.1; Figure 4.2). From this observation, we conclude that the presence of the virus leads to significantly enhanced *F. graminearum* disease levels.

Table 4.2 Experimental fate of twenty-four candidate FgSSPs.

FgSSP	VOX[1]	Gene deletion[2]	Recombinant expression in Nicotiana[3]	Other
FgSSP14		✓		
FgSSP15				Untested
FgSSP16				Untested
FgSSP17				Unable to amplify transcript
FgSSP18				Unable to amplify transcript
FgSSP19				Untested
FgSSP20				Untested
FgSSP21				Untested
FgSSP22	✓		✓	
FgSSP23	✓		✓	
FgSSP24	✓	✓	✓	
FgSSP25				
FgSSP26	✓		✓	
FgSSP27				Untested
FgSSP28				Untested
FgSSP29				Untested
FgSSP30	✓		✓	
FgSSP31				Unable to amplify transcript
FgSSP32	✓	✓	✓	
FgSSP33	✓	✓	✓	
FgSSP34				Unable to amplify transcript
FgSSP35				Unable to amplify transcript
FgSSP36	✓			VOX construct tested in pilot study

[1] FgSSPs tested in the BSMV-VOX system, [2] Single gene deletions of *FgSSPs* generated by split-marker transformation, [3] FgSSPs recombinantly expressed in *N. benthamiana* and screened for ability to induce cell death.

The first two FgSSPs tested using BSMV-VOX were FgSSP23 and FgSSP24, both of which are predicted to be secreted during the symptomless phase of the *F. graminearum*-wheat floral interaction. Overexpression of these two proteins led to an increase in FHB disease symptoms, however, *FgSSP23* and *FgSSP24* transcripts were not detectable in virally-infected wheat ears thereby suggesting that the BSMV:FgSSP23 and BSMV:FgSSP24 vectors were unstable. This instability is most likely attributable to insert size and as such the BSMV:FgSSP23 (173 amino acids) and BSMV:FgSSP24 (161 amino acids) constructs were not further tested. In retrospect, these proteins would have been better suited to expression using the Foxtail Mosaic Virus or via heterologous transformation of *Arabidopsis* – both of which allow expression of larger proteins. *ΔFgSSP24 Fusarium* gene deletion strains were generated by split-marker transformation and phenotypically tested, however, no phenotypic or pathogenic differences were observed when compared to the wild-type. Despite this, *FgSSP24* is still an interesting candidate for further examination due to the high level of transcript expression exhibited during the symptomless phase of *Fusarium* infection. FgSSP23 is also an interesting candidate due to the presence of the Hce2 protein domain (Pfam:14846) – a domain present in the necrosis-inducing effector Ecp2 from *Cladosporium fulvum* (Stergiopoulos et al. 2010).

FgSSP22, a homologue of the well characterised PAF antifungal protein isolated from *Penicillium chrysogenum* (Binder et al. 2010), was tested in three experimental replicates. In two of the experimental replicates, overexpression of FgSSP22 led to a significant reduction in fungal disease symptoms – ultimately resulting in a reduction of 0.7 spikelets at 12dpi

across all three replicates ($p<0.05$). Due to the small margin to which fungal disease symptoms are reduced compared to the viral control, further experimentation would be required to verify the veracity and reliability of this data. As many effectors are predicted to function apoplastically, FgSSP22 was then expressed in the VOX vector lacking a signal peptide to determine whether the signal peptide was integral to the disease reduction phenotype. The BSMV:FgSSP22-SP construct was tested in just one experimental replicate and expression of mature FgSSP22 did not lead to any changes in fungal pathogenicity. FgSSP22 remains of experimental interest.

FgSSP26 and FgSSP30 were tested in experimental replicates three and five, in one of which significant differences to the viral control were observed. *FgSSP26* is one of the more highly expressed candidate effectors, known to be upregulated during the symptomless phase of *F. graminearum* infection (Chapter 3, Figure 3.12). FgSSP26 also shares protein sequence identity with a long chronological lifespan protein which is linked to apoptosis in yeast (Herker et al. 2004). *FgSSP30*, on the other hand, is most highly expressed during the onset and symptomatic phases of *Fusarium* infection in the Affymetrix dataset but most highly expressed in the symptomless phase in the RT-qPCR dataset. Orthologues of FgSSP30 are widespread amongst the *Fusaria* and FgSSP30 is just one of three identified *FgSSPs* that belong to the *F. graminearum* secreted gene cluster IX identified by Brown, Antoniw, and Hammond-Kosack (2012). In the first experimental replicate, overexpression of FgSSP26 and FgSSP30 did not lead to any changes in fungal pathogenicity but, in a second experimental replicate, overexpression of these proteins led to a significant increase in disease symptoms 12dpi.

Across two experimental replicates, ears expressing FgSSP26 exhibited a small but significant ($P<0.05$) increase in *Fusarium* symptoms whereas FgSSP30 did not (0.7 spikelets and 0.2 spikelets, respectively). These proteins were not tested any further in BSMV-VOX experiments and FgSSP26 in particular requires further study.

Figure 4.1 Wheat ears displaying BSMV symptoms after inoculation with various VOX constructs. White arrows point to lesions on the glumes caused by the virus.

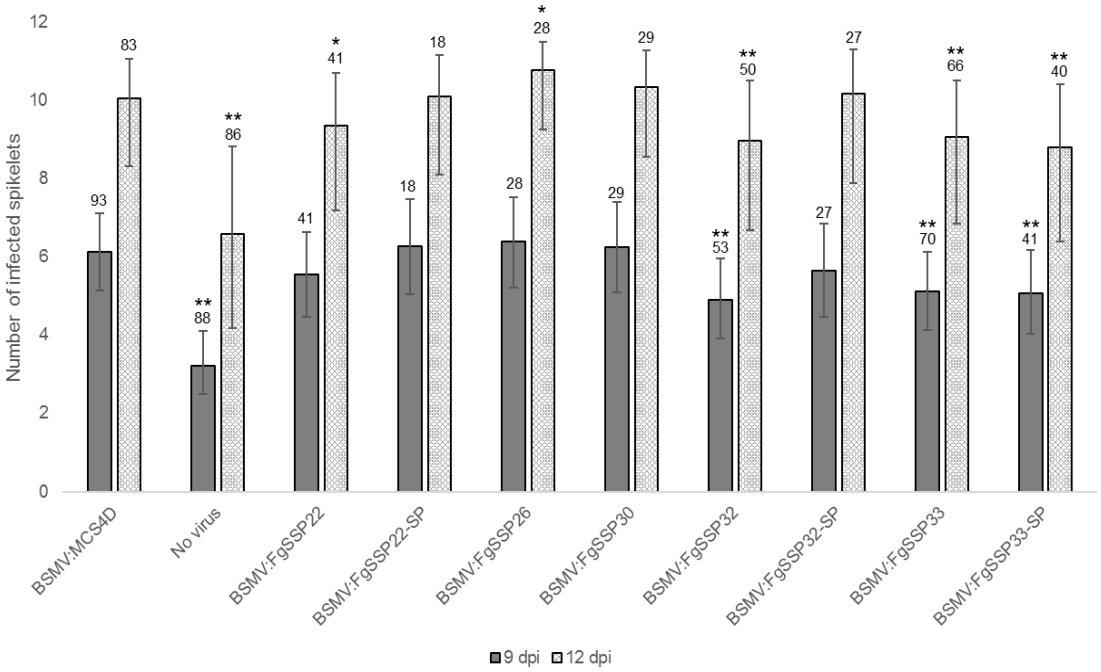

Figure 4.2 Graph representing number of visibly diseased spikelets below the point of *F. graminearum* inoculation in wheat ears at 9 and 12dpi. Numbers above bars represent the total number of wheat ears tested across seven experimental replicates. Asterix denotes treatments that are statistically different to the viral control (BSMV:MCS4D)(* = p<0.05; ** = p<0.01; GLMM analysis).

Table 4.3 List of treatments tested in BSMV-VOX experiments.

	Experiment number							Significant?
Treatment	**1**	**2**	**3**	**4**	**5**	**6**	**7**	
FgSSP22	-	-	**Tested**	-	Tested	-	**Tested**	**Yes**
FgSSP22-SP	-	-	-	-	-	-	Tested	No
FgSSP26	-	-	Tested	-	**Tested**	-	-	**Yes**
FgSSP30	-	-	Tested	-	**Tested**	-	-	No
FgSSP32	**Tested**	**Tested**	-	**Tested**	-	**Tested**	-	**Yes**
FgSSP32-SP	-	-	-	Tested	-	Tested	-	No
FgSSP33	**Tested**	**Tested**	-	**Tested**	-	**Tested**	**Tested**	**Yes**
FgSSP33-SP	-	-	-	Tested	-	**Tested**	**Tested**	**Yes**

Red represents a statistically significant reduction in fungal disease symptoms was observed and green represents a statistically significant increase in fungal disease symptoms. Significant column = significant across all biological replicates.

Figure 4.3 Representative *F. graminearum* disease symptoms on wheat ears expressing FgSSP32 and FgSSP33 +/- signal peptides (SP). Wheat ears were point inoculated with *F. graminearum* conidial suspensions ($1x10^5$spores/ml) at anthesis. The two black dots on neighbouring spikelets indicate the points of fungal inoculation. The photographs in this figure were taken 12 days post *F. graminearum* infection.

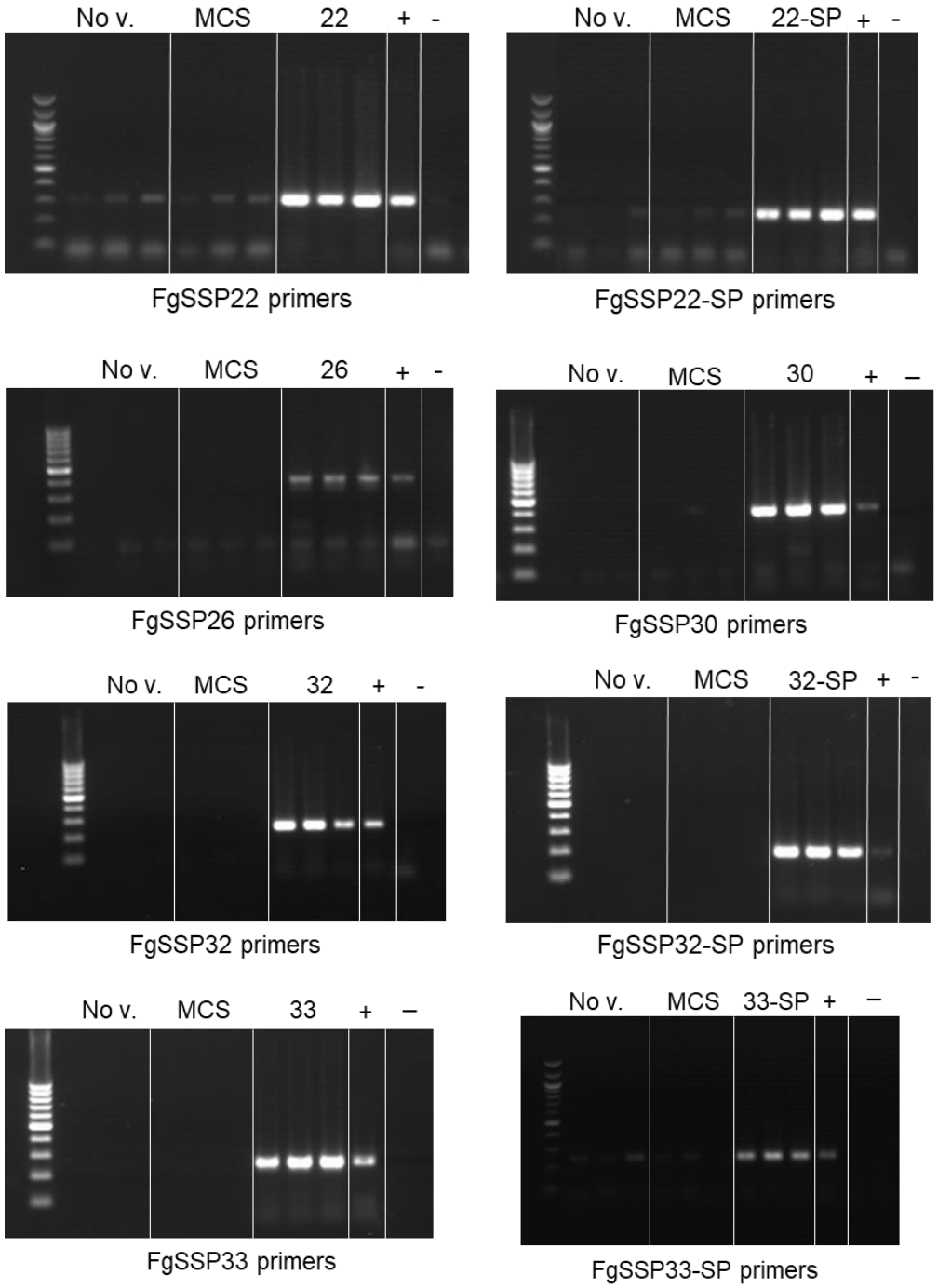

Figure 4.5 Detection of *FgSSP22, FgSSP22-SP, FgSSP26, FgSSP30 , FgSSP32, FgSSP32-SP, FgSSP33,* and *FgSSP33-SP* transcripts from the cDNA of virus-infected wheat ears. Each image depicts a gel electrophoresis gel of each *FgSSP* fragment amplified using *FgSSP* specific primers. + represents. No. v = samples taken from uninfected wheat ears and MCS = samples taken plants infected with BSMV:MCS4D viral control. *F. graminearum*-infected wheat cDNA used as a positive control and – represents the negative water control.

The experiments overexpressing two symptomatic proteins, FgSSP32 and FgSSP33, provide the most robust of the VOX datasets (three and four experimental replicates, respectively). FgSSP32 and FgSSP33 are both unannotated proteins with no sequence identity to any other characterised proteins. In addition to this, the taxonomic distribution of these proteins is restricted to the *Fusarium* genus and, within the *F. graminearum* pan-genome, these proteins are extremely well-conserved. In all experimental replicates, overexpression of full-length FgSSP32 and FgSSP33 led to a significant reduction in FHB disease symptoms. While the extent to which this reduction occurred varied between experiments, across all experiments this reduction was found to be significant and on average resulted in a reduction of 1.07 and 0.99 spikelets, respectively, when compared to the viral control 12dpi ($P<0.01$). Like FgSSP22, FgSSP32 and FgSSP33 were then expressed in the VOX vector lacking their signal peptides. In two experimental replicates, expression of mature FgSSP32 did not lead to any statistical differences in FHB disease thereby suggesting that this protein is secreted using a classical secretion pathway and functions apoplastically (Figure 4.3; Figure 4.4). Overexpression of the BSMV:FgSSP33-SP construct, however, still led to a significant reduction in fungal disease symptoms – although this was variable within experiments. In the first experimental replicate, overexpression of this construct did not lead to any changes in fungal disease symptoms initially suggesting that, like FgSSP32, FgSSP33 is secreted using a classical secretion pathway. In the following two experimental replicates however, overexpression of BSMV:FgSSP33-SP led to a significant reduction in fungal disease symptoms at 9dpi and 12dpi

(P<0.01). This might suggest either a lack of secretion or that an alternative secretion pathway may be used to achieve apoplastic localisation. Further testing is required to definitively determine protein localisation.

In early experiments, plants inoculated with the BSMV:FgSSP32 and BSMV:FgSSP33 virus were observed to exhibit particularly strong viral symptoms. To explore the levels to which each of these viral constructs accumulated in wheat ears, an ELISA was carried out on wheat ears prior to *Fusarium* inoculation. This experiment revealed that the BSMV:FgSSP32 and BSMV:FgSSP33 accumulated to a significantly higher level than the viral control (student's t-test; p<0.05)(Figure 4.5). While only one replicate of this experiment was carried out, this observation leads to further questions about the effect that the expressed protein may have on virus accumulation, particularly if said protein is hypothesised to interfere with host defences.

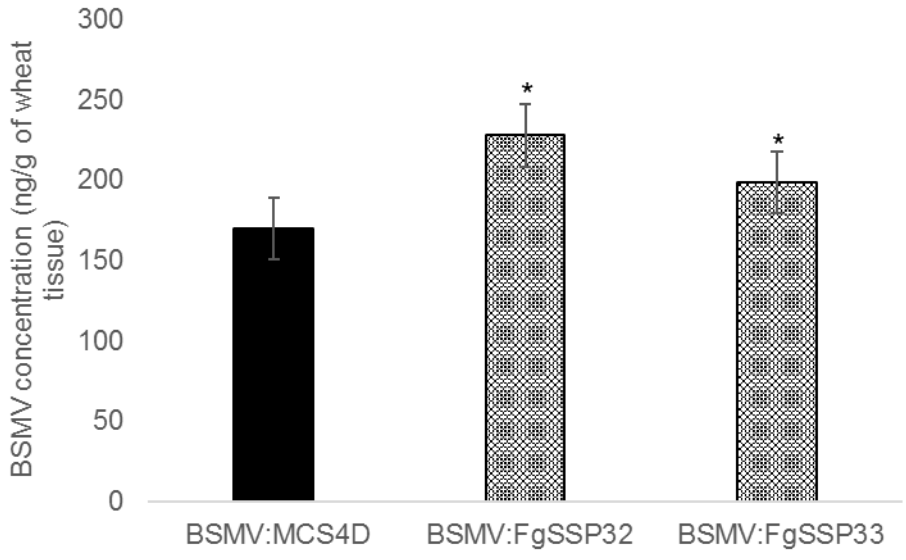

Figure 4.5 Graph showing viral titre of BSMV-infected wheat samples nine days post viral inoculation as determined by DAS-ELISA. Results were statistically analysed using a student's t-test whereby * denotes significance at p<0.05.

4.4 Discussion

In this chapter, the BSMV-VOX system was successfully used to analyse the specific contribution of putative *F. graminearum* effectors to the development of FHB in mature wheat plants. The data from this chapter suggests that the BSMV-VOX system is a particularly effective methodology for teasing out the contribution of individual proteins to virulence – especially subtler contributions that may not be apparent through the generation of single gene deletion mutants. Of the twenty-four bioinformatically-selected putative effectors, seven were tested in this study. The discrepancy between selected and tested FgSSPs is due to the labour-intensive nature of VOX experiments which require the use of category 3 facilities. Despite being undertaken in controlled conditions, VOX experiments can still be greatly affected by the time of year in which experiments are carried out thereby limiting the number of replications that could be carried out throughout my PhD.

Of the seven FgSSPs tested, overexpression of two proteins, FgSSP32 and FgSSP33, consistently led to a significant decrease in fungal disease symptoms across and within experimental replicates ($p<0.01$)(Figure 4.3; Table 4.4). The average reduction in fungal disease symptoms in both cases amounted to approximately one spikelet, although this was variable between experimental replicates. FgSSP32 and FgSSP33 are both unannotated proteins with homologues restricted to the *Fusarium* genus. While only a small number of FgSSP32 homologues exist within very closely-related species, including *F. venenatum* and *F. culmorum*, FgSSP33 exhibits greater expansion in the *Fusaria* with at least twenty known homologues (Figure 3.10). Expression of *FgSSP32* and *FgSSP33* peaks during the symptomatic

phase of the *F. graminearum*-wheat floral interaction leading us to hypothesise that these proteins contribute towards pathogenicity by the activation of host cell death. Premature expression of these proteins using BSMV-VOX may therefore pre-emptively activate host defences, alerting the host to the presence of *Fusarium* prior to fungal inoculation, ultimately leading to a reduction in disease symptoms following subsequent fungal inoculation. To explore this hypothesis further, it would be interesting to see the effect that expression of FgSSP32 and FgSSP33 has on host defence gene expression. While this experiment was considered, it is marred by several technical difficulties – namely the high level of background defence gene expression in full-grown wheat ears and the defence gene expression induced by the presence of BSMV. Alternative approaches could include delivery of modified BSMV by seed imbibition or heterologous transformation of *Arabidopsis* for the generation of stable FgSSP32 and FgSSP33 expressing lines (Cheuk and Houde 2017). Evaluation of defence gene expression by RT-qPCR would be less challenging in younger plants and expression of defence-activating proteins may lead to an observable phenotype. Furthermore, by expressing *Fusarium* proteins in younger plants, seed imbibition of BSMV inoculum could be developed into high throughput way to screen for effector function by screening proteins in the more recently developed wheat coleoptile assay (Jia, Wang, and Tang 2017).

One of the main criteria applied in the bioinformatic pipeline for effector discovery was the presence of a signal peptide predicted to target proteins to the apoplast. To determine FgSSP32 and FgSSP33 protein localisation, both proteins were expressed lacking a signal peptide (BSMV:FgSSP32-SP and

BSMV:FgSSP33-SP). Overexpression of BSMV:FgSSP32-SP did not lead to any reductions in fungal pathogenicity thereby suggesting that activity of FgSSP32 occurs in the apoplast. In contrast, overexpression of BSMV:FgSSP33-SP led to results that, while variable across biological replicates, overall led to a significant reduction in fungal disease symptoms. We therefore cannot conclude that FgSSP33 functions apoplastically, as expected. While conventional secretory pathways rely on the presence of an N-terminal signal peptide to allow selective entry into the Golgi apparatus, FgSSP33 may bypass this pathway and be secreted into the apoplast via an unconventional protein secretion (UPS) pathway (Rabouille 2017). Examples of UPS systems include organelle fusion with the plasma membrane, secretion via multi-vesicular bodies, and secretion via exosomes or intraluminal vesicles (Robinson, Ding, and Jiang 2016). To test this further, specific antibodies could be used to detect the presence of FgSSPs in the wheat apoplast. Further characterisation of FgSSP32 and FgSSP33 is described in chapters 5 and 6.

For several of the FgSSPs tested, the results from the VOX experiments were inconclusive and will require further study. Overexpression of FgSSP22 and FgSSP26 led to a significant decrease and increase in fungal disease symptoms respectively at 12dpi. BSMV:FgSSP22 was tested in three independent biological replicates with overexpression leading to a significant reduction in fungal disease symptoms in two biological replicates. FgSSP22 was also expressed lacking a signal peptide in one biological replicate and found not to affect fungal disease symptoms. FgSSP22 contains an antifungal domain, first isolated and identified from *Penicillium chrysogenum,*

known as PAF (Binder et al. 2010). PAF is one of the most well studied secreted antifungal proteins and has been shown to disrupt Ca^{2+} signalling and homeostasis, the continued disturbance of which can trigger programmed cell death (PCD), which could account for the decrease in disease symptoms. Overexpression of FgSSP26, on the other hand, led to a significant increase in fungal symptoms of 0.7 spikelets compared to the viral control – infection with which already elevates FHB disease levels when compared to the no virus control. While the increase in number of disease spikelets is small, this is an interesting result as FgSSP26 is the only symptomless protein tested in the VOX experiments. As *FgSSP26* is most highly expressed during the symptomless phase of *Fusarium* infection, we hypothesise that FgSSP26 acts as a defence-suppressing effector. It may be the case that expression of this protein in the VOX system is able to suppress host defences to a small extent thereby allowing *Fusarium* to progress down the wheat ear faster than in non-immunocompromised ears. As this phenotype was only observed in one biological replicate, FgSSP26 will require further study to verify its contribution to FHB development. It would also be interesting to co-express this protein with a cell necrosis-inducing effector, such as the *Phytophthora infestans* effector INF1, in *Nicotiana benthamiana* to see whether FgSSP26 is able to suppress INF1-induced necrosis (Bos et al. 2006).

FgSSP30 was also tested in two experimental replicates, and while overexpression was shown to lead to an increase in fungal symptoms in one replicate, across experiments overexpression did not lead to any changes in fungal pathogenicity. *FgSSP30* is an interesting gene for characterisation

due to the fact that it lies within a predicted *F. graminearum* 5.5kb gene cluster of nine members, five of which are predicted to be secreted (Brown, Antoniw, and Hammond-Kosack 2012). In the Affymetrix microarray dataset, expression of *FgSSP30* was found to peak during the onset and symptomatic phases of *F. graminearum* infection. Validation of this dataset by RT-qPCR, described in chapter 3, however, revealed a discrepancy in the profiles of *FgSSP30* during infection with expression of *FgSSP30* peaking during the symptomless phase. The increase in disease symptoms observed may therefore indicate that this protein is secreted during the initial biotrophic phase of *F. graminearum* infection and may therefore, like FgSSP26, act to suppress host defences. As the increase in symptoms observed only amounted to 0.2 spikelets, it is unlikely that this protein individually contributes to virulence in a meaningful way but is likely part of the general repertoire of FgSSP effectors that collectively facilitate infection.

Despite technological advances in the BSMV-VOX system, there are still several limitations affecting the viability of this system as a high through-put screen. Firstly, with the three-component BSMV vector, this system is greatly limited by low cargo capacity for heterologous sequences. Expression of FgSSP23 and FgSSP24 led to genetic instability of the vector due to their size – ratifying previous observations that the cargo limit for this vector is around 160 amino acids. Secondly, the timing of viral inoculation is critical to experiments exploring the contribution of fungal components towards infection. Adult wheat plants must be inoculated between growth stages 37 and 42 but, even within this window, the degree of virus infection can vary greatly. Inoculation at the beginning of this window can lead to a higher viral

load, symptoms of which can obscure the evaluation of FHB development; while inoculation at the end of this period can lead to shortened window for virus accumulation prior to anthesis. The level to which the virus accumulates can have a great impact on plant development, and in some instances, overexpression of FgSSP32 and FgSSP33 was observed to result in a phenotype of a bent peduncle in plants heavily infected with virus. To explore the levels to which modified BSMV was accumulating, the tops of wheat ears were sampled prior to *F. graminearum* infection. Interestingly, BSMV:FgSSP32 and BSMV:FgSSP33 were found to accumulate to a greater level in wheat ears than the virus carrying the BSMV:MCS4D construct (Figure 4.3) . While only one experimental replicate was carried out, the observation that viruses carrying different heterologous sequences differentially accumulate within the wheat ear opens up a plethora of questions in regard to the multitude of interactions occurring in the VOX experiments – particularly, what affect does expression of defence-perturbing compounds have on virus accumulation?

Finally, definitive confirmation of heterologous protein presence within the wheat ear is difficult to achieve. In these experiments, RT-PCR of the cDNA of virally-infected wheat ears prior to *Fusarium* inoculation was carried out. However, as BSMV is an RNA virus it is possible that amplification of *FgSSP* transcripts is from the virus itself and is therefore only a proxy for protein detection. While specific antibodies could be used to detect FgSSPs, this would not represent a cost-effective or high throughput method for functional characterisation. In addition, previous experiments from our laboratory have shown that detection of specific fungal proteins in BSMV-VOX experiments is

extremely difficult (Kanyuka and Lee, unpublished). This is most likely due to the low levels to which proteins are expressed and subsequent sensitivity issues with western-blotting techniques. Further study of the BSMV-VOX system is required to definitively quantify the levels to which proteins are expressed and the variables affecting protein expression.

In conclusion, we report the identification of several putative *F. graminearum* effectors using the BSMV-VOX system. Overexpression of three FgSSPs was found to reduce fungal disease symptoms and overexpression of one was found to increase symptoms. The mechanism through which these differences in pathogenicity were achieved, however, remains unknown. In later chapters, FgSSPs are further characterised, in particular FgSSP32 and FgSSP33, by screening in *Nicotiana benthamiana* and by the generation of gene deletion mutants.

Chapter 5 Screening *Fusarium graminearum* small secreted proteins for necrosis-inducing activity in *Nicotiana benthamiana*

5.1 Introduction

Nicotiana benthamiana is one of the most widely used model dicotyledonous plant species, in part due to the susceptibility of this plant to a diverse array of viruses (Goodin et al. 2008). Over the past few decades, several major technical advances have led to the adoption of *N. benthamiana* as a model species: 1) the ability to express foreign genes from a plant virus vector, 2) the development of virus-induced gene silencing (VIGS) and 3) the development of *Agrobacterium*-based agroinfiltration (Goodin et al. 2008). Agroinfiltration was initially developed as a tool for the study of plant-virus interactions, however, since its conception the applications of agroinfiltration have vastly broadened and this method is now an extremely efficient for the transient expression of recombinant proteins (Chen et al. 2013; Grimsley et al. 1986). Many well-established effectoromics pipelines screen putative effectors for cell death-promoting or defence-suppressing activity in *N. benthamiana* and, beyond this, utilise this highly tractable system for subcellular localisation of fluorescently-tagged effectors (Figure 5.1)(Caillaud et al. 2012; Petre, Saunders, et al. 2016; Marsian and Lomonossoff 2016).

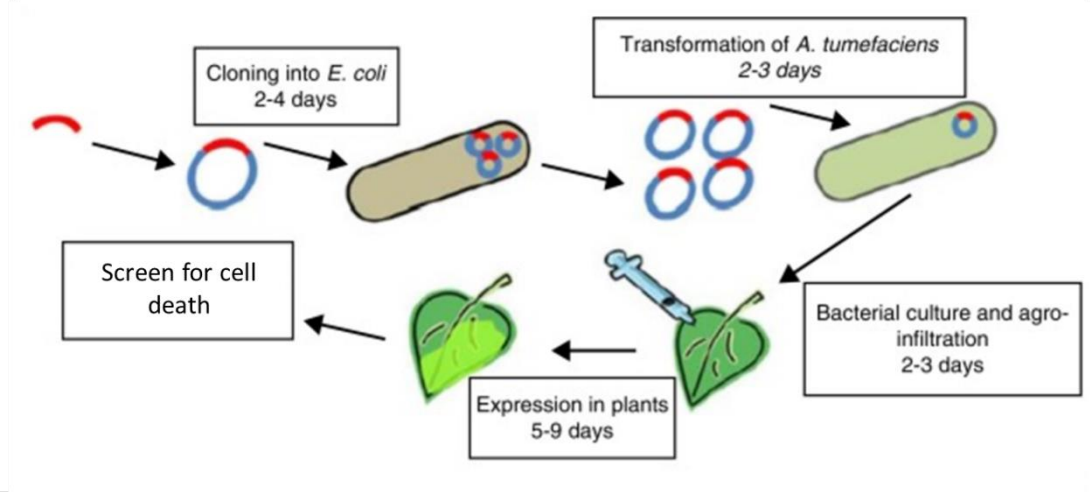

Figure 5.1 Schematic description of transient expression of recombinant effectors in *N. benthamiana* to screen for function. Adapted from Marsian and Lomonossoff (2016).

Programmed cell death lies (PCD) at the centre of the plant immune response to invaders and is essential to developmental processes such as senescence, aging, and cell differentiation (Mukhtar et al. 2016). While several morphologically distinct types of PCD have been described in animal species, the different types of PCD in plants are less easily defined and plant PCD classification remains challenging (Dickman et al. 2017). The most well-characterised form of PCD in animals is apoptosis – a tightly controlled process defined by cell shrinkage, nuclear condensation and fragmentation and break-up of the cell into 'apoptotic bodies' which are subsequently engulfed by phagocytes (Locato and De Gara 2018). While the strict definition of apoptosis centres on the formation of these apoptotic bodies, a phenomenon absent in the plant immune response, several other hallmarks of apoptosis are observed during 'apoptosis-like' PCD (Fukuda 2000).

A specialised and plant-specific form of PCD is the hypersensitive response (HR) - characterised by rapid collapse of living tissues localised to the site of pathogen infection. The HR was first observed at the turn of the 20th century when plant pathologists observed variable responses towards various *Puccinia* rust species in wheat (Ward 1902; Gibson 1904). While variation exists within the HR phenotype, common features of HR include response rapidity (within a few minutes), cytoplasmic clumping and vesiculation, and the reinforcement of cell walls with a variety of autofluorescent phenolic compounds (Routledge et al. 2004; Chaerle et al. 2007).

The HR is commonly initiated when cytoplasmic nucleotide-binding leucine, rich repeat receptors (NLRs) directly or indirectly recognise pathogen effectors, acting to limit the spread of invading pathogens and is thereby a hall-mark of effector-triggered immunity (ETI)(Jones and Dangl 2006). Rice NLRs are now known to integrate unconventional domains into the protein architecture which can bait distinct *Magnaporthe oryzae* effectors to initiate an immune response (Varden et al. 2019). For instance, two rice immune receptor pairs, Pik-1/Pik-2 and RGA5/RGA4, use integrated heavy metal-associated domains to bind two effectors, Avr-Pik and Avr-Pia, belonging to the MAX effector protein family (de Guillen et al. 2015). The initiation of this response is dependent on the cell-surface localised receptor kinase BRI1-associated receptor kinase (BAK1)(Chinchilla et al. 2007; Heese et al. 2007). A key component of brassinosteroid signalling and flagellin recognition, BAK1 functions as a co-receptor cooperating with multiple immune receptors, such as the receptor-like kinase (RLK) SOBIR1 (suppressor of Bir-

1), at the plasma membrane or cytoplasm to modulate pathogen-triggered PCD processes (Gao et al. 2019).

As the HR functions to limit the spread of pathogen invasion, biotrophic pathogens often secrete effectors that act to inhibit the initiation of PCD. The *Cladosporium fulvum* effector Avr2, for instance, inhibits PCD by targeting host cysteine proteases (Rooney 2005). In contrast, initiation of HR is intrinsic to the lifestyle of many necrotrophic pathogens which instead hijack PCD machinery – a strategy that enables the survival of these pathogens on dead plant tissue. During necrotrophic attack, the HR is often initiated by enzymes and toxins secreted by the pathogen. An example of the latter is victorin – a toxin secreted by oat pathogen *Cochliobolus vicotriae* which inhibits glycine decarboxylase, a component of photorespiration (Navarre and Wolpert 1995). Like biotrophs, necrotrophs also secrete effectors which manipulate PCD with the aim, however, of inducing effector-triggered susceptibility (ETS). For example, *Parastagonospora nodorum* effectors induce cell death and necrosis as an outcome of their interaction with a cognate susceptibility gene (Faris et al. 2010) - e.g. the Tox1 effector interacts with Snn1, a membrane-bound wall-associated kinase (WAK), to induce cell death (Shi et al. 2016).

Known classes of fungal proteins that trigger of PCD include: the necrosis- and ethylene-inducing-like peptides (NLPs), cerato-platanins (CPs) and crinkling- and necrosis-inducing proteins (CRNs)(Azmi et al. 2018; Frias, Gonzalez, and Brito 2011; Amaro et al. 2017). Recently, Kettles et al. (2017) identified numerous apoplastic *Z. tritici* effectors with PCD-inducing activity in the non-host *N. benthamiana* – the majority of which have no predicted

function. Perception of these effectors was also shown to be dependent on the presence of the previously described BAK1 and SOBIR1 which the authors speculate may be a hallmark of recognition of apoplastic effectors.

Identification and subsequent deployment of necrotrophic effectors into breeding programmes offers a rapid method to select either qualitatively or quantitatively for resistant germplasm and to probe host germplasm for susceptibility alleles (Lorang 2019). Integration of these effector assays into breeding programmes reduces the need for infection assays and large-scale field trials ultimately saving breeders both time and money (Vleeshouwers and Oliver 2014). Prior to this study, a limited number of proteins with PCD-inducing activity, which include the cerato-platanins FgSSP6 and FgSSP7, had been identified in *F. graminearum* (Ana Machado, Thesis). In the previous chapter, I described the identification of several FgSSPs which, when overexpressed using the BSMV-VOX system, were found to contribute towards the establishment of FHB in wheat (FgSSP22, FgSSP26, FgSSP32 and FgSSP33). The aim of this chapter was therefore to further characterise these proteins through recombinant expression in *N. benthamiana* and to screen these proteins for the ability to induce PCD. While recombinant expression of effectors in *N. benthamiana* is a widely used functional screen, in this chapter we report the first instance of the use of this screen to characterise *F. graminearum* putative effectors. As two FgSSPs were found to induce PCD, a VIGS approach was undertaken to determine whether initiation of PCD was dependent on several immune signalling components previously described to be involved in effector-triggered PCD signalling.

5.2 Materials and methods

5.2.1 Gateway cloning of FgSSPs for *Agrobacterium*-mediated recombinant expression in *Nicotiana benthamiana*

FgSSPs (+/- signal peptide (SP)) were PCR-amplified from cDNA isolated from *F. graminearum*-infected wheat rachis tissue using Phusion polymerase (New England Biolabs). *AttB*-flanked PCR products were cloned into the Gateway-compatible entry vector pDONR207 (Figure S2) using BP clonase II enzyme mix (Thermo Fisher Scientific) as per the manufacturer's instructions. Sequence-verified FgSSPs were then recombined into the binary destination vector pEAQ-HT-DEST3 using the LR clonase II enzyme mix (Thermo Fisher Scientific)(Figure 5.2)(Sainsbury, Thuenemann, and Lomonossoff 2009). All constructs were cloned into chemically competent JM109 cells (Promega) and into the *Agrobacterium tumefaciens* strain GV3101 for agroinfiltration via electroporation. Constructs that were found to induce cell death in *N. benthamiana* were re-cloned into the pEAQ-HT-DEST3 vector without the native SP as determined by SignalP 4.0 (Petersen et al. 2011). For agroinfiltration, transformed *Agrobacteria* were cultured in LB Lennox broth and resuspended in agroinfiltration buffer to an OD_{600} of 1.0. Four-week old leaves of *N. benthamiana* were then infiltrated with constructs carrying FgSSPs of interest, along with the following controls: buffer only, empty vector (EV), GFP and the necrotrophic effector MgNLP(+/-SP). Seven days later, infiltrated leaves were assessed for macroscopic disease symptoms.

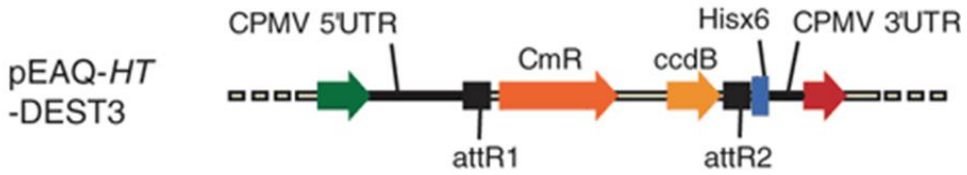

Figure 5.2 Diagrammatic representation of the pEAQ-HT-DEST3 vector. Black boxes represent *attR* GATEWAY recombination sites; green arrow represents the promoter site; orange arrow represents the chloramphenicol resistance gene; yellow arrow represents the *E. coli ccdB* lethal gene; blue box represents a C-terminal His-tag; red arrow represents the terminator sequence. Figure adapted from Sainsbury *et al* (2009).

5.2.2 Virus-induced gene silencing (VIGS) in *N. benthamiana*

All silencing constructs described were based on the *Tobacco rattle virus*-based vector PTV00 (Ratcliff, Martin-Hernandez, and Baulcombe 2001). *Agrobacterium* strains harbouring PTV00:GFP, PTV:NbBAK1, PTV:SGT1, PTV:NbSOBIR1 and PTV:PDS, provided by Paul Birch and Graeme Kettles, were cultured in LB Lennox supplemented with antibiotics overnight at 28°C (Ratcliff, Martin-Hernandez, and Baulcombe 2001; Bos et al. 2006; Heese et al. 2007; Kettles et al. 2017). Cultures were diluted with agroinfiltration buffer to an OD_{600} of 1.0 and mixed at 1:1 ratio with an *Agrobacterium* strain carrying pBINTRA6 (TRV RNA1) which promotes DNA stability. A small region of $5mm^2$ was infiltrated in the leaves of three-week old *N. benthamiana* plants using a 1ml needleless syringe and, two weeks later, upper uninoculated leaves displaying symptoms of viral infection were infiltrated with *Agrobacterium* effector-expressing strains. Leaves were evaluated for the induction of cell death seven days post infiltration.

5.2.4 Photography and multi-spectral imaging

Seven days after agroinfiltration, infiltrated leaves were photographed under white and UV light using a Nikon D80 digital camera. For the fluorescence photography, plants were illuminated with blue light (440–460 nm excitation) using a Dual Fluorescent Protein flashlight (NightSeaA). Long-pass (510 nm) or band-pass (500–555 nm) filters (Midwest Optical Systems) were mounted onto the camera objectives to block blue or blue plus red light, respectively, reflected from the excitation source (Bouton et al. 2018).

To further analyse infiltrated plants, detached leaves were imaged using the multispectral VideometerLab4 using the F3 filter and with UVA light (365nm excitation)(Videometer, Cambridge, UK). In the VIGS experiment, transformations were built to distinguish the following: 1) leaf vs. background, 2) infiltrated region vs uninfiltrated region and 3) FgSSP-induced response vs control treatments. The first two transformations were combined to mask the background and uninfiltrated leaf regions and, then, transformation 3 was used to quantify the proportion of the area exhibiting the FgSSP-induced phenotype.

5.2.5 Statistical analysis

Statistical analysis of the response induced by FgSSPs was carried out using a one way-ANOVA. All data was transformed using the logit function and differences between treatments were deemed significant at $P< 0.05$. Least significant differences were calculated at 1% and 5% thresholds to determine which treatments were statistically different from one another.

For the VIGS data, a regression analysis was carried out on logit-transformed necrosis data whereby both percentage necrosis and total leaf area were fitted as terms in the model. An accumulated ANOVA was then carried out which showed that there was a linear relationship between % necrosis and leaf area ($P=0.026$) and as such leaf area was fitted as a co-variate for further analyses. To then determine whether FgSSPs induced differential levels of necrosis compared to the EV control in the GFP, BAK1, SOBIR1 and SGT1-silenced plants, ANCOVA analysis was performed and differences between FgSSP treatments were deemed significant at $P< 0.05$. GFP, BAK1, SOBIR1 and SGT1 datasets were analysed individually as comparisons between silencing treatments was not possible due to lack of replication.

5.3 Results

5.3.1 FgSSP32 and FgSSP33 induce vascular-associated cell death in *Nicotiana benthamiana*

To further characterise the *Fusarium* proteins screened in the BSMV-VOX system, FgSSPs (FgSSP22, FgSSP26, FgSSP32 and FgSSP33) were recombinantly expressed in *N. benthamiana* and screened for cell death-inducing activity. To achieve high levels of long-lasting protein expression, FgSSPs were expressed using the pEAQ-HT-DEST3 vector – a system particularly well-suited at identifying less potent effector interactions (Kettles et al. 2017). The pEAQ-HT-DEST3 vector system utilises the Cowpea Mosaic Virus (CPMV) promoter and contains the p19 gene silencing suppressor allowing higher levels of protein expression (Peyret and Lomonossoff 2013). Several controls were tested in these experiments including a buffer control, EV control, GFP and the *Zymoseptoria tritici* effector MgNLP. MgNLP is a cytotoxic protein which belongs to the NLP family - known to induce cell necrosis when recombinantly expressed in *N. benthamiana* (Kettles et al. 2017; Qutob et al. 2006).

As agroinfiltration required mechanical wounding of the leaf tissue, small amounts of necrosis were observed around the puncture site in the controls which were not attributable to treatment (Figure 5.3). Strong GFP expression and MgNLP-induced necrosis were observed as early as 2 days post infiltration (dpi) providing evidence that the vector was driving rapid, high levels of protein expression. Leaves were then assessed for macroscopic disease symptoms under normal and UV light at seven days post agroinfiltration – the latter of which is possible due to the accumulation of

stress-induced autofluorescent compounds induced during cell necrosis (Dixon and Paiva 1995).

Recombinant expression of FgSSP26 did not lead to the appearance of any macroscopic symptoms under normal or UV light. As the gene encoding FgSSP26 is upregulated during the symptomless phase of the *F. graminearum*-wheat floral interaction, we hypothesise that this protein contributes towards virulence in a biotrophic manner and is therefore unlikely to induce PCD. Like FgSSP26, FgSSP22 did not induce PCD-symptoms. However, FgSSP22 was observed to induce small amounts of chlorosis within the leaf which correlated with the accumulation of autofluorescent compounds (Figure 5.3). Due to time constraints, this possible chlorosis was not further studied.

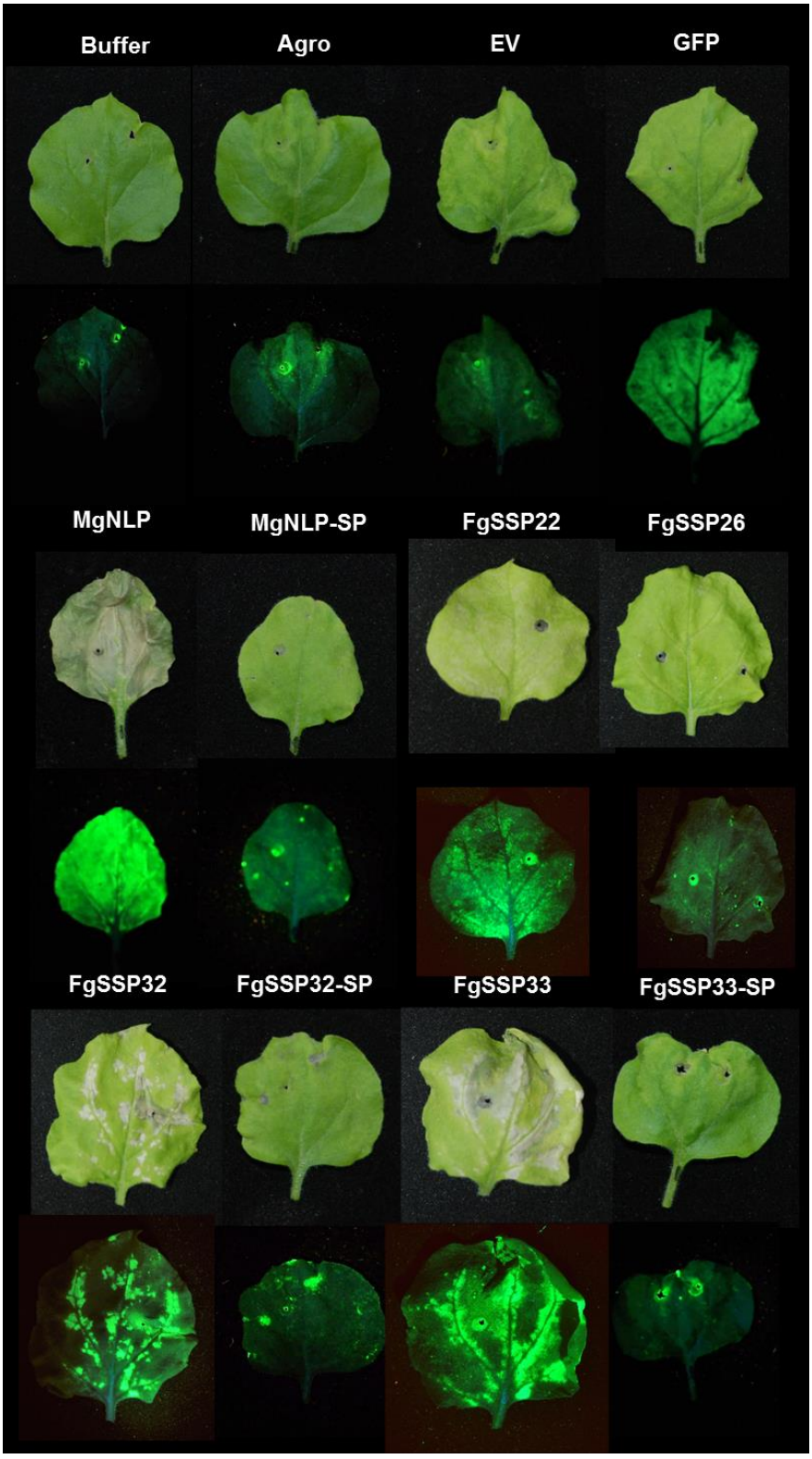

Figure 5.3 Recombinant expression of FgSSPs in *Nicotiana benthamiana* driven by the pEAQ-HT-DEST3 vector system. Photos taken seven days post infiltration and taken under white (top panel) and UV light (bottom panel). Agro = *Agrobacterium tumefaciens* infiltration only, EV = empty vector infiltrated.

Interestingly, recombinant expression of FgSSP32 or FgSSP33 led to the induction of cell necrosis which preferentially accumulated around the vasculature tissue of the leaf. The severity of symptoms varied between experiments but FgSSPP33 induced the strongest and most consistent symptoms (Figure 5.3). Macroscopic symptoms appeared as early as 3pi at the vasculature tissue, eventually spreading to surrounding tissue in leaves exhibiting higher levels of necrosis. While the symptoms induced by expression of FgSSP32 were less severe than those induced by FgSSP33, symptoms of cuticle thinning were consistently apparent on the abaxial side of infiltrated leaves (Figure 5.4). This phenotype is the beginning of the establishment of necrosis in the leaf and has been termed the ‘pre-necrosis’ phenotype throughout the rest of this study.

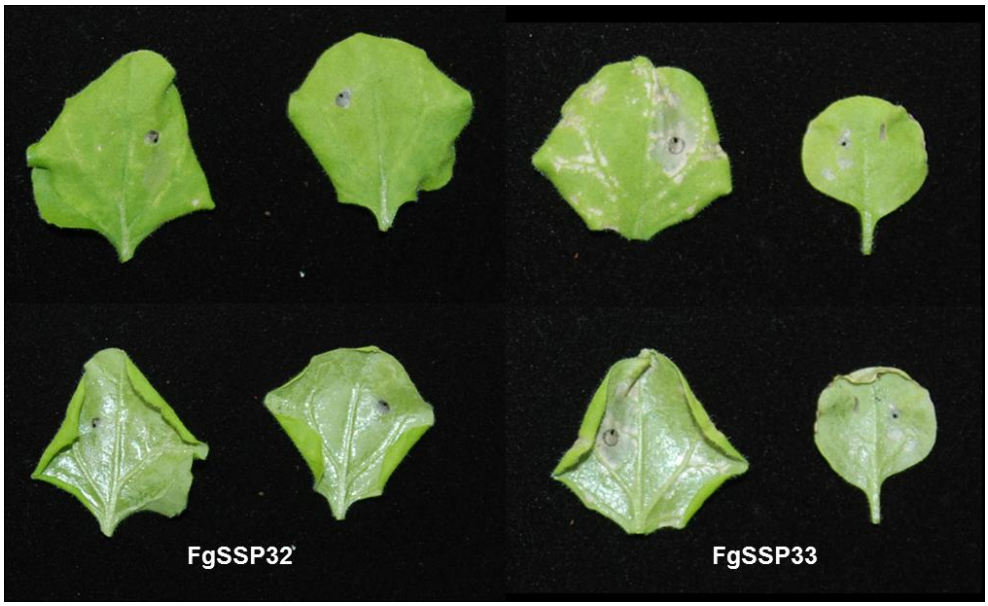

Figure 5.4 Recombinant expression of FgSSP32 and FgSSP33 leads to the induction of vascular-associated necrosis. Prior to the appearance of symptoms on the adaxial side of the lead, thinning of the waxy cuticle layer of the leaf on the abaxial side occurs.

To explore the ‘pre-necrosis’ phenotype further and quantify both the ‘necrosis’ and ‘pre-necrosis’ phenotypes, agroinfiltrated leaves expressing FgSSP32 and FgSSP33 were detached and multi-spectral images of each leaf were taken (Figure 5.5). The VideometerLab4 software was trained to recognise this response enabling quantification of both ‘pre-necrosis’ and ‘necrosis’, which in this study will be termed ‘FgSSP-induced’ symptoms given as a percentage of the total leaf area. The buffer control and EV controls induced very small amounts of FgSSP-induced symptoms (1.2% and 7.8% of the total leaf area, respectively) when compared to leaves expressing FgSSP32 and FgSSP33 which exhibited FgSSP-induced symptoms across 47.8% and 65.6% of the total leaf area (Figure 5.6).

Interestingly however, multispectral imaging also revealed a third unexpected phenotype. Around the site of infiltration, a response in the EV control was observed which we attributed to the plant response to *Agrobacterium* infection (17.8% of the total leaf area)(Figure 5.5; Figure 5.7). Unexpectedly, this response was not observed to such a strong extent in FgSSP32 and FgSSP33-infiltrated plants (2.2% and 3.2% of the total leaf area, respectively). This may suggest that FgSSP32 and FgSSP33 in some way inhibit the response induced by *Agrobacterium*.

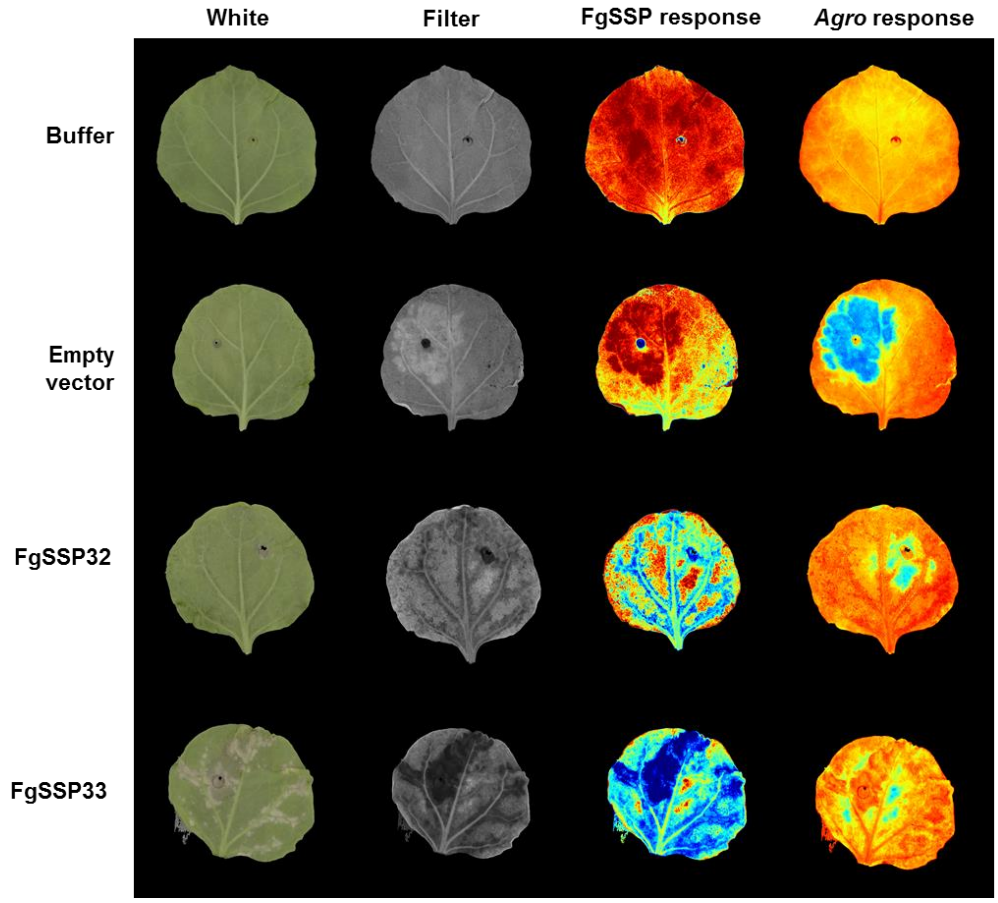

Figure 5.5 Multispectral imaging of *N. benthamiana* leaves recombinantly expressing FgSSP32 and FgSSP33. Column 1 shows images of leaves taken under white light; Column 2 shows images of leaves taken under a wavelength of 365nm with an F3 filter; Column 3 demonstrates the transformation built to recognise the FgSSP-induced response; Column 4 demonstrates the transformation built to recognise the host response to agroinfiltration. The blue pixels in columns 3 and 4 represent the host response to either expression of FgSSP32 and FgSSP33 or to *Agrobacterium* infection.

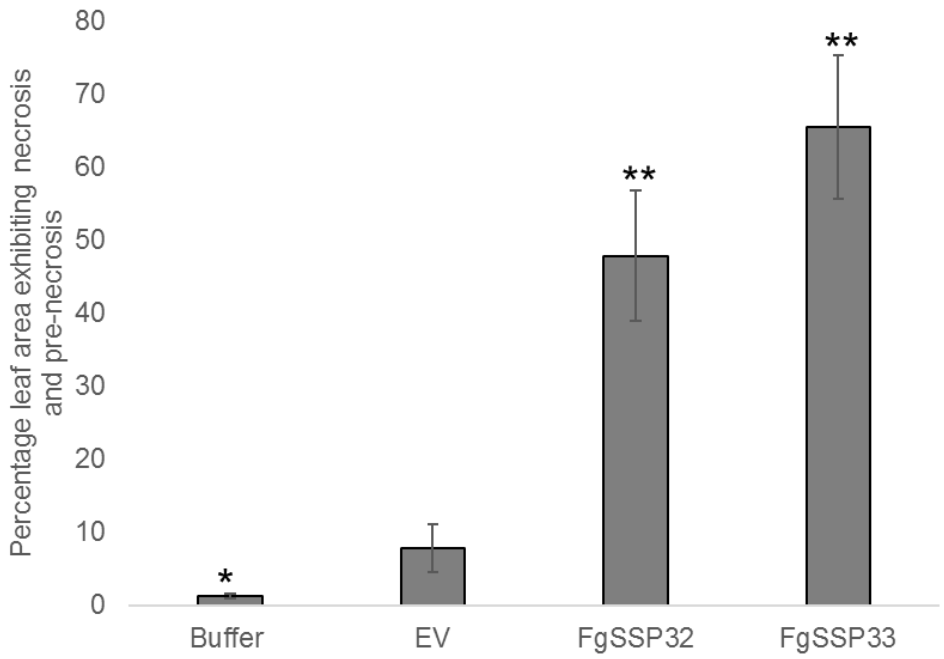

Figure 5.6 Graph showing the percentage of total leaf area exhibiting a 'necrotic' or 'pre-necrotic' response to FgSSPs. Data analysed using a one-way ANOVA on logit-transformed data. Comparisons made between treatments using LSDs on the logit scale (N=3). * denotes treatments that are significantly different from EV at P<0.05. ** denotes treatments that are significantly different from EV at P<0.01. Untransformed data is presented in this graph and error bars represent SEM.

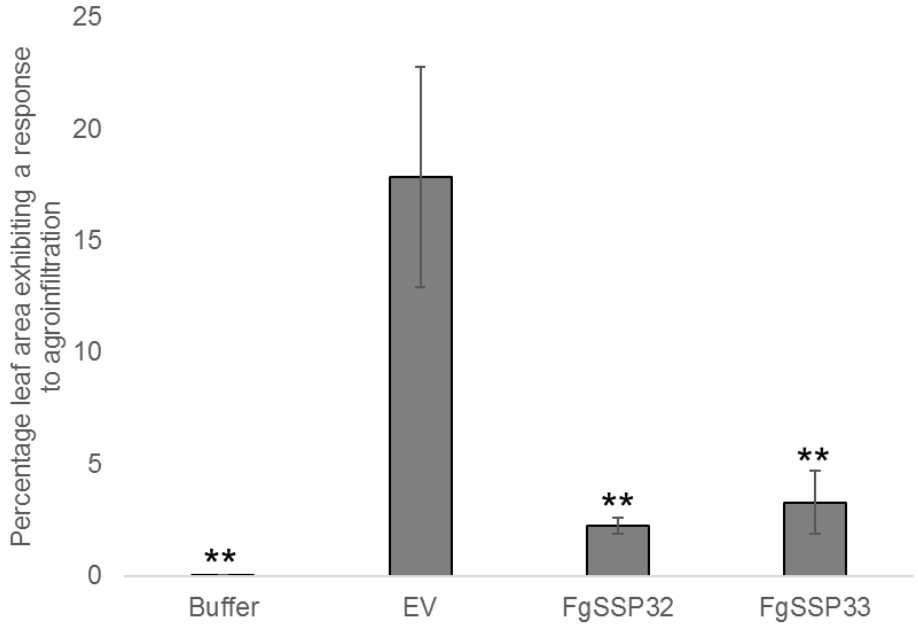

Figure 5.7 Graph showing the percentage of total leaf area exhibiting a response to *Agrobacterium* infection / agroinfection. Data analysed using a one-way ANOVA on logit-transformed data. Comparisons made between treatments using LSDs on the logit scale. ** denotes treatments that are significantly different from the EV control (P<0.01, n=3). Untransformed data is presented in this graph and error bars represent SEM.

5.3.2 FgSSP32 and FgSSP33-induced cell death is dependent on secretion into the apoplast

As FgSSP32 and FgSSP33 were both found to induce necrosis in *N. benthamiana,* both proteins were then expressed lacking a signal peptide (SP) to determine whether secretion was essential to the necrosis phenotype. Expression of the mature portions of FgSSP32 and FgSSP33 did not lead to the induction of necrosis suggesting that secretion of these proteins in the apoplast is essential to the necrosis-inducing activity observed (Figure 5.3).

5.3.3 Expression of FgSSP32 and FgSSP33 in *NbBAK1, NbSOBIR1 and NbSGT1* silenced plants shows a trend towards reduced FgSSP-induced symptoms

The presence of the signal peptide of FgSSP32 and FgSSP33 was shown to be a requirement for effector-induced cell death. To test whether localisation is important due to effector recognition in the apoplast by unknown RLKs or RLPs that interact with the known co-receptors BAK1 and SOBIR1, these genes were silenced in three-week-old *N*. *benthamiana* plants using a TRV-based silencing system. In this experiment, another important immune signalling component was also silenced - the ubiquitin-ligase associated protein SGT1 (suppressor of G2 allele of *skp1*) which is known to be required for plant cell death responses, including those involved in *R*-gene-mediated disease resistance (Azevedo et al. 2006). After two weeks, a window allotted to allow for silencing to occur, FgSSP32 and FgSSP33 were expressed in silenced plants using the pEAQ-HT-DEST3 vector system and assessed for disease symptoms.

In the previous agroinfiltration experiments described, the necrosis induced by FgSSP32 and FgSSP33 was observed in four-week-old plants. In the VIGS experiment, six-week-old pants were instead infiltrated with the pEAQ:FgSSP32 and pEAQ:FgSSP33 constructs. At this later time point, FgSSP-induced necrosis was difficult to observe under normal and UV light. To overcome this, multispectral images of silenced leaves expressing recombinant effectors were taken using the VideometerLab4. The VideometerLab4 software was trained to recognise the total leaf area and then to recognise the leaf response towards both FgSSP32 and FgSSP33.

In TRV:*GFP* control plants, the phenotypes induced by pEAQ:EV, pEAQ:FgSSP32 and pEAQ:FgSSP33 were explored and representative images of these treatments are shown in figure 5.9a. The percentage of the total leaf area of TRV:*GFP* plants exhibiting the FgSSP-induced response was 11% and 5% in plants expressing FgSSP32 and FgSSP33, respectively (Figure 5.8). The severity of symptoms induced by FgSSP32 and FgSSP33 was therefore much milder compared to those seen in younger and non-silenced plants (as shown in figure 5.5). Expression of pEAQ:EV in some TRV:*GFP* plants also induced a similar response to the plants expressing FgSSP32 and FgSSP33, although to a lesser extent (2% of the total leaf area). While the assessment of the silenced leaves was challenging, based on 1) the localisation of the response to FgSSP32 and FgSSP33 to the vasculature, 2) the similarity to the previously defined FgSSP-induced response shown in figure 5.5, and 3) the increased proportion of the leaf area exhibiting this response compared to plants expressing the EV, it is probable that the response identified is FgSSP-induced. The difference

observed between pEAQ:EV and pEAQ:FgSSP treatments was, however, not statistically significant with a P value of 0.073. As this value is close to the significance value of $P<0.05$ we can therefore say that, in plants expressing FgSSP32 and FgSSP33 in TRV:*GFP* plants, there is a trend towards increased levels of 'necrosis' when compared to the EV control.

In TRV:*GFP*, TRV:*SOBIR1* and TRV:*SGT1* plants, the symptoms induced by pEAQ:EV remained at a similar level (2% of the total leaf area). In TRV:*BAK1* plants, however, 5% of the total leaf area exhibited a response to infiltration with pEAQ:EV. This increase may be attributable to the altered morphology of *BAK1*-silenced plants which were dwarfed and crinkled compared to the TRV:*GFP* control leaves – a phenotype reported in other studies (Chakravarthy et al. 2010) – rather than by agroinfiltration with pEAQ:EV.

When FgSSP32 and FgSSP33 were expressed in *BAK1*-silenced plants, 4.1% and 4.2% of the total leaf area exhibited an FgSSP-induced response respectively thus representing a decrease from the response induced in TRV:*GFP* control plants (11% and 5% respectively) and also a reduction compared to TRV:*BAK1* plants expressing EV (5%). The reduction of FgSSP-induced necrosis observed in TRV:*BAK1* plants expressing FgSSP32 and FgSSP33 compared to EV was not significant ($P=0.142$). However, as there appears to be a reduction in the symptoms induced by FgSSP32 and FgSSP33 in TRV:*BAK1* plants compared to TRV:*GFP* it may be that FgSSP32 and FgSSP33-induced necrosis is dependent on the presence of BAK1.

In TRV:*SOBIR1* plants, the response induced by pEAQ:FgSSP32 and pEAQ:FgSSP33 follows a similar pattern as seen in TRV:*GFP.* Expression of pEAQ:FgSSP32 and pEAQ:FgSSP33 induced a response that amounted to 4% and 2.4% of the total leaf area when compared to pEAQ:EV which induced 2%. The differences between treatments in TRV:*SOBIR1* plants was not significant (P=0.508) suggesting that FgSSP32 and FgSSP33 do not induce a differential response when compared to EV. When compared to TRV:*GFP* plants, *SOBIR1*-silenced plants showed a reduction in FgSSP32 and FgSSP33 induced-symptoms (11% and 5%, respectively, in TRV:*GFP* plants). This may therefore suggest that FgSSP32 and FgSSP33 are recognised by an unknown RLK or RLP interacting with SOBIR1. Further experimentation is required to explore this possibility.

In TRV:*SGT1* plants, the response induced by pEAQ:FgSSP32 and pEAQ:FgSSP33 also showed a trend towards reduced symptoms plants (6% in plants expressing pEAQ:FgSSP32 and 2% in plants expressing pEAQ:FgSSP33). While SGT1 is known to be involved in NBS-LRR folding, SGT1 is also required for immune responses triggered by non-NLR sensors such as the tomato *R* proteins Cf4 and Cf9 (Peart et al. 2002; Shirasu and Schulze-Lefert 2003; Takahashi et al. 2003). Replication of all experiments is required to explore whether the FgSSP-induced phenotype is truly dependent on the presence of each protein.

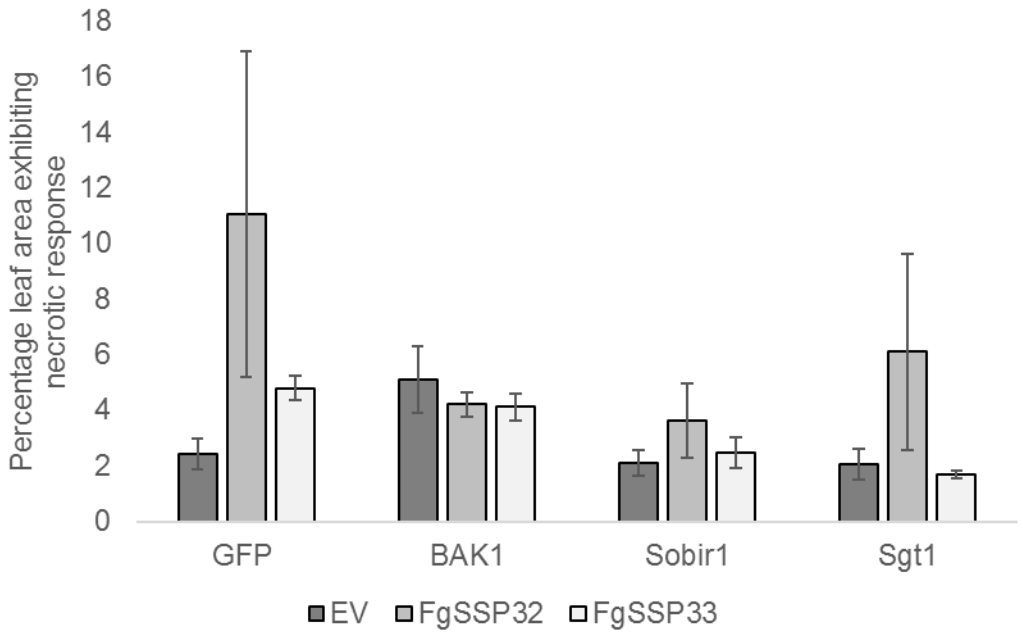

Figure 5.8 Graph showing the percentage of the total leaf area exhibiting a response to FgSSP32 and FgSSP33 in VIGS plants. Silenced plants were statistically analysed independently of each other. Data was analysed using ANCOVA analysis whereby leaf area was fitted as a co-variate and logit-transformed % necrosis was fit as the main variate. The P values for the ANCOVA analysis for each group of silenced plants, GFP, BAK1, SOBIR1 and SGT1, are 0.073, 0.142, 0.508, 0.858 respectively.

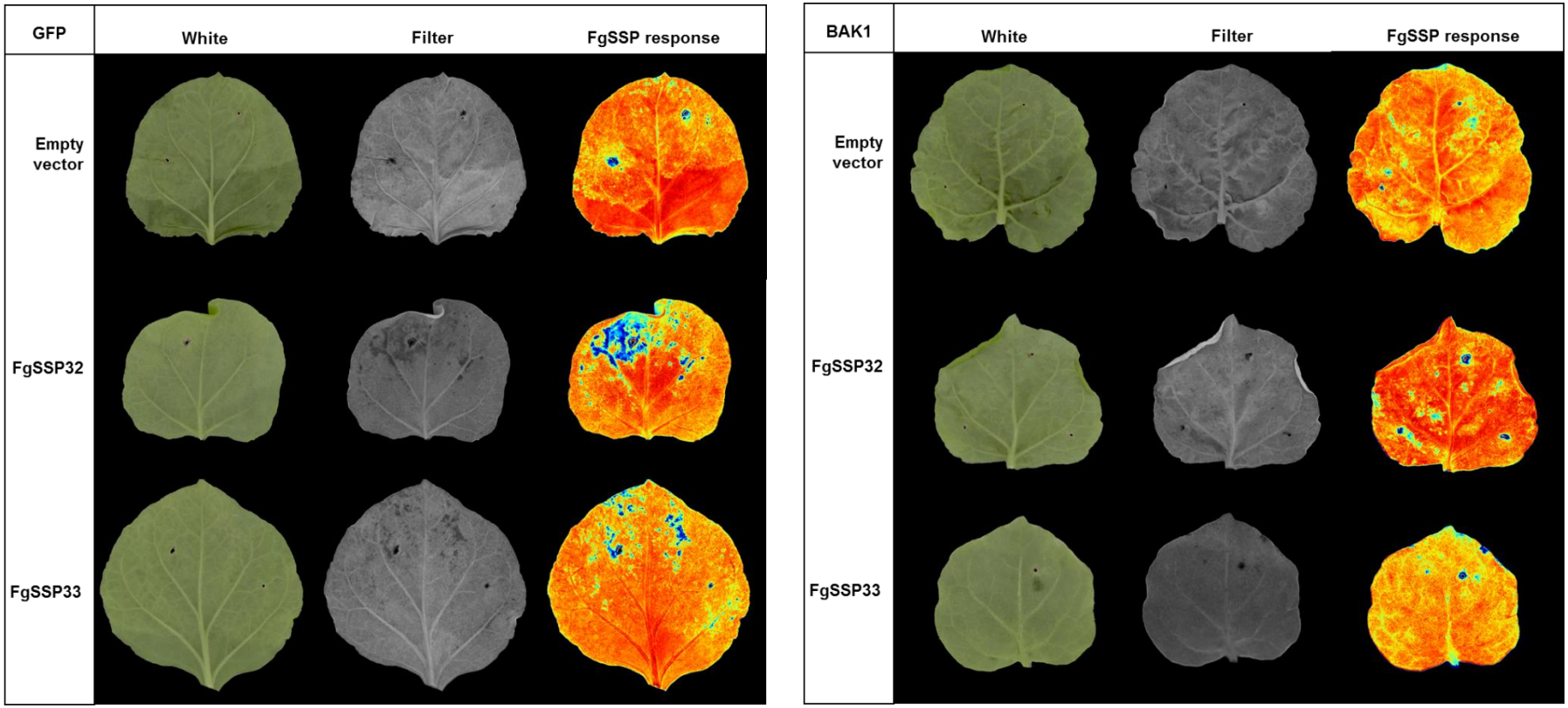

Figure 5.9a Multispectral imaging of *N. benthamiana* leaves recombinantly expressing FgSSP32 and FgSSP33 in *BAK1*-silenced plants. The *Tobacco Rattle Virus* (TRV)-based VIGS vector PTV00 derivatives were used to initiate gene silencing. TRV:*GFP* was used as a control treatment. Column 1 shows images of leaves taken under white light; Column 2 shows images of leaves taken under a wavelength of 365nm with an F3 filter; Column 3 demonstrates the transformation built to recognise the FgSSP-induced response. The blue pixels in column 3 represent the host response to either expression of FgSSP32 and FgSSP33.

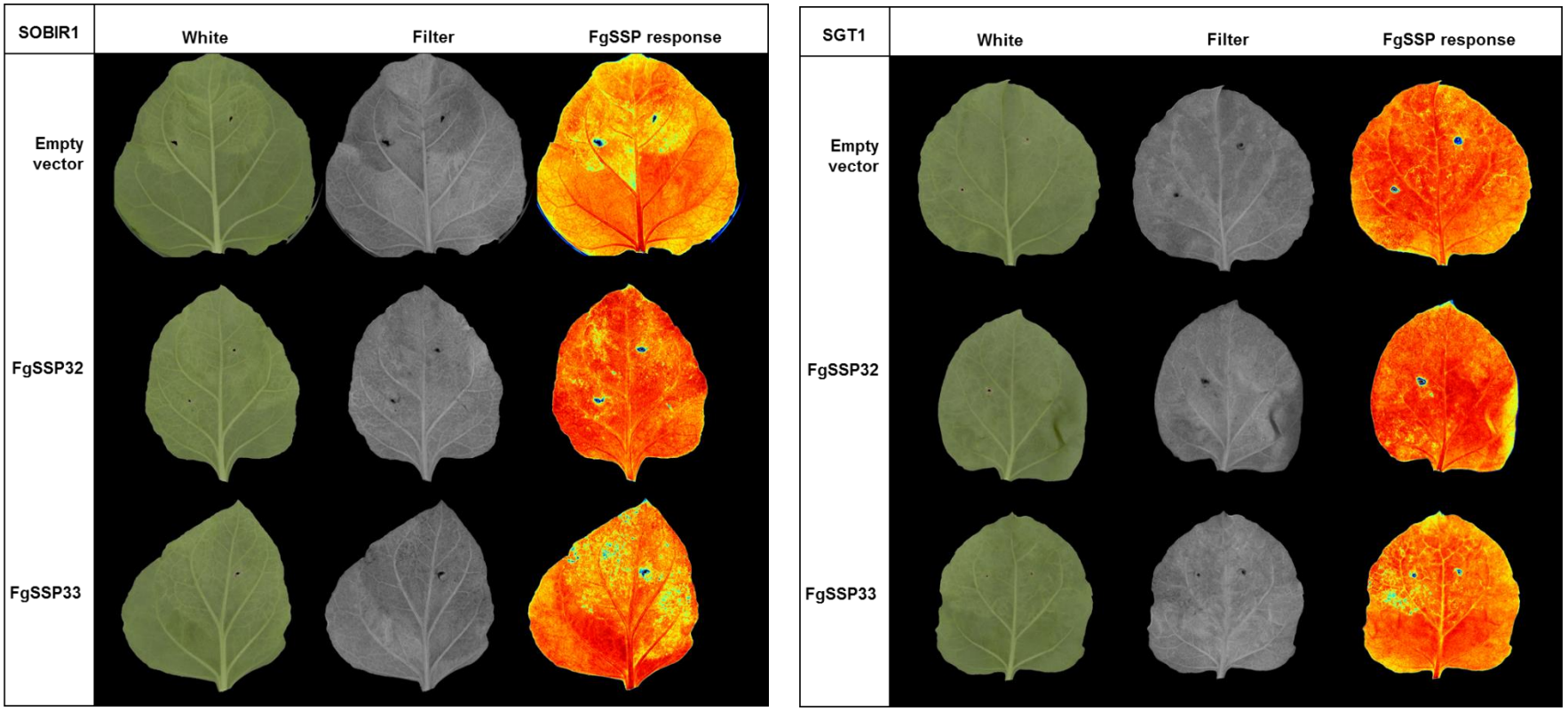

Figure 5.9b Multispectral imaging of *N. benthamiana* leaves recombinantly expressing FgSSP32 and FgSSP33 in *SOBIR1* and *SGT1*-silenced plants. The *Tobacco Rattle Virus* (TRV)-based VIGS vector PTV00 derivatives were used to initiate gene silencing. TRV:*GFP* was used as a control treatment. Column 1 shows images of leaves taken under white light; Column 2 shows images of leaves taken under a wavelength of 365nm with an F3 filter; Column 3 demonstrates the transformation built to recognise the FgSSP-induced response. The blue pixels in columns 3 represent the host response to either expression of FgSSP32 and FgSSP33.

5.4 Discussion

In the previous chapter, I described the use of BSMV-VOX as a screening tool for *F. graminearum* putative effectors which led to the identification of several proteins which contribute towards the establishment of FHB in the wheat ear. To study the contribution of these proteins towards *F. graminearum* pathogenicity further, FgSSP22, FgSSP26, FgSSP32 and FgSSP33 were screened for cell death-inducing activity in *N. benthamiana*. Recombinant expression of putative effectors in *N. benthamiana* is a widely used screen for a range of plant pathogens, however, prior to this study this screen had not been utilised for the study of *F. graminearum* effectors (Bos et al. 2010; Kettles et al. 2017; Wei et al. 2007). In this study, proteins were only screened for cell death-inducing activity but, in the future, this assay could be expanded to include screening for proteins with defence-suppressing activity. The *Phytophthora infestans* elicitor INF-1 is widely used in such studies whereby other effectors are screened for the ability to suppress the INF-1-induced defence response (Kamoun et al. 1998).

Of the four proteins screened for activity, recombinant expression of two led to the induction of cell necrosis – FgSSP32 and FgSSP33. Perhaps unsurprisingly, recombinant expression of FgSSP26 did not lead to any detectable response. As the gene encoding FgSSP26 is upregulated during the symptomless phase of infection, it is likely that this protein instead contributes towards the establishment of disease in a biotrophic manner and is therefore unlikely to induce cell death. In future experiments, FgSSP26 should be tested for the ability to suppress INF-1 induced defences as previously described (Kamoun et al. 1998). Expression of FgSP22 appeared

to induce some form of chlorosis, although this phenotype was not properly explored due to time constraints. The chlorosis was accompanied by an accumulation of autofluorescent compounds suggesting that a host response towards FgSSP22 was occurring. Multispectral imaging of leaves expressing FgSSP22 would have helped to reveal how widespread this phenotype was and enabled quantification of the host response. In addition, changes to the photosynthetic capacity (A_{max}) post infiltration could also have been explored by measuring carbon dioxide exchange and chlorophyll fluorescence (Dahal et al. 2014).

In the BSMV-VOX experiments, overexpression of FgSSP32 and FgSSP33 consistently led to a significant reduction in fungal disease symptoms in wheat. As the genes encoding both proteins are expressed during the symptomatic phase of the *F. graminearum*-wheat floral interaction, FgSSP32 and FgSSP33 were hypothesised to contribute towards fungal pathogenicity by inducing localised cell death thus leading to the release of nutrients for fungal sequestration. The ability of both proteins to induce cell death in *N. benthamiana* further supports this hypothesis. Further experimentation is required to determine the range of hosts and tissues that these proteins can induce this phenotype, for example, wheat leaf or stem base tissue. It is important to note that expression of FgSSP32 and FgSSP33 via the BSMV-VOX vector did not lead to the induction of necrosis in *N. benthamiana*. The lack of necrosis may be due to the lower levels to which the VOX vector expresses recombinant protein compared to the highly expressing pEAQ vector. The necrosis-induced by FgSSP32 and FgSSP33 may therefore be dose-dependent.

Interestingly, the patterning of necrosis induced by both FgSSP32 and FgSSP33 localised to the vascular tissues of the host. This spatial patterning was not observed in plants expressing the *Z. tritici* effector MgNLP, which induced indiscriminate necrosis across the whole leaf. The phenotype induced by MgNLP Is extremely common when screening for effectors for cell death and the majority of effectors induce necrosis across the whole leaf panel in which they are infiltrated (Yoshino et al. 2012; Bozkurt et al. 2011; Ma et al. 2012).

Several hypotheses can be made as to how this vascular-associated phenotype may develop. Firstly, there is a possibility that agroinfiltration is perhaps more effective around vascular tissues and that this phenotype is an artefact of this phenomena. However, as agroinfiltration with MgNLP induces a whole leaf response, this is unlikely and would be widely reported in the literature.

Studies on senescence in the daylily, *Hemerocallis* hybrid cv Stella d'Oro, revealed that cell death is in part controlled by the specific decrease in activities of protective enzymes such as catalase and ascorbate peroxidase and an increase in peroxidase (POX)-specific activities. In this study, POX activity appeared to be concentrated around the vascular tissues of petals and preferential accumulation of POX to the abaxial rather than the adaxial side of leaves was also observed (Panavas and Rubinstein 1998). Similarly, prior to the appearance of necrosis, a response to FgSSP32 and FgSSP33 could be observed on the abaxial side of the leaf where the leaf appears to have a 'silvery' appearance – best demonstrated by multispectral imaging (Figure 5.5). This 'silvery' phenotype and subsequent necrosis around the

vasculature may also be a result of preferential accumulation of enzymes, such as POX, in these regions. To test this hypothesis, DAB staining could be utilised. Alternatively, the ‘silvery’ phenotype could be due to water loss, as a consequence of the supra-optimal opening of stomata caused by the activation of proton-ATPase pump as observed in the Cf-9–Avr9 interaction (Hammond-Kosack et al. 1996; Hammond-Kosack, Harrison, and Jones 1994). Alternatively, FgSSP32 and FgSSP33 may preferentially localise or be transported to the vasculature tissue by chaperone proteins (Boston, Viitanen, and Vierling 1996). As both FgSSP32 and FgSSP33 have several predicted protease cleavage sites, it is possible that proteases may cleave FgSSPs in the main panel of the leaves prior to transport to the vasculature.

In the *F. oxysporum*-tomato interaction, the apoplastic effector Avr2 was reported to trigger necrosis which ‘trailed around the vasculature’ – a phenotype that was dependent on the presence of the resistance protein I-2 (Houterman et al. 2009; Cao et al. 2018). I-2 is a classical NB-LRR resistance protein which is specifically expressed in the vascular tissue (Ori et al. 1997; Mes et al. 2000). While FgSSP32 and FgSSP33 are sequence unrelated to Avr2 (10.8% and 14.2% shared protein amino acids, respectively), it is possible that FgSSP32 and FgSSP33 are therefore recognised by receptors specifically expressed in the vascular tissue as seen with Avr2 and I-2.

The second instance of this vascular-associated phenotype has been reported in the *Xanthomonas campestris*-Arabidopsis interaction. The bacterial pathogen *X. campestris* is the causal agent of black rot, a vascular disease of cruciferous plants. The *X. campestris* leucine-rich repeat (LRR)

domain-containing effector AvrAC is known to trigger ETI specifically in vascular tissues (Xu et al. 2008; Feng et al. 2012). AvrAC uridylates and inhibits several plant RLKs including BIK1 – a critical component of multiple pattern recognition receptor (PRR) complexes (Feng et al. 2012; Lu et al. 2010). A homolog of BIK1, PBL2, is required for ETI induced by AvrAC (Guy et al. 2013). Yeast2Hybrid analysis could be carried out between FgSSP32, FgSSP33 and RLKs, such as BIK1, known to interact with AvrAC to test whether these proteins function in a similar manner. While not a strictly vascular pathogen like *X. campestris*, *F. graminearum* heavily colonises vascular tissues during the symptomatic phase of intercellular growth in wheat rachis tissue (Brown et al. 2010). The loss of vascular integrity in wheat ears results in the premature bleaching which characterises FHB disease. As both *FgSSP32* and *FgSSP33* are expressed during the symptomatic phase of the *F. graminearum*-wheat floral interaction, we could hypothesise that FgSSP32 and FgSSP33 somehow contribute towards vascular colonisation.

Unexpectedly, infection with *Agrobacterium*-induced a response which was greatly reduced in plants expressing FgSSP32 and FgSSP33 (Figure 5.5; Figure 5.6). Presumably, this is a PTI response arising from the recognition of one or more *Agrobacterium* PAMPs. Using multispectral imaging, a response to *Agrobacterium* infection around the site of agroinfiltration was observed. As this response was not observed in the buffer control treatment, we can assume that the response occurs because of *Agrobacterium* infection rather than mechanical wounding. While a response to *Agrobacterium* infection was observed in plants expressing FgSSP32 and FgSSP33, this

response was greatly reduced. While it is possible that the response induced by FgSSP32 and FgSSP33 masks the *Agrobacterium* infection response, it could also be possible that FgSSP32 and FgSSP33 function to suppress the immune response induced by *Agrobacterium*. Transcriptional profiling of *N. benthamiana* expressing FgSSP32 and FgSSP33 could provide insights into how the host immune response is coordinated in these experiments.

Expression of FgSSP32 and FgSSP33 lacking a signal peptide did not lead to the induction of necrosis thereby suggesting that secretion of these proteins into the apoplast is essential to function. In the BSMV-VOX experiments (Chapter 4, Figure 4.3), overexpression of FgSSP32 lacking a signal peptide did not lead to any changes in fungal pathogenicity compared to the viral control used. Both datasets therefore support the hypothesis that FgSSP32 functions as an apoplastic effector. In contrast, overexpression of FgSSP33 lacking a signal peptide in the BSMV-VOX experiments led to a significant reduction in fungal disease symptoms – although this reduction was variable across experiments.

As the results from the experiments described in this chapter indicated that both FgSSP32 and FgSSP33 function apoplastically, a VIGS experiment was carried out to determine whether the FgSSP-induced necrosis was dependent on the presence of the membrane-bound RLKs BAK1 and SOBIR1. As important immune signalling components, BAK1 and SOBIR1 facilitate intracellular signalling following recognition of PAMPs and apoplastic effectors (Albert et al. 2015). The results from this experiment revealed an overall trend towards the requirement of BAK1 and SOBIR1 for the induction of an FgSSP-induced response, although the differences

observed were quantitative as silencing of these genes did not lead to total abolishment of the FgSSP-induced response. TRV:*GFP* plants exhibited a variable response to recombinant expression of FgSSP32 and as such it is difficult to interpret whether or not FgSSP32-induced necrosis is dependent on the presence of BAK1 or SOBIR1. A reduction in FgSSP33-induced symptoms was also observed in *BAK1* and *SOBIR1*-silenced plants however, as this reduction was small and insignificant, it is also not possible to say whether FgSSP33-induced necrosis is dependent on these RLKs.

In this VIGS experiment, *SGT1* was also silenced to determine whether effector perception relied on the presence of this gene. A ubiquitin-ligase associated protein, SGT1 (suppressor of G2 allele of *skp1*) forms a chaperone complex with HSP90 (heat shock protein 90 kDa) functioning to stabilise NLRs (Shirasu 2009). SGT1 and HPS90 are therefore required for the activation of resistance mediated by several NLRs and the *Phytophthora infestans* effector AVR3a is unable to induce HR in *SGT1*-silenced plants (Bos et al. 2006). In *SGT1*-silenced plants, there was a large amount of variability in the symptoms induced by FgSSP32 although there appears to be trend towards a reduction in symptoms. Recombinant expression of FgSSP33 in *SGT1*-silenced plants, however, resulted in a reduction in the FgSSP33-induced response although this reduction was not significant. This may therefore indicate that the induction of FgSSP33-induced necrosis may be mediated by an unidentified NLR. Further work is required to confirm the role of BAK1, SOBIR1 and SGT1 in mediating FgSSP32 and FgSSP33-induced necrosis. To alleviate some of the technical difficulties in setting up this VIGS experiment, CRISPR-generated BAK1 *N. benthamiana* lines (Jane

Parker lab, Max Planck Institute Cologne, Germany) could be used for effector expression assays to permit confirmation of the results reported in this study.

Finally, considering the rarity of the vascular-associated response induced by FgSSP32 and FgSSP33 in the literature, and the lack of sequence relatedness of the two proteins, it is important to consider how these two proteins could induce the same response. FgSSP32 and FgSSP33 share a pairwise identity of 20.5% and have four conserved cysteine residues. Apart from these cysteine residues, no shared motifs within these proteins are present leading us to question why two seemingly unrelated proteins induce the same rare phenotype. Recent work by Varden et al. (2019) demonstrated how unconventional integrated domains within a single NLR can bait multiple pathogen effectors. The existence of either an NLR or an RLP which can recognise both FgSSP32 and FgSSP33 is, however, purely speculative. While supported by the initiation of the HR in response to FgSSP32 and FgSSP33 expression, further work is required to elucidate the receptors that recognise these proteins to initiate the observed response. Identification of the host proteins which interact with FgSSP32 and FgSSP33 is therefore integral to gaining an understanding as to the mode of action of these proteins. Recently, Schultink et al. (2019) used a forward genetics approach to identify the *Nicotiana* NLR responsible for perception of the *Xanthomonas perforans* effector XopJ4. The authors of this study used ethyl methanesulfonate (EMS) mutagenesis to generate an *N. benthamiana* mutant library which they then screened for loss-of-function. Prior to this study, forwards genetics approaches have not been widely utilised in *N.*

benthamiana due to the plants allotetraploid genome (3.1GB) and incomplete reference genome (Naim et al. 2012). Four draft genomes are currently available for *N. benthamiana* (Niben 1.0.1; Niben 0.4.4; Nbv0.5; and Nbv0.3) and, recently, Kourelis et al. (2018) reanalysed these genomes and improved the quality of the current annotations (Bombarely et al. 2012; Naim et al. 2012; Nakasugi et al. 2014). Screening of *N. benthamiana* mutants for loss of ability to perceive FgSSP32 and FgSSP33 would be an interesting approach to identify the host network responsible for immune signalling against these effectors.

Chapter 6 Further characterisation of the necrosis-inducing proteins FgSSP32 and FgSSP33

6.1 Introduction

Characterisation of novel proteins can be challenging – particularly those that lack sequence similarity to other characterised proteins. Fortunately, a wide range of molecular, biochemical and imaging techniques can now be exploited to gain insight into protein structure, function, and protein-protein interactions. In the previous chapter, I describe the identification of two novel *F. graminearum* proteins with necrosis-inducing ability in *N. benthamiana*, namely FgSSP32 and FgSSP33 (Chapter 5). While both FgSSP32 and FgSSP33 have homologues distributed within the *Fusarium* genus, none of these homologues have been characterised and the amino acid sequence of these proteins does not contain any known functional domains (Chapter 3). In this chapter efforts were made to uncover the mechanisms through which FgSSP32 and FgSSP33 may function using the techniques outlined below.

In recent years, the accumulation of next generation sequencing data has prompted advances in diverse mass-spectrometry (MS) coupled techniques from which structural information, and consequently protein dynamics, can be inferred (Pi and Sael 2013). With the help of colleagues at Rothamsted, Drs David Withall and John Caulfield, high performance-liquid chromatography (HPLC) and liquid-chromatography mass-spectrometry (LCMS) was used to chemically analyse the *N. benthamiana* response to recombinant expression of FgSSP32 and FgSSP33. While both techniques enable the separation of hundreds of compounds and metabolites from a single plant extract, LCMS additionally enables the identification of these

compounds via resolution of the mass-to-charge (m/z) ratio (Fiehn et al. 2000; Proestos, Sereli, and Komaitis 2006). LCMS has proven particularly useful for the separation and detection of plant secondary metabolites and, in addition, is extremely sensitive and reliable (Moco et al. 2006). When further coupled with nuclear magnetic resonance (NMR), resolution of the molecular structure of individual compounds can be confidently determined (Kim, Choi, and Verpoorte 2011). Application of comprehensive metabolomic and proteomic approaches to the study of pathogen-host interactions can lead to the detection of biochemicals, such as resistance gene products, involved in the disease response (Kushalappa and Gunnaiah 2013). As recombinant expression of FgSSP32 and FgSSP33 independently of *F. graminearum* leads to cell necrosis, exploration of the metabolomic host response to these proteins may offer key insights into protein function. Like many other necrotrophic effectors, FgSSP32 and FgSSP33 induce the accumulation of unidentified autofluorescent compounds, facilitating the widespread use of the *N. benthamiana* cell death screen (Kettles et al. 2017). Biochemical profiling of *N. benthamiana* leaves recombinantly expressing FgSSP32 and FgSSP33 may therefore lead to the identification of these compounds.

In this chapter I also describe the morphological characterisation of the *N. benthamiana* response to FgSSP32 and FgSSP33 as determined by light microscopy. Additionally, efforts were taken to localise FgSSP33 using immunogold labelling. Although a laborious and low throughput technique, transmission electron microscopy (TEM)-immunocytochemistry enables high-resolution of effectors to subcellular compartments – as demonstrated by the localisation of *Colletrotrichum higginsianum* effectors to the appressorial pore

(Kleemann et al. 2012). Effector localisation to either the apoplast, cytoplasm, or other sub-cellular compartments provides clues as to the potential mode of action of these proteins. Resolution of effector localisation is therefore a key step in the determination of novel protein function.

6.2 Materials and methods

6.2.1 Chemical analysis of FgSSP32 and FgSSP33-induced compounds in *N. benthamiana*

6.2.1.1 Methanolic extraction of compounds

Four-week old *N. benthamiana* plants were agroinfiltrated with *A. tumefaciens* pEAQ-HT-DEST3 strains recombinantly expressing FgSSP32 and FgSSP33 as described in chapter 5. Two negative controls were used in these experiments – healthy, uninfiltrated plants and plants infiltrated with the pEAQ-HT-DEST3:Empty vector (EV) construct. Leaves were harvested three days post infiltration. Samples were snap-frozen in liquid nitrogen and homogenised using steel ball bearings. Ground tissue (approx. 100 mg) was then resuspended in 1ml of a 4:1 mixture of HPLC-grade methanol and HPLC-grade water. Samples were centrifuged to pellet debris and the supernatant was recovered and decanted into glass vials. Samples were then kept at -20°C for further analysis.

6.2.1.2 High-performance liquid chromatography (HPLC) analysis

HPLC analysis was performed on a Shimadzu UFLC XR HPLC instrument fitted with a HICHROM C18-HL column (250x4.66mm, 90Å pore size, 25°C) with a flow rate of 1ml per min. Samples were monitored at 180-800 nm and run along a methanol : water gradient (Table 6.1). Aliquots of 15µl of each sample were injected onto the column.

Table 6.1 HPLC conditions used for analysis of *N. benthamiana* samples.

Time (min)	Water %	Methanol%
0.01	95	5
5.00	95	5
50.00	0	100
55.00	0	100
60	95	5

6.2.1.3 Liquid chromatography and mass spectrometry (LCMS)

LCMS analysis was carried out using an Acquity ultra-high-pressure liquid chromatography (UPLC) system coupled to a Synapt G2Si Q-Tof mass spectrometer with an electrospray ionization source (Waters, UK). The system was controlled through Masslynx 4.1 software (Waters). Chromatographic separation was carried out at a flow rate of 0.21mL min^{-1} using a UPLC BEH C18 column (2.1 x 150mm, 1.7 µm, Waters) coupled to a C18 Vanguard pre-column (2.1 x 5mm, 1.7µm, Waters). The mobile phase consisted of solvent A (0.02% formic acid v/v, water) and solvent B (0.02% formic acid v/v in methanol) with the following gradient: initial conditions 95% A, 0 – 2.4 min 95% A, 2.4 – 29.4 min 5% B to 100% B, 29.4 – 32.4 min 100% B, 32.4 – 35.4 100% B to 95% A, 35.4 – 38 min 95% A. The column was maintained at 50°C and the injection volume was 3µl. Samples were run in positive and then negative modes with two consecutive injections of methanol between modes to allow for stabilization.

An Acquity photodiode array (PDA) detector was used to monitor the UV trace (range 200-450nm), sampling rate of 10 points s^{-1} with resolution set to 2.4nm. The Synapt was operated in high resolution mode and set to a mass

range of 50 – 1200 Da and scan time = 0.1s, in both ionization modes. The system was operated in MS1 mode with the following conditions: capillary voltage – 2.5KV, sample cone voltage 30V, sample offset 80V, source temperature 100°C, desolvation temperature 300°C, desolvation gas flow 800L h^{-1}, cone gas flow 57L h^{-1}. The Synapt MS system was calibrated by infusing sodium formate solution and accurate mass detection was made by infusing the internal lockmass reference peptide leucine enkephalin during the runs. Tentative peak identifications were then made by comparing mass spectra with the METLIN database (https://metlin.scripps.edu)(Guijas et al. 2018).

6.2.2 Immunodetection of FgSSP33 in *E. coli* and *Nicotiana benthamiana*

6.2.2.1 Synthesis of specific antibodies

A specific polyclonal antibody to FgSSP33, anti-FgSSP33, was synthesised by Eurogentec Ltd. (Belgium) using their anti-peptide 28-day speedy polyclonal package. The antigen peptide sequence was generated from the regions of the peptide predicted to be surface-exposed. The FgSSP33 peptide sequence generated was nh2-CNNGGLYYSDPKTLEP–conh2. No peptide was possible with a high enough antigenic index for FgSSP32 and as such an antibody to this protein was not raised.

6.2.2.2 Expression of recombinant FgSSP33 in *E. coli*

Expression of recombinant FgSSP33 in *E. coli* was achieved using Gateway cloning technology. Transcripts of *FgSSP33* were amplified from *F. graminearum*-infected wheat using Phusion PCR as previously described in chapter 5. Primers amplifying these constructs were designed with *attB*-

flanking sites to enable Gateway cloning into the pDEST17 expression vector which contains an N-terminal His tag sequence (Figure S3). The predicted signal peptide at the 5' end of the *FgSSP33* coding sequence was removed to prevent the N-terminal His tag from interfering with protein secretion. Expression of the pDEST17 vector is under the control of the phage T7RNA polymerase-regulated T7 promoter. T7RNA polymerase is under the control of the lacUV5 promoter and target protein expression is thereby induced by lactose or the non-hydrolysable analogue of lactose, isopropyl β-D-1-thiogalactopyranoside (IPTG). Sequence-verified clones were grown in LB-Miller overnight at 30°C under constant shaking conditions (250RPM). An aliquot of cells was transferred to fresh LB Miller and diluted by 1:100 and grown until cells reached an OD_{600} of 0.4. To induce protein expression, IPTG (50mM) was added to cultures and grown overnight at 16°C. Cells were harvested by centrifugation at 13000 RPM for 2 mins. For extraction of soluble proteins, cells were lysed with glass beads to enable membrane breakage. Protein extracts were then run on a sodium dodecyl sulfate–polyacrylamide gel electrophoresis (SDS-PAGE) gel and subject to western blot analysis.

6.2.2.3 Protein extraction from plant tissues

N. benthamiana leaf tissue was snap-frozen in liquid nitrogen and ground by pestle and mortar with 270µl of Sainsbury's extraction buffer (50mM Tris-HCl pH 7.5, 150mM NaCl, 2mM ethylenediaminetetraacetic acid (EDTA), 1% v/v Protease Cocktail Inhibitor (Merck, NJ, USA), 0.1% Tween-20). Lysates were clarified by centrifugation and separated on a 16% SDS-PAGE gel under reducing conditions.

6.2.2.4 Recovery of apoplastic wash fluid from infiltrated *N. benthamiana* leaves

Apoplastic washing fluid (AWF) from leaf tissue using the infiltration-low speed centrifugation method described by O'Leary et al. (2014). *N. benthamiana* leaves were detached from the plant and washed with distilled water to remove leaf surface contaminants. Leaves were gently dried to remove excess water and rolled into a 50ml needless syringe. The syringe was then filled up with water until the 40ml mark and, by covering the syringe tip, negative pressure was created by pulling back the syringe until the 60ml mark and slowly releasing until the whole leaf was infiltrated with water. The syringes containing infiltrated leaves were then centrifuged inside a 50ml falcon tube for 10 min at 1,000x*g* in a swinging bucket rotor at 4°C. The recovered AWF was then recovered and spun again to remove any remaining debris. To concentrate AWF for downstream applications, samples were centrifuged in an Amicon® Ultra-15 Centrifugal Filter unit as per the manufacturer's instructions.

6.2.2.5 Western blot analysis

Prior to SDS-PAGE, protein extracts were supplemented with loading buffer (8% [w/v] SDS, 20% [v/v] 2-mercaptoethanol, 40% [w/v] glycerol, 0.008% [w/v] Bromophenol Blue, and 0.25 M Tris-HCl, pH 6.8) and incubated at 95°C for 10 mins to allow for protein denaturation. Proteins were separated by electrophoresis in running buffer (25 mM Tris, 192 mM Gly, and 0.1% (v/v) SDS) before being electroblotted onto a nitrocellulose membrane for 1h at RT (Hybond ECL, Amersham) in transfer buffer (20mM Tris, 192 mM Gly, and 20% (v/v) methanol). Membranes were then stained with Ponceau S

solution to verify equal protein loading across samples. Membranes were then destained using PBS-T buffer (50 mMTris, 150 mM NaCl, and 0.1% [v/v] Tween 20) and blocked in PBS-T supplemented with 5% (w/v) dry milk for 1h at room temperature and under constant shaking (20 rpm). Membranes were then incubated overnight at 4°C with the a 1:500 dilution of anti-FgSSP33 primary antibody in PBS-T and milk solution. Membranes were then washed in PBS-T for 10 mins with shaking. This washing step was repeated five times. Washed membranes were then incubated at RT with a 1:10,000 dilution of the secondary antibody (Anti-rabbit horseradish peroxidase, New England Biolabs). Specific antibody binding was detected using the ECL Prime kit (GE Healthcare Life Sciences, IL, USA). Chemiluminescence signals were then visualised using either Hyperfilm ECL (GE Healthcare Life Sciences, IL, USA) or the Azure C600 Instrument (Azure Biosystems, CA, USA).

6.2.3 Light microscopy and transmission electron microscopy (TEM)

6.2.3.1 Tissue preparation and sectioning

Four-week old *N. benthamiana* plants were agroinfiltrated with pEAQ-HT-DEST3 compounds recombinantly expressing FgSSP33. Three days post infiltration, three small samples (6mm^2) were taken from one leaf per plant. Six plants were used per treatment. Samples were cryo-frozen using a Leica EPM HPM100 high-pressure freezing system and then subject to freeze substitution in ethanol allowing dehydration of tissue samples. Freeze substitution was performed using the Leica Reichard AFS embedding system under the following conditions: -160°C for 0.5h, temperature increased by 15°C per hour for 5h, temperature kept at -85°C for 24h, temperature

increased by 15°C per hour for 5h, until the temperature was gradually brought to 0°C. Freeze-substituted samples were then gradually infiltrated in increasing concentrations of LR-white resin (Ethanol 100% : LR White – 3:1 1h5, 2:2 1hr, 1:3 1hr, 0:4 1hr) before finally being embedded in 100% resin and oven-baked at 55°C for 18h. Transverse 1µm sections were cut using a Leica EM U7 Rotary Microtome, collected on a polysine coated glass slides (Agar Scientific, UK) for staining. Sections were then stained with aqueous 0.1% toluidine blue (TBO) in 1% sodium tetraborate (w/v) pH 9.0 and mounted in DPX mounting media and imaged using a Zeiss Axiophot light microscope. Transverse 50-100nm sections were cut using a Diatom diamond knife (45°C) and placed onto Formvar-coated nickel grids (3.05mm grid size, AgarScientific) for imaging via TEM.

6.2.3.3 Immunogold labelling and TEM

Ultrafine-sections on nickel grids were blocked on 1% bovine serum albumin (BSA) for 30 mins at RT. Grids were then incubated with the FgSSP33-specific primary antibody, diluted in PBS-T by 1:50 for 2h at RT. Grids were then washed in PBS-T three times before blocking again in 1% BSA for 30 mins at RT. Grids were then incubated with 10nm gold-conjugated secondary antibody (Goat anti-rabbit IgG)) diluted 1:50 in PBS-T for 2 hrs at RT. Drops of 5% uranyl acetate (UA) were placed onto wax and the grids were placed on top of these UA droplets, with the section sample facing down, and incubated in darkness for twenty minutes. Grids were then washed in distilled water before staining with lead citrate for 3 minutes in the same conditions as the UA staining. Grids were washed again, dried on filter

paper and imaged by TEM using the Jeol JEM 2011Transmission electron microscope (Tokyo, Japan).

6.2.4 Generation of *FgSSP32* and *FgSSP33* single deletions in *F. graminearum*

To generate *F. graminearum* single gene deletions of *FgSSP32* and *FgSSP33*, the ‘split-marker’ approach for transformation of fungal protoplasts was employed. This approach requires the generation of two constructs per transformation – each construct containing a flank of the target gene and approximately two thirds of a selectable marker cassette. The 5’ and 3’ 1kb flanking regions of *FgSSP32* and *FgSSP33* were PCR amplified from the gDNA of the American wild-type isolate of *F. graminearum* PH-1 cultured in potato dextrose broth (PDB). The first two-thirds and the latter two-thirds of the hygromycin resistance gene (*hyg*) were also PCR-amplified from the pHYG plasmid. The purified fragments were then cloned into the EcoRV restriction site of pGEM®-T Easy Vector (Promega, WI, USA) using the Gibson assembly kit (New England Biolabs, MA, USA) as per the manufacturer's instructions. The two fusion cassettes were then used simultaneously to transform *F. graminearum* strain PH-1 protoplasts as previously described by Catlett et al. (2003). Resistant transformants were selected in REG medium (0.7% agarose, 0.2% yeast extract, 0.2% casein-hydrolysate (N-Z-Amine A), 0.8M sucrose). Transformants were then screened using the primers listed in chapter 2 in table 2.1.

Gene deletions were then tested for changes in pathogenicity in the coleoptile and wheat ear assays. For the coleoptile assay, wheat (cv. Bobwhite) seeds were germinated on perlite, soaked with water, in a closed

container. After 3 days, 1-2mm of the coleoptile tip was carefully removed using a sterile razor blade. A 1cm x 3cm piece of filter paper was then soaked with *F. graminearum* spore suspensions ($5x10^5$ spores/ ml) and wrapped around the coleoptile tip and contained using a pipette tip. The seedlings were then incubated with the filter paper for 3 days in the closed container and kept in darkness at 25°C. After 3 days, the container was opened, and plants were grown at 25°C with a 16h light period and at 80% RH. Seven days after inoculation, photographs of infected coleoptiles were taken and lesion size (mm^2) was determined using ImageJ (Schneider, Rasband, and Eliceiri 2012). Data was then analysed using a one-way ANOVA where lesion size was fitted as the variate and the *F. graminearum* strain used was fitted as a factor. Differences between strains were deemed significant at a $P<0.05$.

For the wheat ear assay, mature wheat ears were point inoculated as described in chapter 2.3. The number of spikelets exhibiting *F. graminearum* disease symptoms was scored every three days until the whole ear was infected. The proportion of spikelets showing macroscopic *F. graminearum* disease symptoms was analysed using generalised linear modelling (GLM) assuming a binomial distribution with a logit link function. The variate modelled was the number of diseased spikelets as a proportion of total diseased spikelets below the point of *F. graminearum* inoculation. Individual batches of plants, where batch means groups of plants inoculated at the same time, were termed as blocks in the model. Significance of the model was assessed using an approximate chi-squared test deemed significant at $P \leq 0.05$. To determine whether treatments (e.g. *F. graminearum* strains)

were significantly different from one another, the least significant difference (LSD) was calculated at a 5% significance level.

6.3 Results

6.3.1 Chemical analysis of plants expressing FgSSP32 and FgSSP33

In chapter 5, I described how recombinant expression of FgSSP32 and FgSSP33 in *N. benthamiana* led to the induction of vascular-associated necrosis – a phenotype that was also detectable under UV light due to the accumulation of defence-related autofluorescent compounds (Dixon and Paiva 1995). While detection of these autofluorescent compounds is widely used in effector screens, little work has been done to characterise these compounds (Kettles et al. 2017). The aim of the following experiments was therefore to identify autofluorescent compounds induced and, more broadly, to employ a chemical profiling approach of *N. benthamiana* plants recombinantly expressing FgSSP32 and FgSSP33. Identification of host compounds induced in response to these effectors may shed light on the mechanisms through which they function.

To determine whether the chemical profiles of *N. benthamiana* plants expressing FgSSP32 and FgSSP33 were different to the control treatments (healthy & EV), HPLC analysis was carried out on leaf extracts taken three days post agroinfiltration. Across all treatments, three peaks with retention times of 16 mins, 22 mins and 38 mins were present in the chromatogram in all samples. In plants expressing FgSSP32 and FgSSP33 a large peak was consistently observed in samples with a retention time of ~47 mins. This peak was also observed in EV control samples but to a much lesser extent and was not present in healthy leaves (Figure 6.1). Other peaks were identified in the chromatogram that were induced in response to FgSSP32

and FgSSP33, however, these peaks were less consistently induced and as such were not further explored due to time constraints.

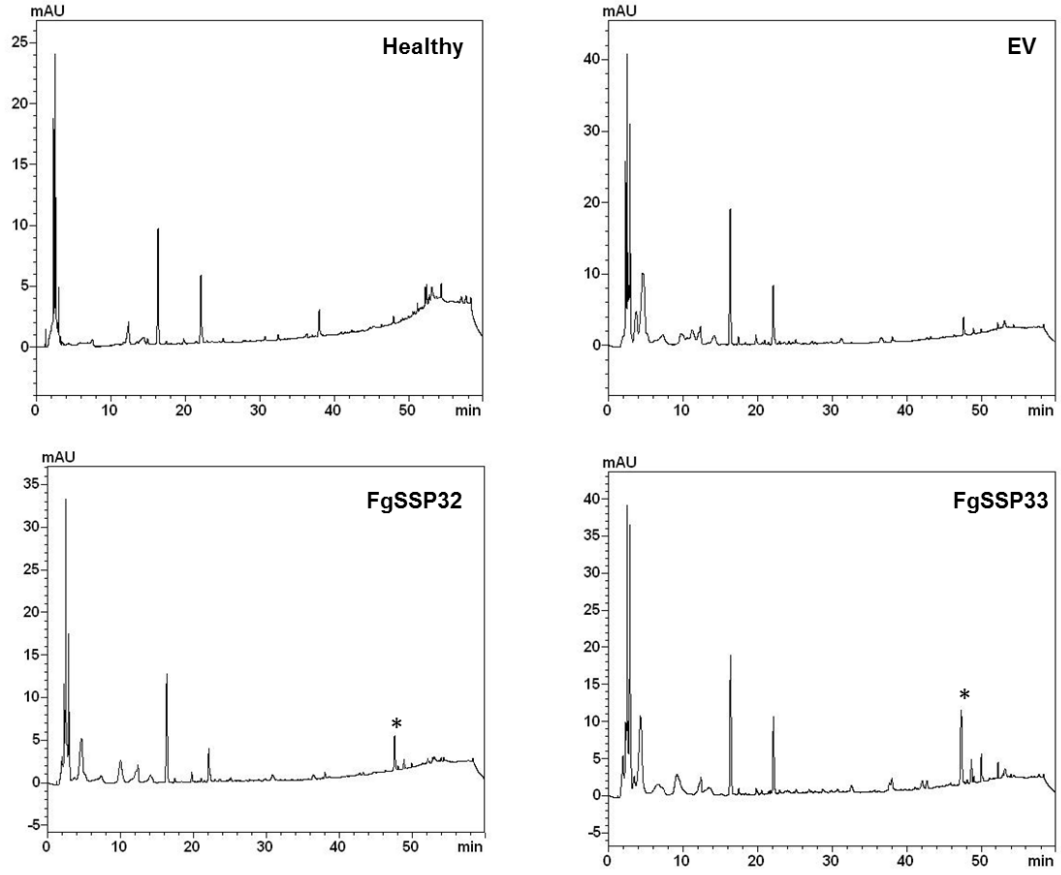

Figure 6.1 A comparison of representative HPLC chromatograms observed between the healthy and EV controls and *N. benthamiana* plants expressing FgSSP32 and FgSSP33. * denotes the peak observed at 47 mins present in plants expressing FgSSP32 and FgSSP33.

HPLC analysis therefore revealed that plants expressing FgSSP32 and FgSSP33 had different biochemical profiles compared to the two controls. Samples were therefore then analysed by LCMS allowing the determination of the m/z of FgSSP32 and FgSSP33-induced compounds. Two chromatograms were generated per sample: 1) a PDA chromatogram which detects UV and allows comparisons to be made against the HPLC data 2) and the LCMS chromatogram. As retention time shifts can occur depending on the column and the instrument used to analyse samples, the peaks identified in the HPLC data had to be matched up to the data generated by the LCMS. The peaks identified at 16, 22, and 38 mins on the HPLC were identified in the LCMS data at 11.09, 13.01, and 17.2 mins, respectively (Figure 6.2; Figure 6.3).

A peak with a retention time of 28.32 mins was present in FgSSP32 and FgSSP33-expressing plants and presumed to be the 47-minute peak identified in the HPLC data (Figure 6.1; Figure 6.2; Figure 6.3). MS analysis of this peak revealed that this compound had a m/z = 291.1955 mass units (Figure 6.3 and Figure 6.4). Using the Metlin MS database (Guijas et al. 2018), the most likely chemical formula of this compound is $C_{18}H_{28}O_3$. Many compounds with this chemical formula are components of the jasmonic acid pathway including the compounds 13-epi-12-oxo-phytodienoic acid and 12-oxo-phytodienoic acid (12-OPDA)(Figure 6.5; Figure 6.6). Attempts were made to confirm which of these compounds was being produced by nuclear magnetic resonance (NMR). Several months after compound extraction and analysis, samples were re-run on the HPLC and the peak identified at 47

mins was nearly undetectable. The peak identified at 47 mins in the HPLC experiment was collected from multiple samples and concentrated and then used for NMR but were still not detectable. The FgSSP-induced compound therefore proved to be extremely unstable even when extracts were stored at -20°C in solvent.

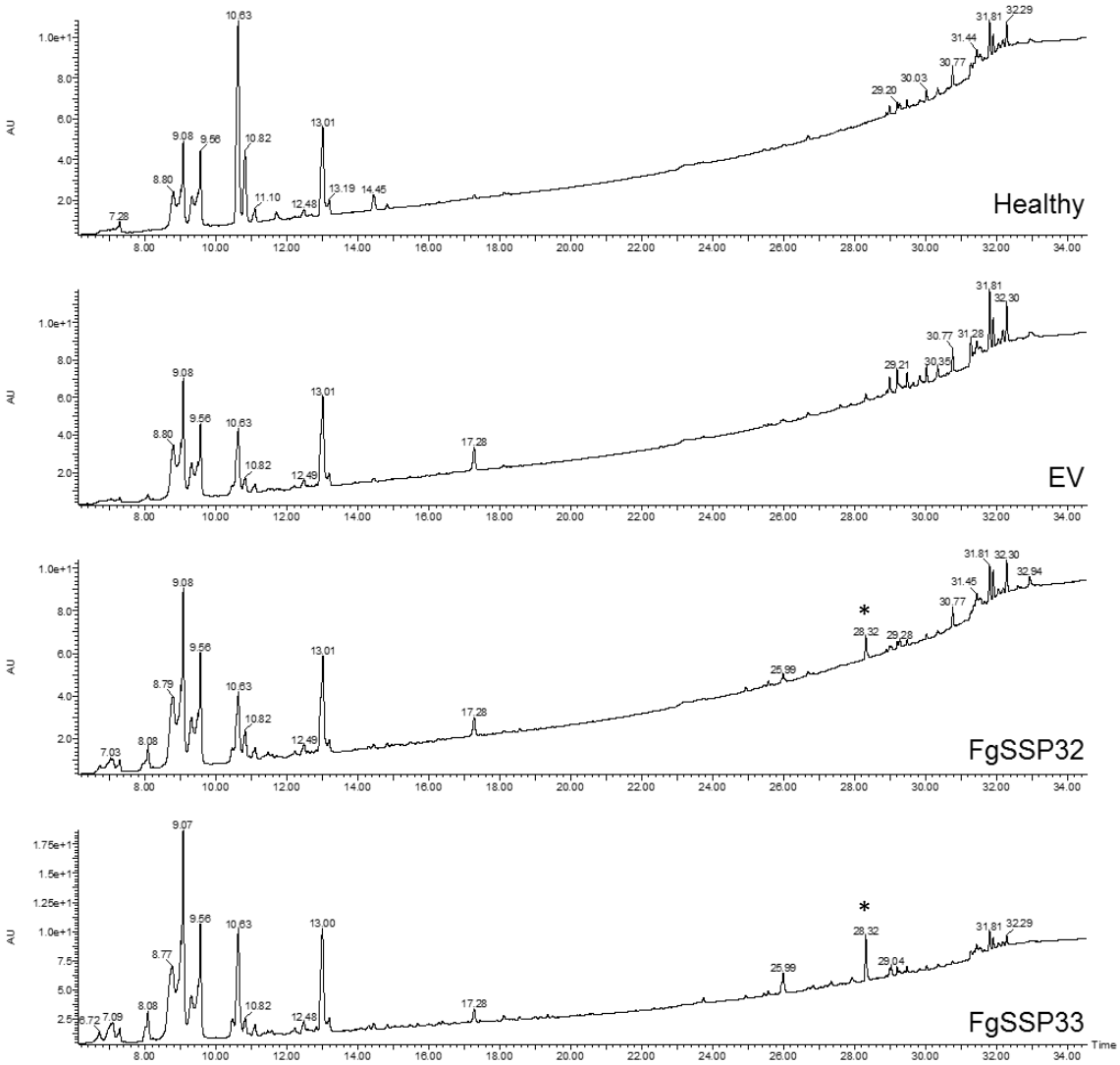

Figure 6.2 A comparison of representative PDA chromatograms observed between the healthy and EV controls and *N. benthamiana* plants expressing FgSSP32 and FgSSP33. * denotes the peak observed at 28.32 minutes present in plants expressing FgSSP32 and FgSSP33.

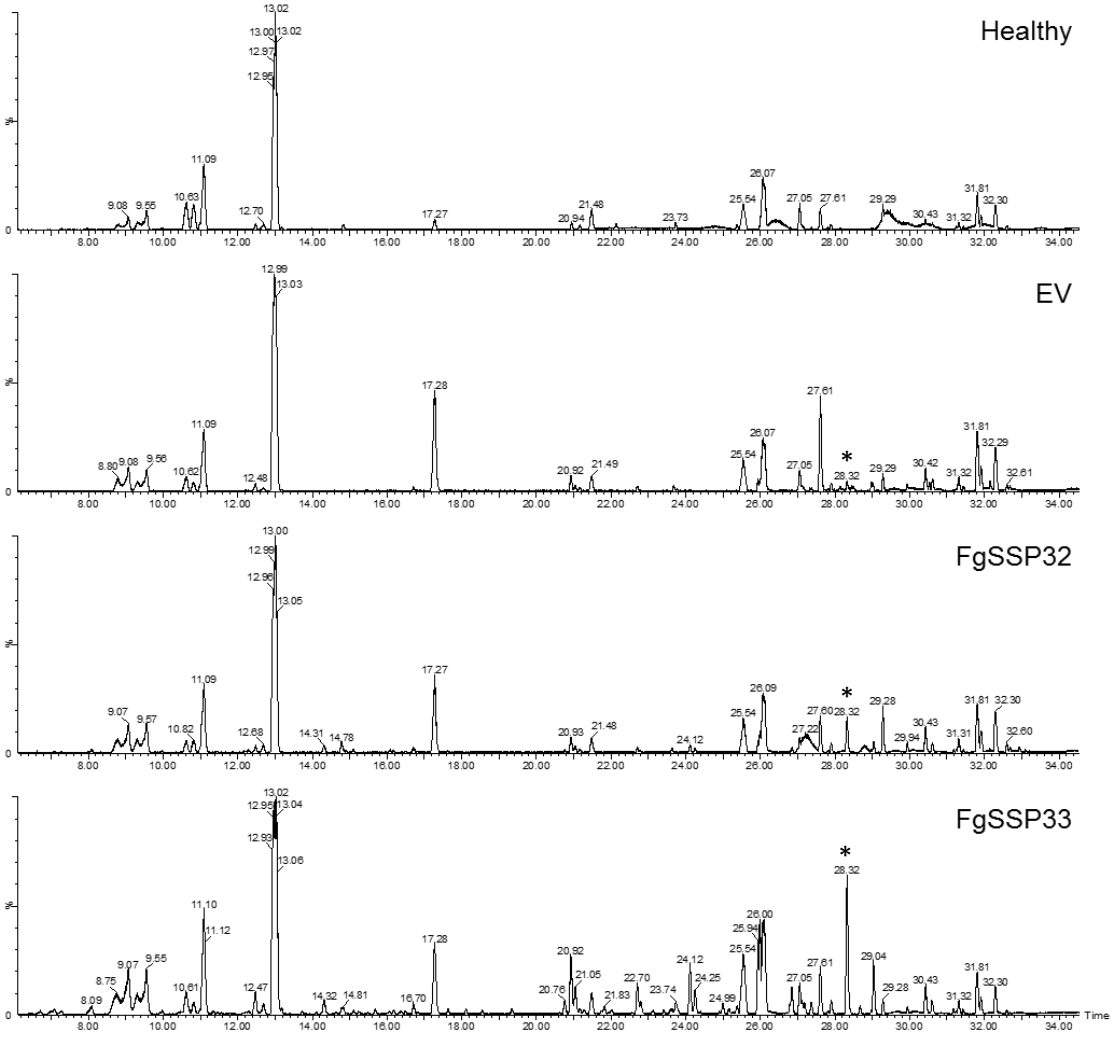

Figure 6.3 A comparison of representative extracted LCMS chromatograms of healthy and EV controls and *N. benthamiana* plants expressing FgSSP32 and FgSSP33. * denotes the peak observed at 28.32 minutes present in plants expressing FgSSP32 and FgSSP33, and to a much lower level in the EV sample.

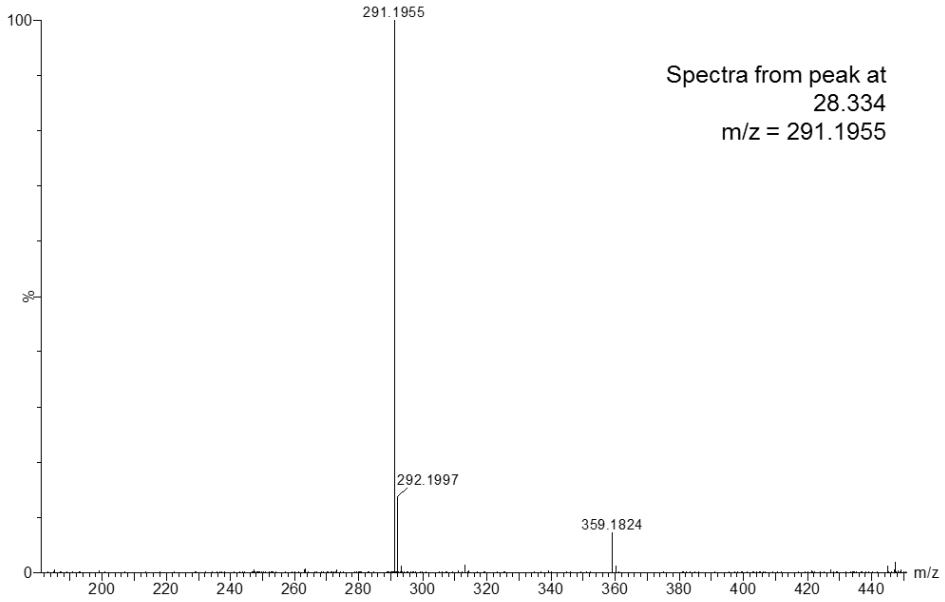

Figure 6.4 The mass spectra of the peak observed at 28.334 minutes by GS-MS analysis. The m/z of the largest peak is 291.1955.

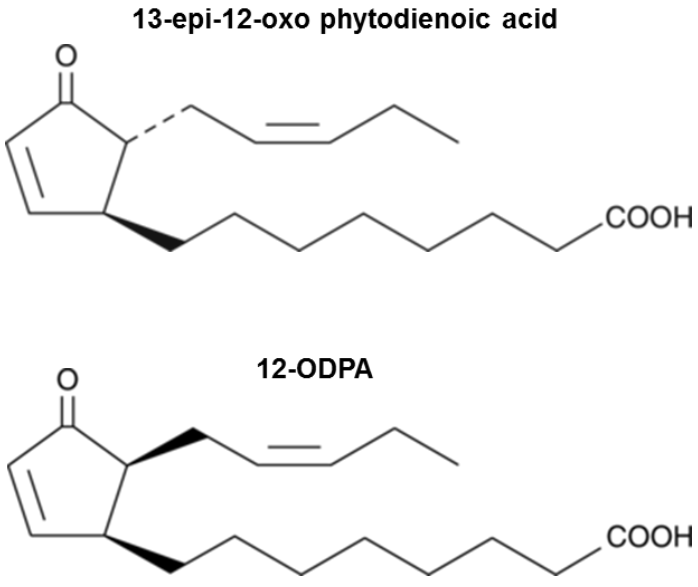

Figure 6.5 Possible compounds with a m/z of 291.1955.

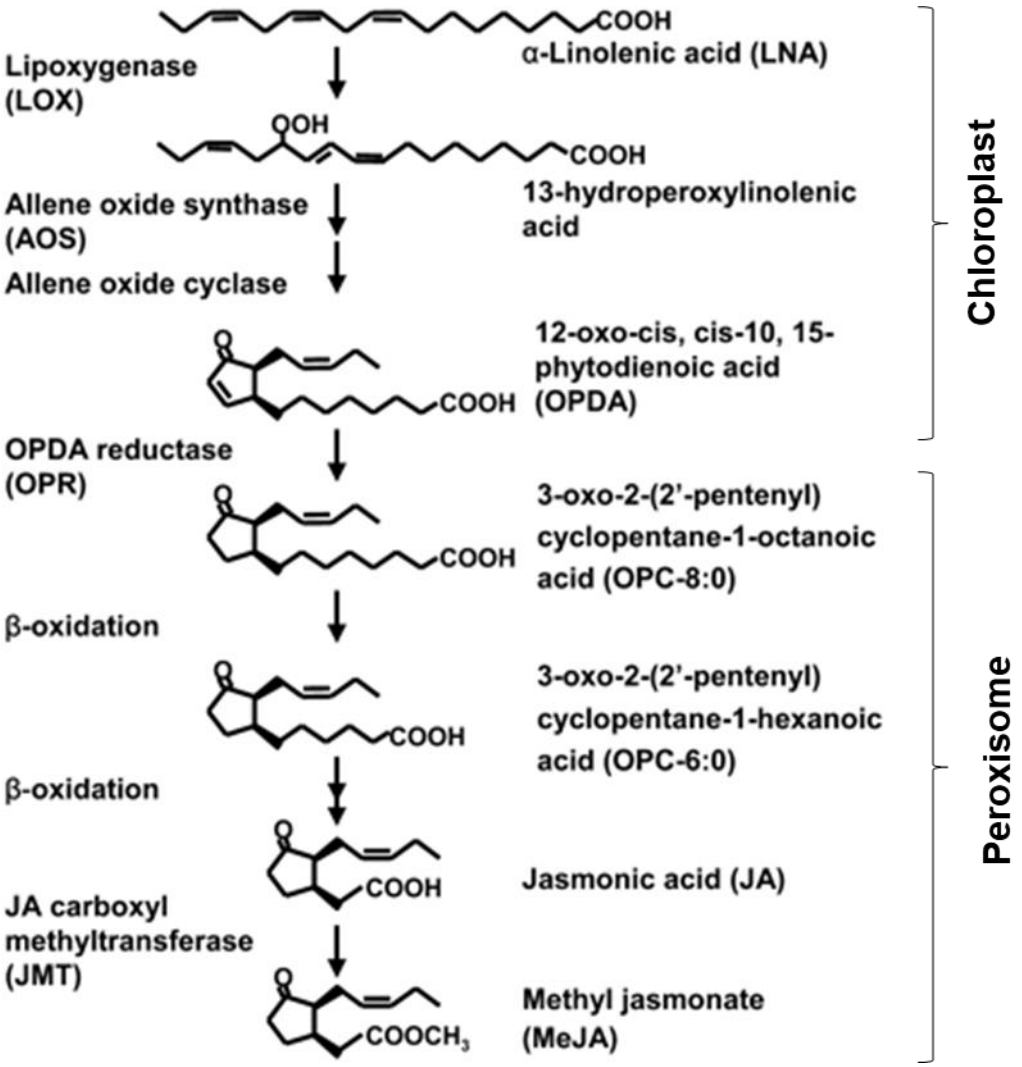

Figure 6.6 The jasmonate biosynthetic pathway. JA biosynthesis begins in the plastid with the release of octadecatrienoic acid or hexadecatrienoic acid from membrane lipids by lipases. Cis-OPDA is then formed by sequential steps catalysed by LOX and AOS and AOC. Cis-OPDA is then transported into the peroxisome where, following several rounds of oxidation, is transformed into JA. Adapted from Taki et al (2005).

6.3.2 *In planta* detection of *FgSSP33*

A polyclonal antibody was raised to enable the detection of FgSSP33 *in planta*. Unfortunately, as no regions within FgSSP32 had a high enough antigenic index, it was not possible to raise an antibody towards this protein. To test whether the FgSSP33-specific antibody was able to detect FgSSP33 *in vitro*, FgSSP33 was recombinantly expressed in *E. coli* using a lac-inducible plasmid. Western blot analysis was carried out on protein extracts from *E. coli* cultures and FgSSP33 was detectable in total protein extracts of induced *E. coli*. FgSSP33 was not, however, detectable in the soluble protein extracts of induced *E. coli* cultures suggesting that this protein is not soluble when produced in *E. coli* (Figure 6.7).

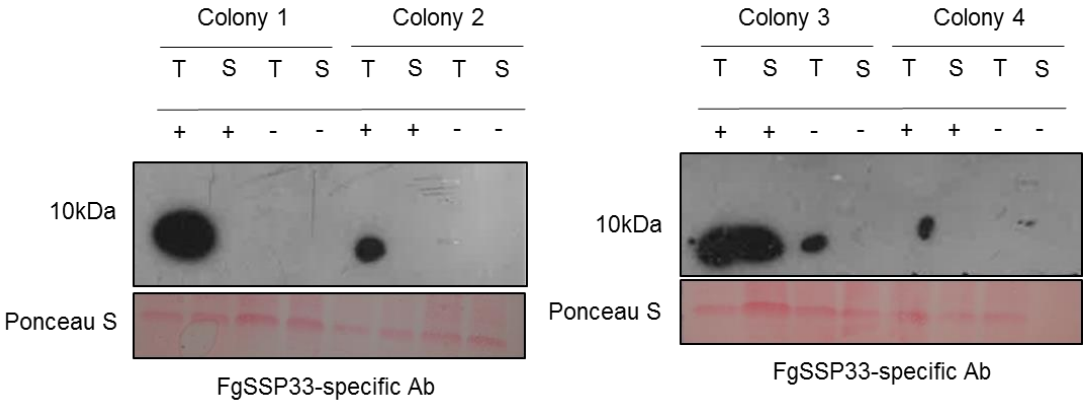

Figure 6.7 Immunodetection of FgSSP33 recombinantly expressed by several *E. coli* strains for validation of the FgSSP33-specific polyclonal antibody. Band detected below 10kDa and the predicted size of FgSSP33 without a signal peptide is 5.44 kDa. Protein loading was verified using Ponceau S stain. T = total protein, S = soluble protein, + = IPTG added, and - = no IPTG added.

Attempts were then made to detect FgSSP33 in the total protein and AWF extracts of *N. benthamiana* plants recombinantly expressing the protein using the pEAQ-HT-DEST3 vector. Unfortunately, I was unable to detect FgSSP33 *in planta* as several non-specific bands were observed in total protein extracts of healthy plants. This therefore suggests that the FgSSP33-specific antibody has bound to another *N. benthamiana* protein and is not specific towards FgSSP33 (Figure 6.8).

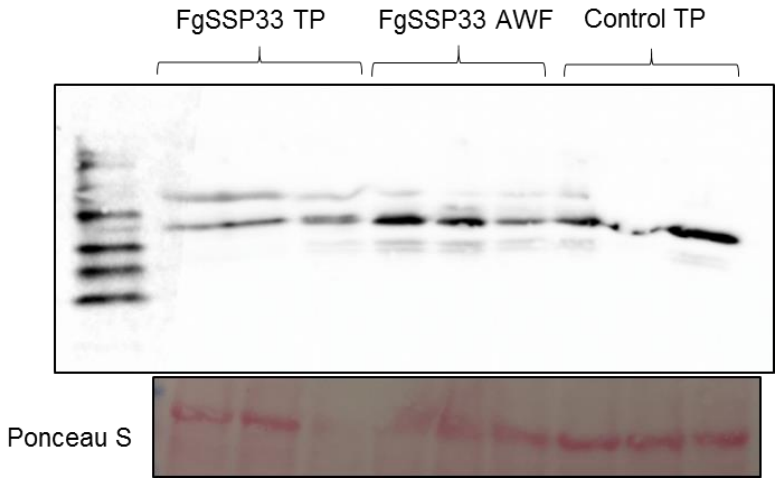

Figure 6.8 Immunodetection of FgSSP33 recombinantly expressed in *N. benthamiana* using the pEAQ-HT-DEST3 vector. Uninfiltrated plants were used as the control in these experiments. Several band detected around 25kDa and the predicted size of FgSSP33 with a signal peptide is 7.17 kDa.TP = total protein and AWF = apoplastic wash fluid. Protein loading was verified using Ponceau S stain.

6.3.3 Light microscopy and TEM analysis of *N. benthamiana* plants expressing FgSSP32 and FgSSP33

Morphological analysis of *N. benthamiana* plants expressing FgSSP33 was undertaken by obtaining light microscopy images of leaf samples. Initially, these experiments were set-up to carry out immunogold labelling to enable localisation of FgSSP33 using the FgSSP33-specific antibody and as such FgSSP32 was not included as treatment in this experiment. Sections of *N. benthamiana* leaves infiltrated with FgSSP33 were taken and images were compared to an EV control. As the cell death phenotype observed in chapter 5 localised to the vascular tissue of *N. benthamiana,* focus was placed upon looking at the morphology of the vasculature. In three out of six replicates, expression of FgSSP33 led to what appears to be the accumulation of secreted polymers, such as lignin or suberin, into the intercellular spaces thereby indicating a host reaction towards FgSSP33 (Figure 6.9). At the point of sampling, it also appears that the xylem and phloem parenchyma were still intact in FgSSP33-treated leaves.

As previously mentioned, efforts were also made to use the FgSSP33-specific antibody using immunogold labelling despite unsuccessful attempts to identify this antibody *in planta* using western blotting techniques (Figure 6.8). Several technical difficulties were encountered in these experiments which ultimately meant that localisation of FgSSP33 was unsuccessful. The first difficulty encountered was that, during immunogold labelling, crystals formed and other sources of dirt were deposited onto the section (Figure 6.10b and c). While this would not be a problem in light microscopy, due to the high levels of magnification required to identify gold labels in TEM these

dirt deposits obscured many of the subcellular structures. As the dirt deposits were dark in colour, this also meant that resolution of subcellular structures was poor as well. In addition to obscuring the subcellular structures, gold labels were found to cluster around dirt and crystal deposits which could lead to the false positive gold labelling (Figure 6.10d). Another limitation of these experiments was that resin tearing was observed around cell wall structures making it difficult to isolate intact regions of cellular material (Figure 6.10e). This made it difficult to make comparisons between control and FgSSP33-treated plants in terms of gold particle clustering. Some regions of samples were however useable and in these samples gold particles appeared to localise to the cell wall in *N. benthamiana* leaves expressing FgSSP33 (Figure 6.10f and g). It is not possible to say whether this is representative of the true localisation of FgSSP33. In some samples, including both control and FgSSP33 samples, gold particle clustering was also observed in chloroplasts (Figure 6.10h). It is likely that this is background labelling but, due to the poor sample quality and time and cost constraints, this was not explored further.

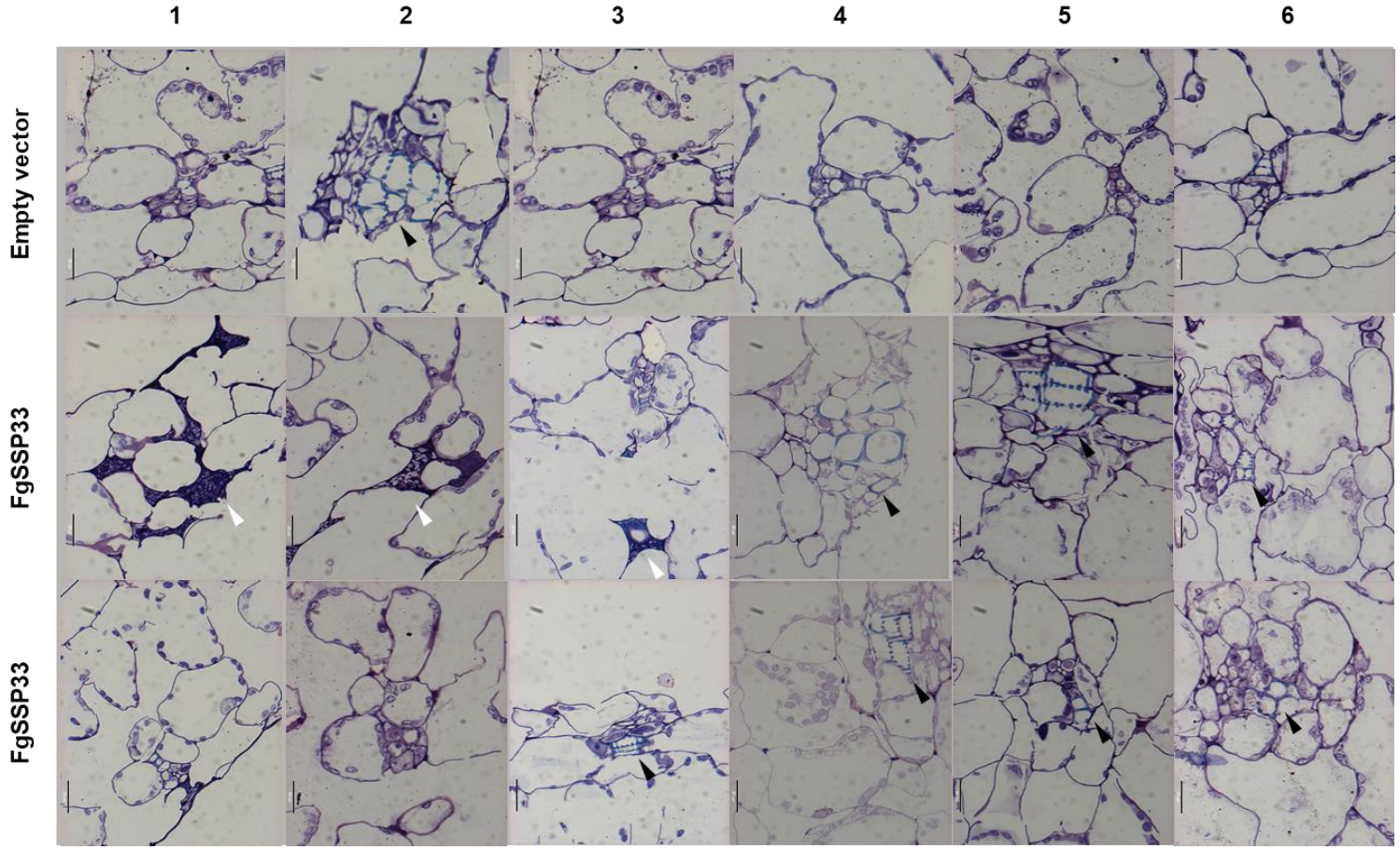

Figure 6.9 Light micrographs of transverse sections of *N. benthamiana* tissue expressing EV and FgSSP33. The top row illustrates vascular tissue in *N. benthamiana* leaves infiltrated with empty vector. The second and third rows illustrate vascular tissue in *N. benthamiana* leaves recombinantly expressing FgSSP33. White arrowhead indicates accumulation of unidentified polymers in response to expression of FgSSP33. Black arrowhead indicates the intact phloem and xylem parenchyma. Bar = 20µm. Numbers on the top row indicate replicate number.

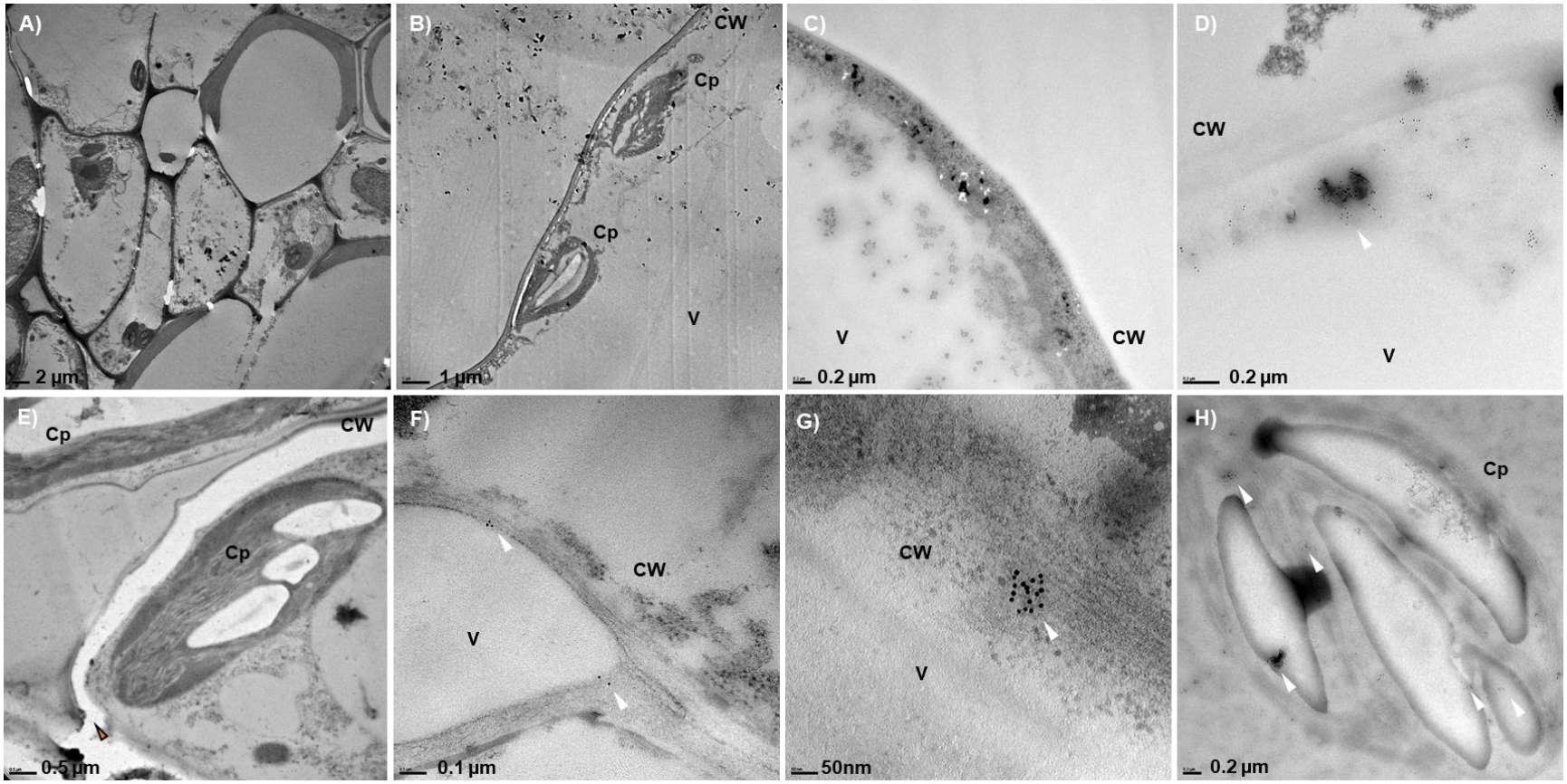

Figure 6.10 Electron micrographs of *N. benthamiana* leaves expressing EV and FgSSP33. A) Vascular region of an unlabelled *N. benthamiana* leaf. B) Image depicts accumulation of dirt on a section that is deposited during immunogold labelling. C) Cell wall of *N. benthamiana* lead expressing FgSSP33. Potential labelling obscured by crystals that appear during the immunolabelling process. D) Cell wall obscured by crystal formation. Clustering of gold labelling occurs where dirt has stuck to the section in control plants. E) Image depicts resin tearing around the cell wall. F and G) *N. benthamiana* expressing FgSSP33 and immunogold labelled using FgSSP33-specific antibody. H) Clustering observed in chloroplasts from EV samples. White arrow illustrates gold labelling. Orange arrows indicate resin disintegration around cell walls. Cp = chloroplast, V = vacuole, CW = cell wall.

6.3.4 *FgSSP32* and *FgSSP33* fungal gene deletion mutants exhibit wildtype pathogenicity

Overexpression of FgSSP32 and FgSSP33 in mature wheat tissues led to a consistently significant reduction in FHB symptoms in BSMV-VOX experiments and therefore contribute towards fungal pathogenicity (Chapter 4). To determine whether these proteins are essential to *F. graminearum* pathogenicity, single gene deletion mutants of *FgSSP32* and *FgSSP33* were generated by split-marker transformation and verified using a PCR-based approach (Figure 6.11).

Two independent *ΔFgSSP32* and *ΔFgSSP32* mutants were selected for *in vitro* and *in planta* characterisation (*FgSSP32.1, FgSSP32.5, FgSSP33.2 and FgSSP33.3* (Figure 6.11). The gene deletion strains were grown on nutrient-poor SNA to assess growth and no differences were observed when compared to the wildtype PH-1 strain (Figure 6.12). Strains were then tested in coleoptile and wheat ear assays to test for any changes in fungal pathogenicity. In the coleoptile assay, lesion size was determined by ImageJ analysis 7 dpi and, while differences between treatments were observed, these differences were not statistically significant and most likely attributable to the inclusion of several replicates which *F. graminearum* was unable to infect (Figure 6.13). Deletion strains were then tested for the ability to cause disease in wheat ears and were shown to exhibit similar pathogenicity to the PH-1 (Figure 6.14). The results from the coleoptile and the wheat ear assay suggest that these proteins are not essential for fungal virulence.

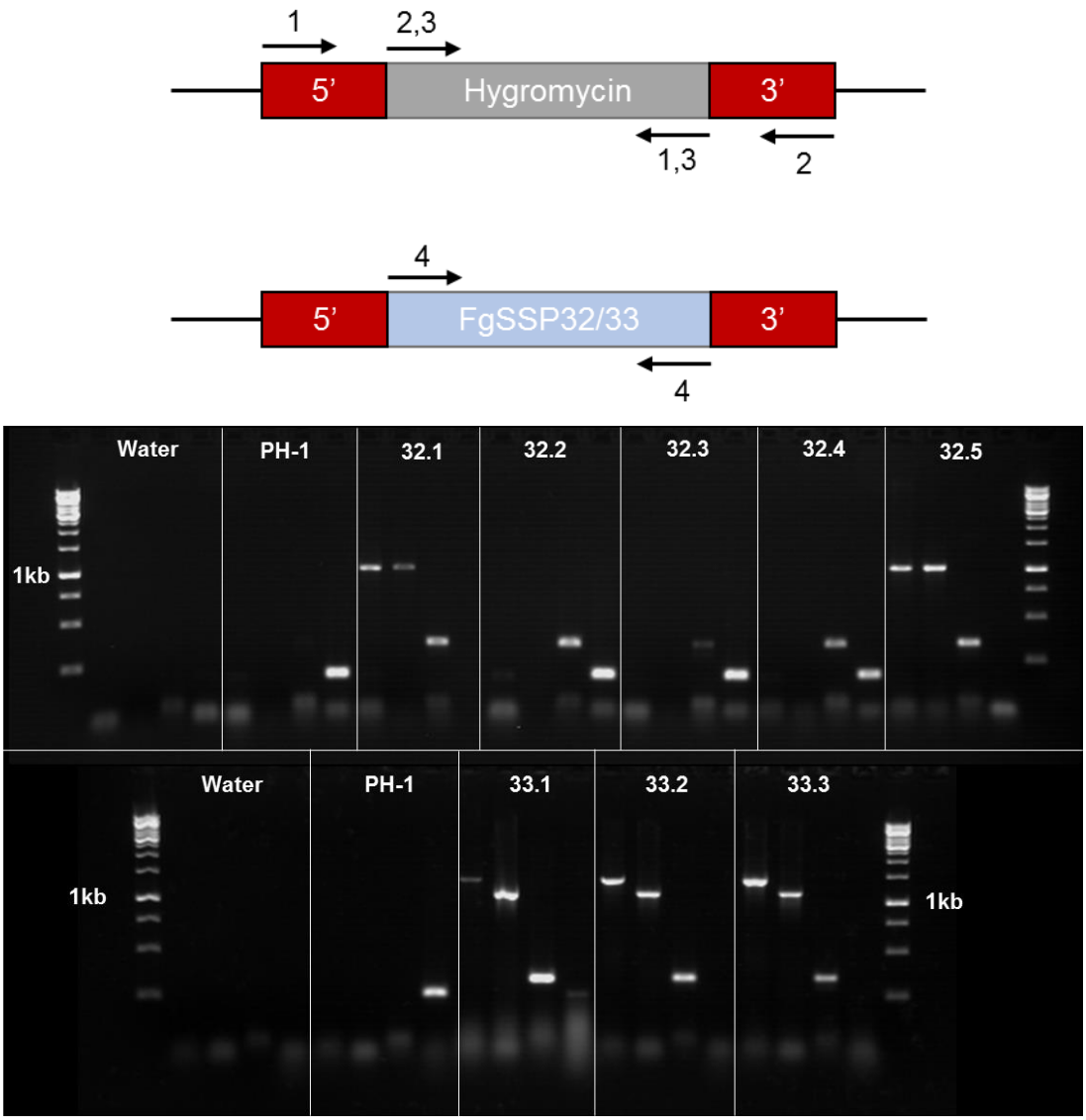

Figure 6.11 Confirmation PCR schematic and analysis of transformed *F. graminearum* FgSSP32 and FgSSP33 gene deletion mutants. For each strain tested four PCR analyses were carried out which amplified: column 1) the 5' flank of the deleted genes; column 2) the 3' flank of the deleted gene; column 3) a fragment within the hygromycin gene and column 4) the deleted gene. Water and the wild-type strain PH-1 were used as controls.

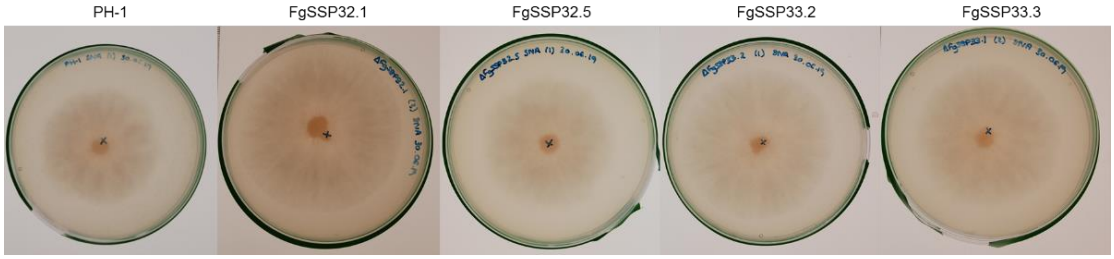

Figure 6.12 Images of representative colony growth on SNA after 5 days of growth.

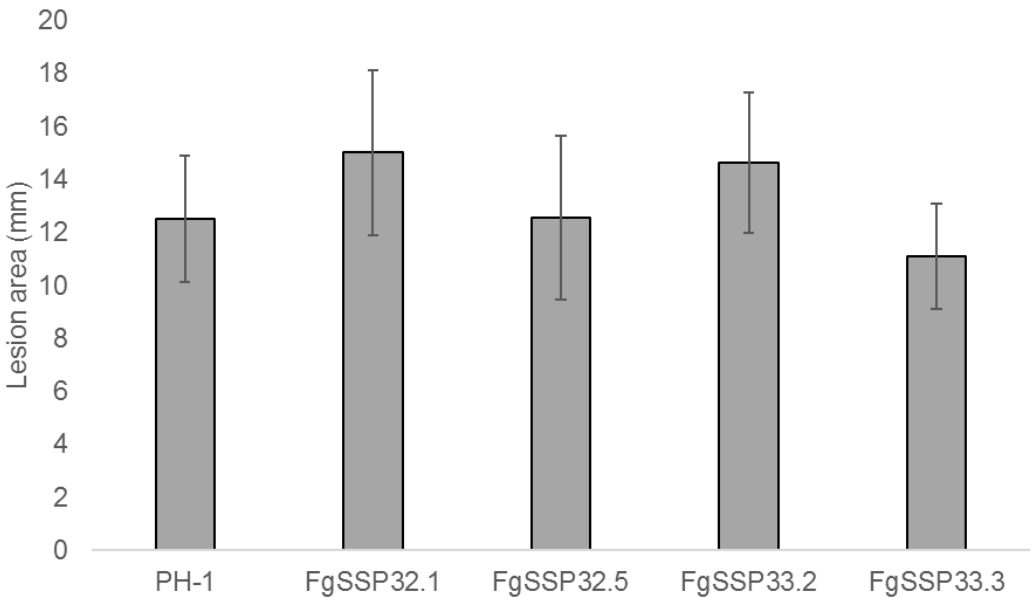

Figure 6.13 Graph showing the average lesion size of coleoptiles infected with *F. graminearum FgSSP32* and *FgSSP33* gene deletions, *ΔFgSSP32.1*, *ΔFgSSP32.5*, *ΔFgSSP33.2* and *ΔFgSSP33.3,* 7dpi. Data analysed by one-way ANOVA and differences between treatments found to be non-significant (p=0.835, S.E.D= 3.77).

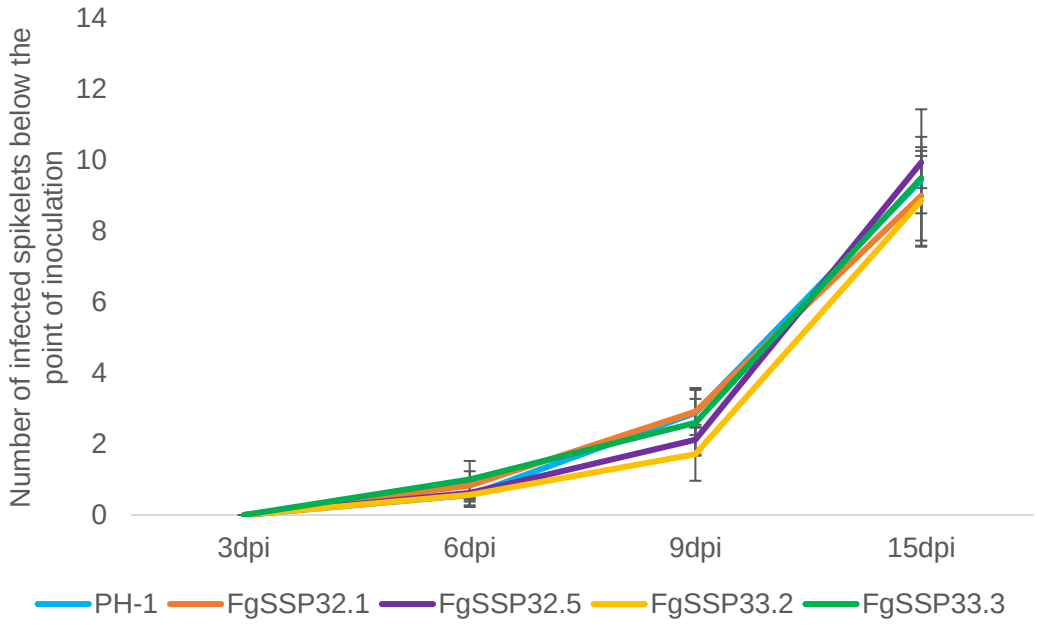

Figure 6.14 Graph showing the number of infected spikelets below the point of inoculation in wheat ears infected with wild-type PH-1 and the gene deletion strains, *ΔFgSSP32.1*, *ΔFgSSP32.5*, *ΔFgSSP33.2* and *ΔFgSSP33.3*. Data was analysed using a generalised linear model and differences between strains were not significant.

6.4 Discussion

In the previous chapters (Chapter 4 & 5), I described the discovery of two novel necrosis-inducing *F. graminearum* effectors which exhibit functionality in both wheat and *N. benthamiana.* When recombinantly expressed in *N. benthamiana,* both proteins induced necrosis which localised to the vasculature – an uncommon phenotype only briefly reported in the literature in two pathosystems (Houterman et al. 2009; Cao et al. 2018; Xu et al. 2008; Feng et al. 2012). Screening of effectors for necrosis-inducing ability is often facilitated by the detection of autofluorescent compounds visible under UV light (Kettles et al. 2017). While detection of these compounds is widely utilised, and these compounds are presumed to be phenylpropanoids, this response has not yet been fully chemically characterised (Dixon and Paiva 1995). In the first part of this chapter, we therefore made efforts to identify these autofluorescent compounds and, following this, took a broader explorative approach to identify compounds induced by FgSSP32 and FgSSP33.

Through HPLC and LCMS analysis, we found that recombinant expression of FgSSP32 and FgSSP33 in *N. benthamiana* induced the production of compounds predicted to be involved in jasmonic acid synthesis such as 12-OPDA. Attempts were made to confirm which compounds were being produced by NMR, however, the peak identified in HPLC and LCMS analysis proved to be very unstable. This instability may be due to the 1-4-diene chemical arrangement present in both 12-OPDA and its isomers. Glutathione is known to exhibit activity towards 1-4-diene arrangements (David Withall, personal communication) and elevated levels of glutathione have been

observed in *N. benthamiana* plants in response to fungal infection (Dean, Goodwin, and Hsiang 2005). It is also possible that, as we did not include a denaturation step in sample preparation, that some plant enzymes remained active in methanol at -20°C and these JA precursors were therefore rapidly degraded or isomerised. All the plausible compounds with a m/z ratio of 291.1955 identified in mass spectral databases were precursors to JA such as 12-OPDA and its isomers. While NMR of the identified compound was unsuccessful, in future experiments, a LCMS approach will be undertaken on 12-OPDA chemical standards to determine if this standard has the same retention time as the peak identified in this study.

While the observation that FgSSP32 and FgSSP33 expression induces JA precursor production in *N. benthamiana* is tentative and yet to be confirmed, hypotheses can be made as to why these proteins induce this pathway. Along with salicylic acid and ethylene, JA and JA derivatives are recognised as major plant defence hormone signals and are produced in response to insect-wounding and necrotrophic pathogens (Glazebrook 2005). A common target of effectors (Jiang, Yao, et al. 2013), the JA signalling network coordinates large scale defence responses including the production of secondary metabolites and defence-related proteins (Hickman et al. 2017). While endogenous JA levels are known to increase during effector-triggered immunity (ETI), ultimately triggering programmed cell death (PCD), the exact role of JA in ETI remains unclear (Kenton et al. 1999; Mur et al. 2006). Studies in *Arabidopsis* have shown that JA pathway mutants are hyper-resistant to *F. graminearum* and that JA signalling in fact facilitates early infection (Makandar et al. 2010; Nalam et al. 2015). In contrast however, JA

is known to directly inhibit *F. graminearum* growth *in vitro* and functional analysis of FHB resistant wheat lines suggests that defence pathways are regulated by JA (Qi et al. 2016; Li and Yen 2008). While 12-OPDA is a cyclopentenone precursor of JA, it is important to note that 12-OPDA is not just a metabolic intermediate but a signalling molecular with overlapping and distinct functions from JA (Taki et al. 2005). While studies have shown that JA is the active signalling molecule in this pathway, treatment of *Arabidopsis* with 12-OPDA induces the expression of specific sets of genes which encode signalling components, transcription factors and stress-related response genes functioning independently of JA signalling (Taki et al. 2005).

As both FgSSP32 and FgSSP33 induce necrosis in *N. benthamiana*, induction of JA may support the hypothesis that FgSSP32 and FgSSP33 trigger ETI via effector recognition by an unidentified NLR (Maekawa, Kufer, and Schulze-Lefert 2011). It is also possible that FgSSP32 and FgSSP33 stimulate JA signalling independently of NLRs. Whether FgSSP32 and FgSSP33 induce JA signalling in wheat remains unknown and these proteins may function differentially in wheat depending on the presence / absence of interacting host proteins. To determine whether FgSSP32 and FgSSP33 induce JA signalling in wheat, it would be useful to develop a transient expression assay in wheat leaves to compare the response between *N. benthamiana* and wheat. If FgSSP32 and FgSSP33 do induce JA in wheat, as the genes encoding FgSSP32 and FgSSP33 are upregulated during the symptomatic / necrotrophic phase of the *F. graminearum*-wheat floral interaction (Chapter 3), FgSSP32 and FgSSP33 may facilitate the symptomatic phase of infection by triggering the JA pathway and inducing

localised cell death. The importance of JA signalling to the induction of the FgSSP32 and FgSSP33-induced necrosis could be explored through the generation of *N. benthamiana* lines deficient in sequential steps of the JA pathway. As previously mentioned, the initial experimental question in this biochemical screen was whether we could identify the autofluorescent compounds which facilitate the widely-used necrotrophic screen. Further work is required to determine whether the JA precursors identified are the autofluorescent compounds detected in cell death screens in *N. benthamiana*. This could be determined through infiltration of *N. benthamiana* with purified 12-OPDA to see whether autofluorescence is detected.

In this study, a polyclonal antibody was raised towards FgSSP33 with the expectation that this antibody would enable the detection of FgSSP33 *in planta*. Unfortunately, *in planta* detection of FgSSP33 in *N. benthamiana* using western blotting failed in these experiments despite validation of this specific antibody using *E. coli* strains recombinantly expressing FgSSP33. If this antibody had been functional in *N. benthamiana,* this could have enabled the identification of FgSSP33 host interactors using a variety of biochemical and MS-based approaches. For instance, tandem affinity purification (TAP) enables rapid purification of protein complexes under native conditions and components within this purified protein complex can then be identified by MS (Adelmant et al. 2019). Alternatively, co-immunoprecipitation (Co-IP) using the FgSSP33-specific antibody could be employed to identify the primary target of FgSSP33 and other interacting proteins – a technique widely employed in effector biology (Kanzaki et al. 2012; Sarris et al. 2015; Fujisaki

et al. 2015). As previously mentioned, several *E. coli* strains were generated which recombinantly expressed both FgSSP32 and FgSSP33 and were used to validate the FgSSP33-specific antibody. These strains could be further exploited for the purification of recombinant FgSSP32 and FgSSP33 and subsequent crystallisation to determine protein structure (Spanu et al. 2018). Alternatively, the FgSSPs could be tagged with fluorescent proteins such as GFP and RFP and antibodies specific to these fluorescent tags could be used to identify interacting proteins.

Despite difficulties detecting FgSSP33 using western blotting techniques, attempts were made to detect and localise FgSSP33 through immunogold labelling. Unfortunately, this also proved unsuccessful due to background labelling in the controls and technical difficulties encountered regarding cleanliness of ultra-fine sections. Throughout immunogold labelling experiments, crystals formed which obscured sub-cellular structures. Attempts were made to identify the source of these crystals which were not present on sections that had not been subject to immunogold labelling. During immunogold labelling, sections are incubated in PBS-Tween, BSA and in primary and secondary antibody. Incubation of sections in PBS-Tween and BSA alone did not lead to the formation of crystals and the introduction of dirt onto the section. As such, we currently hypothesise that the source of crystal formation in these experiments was from the glycerol in which the primary antibody was stored.

While immunodetection of effectors by EM has proven useful for the characterisation of effectors, such as the *U. maydis* effector Cmu1, this approach has several limitations (Djamei et al. 2011) – particularly cost. In

future experiments, FgSSPs should be tagged with fluorophores to enable live cell imaging via confocal microscopy. While the addition of tags such as RFP and GFP was considered during the experimental design process, we were initially concerned that tagging small proteins with large fluorophores may affect functionality and localisation of these proteins. Similarly, Tanaka et al. (2014) speculated that large fluorescent tags fused to effectors expressed in *U. maydis* prevented correct uptake thereby affecting localisation of effectors. While this concern may be valid when tagging effectors within the host fungus, this does not appear to be a problem when expressing effectors in a binary vector as evidenced by the now widespread use of this technique in the effector community (Guo et al. 2019; Asai et al. 2018).

Alongside immunogold labelling, a morphological characterisation of plants expressing FgSSP33 was also undertaken by light microscopy. In plants expressing FgSSP33, an accumulation of unidentified polymers was observed in the intercellular spaces. A similar response was observed in a study undertaken by Dilks et al. (2019) which characterised the wheat response towards *F. graminearum* mutants lacking G protein-coupled receptors. A mutant which exhibited defects in the establishment of the symptomless phase of the *F. graminearum*-wheat floral interaction induced the formation of ‘apoplastic occlusions’ in wheat rachis tissue which are hypothesised to impede infection (Figure 6.15). The ability of FgSSP33 to induce these apoplastic occlusions in *N. benthamiana* demonstrates that similar responses towards *F. graminearum* infection occur in both wheat and *N. benthamiana*. Further work should be undertaken to characterise the

nature of this response to answer 1) what compounds are being produced in these occlusions, 2) what signalling pathways lead to their induction and 3) does the production of these structures facilitate or hinder the symptomatic phase of infection?

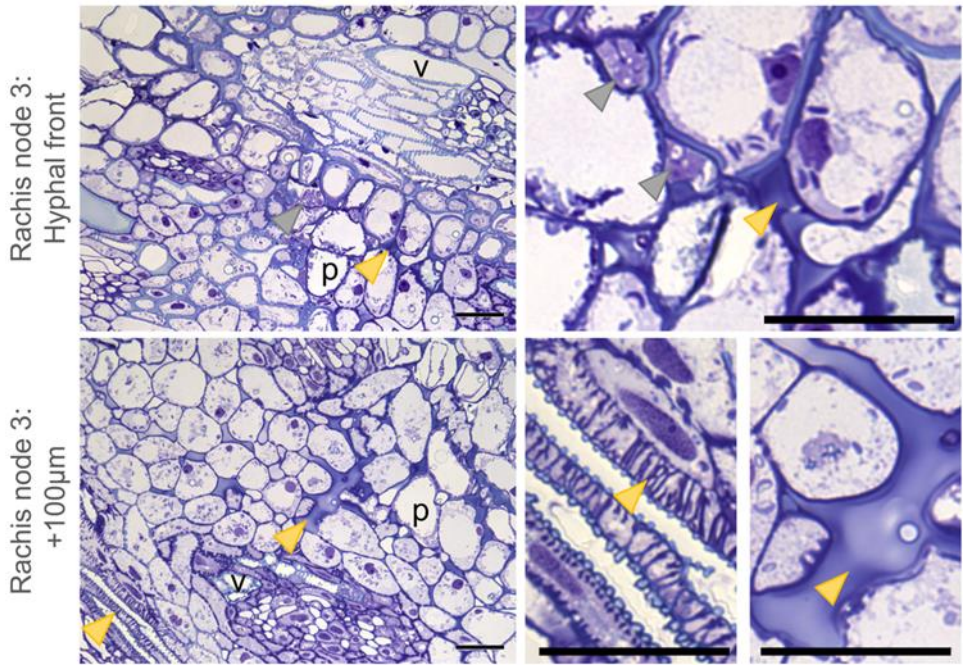

Figure 6.15 Apoplastic occlusions induced in wheat rachis tissues infected with a mutant strain of *F. graminearum* (*ΔFgRRES_16221*) impaired in symptomless infection. Light micrographs of transverse sections of the Δ16221_3 infected 3rd rachis node revealing the appearance of infection at the advancing hyphal front, plus ahead (+100 µm) and behind (-100 µm) the hyphal front. Behind the hyphal front, Δ16221_3 accumulates within intercellular spaces between a mixture of live and dead plant cells. At the hyphal front, a limited amount of intercellular hyphae are surrounded by active live plant cells. In advance of the hyphal front, the plant cells are responding to infection resulting in cell fortifications and the occlusion of the intercellular spaces. Arrows: grey = fungal hyphae, yellow = wheat cells responding to infection. Bar = 50 µm. P = parenchyma. V = vasculature. Figure adapted from Dilks et al. (2019).

Finally, single *FgSSP32* and *FgSSP33* gene deletion *F. graminearum* mutants were generated using a split-marker approach to determine whether *ΔFgSSP32* and *ΔFgSSP33* mutants exhibited any changes in pathogenicity compared to the wild-type strain PH-1 (Catlett et al. 2003). Wheat ear and coleoptile pathogenicity assays revealed that these gene deletions exhibited disease-causing capabilities comparable to PH-1. This is perhaps not surprising considering that identification of *F. graminearum* gene deletions with reduced disease-causing capabilities is rare for sequences coding for secreted proteins (Brown and Hammond-Kosack 2015). This may be attributable to genetic redundancy within the pathosystem as *F. graminearum* encodes more than 200 putative effectors - 36 of which exhibit a similar expression profile to *FgSSP32* and *FgSSP33*. Removal of either FgSSP32 or FgSSP33 from the pathosystem may therefore lead to compensation from other effectors (Brown et al. 2017; Sperschneider et al. 2018). It would be interesting to see whether an *FgSSP32* and *FgSSP33* double mutant exhibits any changes in fungal pathogenicity to overcome genetic redundancy.

In conclusion, in this chapter we report further attempts to biochemically characterise the *N. benthamiana* response to FgSSP32 and FgSSP33. It is highly likely that recombinant expression of FgSSP32 and FgSSP33 leads to the production of JA precursors such as 12-OPDA. While attempts to localise FgSSP33 using specific antibodies were unsuccessful through western blotting and immunogold labelling, a morphological characterisation of *N. benthamiana* recombinantly expressing FgSSP33 revealed that FgSSP33 induces the production of apoplastic occlusions. These occlusions likely

function to restrict the spread of fungal infection. In addition, it was also determined that *FgSSP32* and *FgSSP33* single gene deletions do not exhibit any changes in fungal pathogenicity compared to the wildtype strain which may indicate a degree of functional redundancy in the *F. graminearum*-wheat pathosystem.

Chapter 7 General Discussion

7.1 Summary of key findings

Prior to 2010, *F. graminearum* was considered a classic necrotroph. However, a detailed microscopic investigation of the infection biology of *F. graminearum* in fact revealed that *F. graminearum*, like many other necrotrophs, has a substantial phase of intercellular hyphal growth maintained at the advancing infection front (Brown et al. 2011). The discovery of this symptomless phase provided new insights into the mechanisms utilised by *F. graminearum* during wheat ear infection and a recent transcriptomic investigation exploring biphasic infection further refined our understanding of the *F. graminearum* infection model (Brown et al. 2017). During both the symptomless and symptomatic phases of the *F. graminearum* infection, unique subsets of genes encoding small, secreted proteins, or putative effectors, are upregulated. The aim of this thesis was to therefore refine the model proposed by Brown et al. (2017) further by elucidating the contribution of effectors to infection. In this thesis, I have examined the contribution of several putative *F. graminearum* effectors to fungal pathogenicity in model and non-model host species. Using an array of bioinformatics and functional genomics techniques, I have characterised two *F. graminearum* necrotrophic effectors, FgSSP32 and FgSSP33, which contribute towards the establishment of FHB within the wheat ear. Below, I will outline how we hypothesise these effectors function in relation to our current working model of *F. graminearum* infection and explore the limitations of this study.

7.1.1 The establishment of an effective bioinformatic pipeline for *F. graminearum* effector discovery and future pipeline improvements

In chapter 3, I described the *in silico* techniques used to generate a bioinformatic pipeline for effector discovery. These techniques were used in conjunction with *in planta* transcriptome data exploring *F. graminearum* gene expression during wheat infection and ultimately led to the identification of FgSSP32 and FgSSP32.The genes encoding FgSSP32 and FgSSP33, two *Fusarium*-specific and novel proteins, were found to be upregulated during the symptomatic phase of infection. While both *FgSSP32* and *FgSSP33* are highly expressed during the symptomatic phase of infection and expressed to much lower levels in the symptomless phase, *FgSSP33* was also found to be highly expressed during the 'onset' phase of infection (Figure 3.12b). The 'onset' phase was characterised as the transition between the symptomless and symptomatic phase and the observation that *FgSSP33* is highly expressed in 'onset' rachis tissues may suggest that FgSSP33 facilitates the transition into the symptomatic phase. Overall, the expression profiles of *FgSSP32* and *FgSSP33* led us to hypothesise that these FgSSPs may function in a manner reminiscent of other necrotrophic effectors, facilitating cell death to enable the release of nutrients for fungal sequestration.

Like many other bioinformatic pipelines, one of the most important criteria applied when selecting putative effectors was *in planta* expression. Removal of genes which were more highly expressed *in vitro* than *in planta* reduced the number of candidate effectors from 563 to 439 (Figure 3.2). Interestingly however, while effectors are traditionally defined as being upregulated *in planta,* a recent study by Thomma et al (2019) revealed that this may not

always be the case. Two *Verticillium dahliae* effectors, Ave1 and vAMP2, were both shown to contribute towards pathogenicity despite exhibiting expression profiles contrary to the traditional effector expression profile. While Ave1 is ubiquitously expressed, vAMP2 is only expressed in soil and, as such, these two bona fide effectors would slip through the net of most bioinformatic effector selection pipelines. This discovery raises important questions about the limitations imposed by stringent bioinformatic criteria and, also, brings to light the potential role of effectors in mediating interactions with other microbes. In future, a broader and more integrative approach could be taken for *F. graminearum* effector selection including ubiquitously expressed effectors, effectors expressed *in vitro*, and proteins with less stringent size limits. Identification of candidate effectors could further be bolstered by integration of genomic and metabolomic approaches, rather than sole reliance on bioinformatic prediction. Recently, Zhong et al. (2017) used a combination of genome-wide association studies (GWAS) and classic linkage mapping to identify the *Z.tritici* effector AvrStb6. As whole-genome analysis of large pathogen populations becomes more achievable, exploitation of GWAS to screen for phenotypic variation within the pangenome proffers a powerful method for the discovery of effectors and in addition sheds light on the evolutionary dynamics at effector loci (Sanchez-Vallet et al. 2018).

7.1.2 Using the BSMV-VOX to characterise the role of effectors within the establishment of FHB

In chapter 4, seven of the twenty-four bioinformatically-selected FgSSPs were overexpressed in wheat using the BSMV-VOX system and screened for

the ability to increase or decrease *F. graminearum* pathogenicity. Despite the widespread use of the BSMV-VIGS vector in wheat pathogenomics studies (Lee et al. 2015; Bennypaul et al. 2012; Cakir, Gillespie, and Scofield 2010), there are a paucity of studies which utilise the VOX vector to study the contribution of individual proteins to the pathogenicity of fungi which infect wheat floral tissue. In this study, this system was successfully utilised to identify several FgSSPs – the overexpression of which led to differential *F. graminearum* pathogenicity. Overexpression of FgSSP32 and FgSSP33 led to a consistent, albeit subtle, reduction in the number of infected spikelets thereby suggesting that both proteins contribute towards the establishment of FHB in the wheat ear. As the genes encoding FgSSP32 and FgSSP33 were shown to be upregulated during the symptomatic phase of the *F. graminearum*-wheat floral interaction, we hypothesised that these proteins contribute towards pathogenicity by inducing localised cell death which acts to prime the host for subsequent fungal infection. This hypothesis is supported by the observation that FgSSP32 and FgSSP33 induce vascular-associated necrosis in the non-natural host *N. benthamiana* as described in chapter 5.

Overexpression of FgSSP22, a *Penicillium chrysogenum* antifungal (PAF) protein homologue, also led to a significant decrease in fungal pathogenicity. *FgSSP22* is upregulated during the onset and symptomatic phases of infection and as such is likely to function as a defence-activating effector hence the subsequent decrease in fungal disease symptoms. Previous work undertaken in our group focused on the characterisation of two cerato-platanins (CPs), FgSSP6 and FgSSP7, which are secreted throughout

infection. In contrast to FgSSP32 and FgSSP33, overexpression of FgSSP6 and FgSSP7 led to a significant increase in disease symptoms. FgSSP6 and FgSSP7 were hypothesised to aid adhesion of hyphae to plant cells and to bind chitin fragments released by plant chitinases (Machado, A, thesis). Overexpression of these CPs therefore led to an increase in FHB disease symptoms as they function to hamper PTI. The observation that *FgSSPs* upregulated during different phases of infection have a differential impact on *F. graminearum* pathogenicity in BSMV-VOX experiments lends weight to the hypothesis that these effectors function either biotrophically or necrotrophically in this infection model.

Interestingly, while recombinant expression of FgSSP32 and FgSSP33 in *N. benthamiana* using the pEAQ-HT-DEST3 vector led to the induction of cell necrosis (Chapter 5), none of the proteins overexpressed using the BSMV-VOX vector induced a visible phenotype in *N. benthamiana*. This lack of phenotype may be attributable to a discrepancy in the level of protein expression achieved by each vector as the pEAQ-HT-DEST3 vector is known to drive high and long-lasting expression (Sainsbury, Thuenemann, and Lomonossoff 2009). This, however, was not thoroughly tested and, in future, the multi-spectral imaging utilised in chapter 5 could be used to determine whether overexpression of FgSSPs using the BSMV-VOX vector led to any discernible changes in the spectral profile of *N. benthamiana* leaves.

Through the identification of FgSSP32 and FgSSP33, BSMV-VOX has proven to be a valuable tool for screening *F. graminearum* proteins *in planta*. The generation and full evaluation of transgenic wheat lines overexpressing

seven different FgSSPs would have been both significantly more time-consuming and costly. Despite advances in stable transformation, namely CRISPR-Cas technologies, transient expression using BSMV-VOX still offers the most rapid method of heterologous protein expression in mature wheat. Even so, the BSMV-VOX system has several limitations. Perhaps the most constricting is the size limitation imposed in the BSMV-VOX system, with inserts larger than 160 amino acid resulting in vector instability. In future experiments, the recently developed and improved Foxtail Mosaic Virus vector could be utilised which can be used to express proteins as large as 600 amino acids as described in chapter 4 (Bouton et al. 2018).

A lesser explored limitation of the BSMV-VOX system is the effect of viral infection on subsequent fungal infection. The effect of BSMV infection in these experiments could be threefold. Firstly, the symptoms of BSMV can obscure FHB symptoms which may lead to mis-phenotyping of fungal proteins. To overcome this in the BSMV-VIGS system, with particular focus on the effect that BSMV infection has on the obscuration of FHB symptoms, Buhrow, Clark, and Loewen (2016) developed an attenuated version of the BSMV-VIGS vector. Infection with attenuated BSMV led to a reduction in abscisic acid, JA and SA accumulation upon co-infection with *F. graminearum* when compared to the wild-type BSMV. An attenuated version of the BSMV-VOX vector was tested in our group by Wing-Sham Lee, however, the use of this vector was not found to reduce viral symptoms upon visual inspection (Wing-Sham Lee, personal communication). Secondly, as BSMV accumulates in the wheat ear, BSMV may induce the same defence pathways triggered by *Fusarium* hyphae. RNA-seq analysis of BSMV-

infected *Brachypodium distachyon* revealed that, in a compatible interaction, SA signalling is activated while the genes encoding jasmonate and ethylene-responses are repressed (Wang, Wang, et al. 2017). Tufan et al. (2011) also found that infection with the BSMV-VIGS vector led to the induction of several barley genes implicated in the defence response against fungal pathogens, including *PR1, PR4, PR5, PR10* and *PAL*. The authors of this study also found that wheat was less susceptible to *M. oryzae* following treatment with BSMV:GFP in a VIGS experiment. In addition, viral replication of BSMV takes place in the vesicular invaginations of the chloroplast, damaging chloroplasts and affecting functionality (Torrance et al. 2006; Li et al. 2016). As the sites of SA and JA production, chloroplasts play a critical role in the co-ordination of immune signalling responses to plant pathogens (Grant and Jones 2009; Nomura et al. 2012). Disruption of chloroplast functionality may therefore have an uncharacterised impact on host susceptibility to fungal infection. That said, the lack of an effect on the feeding and colonisation of obligate biotroph fungal rusts suggests that the impacts of BSMV can either be ‘re-corrected’ by certain pathogens or are localised and short lived (Panwar, McCallum, and Bakkeren 2013).

There may also be other uncharacterised interactions occurring in the BSMV-VOX interaction. For example, if a biotrophic effector with defence-suppressing activity is expressed in wheat or *N. benthamiana*, will defence suppression allow for greater viral accumulation, and consequently, differential protein production? The viral titre of wheat ears infected with BSMV strains overexpressing FgSSP32 and FgSSP33 were found to be significantly higher than ears infected with the MCS4D control, contrary to

the previously described hypothesis. This observation leads to question as to why BSMV vectors carrying FgSSP32 and FgSSP33 replicate and accumulate in the wheat ear to a higher level. As FgSSP32 and FgSSP33 are now known to induce the JA pathway, which acts antagonistically to the SA pathway, the repression of SA-associated defences may allow for greater viral accumulation. SA is well known to mediate the outcome of plant-virus interactions and mutations in the SA pathway render plants more susceptible to viral infection (Baebler et al. 2014; Takahashi et al. 2004). Expression of FgSSP32 and FgSSP33 may therefore create a positive feedback loop whereby FgSSP32 and FgSSP33 block SA defences allowing for greater viral accumulation and therefore increase recombinant protein production. These observations reinforce the importance of using the BSMV:MCS4D viral control as the main control when making comparisons between treatments.

Finally, another important limitation of the BSMV-VOX experiments carried out is the lack of definitive proof that the FgSSPs tested are truly being expressed. In this thesis, transcripts of each *FgSSP* from BSMV-infected wheat ears were amplified by RT-PCR. While the transcripts from each *FgSSP* were present in wheat tissues, transcript detection is not a proxy for protein detection – especially as BSMV is an RNA virus (Petty et al. 1989). Previous experiments at Rothamsted have utilised FgSSP-specific antibodies for protein detection which is an extremely costly process which has not proven successful in the past (Machado, A, thesis). Alternatively, a mass-spectrometry (MS)-based approach could be taken to identify overexpressed proteins - a route that should be considered in the future – or,

expression of tagged effectors using the FoMV virus could also aid detection e.g. by using GFP or HA-tag antibodies.

7.1.3 Exploitation of the model species *N. benthamiana* for *F. graminearum* effector screening

In chapter 5, FgSSPs previously characterised using BSMV-VOX were recombinantly expressed in *N. benthamiana* and screened for cell death-inducing activity. While this cell death screen is widely used among the effector community (Kettles et al. 2017; Wei et al. 2007; Bos et al. 2006), prior to the experiments described in this thesis, *F. graminearum* effectors had not been expressed in this model species. The use of this heterologous screen led to the discovery that FgSSP32 and FgSSP33 induce vascular-associated necrosis – a discovery that was further explored in chapter 6. The necrosis induced by FgSSP32 and FgSSP33 in *N. benthamiana* was dependent on the presence of a signal peptide which thereby suggests that secretion of these proteins into the apoplast is essential to their functionality. It may be that cell surface-localised receptors, such as RLKs, RLPs and NLRs, recognise FgSSP32 and FgSSP33 leading to the induction of necrosis.

While heterologous effector expression systems provide a wealth of information about effector function, it is still important to consider the biological relevance of these systems which often focus on the interaction between a pathogen and non-host. For example, while *F. graminearum* can infect *N. benthamiana* under artificial conditions, *N. benthamiana* is not considered a ‘natural host’ of *F. graminearum* (Urban et al. 2002). In some instances, limited conclusions can be drawn from these screens which may

lead to protein misfolding or mis-localisation. Furthermore, *N. benthamiana* may lack critical interactors present in the native system and, as such, sole reliance on heterologous screens will limit our understanding of the true function of effectors in pathogenicity (Lorrain, Petre, and Duplessis 2018).

The vascular-associated phenotype induced by FgSSP32 and FgSSP33 was highly unusual and unexpected. This phenotype has only been reported in the literature twice before, namely the *X. campestris* AvrAC effector and the *F. oxysporum* f. sp. *lycopersici* Avr2 effector are able to induce this response in Arabidopsis and tomato, respectively (Houterman et al. 2009; Xu et al. 2008). Avr2 interacts with the cognate resistance protein I2 (an NBS-LRR protein) to induce vascular-associated cell death leading us to question whether FgSSP32 and FgSSP33 induce necrosis in a similar manner. All known resistance towards *F. graminearum* in wheat is quantitative and, as such, the identification of a single receptor that recognises classic effector proteins is hugely promising. Much more work is required to identify the FgSSP32 and FgSSP33 interacting proteins, most likely using a Y2H or MS-based approach. Further exploration of the vascular-associated phenotype could also be achieved by transcriptomic analysis of *N. benthamiana* plants expressing both FgSSP32 and FgSSP33 to identify the genes differentially expressed in response to these proteins.

Compared to *Arabidopsis*, little is still known about the origins, genetic variation and ecology of the *N. benthamiana* lines used in the research community (Goodin et al. 2008). Despite the rise of *N. benthamiana* as a model system for studying plant-pathogen interactions, the generation of genomic and transcriptomic studies has been slow due to the complex and

large allotetraploid genome (3.1Gb)(Bally et al. 2018). In 2012, two independent draft genomes were assembled which are publicly available online (https://solgenomics.net/ and http://benthgenome.com/)(Bombarely et al. 2012; Naim et al. 2012). Efforts however still need to be made to fill in the sequence gaps between genes to reduce the number of scaffolds and to identify and differentiate the homeologs. As the mode of infection through which *F. graminearum* infects the wheat ear shows high levels of host and tissue specificity, it would be interesting to explore the level of synteny and orthology shared between *N. benthamiana* and wheat – particularly regarding shared immune signalling components.

In chapter 5, efforts were also made to discern the importance of several defence-related genes to the ability of FgSSP32 and FgSSP33 to induce necrosis. A VIGS approach was taken to silence *BAK1*, *SOBIR1* and *SGT1,* however the effect of silencing these genes and the viral symptoms of TRV infection obscured the phenotype induced by FgSSP32 and FgSSP33. The generation of a library of transgenic *N. benthamiana* defence gene mutants would be particularly useful for screening assays looking at the ability of these mutants to recognise FgSSP32 and FgSSP33. For example, *NbEDS1, NbPAD4* and *NbSAG101* mutants have been generated by Ordon et al. (2017) and Gantner et al. (2019) using a GE approach. Backcrossing of these mutant lines to create double, triple and quadruple *N. benthamiana* mutant lines has proven useful for the study of TNL-triggered cell death and pathogen growth restriction (Lapin et al. 2019).

Transient and stable expression of the Cas9 enzyme and guide RNAs has enabled rapid gene editing in *N. benthamiana* leaf tissues (Jiang, Zhou, et al.

2013; Nekrasov et al. 2013). Recently, Ali et al. (2018) developed *N. benthamiana* lines constitutively expressing the Cas9 enzyme and delivered guide RNAs using TRV. This is a highly promising, high throughput system for gene editing although again, in the case of effector studies, TRV infection may obscure phenotyping. As silencing of *BAK1* led to particularly strong developmental defects, it is highly likely that stable *BAK1* mutants would be severely crippled. An alternative method of silencing *BAK1* could be co-infiltration of FgSSP32 and FgSSP33 with a silencing hairpin construct (Johansen and Carrington 2001). Through the implementation of the techniques outlined above, it would be possible to generate a library of *N. benthamiana* lacking specific immune signalling components. Screening FgSSP32 and FgSSP33 in these lines would be an interesting strategy for elucidating the contribution of different immune signalling components to the perception of these proteins.

7.1.4 Application of biochemical and bioimaging approaches for the characterisation of novel *Fusarium* effectors

The establishment of *N. benthamiana* as a suitable system for the characterisation of *F. graminearum* effectors opens numerous avenues regarding further characterisation of these proteins. In chapter 6, a biochemical approach was therefore undertaken to characterise the *N. benthamiana* response towards FgSSP32 and FgSSP33 using a combination of HPLC and MS.

Biochemical analysis of *N. benthamiana* leaves expressing FgSSP32 and FgSSP33 led to the induction of a compound tentatively identified as 12-OPDA. 12-OPDA is the final product of the plastid-localised part of the JA

biosynthesis pathway and is translocated into the peroxisome for JA synthesis (Schaller and Stintzi 2009). The observation that FgSSP32 and FgSSP33 induce the production of compounds involved in JA biosynthesis is perhaps not surprising considering that JA is known to govern defence responses towards necrotrophs and both proteins exhibit necrosis-inducing ability. It is important to note, however, that 12-OPDA does not just function as a metabolic intermediate but as a signalling molecule with overlapping and distinct functions from JA (Taki et al. 2005). For example, 12-OPDA has been shown to play a key role in governing *Arabidopsis* susceptibility towards the root-knot nematode *Meloidogyne hapla*. By using *Arabidopsis* mutants in the JA biosynthetic pathway, the authors of this study showed that, even in the absence of JA, 12-OPDA plays a critical role in defence signalling against nematodes. A similar approach could be undertaken to elucidate the role of 12-OPDA and JA in the induction of the FgSSP32 and FgSSP33-induced response in *N. benthamiana.* For example, JA pathway *N. benthamiana* mutants could be generated through gene editing and screened for loss or retention of FgSSP32 and FgSSP33-induced vascular-associated necrosis.

JA is well known to play a decisive role in the defence response against necrotrophic fungi and contributes towards the partial resistance exhibited by Sumai 3 to FHB (Glazebrook 2005; Li and Yen 2008). Metabolic profiling of the wheat rachis during infection with PH-1 and *ΔTri5* revealed that the spread of the DON-deficient mutant was blocked in a JA-related defence reaction. Induction of JA signalling by FgSSP32 and FgSSP33 prior to *F. graminearum* inoculation may therefore be the mechanism through which

wheat is primed for fungal inoculation in the BSMV-VOX experiments. The ability of FgSSP32 and FgSSP33 to induce 12-OPDA in wheat tissues has not yet however been tested.

While the role of phytohormones in FHB resistance has been well explored, no studies have focused on how *F. graminearum* may manipulate phytohormones in a phase-specific manner. As both biotrophic and necrotrophic effectors are known to act as key modulators of phytohormones, manipulating phytohormone signalling pathways to aid infection, it would be interesting to determine whether JA manipulation is one of the mechanisms utilised by these proteins when contributing to infection in wheat. In the *F. graminearum-Arabidopsis* pathosystem, contrasting conclusions have been drawn from experiments studying the role of JA in this interaction. One study has found that JA signalling mutants are more susceptible to *F. graminearum* infection indicating a role for JA during initial infection and internal colonisation of *Arabidopsis* leaves (Makandar et al. 2010). Furthermore, the authors of this study suggested that during early stages of infection JA signalling contributed towards susceptibility while in the later stages of infection provided resistance (Brewer and Hammond-Kosack 2015).

One of the most interesting discoveries in these experiments was that expression of FgSSP32 and FgSSP33 in *N. benthamiana* leads to the induction of vascular-associated necrosis. This observation led us to hypothesise that these proteins function in the *F. graminearum*-wheat floral interaction by inducing localised cell death within cells in the vascular bundle or in tissues surrounding the vascular tissues in the wheat rachis. Questions

remain, however, as to how this may aid fungal infection and these observations must therefore be placed in the context of the cell biology of *F. graminearum* infection. During wheat ear infection, *F. graminearum* uses the vascular tissue in the rachis and rachilla to spread from spikelet to spikelet, achieving systemic colonisation (Trail 2009). In-depth characterisation of the *F. graminearum* infection pathway using thin sectioning of fixed tissue and light microscopy and was carried out by Brown et al. (2011) and closely explored the process through which *F. graminearum* enters the vasculature. At the advancing infection front, colonisation of the host cortex occurs ahead of vascular colonisation. Behind the advancing infection front, hyphae become abundant in the vasculature tissue and the cortex, growing through the pit fields of thick-walled cells. All cell types of the vasculature are heavily colonised during the late stages of infection and hyphae with a large diameter can be found in the collapsed phloem while smaller hyphae can be found in the xylem. While entry into the vasculature aids systemic colonisation, vascular bundles are also an important link between the developing grain containing the embryo, endosperm and aleurone and the rachis, with colonisation spreading outwards from the vascular tissue to the epidermis (Rittenour and Harris 2010; Guenther and Trail 2005). Secretion of FgSSP32 and FgSSP33 into the apoplast surrounding the vascular tissue may in some way aid intracellular colonisation of these cell types ultimately leading to systemic colonisation.

Efforts were also made in this thesis to localise FgSSP33 using a custom made FgSSP33-specific antibody. Unfortunately, in several *in planta* experiments FgSSP33 was not detectable using the FgSSP33-specific

antibody and in one experiment non-specific bands were detected (Figure 6.8). Attempts were made to use the antibody to carry out immunogold labelling but background labelling within the EV control and poor sample quality meant that comparisons between plants expressing FgSSP33 were not feasible. FgSSP-specific antibody sensitivity issues have been described before, particularly in wheat tissues which may have also contributed to the lack of success in these experiments (Ana Machado, personal communication). In this study, *E. coli* strains were generated which recombinantly expressed FgSSP33. Protein detection using *E. coli* extracts was possible in these strains and it would therefore be interesting to see whether FgSSP33 was detectable in *N. benthamiana* plants infiltrated with these FgSSP33-expressing *E. coli* strains.

One of the biggest challenges in researching effector biology in non-model systems is fungal effector visualisation following secretion from the mycelium into the apoplast (Fudal, Balesdent, and Rouxel 2018). In model systems, live cell imaging of fluorescently tagged effectors provides a powerful method for viewing subcellular localisation and protein movement between cells and between organisms (Van den Ackerveken 2017). For example, Wang, Boevink, et al. (2017) used live cell imaging to visualise the *P. infestans* effectors EPIC1 and Pi04314 during effector secretion providing key insights into the mechanisms of effector translocation. The advantage of this approach is that effectors can be visualised in their native state, secreted directly from the pathogen. This relies upon appropriate fungal transformation techniques being in place to enable tagging of effectors at their native locus and, unfortunately, this technique has proven to be

effective for a very limited number of pathogens (Lo Presti et al. 2015; Giraldo et al. 2013).

Alternatively, visualisation of effectors can be achieved by heterologous expression of fluorescently-tagged fungal effectors in model species and subsequent imaging through confocal microscopy. While a widely used technique for effector localisation, the rationale for not taking this approach in this study was that large fluorescent tags may affect functionality and localisation of small effectors (Tanaka et al. 2014). In future *F. graminearum* effector characterisation pipelines, FgSSPs could be expressed in vectors carrying a range of fluorescent tags to determine whether this would be an appropriate technique for effector localisation.

While immunogold labelling experiments in this study were unsuccessful, morphological characterisation of the host response towards FgSSP33 revealed that FgSSP33 induced the formation of apoplastic occlusions in *N. benthamiana* leaf tissue. While unconfirmed, it is likely that these occlusions are formed from lignin, suberin or another unidentified polymer. A similar response was observed in wheat rachis tissue in response to infection with an *F. graminearum* mutant lacking a class X G protein-coupled receptor (GPCR)(Dilks et al. 2019). This mutant was found to be deficient in the ability to establish the symptomless phase of infection leading to the induction of defences predicted to restrict the spread of fungal hyphae within the wheat rachis. The ability of FgSSP33 to induce the formation of these occlusions indicates that *N. benthamiana* recognises FgSSP33 as a biotic threat supporting the hypothesis that FgSSP33 is recognised by a host receptor. Whether FgSSP32 also induces the formation of apoplastic occlusions has

not been determined and the ability of FgSSP33 to induce these occlusions in wheat has also not yet been tested.

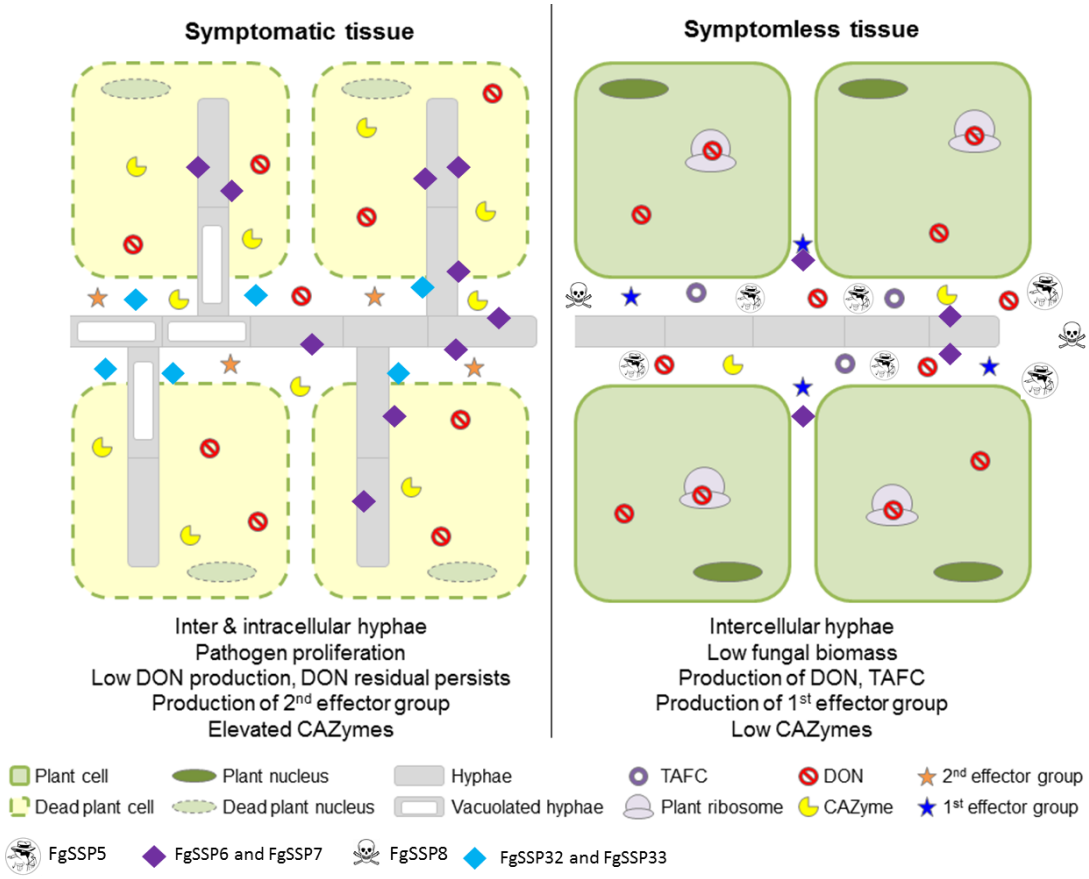

Figure 7.1. A spatial temporal model for *F. graminearum* infection of wheat floral tissue adapted from Brown et al. (2017). The model describes the contribution of DON, TAFC, CAZymes, several previously characterised effectors (FgSSP5, FgSSP6, FgSSP7, FgSSP8) and FgSSP32 and FgSSP33 to the biphasic *F. graminearum* infection process. DON = deoxynivalenol, TAFC = triacetyl fusarinine C; CAZymes = carbohydrate-active enzymes.

7.4 Future work

One of the biggest unanswered questions in this study is whether there are receptor proteins in wheat or *N. benthamiana* or Arabidopsis that recognise FgSSP32 and FgSSP33. The observation that FgSSP32 and FgSSP33 trigger the HR in *N. benthamiana* lends weight to the hypothesis that detection of these proteins by unidentified receptors facilitates this phenotype and may therefore facilitate the phenotype observed in the BSMV-VOX experiments. Interacting proteins could be identified through Y2H or by carrying out a forward genetic screen in *N. benthamiana* as done by Schultink et al. (2019). Identification of a receptor in *N. benthamiana* could then enable the identification of the wheat homologue. A BSMV-VIGS approach could then be taken to see whether silencing the receptor leads to a change in fungal pathogenicity. Alternatively, a bimolecular fluorescence complementation (BiFC) approach could be used to confirm effector and host protein-protein interactions identified using Y2H or MS-based techniques (Lee and Gelvin 2014).

Prior to these experiments, it would be of great interest to determine whether FgSSP32 and FgSSP33 are able to induce necrosis in wheat tissues. During the BSMV-VOX experiments, no necrosis was observed in the wheat ear or in wheat leaves which may be attributable to obscuration of necrosis by viral symptoms or due to the lower levels of protein expression driven by the BSMV-VOX vector compared to the pEAQ-HT-DEST3 vector. Several techniques are available for recombinant protein expression in wheat leaves. Recently, See et al. (2019) expressed two *Pyrenophora tritici-repentis* effectors, ToxA and ToxB, in *E. coli* and in *Pichia pastoris* and the bioactivity

of the effectors was assayed by infiltrating purified protein into young wheat leaves (two weeks old). Expression of effectors in heterologous systems such as this, subsequent purification and assaying for bioactivity is a useful tool for effector characterisation. One of the advantages this technique holds over both VOX and agroinfiltration is that it removes the confounding factor of other biotic stresses e.g. *Agrobacterium* and BSMV. It would have been interesting to see whether infiltration with purified FgSSP32 and FgSSP33 induced cell necrosis, as described in chapter 5, and whether the necrosis induced was dose-dependent. Alternatively, effector delivery in young wheat leaves could be achieved by expression in a non-pathogenic strain of *Pseudomonas fluorescens,* taking advantage of the bacterial type III secretion system (Upadhyaya et al. 2014).

Generation of stable transgenic wheat and *Arabidopsis* lines expressing *FgSSP32* and *FgSSP33* under an inducible promoter could also provide a valuable tool for further characterising these genes. Transcriptomic and metabolomic analysis of uninfected and infected tissues from these transgenic lines would provide great insights into the impact of expression of these proteins on the host. It is possible that constitutive expression of *FgSSP32* and *FgSSP33* using both a weak and a strong promoter could be explored. This may lead to host developmental defects as seen when the *M. larcini-populina* effector Mlp124478 was overexpressed in *Arabidopsis*, likely due to elevated defence levels (Ahmed et al. 2018). Transgenic lines overexpressing FgSSP32 and FgSSP33 could also be used for infection assays to determine whether overexpression leads to enhanced resistance

as seen in the BSMV-VOX experiments and to further characterise this resistance.

In this study, *ΔFgSSP32* and *ΔFgSSP33* single gene deletions did not exhibit any changes in pathogenicity when assayed on wheat ears and coleoptiles. It is therefore likely that *F. graminearum* exhibits some level of functional redundancy regarding effectors. As expression of FgSSP32 and FgSSP33 in both wheat and *N. benthamiana* induces the same phenotype, it would be interesting to see whether an *F. graminearum ΔFgSSP32 ΔFgSSP33* double mutant would behave in these pathogenicity assays. It is possible that removing both proteins from the pathosystem would lead to a reduction in pathogenicity. Alongside this work, an *in planta* transcriptomic analysis could be taken on *F. graminearum* mutants to see how the expression of other effector changes when FgSSP32 and FgSSP33 are removed from the pathosystem. The generation of *F. graminearum* lines constitutively overexpressing FgSSP32 and FgSSP33 could also be utilised in several assays. Overexpression in both wild-type strains and the *ΔTri5* mutant may shed some light onto how these effectors compensate for the loss of DON production.

7.4.2 What role does FgSSP22 play in *F. graminearum* infection?

One of the FgSSPs characterised in both the BSMV-VOX and *N. benthamiana* experiments was FgSSP22 – a protein containing a predicted antifungal domain from *P. chrysogenum*. In two of three BSMV-VOX experiments, overexpression of FgSSP22 led to a significant reduction in fungal disease symptoms and further replication is therefore required to determine whether this reduction is consistent. As FgSSP22 is secreted

during the symptomatic phase of the *F. graminearum*-wheat floral interaction, the observation that overexpression of this protein leads to a reduction in fungal symptoms is in-keeping with our current hypothesis that premature expression of symptomatic effectors primes wheat for subsequent fungal inoculation. While recombinant expression of FgSSP22 in *N. benthamiana* did not lead to visible necrosis, a slight yellowing of the leaf was observed. However, this phenotype was not quantified or explored further. At a later stage in this experiment, multispectral imaging was used to quantify the host response towards recombinant expression of FgSSP32 and FgSSP33. In future. This approach should be taken to probe the response observed in leaves expressing FgSSP22.

The *P. chrysogenum* PAF homologue is one of the most well studied antifungal proteins and has been shown to disrupt Ca^{2+} signalling and homeostasis, the continued disturbance of which can trigger PCD (Binder et al. 2010). While FgSSP22 failed to induce PCD in *N. benthamiana*, it is possible, although highly speculative, that FgSSP22 may disrupt Ca^{2+} signalling leading to the appearance of chlorosis. The importance of Ca^{2+} signalling to plant immunity is well-established and disruption of this signalling has been shown to result in chlorosis in *Arabidopsis* (Du et al. 2009). To explore this hypothesis further, transgenic *Arabidopsis* lines could be generated which overexpress FgSSP22 and tested for morphological differences and enhanced disease resistance or susceptibility to *F. graminearum* and other pathogens. In addition, transgenic *Arabidopsis* lines expressing aequorin markers, facilitating *in vivo* calcium measurements,

could be infiltrated with FgSSP22 to see whether any changes in Ca^{2+} signalling occurs (Mehlmer et al. 2012).

7.5 Conclusions

As the severity of FHB epidemics are strongly influenced by meteorological factors, climate change is predicted to acutely intensify the risk of these epidemics, further compromising small grain security and safety (Vaughan, Backhouse, and Del Ponte 2016). As FHB is responsible for worldwide small grain yield losses amounting to more than a billion dollars a year, the development of durable and sustainable disease control measures is integral to stable food systems (Wegulo et al. 2015). Unfortunately, current disease control strategies are limited due to the complex genetics of disease resistance and the inefficacy of available fungicides. Greater understanding of the molecular interactions underpinning *F. graminearum* infection will be integral to the establishment of novel disease management strategies. Identification of novel fungal effector targets that contribute towards *F. graminearum* pathogenicity could become chemical or RNAi fungicide targets and, furthermore, an effectoromics approach could be taken to identify interacting host proteins.

The results generated in this thesis contribute towards a greater understanding of the molecular mechanisms underpinning *F. graminearum* pathogenicity. The discovery that two necrotrophic effectors, FgSSP32 and FgSSP33, secreted during the symptomatic phase of *F. graminearum* infection contribute towards fungal pathogenicity on wheat supports the current model for infection proposed by Brown et al. (2017). FgSSP32 and FgSSP33 represent the first classic, small, cysteine-rich proteinaceous

effectors discovered and characterised in *F. graminearum*. Characterisation of these effectors involved a range of functional genomics techniques. The coupling of BSMV-VOX and the *N. benthamiana* heterologous expression screen combined high-throughput experiments with biological relevance, offering a global view of how effectors function in host and non-host systems. The functionality of FgSSP32 and FgSSP33 in *N. benthamiana* opens many avenues regarding further characterisation of these proteins; avenues, which if well exploited, may lead to the identification of interacting host proteins which could contribute towards FHB resistance breeding programmes.

Appendix 1: Primers used in this study

Table 1.1 Sequences underlined are adaptor sequences for ligation-independent cloning (LIC).

Primer name	Sequence: 5'-3'	Orientation	Application
FgActin_qPCR_F	ATGGTGTCACTCACGTTGTCC	F	qPCR normalisation
FgActin_qPCR_R	CAGTGGTGGAGAAGGTGTAACC	R	qPCR normalisation
FgSSP14_qPCR_F	TTCTTTGTCTTCCATCTCGCCA	F	qPCR analysis of FgSSP14
FgSSP14_qPCR_R	CCTTGCATCTTCCATAGGAGCA	R	qPCR analysis of FgSSP14
FgSSP17_qPCR_F	CTTTCCATTCTCACTTTCGCCC	F	qPCR analysis of FgSSP17
FgSSP17_qPCR_R	TGGTCTTCCAGTTGTAGCTGAC	R	qPCR analysis of FgSSP17
FgSSP23_qPCR_F	CGTCGATATCGTCAAGTCTGGT	F	qPCR analysis of FgSSP23
FgSSP23_qPCR_R	GAGTTGTTGAGAACCGCCTTTC	R	qPCR analysis of FgSSP23
FgSSP24_qPCR_F	AGCAGCAACAAGAACATCAACG	F	qPCR analysis of FgSSP24
FgSSP24_qPCR_R	AGGCTGAATGTGACTTGGTTCT	R	qPCR analysis of FgSSP24
FgSSP26_qPCR_F	GGGCTTTTTCGACCAGATGTTC	F	qPCR analysis of FgSSP26
FgSSP26_qPCR_R	TCAGGGCAGAGGTATTTATCGC	R	qPCR analysis of FgSSP26
FgSSP30_qPCR_F	GCTACGTGGTCAGAGTACATGG	Anti-sense	qPCR analysis of FgSSP30
FgSSP30_qPCR_R	AGCAAATATCCTGGTAGTCGCC	Sense	qPCR analysis of FgSSP30
FgSSP32_qPCR_F	GCTCTCATCGGCTCTTCTACAG	Anti-sense	qPCR analysis of FgSSP32

FgSSP32_qPCR_R	AGTCCAGTACTCCAGTTGCAAG	Sense	qPCR analysis of FgSSP32
FgSSP33_qPCR_F	TTGTCAGCATCTTGGCTATTGC	Anti-sense	qPCR analysis of FgSSP33
FgSSP33_qPCR_R	ACATTCAGATTTGCAAGGCTCG	Sense	qPCR analysis of FgSSP33
LIC_FgSSP22_F	CCAACCCAGGACCGTTGATGCAGTTCTCAACTATCATTCCT	Sense	Cloning FgSSP22 for VOX
LIC_FgSSP22_R	AACCACCACCACCGCTATTAGTAGCAGGTGAGCGCTT	Anti-sense	Cloning FgSSP22 for VOX
LIC_FgSSP22-SP_F	CCAACCCAGGACCGTTGATGACCCCCGTCAACTCTCCAGC	Sense	Cloning FgSSP22-SP for VOX
LIC_FgSSP23_F	CCAACCCAGGACCGTTGATGCGTTTCGTCAACCTCAT	Sense	Cloning FgSSP23 for VOX
LIC_FgSSP23_R	AACCACCACCACCGCTATTAATAGCCAGTTGACTCAATCCC	Anti-sense	Cloning FgSSP23 for VOX
LIC_FgSSP24_F	CCAACCCAGGACCGTTGATGCACTTCACTACCTTCCT	Sense	Cloning FgSSP24 for VOX
LIC_FgSSP24_R	AACCACCACCACCGCTATTAGACGGAGTATTGACAGG	Anti-sense	Cloning FgSSP24 for VOX
LIC_FgSSP26_F	CCAACCCAGGACCGTTGATGCGCTATATCATCGCCTT	Sense	Cloning FgSSP26 for VOX
LIC_FgSSP26_R	AACCACCACCACCGCTATCACAGTAGGCCTTTTCGTG	Anti-sense	Cloning FgSSP26 for VOX
LIC_FgSSP30_F	CCAACCCAGGACCGTTGATGTTCCCCACCATGAACCT	Sense	Cloning FgSSP230 for VOX
LIC_FgSSP30_R	AACCACCACCACCGCTATTAGCAAATATCCTGGTAGTCGC	Anti-sense	Cloning FgSSP30 for VOX
LIC_FgSSP32_F	CCAACCCAGGACCGTTGATGCAGTTCAGCTCTACTTTCCT	Sense	Cloning FgSSP32 for VOX
LIC_FgSSP32 R	AACCACCACCACCGCTATTAGCGTTGAGGCTGAGAGC	Anti-sense	Cloning FgSSP32 for VOX

LIC_FgSSP32-SP_F	CCAACCCAGGACCGTTGATGCAGGGCAACGGACTC	Sense	Cloning FgSSP32-SP for VOX
LIC_FgSSP33_F	CCAACCCAGGACCGTTGATGCAGTTCTCTATTGTCAGCATC	Sense	Cloning FgSSP33 for VOX
LIC_FgSSP33_R	AACCACCACCACCGCTAACATGTGCACTTGGCCA	Anti-sense	Cloning FgSSP33 for VOX
LIC_FgSSP33-SP_F	CCAACCCAGGACCGTTGATGGCTCCTAAAGCCGCTTG	Sense	Cloning FgSSP33-SP for VOX
LIC_FgSSP22_F	CCAACCCAGGACCGTTGATGCAGTTCTCAACTATCATTCCT	Sense	Cloning FgSSP22 for VOX
LIC_FgSSP22_R	AACCACCACCACCGCTATTAGTAGCAGGTGAGCGCTT	Anti-sense	Cloning FgSSP22 for VOX
LIC_FgSSP22-SP_F	CCAACCCAGGACCGTTGATGACCCCCGTCAACTCTCCAGC	Sense	Cloning FgSSP22-SP for VOX
LIC_FgSSP23_F	CCAACCCAGGACCGTTGATGCGTTTCGTCAACCTCAT	Sense	Cloning FgSSP23 for VOX
LIC_FgSSP23_R	AACCACCACCACCGCTATTAATAGCCAGTTGACTCAATCCC	Anti-sense	Cloning FgSSP23 for VOX
LIC_FgSSP24_F	CCAACCCAGGACCGTTGATGCACTTCACTACCTTCCT	Sense	Cloning FgSSP24 for VOX
LIC_FgSSP24_R	AACCACCACCACCGCTATTAGACGGAGTATTGACAGG	Anti-sense	Cloning FgSSP24 for VOX
LIC_FgSSP26_F	CCAACCCAGGACCGTTGATGCGCTATATCATCGCCTT	Sense	Cloning FgSSP26 for VOX
LIC_FgSSP26_R	AACCACCACCACCGCTATCACAGTAGGCCTTTTCGTG	Anti-sense	Cloning FgSSP26 for VOX
LIC_FgSSP30_F	CCAACCCAGGACCGTTGATGTTCCCCACCATGAACCT	Sense	Cloning FgSSP230 for VOX
LIC_FgSSP30_R	AACCACCACCACCGCTATTAGCAAATATCCTGGTAGTCGC	Anti-sense	Cloning FgSSP30 for VOX

Agro_Nb_FgSSP22_F	GGGGACAAGTTTGTACAAAAAAGCAGGCTTAATGCAGTTCTCAACTATCATTCCT	Anti-sense	Gateway cloning of FgSSP22 for recombinant protein expression
Agro_Nb_FgSSP22_R	GGGGACCACTTTGTACAAGAAAGCTGGGTATTAGTAGCAGGTGAGCGCTT	Sense	Gateway cloning of FgSSP22 for recombinant protein expression
Agro_Nb_FgSSP26_F	GGGGACAAGTTTGTACAAAAAAGCAGGCTTAATGCGCTATATCATCGCCTT	Anti-sense	Gateway cloning of FgSSP26 for recombinant protein expression
Agro_Nb_FgSSP26_R	GGGGACCACTTTGTACAAGAAAGCTGGGTATCACAGTAGGCCTTTTCGTGC	Sense	Gateway cloning of FgSSP26 for recombinant protein expression
Agro_Nb_FgSSP30_F	GGGGACAAGTTTGTACAAAAAAGCAGGCTTAATGTTCCCCACCATGAACCTC	Anti-sense	Gateway cloning of FgSSP30 for recombinant protein expression
Agro_Nb_FgSSP30_R	GGGGACCACTTTGTACAAGAAAGCTGGGTATTAGCAAATATCCTGGTAGTCGCC	Sense	Gateway cloning of FgSSP30 for recombinant protein expression
Agro_Nb_FgSSP32_F	GGGGACAAGTTTGTACAAAAAAGCAGGCTTAATGCAGTTCAGCTCTACTTTCCT	Anti-sense	Gateway cloning of FgSSP32 for recombinant protein expression
Agro_Nb_FgSSP32_R	GGGGACCACTTTGTACAAGAAAGCTGGGTATTAGCGTTGAGGCTGAGAGC	Sense	Gateway cloning of FgSSP32 for recombinant protein expression
Agro_Nb_FgSSP33_F	GGGGACAAGTTTGTACAAAAAAGCAGGCTTAATGCAGTTCTCTATTGTCAGCA	Anti-sense	Gateway cloning of FgSSP33 for recombinant protein expression
Agro_Nb_FgSSP33_R	GGGGACCACTTTGTACAAGAAAGCTGGGTACTAACATGTGCACTTGGCCAG	Sense	Gateway cloning of FgSSP33 for recombinant protein expression
Agro_Nb_FgSSP32-SP_F	GGGGACAAGTTTGTACAAAAAAGCAGGCTTAATGCAGGGCAACGGACTC	Anti-sense	Gateway cloning of FgSSP32-SP for recombinant protein expression
Agro_Nb_FgSSP33-SP_F	GGGGACAAGTTTGTACAAAAAAGCAGGCTTAATGGCTCCTAAAGCCGCTTG	Anti-sense	Gateway cloning of FgSSP33-SP for recombinant protein expression
PGEM_LB_FgSSP32_F	CCGCGGGAATTCGATGCTTCATCAACAGTACCC	Anti-sense	Amplification of 5' flank of FgSSP32 for gene deletion

FgSSP32_LB_HY_R	GTTATCGAATTTGTCTCAATGCAAGTAAGAC	Sense	Amplifying 5' flank of FgSSP32 for gene deletion
FgSSP32_LB_HY_F	TTGAGACAAATTCGATAACTGATATTGAAGGAGCATTTTTT	Anti-sense	Amplifying 5' two thirds of hygromycin for FgSSP32 gene deletion
HY_PGEM_R	GCGAATTCACTAGTGATGGATGCCTCCGCTCGAAG	Sense	Amplifying 5' two thirds of hygromycin for FgSSP32 gene deletion
PGEM_YG_F	CCGCGGGAATTCGATCGTTGCAAGACCTGCCTG	Anti-sense	Amplifying 3' flank of FgSSP32 for gene deletion
YG_FgSSP32_RB_R	GAATACCATCTCGAGGTCGACGGTATC	Sense	Amplifying 3' flank of FgSSP32 for gene deletion
YG_FgSSP32_RB_F	ACCTCGAGATGGTATTCGAACGATTAGC	Anti-sense	Amplifying 3' two thirds of hygromycin for FgSSP32 gene deletion
FgSSP32_RB_PGEM_R	GCGAATTCACTAGTGATTGTTTGTATCCCCTATGG	Sense	Amplifying 3' two thirds of hygromycin for FgSSP32 gene deletion
PGEM_LB_FgSSP33_F	CCGCGGGAATTCGATCCGAAAAGGATGGGGCTG	Anti-sense	Amplifying 5' flank of FgSSP33 for gene deletion
FgSSP33_LB_HY_R	GTTATCGAATTGATAATTGGATAGATTGTTTAAATTGTTTC	Sense	Amplifying 5' flank of FgSSP33 for gene deletion
FgSSP33_LB_HY_F	CCAATTATCAATTCGATAACTGATATTGAAGGAGCATTTTTT	Anti-sense	Amplifying 5' two thirds of hygromycin for FgSSP33 gene deletion
HY_PGEM_R	GCGAATTCACTAGTGATGGATGCCTCCGCTCGAAG	Sense	Amplifying 5' two thirds of hygromycin for FgSSP33 gene deletion
PGEM_YG_F	CCGCGGGAATTCGATCGTTGCAAGACCTGCCTG	Anti-sense	Amplifying 3' flank of FgSSP33 for gene deletion
YG_FgSSP33_RB_R	CAGACACACATCTCGAGGTCGACGGTATC	Sense	Amplifying 3' flank of FgSSP33 for gene deletion
YG_FgSSP33_RB_F	ACCTCGAGATGTGTGTCTGGATATGATGG	Anti-sense	Amplifying 3' two thirds of hygromycin for FgSSP33 gene deletion

FgSSP33_RB_PGEM_R	GCGAATTCACTAGTGATATTCGAATTGCTGGGGTG	Sense	Amplifying 3' two thirds of hygromycin for FgSSP33 gene deletion

Appendix 2: Bioinformatics outputs

Table 1. Expression profiles of candidate *FgSSPs* in publicly other transcriptome datasets.

FgSSP	IN2 RPKM[1]	IN3 RPKM[1]	IN2 rank[2]	IN3 rank [2]	*ΔTri6*[3]	*ΔTri10*[3]	*ΔFgp1 in vitro*[4]	*ΔFgp1 in planta*[4]	Wheat ear-PH-1[5]	Wheat coleoptile-PH1[6]	Barley spikes-Butte86AD[7]
FgSSP13	2.01	0	9070	11297	Up	-	-	-	Mock	64h	48hr
FgSSP14	6.59	3.63	7523	8543	Up	-	Up	Up	Mock	0h	Mock
FgSSP15	95.46	38.90	1593	3547	Up	-	-	Down	144hr	40h	144hr
FgSSP16	11.28	14.15	6673	6251	Down	Down	Up	-	96hr	240h	144hr
FgSSP17	19.63	5.46	5437	7970	-	-	Down	-	48hr	40h	144hr
FgSSP18	101.02	169.92	1521	953	Up	Up	Down	Down	192hr	64h	96hr
FgSSP19	316.44	98.51	502	1639	-	-	Up	Down	48hr	64h	96hr
FgSSP20	23.30	56.10	4970	2643	-	-	-	Down	96hr	64h	96hr
FgSSP21	1271.66	1703.91	162	121	Down	Down	-	Down	96hr	64h	72hr
FgSSP22	106.50	1037.54	1454	201	Down	Down	-	Down	96hr	64h	144hr
FgSSP23	34.02	59.39	3864	2518	Up	-	-	-	Mock	16h	24h
FgSSP24	3886.19	2374.52	18	65	Up	-	Down	-	72hr	64hr	72hr
FgSSP25	64.73	732.94	2307	275	Up	Up	Up	Up	48hr	40h	24hr
FgSSP26	81.46	47.50	1883	3013	-	-	-	-	96hr	64h	72hr

FgSSP27	8.73	1.26	7102	9844	-	Up	Up	Up	Mock	16h	24hr
FgSSP28	99.72	134.33	1539	1226	-	-	Down	-	48hr	YPD	72hr
FgSSP29	16.63	17.14	5864	5804	-	Up	Up	Up	144hr	64h	144hr
FgSSP30	8.614	294.69	7120	579	-	-	-	Down	192hr	64h	144hr
FgSSP31	254.19	200.40	611	817	Up	Up	-	-	48hr	16h	24hr
FgSSP32	n.d	n.d	n.d	n.d	-	-	-	n.d	96hr	240h	Water
FgSSP33	n.d	n.d	n.d	n.d	Up	Up	Up	n.d	96hr	64h	96hr
FgSSP34	n.d	n.d	n.d	n.d	-	Up	Down	n.d	48hr	16h	24hr
FgSSP35	n.d	n.d	n.d	n.d	-	-	-	n.d	Mock	40h	Water
FgSSP36	n.d	n.d	n.d	n.d	-	Up	-	n.d	48hr	64h	24hr
FgSSP6	1057.81	2564.79	192	56	-	-	Up	Up	72hr	0h	96hr
FgSSP7	148.82	1187.15	1049	178	-	-	Up	Up	96hr	40h	72hr
TRI4	8855.36	4942.54	1	13	Down	Down	Down	Down	72hr	40h	72hr
TRI5	4289.99	1804.19	16	111	Down	Down	Down	Down	72hr	YPD	72hr

[1] Data from an RNA-seq experiment exploring gene expression in IN2 and IN3 below the point of inoculation 5dpi. IN3 represents the symptomless phase of infection and IN2 the symptomatic. IN= internode sample.

[2] RNA-seq data ranked on expression with the lowest number being the most highly expressed gene in the transcriptome.

[3] Up and down signifies up- or downregulation of *FgSSPs* in the *ΔTri6* and *ΔTri10* transcription factor mutants compared to wild-type PH-1 *in vitro* (Seong et al. 2009a).

[4] Up and down signifies up- or downregulation of *FgSSPs* in *ΔFgp1* mutant in both *in vitro* and *in planta* conditions (Jonkers et al. 2012).

[5] Time during which *FgSSP* expression peaks during a wheat ear-PH-1 time-course experiment running from 24h, 48h, 72h, 96h, 144h, and 192h inoculation (Lysoe, Seong, and Kistler 2011). The mock used in this experiment was a wheat ear infected with water.

[6] Time during which *FgSSP* expression peaks during a wheat coleoptile-PH-1 time-course experiment running from 0h, 16h, 40h and 64h after inoculation (Zhang et al. 2012a). In vitro comparisons were made to *F. graminearum* cultured in YPD.

[6] Time during which *FgSSP* expression peaks during a barley spike-*F. graminearum* (Butte86AD isolate) time-course experiment running from 24h, 48h, 72h, 96h, and 144h after inoculation. The mock used in this experiment was a wheat ear infected with water.

N.d. = no data available.

Colour represents phase during which FgSSPs are upregulated. Blue = highly expressed in mocks or *in vitro*. Green = highly expressed during earlier stages of infection. Yellow = highly expressed during mid-infection. Red = highly expressed during later stages of infection.

Table 2 Transcriptomic profiles of *FgSSP* candidates exploring gene expression in *F. graminearum*-infecting both living and dead wheat tissues (Boedi et al. 2016).

FgSSP	Peak expression[1]	Dead vs Media[2]		Dead vs Live[3]		Live vs Media[4]	
		Log fold change	Upregulated in	Log fold change	Upregulated in	Log fold change	Upregulated in
FgSSP13	Symptomless	5.583870454	Media	-3.964126574	Dead	0.043372982	Media
FgSSP14	Symptomless	1.721201639	Media	-0.605404946	Dead	1.042994641	Media
FgSSP15	Symptomless	0.883138057	Media	2.149779769	Live	3.129038537	Media
FgSSP16	Symptomatic	6.551764222	Media	1.238940523	Live	5.900707501	Media
FgSSP17	Symptomless	-7.876292687	Dead	5.4604417	Live	-2.557803048	Live
FgSSP18	Symptomatic	-1.303769693	Dead	3.624588635	Live	2.340645362	Media
FgSSP19	Symptomatic	7.103422172	Media	-5.18529928	Dead	1.885239832	Media
FgSSP20	Symptomatic	9.045524704	Media	-3.274641662	Dead	5.616997985	Media
FgSSP21	Symptomatic	0.987893508	Media	1.327481409	Live	2.402160316	Media
FgSSP22	Onset	8.726165773	Media	-7.232352765	Dead	0.683975107	Media
FgSSP23	Symptomless	-0.332303029	Dead	0.516799726	Live	0.290859405	Media
FgSSP24	Symptomless	-2.120886962	Dead	0.713277842	Live	-1.305203707	Live
FgSSP25	Symptomatic	-4.46240081	Dead	2.344460368	Live	-1.957659043	Live
FgSSP26	Symptomless	-0.769674443	Dead	0.541992616	Live	-0.113341	Live
FgSSP27	Symptomless	-2.034515791	Dead	1.537706008	Live	-0.06287093	Live
FgSSP28	Onset	0.355640736	Media	-1.772889647	Dead	-1.299105328	Live
FgSSP29	Symptomatic	5.057999218	Media	-3.308507002	Dead	1.27591992	Media
FgSSP30	Onset	7.940667931	Media	-5.910499523	Dead	0.043372982	Media
FgSSP31	Symptomless	4.205216333	Media	1.447012536	Live	3.276539213	Media
FgSSP32	Symptomatic	4.300038022	Media	-0.315925384	Dead	2.388329244	Media
FgSSP33	Symptomatic	-1.022927439	Dead	-1.142656552	Dead	-2.020356588	Live

FgSSP34	Symptomless	-0.176430546	Dead	4.401122229	Live	4.272019394	Media
FgSSP35	Symptomless	8.503940062	Media	-5.220246601	Dead	n.d.	n.d.
FgSSP36	n.d	n.d	n.d	n.d	n.d	n.d	n.d
FgSSP6	Symptomatic	-0.139918032	Dead	-0.334239652	Dead	-0.361265758	Live
FgSSP7	Symptomatic	-0.624408228	Dead	-2.987678635	Dead	-3.482781599	Live
Tri4	Symptomless	-8.259672289	Dead	5.885103398	Live	-2.226887777	Live
Tri5	Symptomless	-7.929661657	Dead	5.853327533	Live	-2.15602048	Live

[1] Peak expression indicates the phase during which candidate FgSSP expression peaks in the Brown et al. (2017) dataset.

[2] Comparison in gene expression between *F. graminearum* infecting dead tissue vs. gene expression in *vitro.*

[3] Comparison in gene expression between *F. graminearum* infecting dead tissue vs. *F. graminearum* infecting live tissue.

[4] Comparison in gene expression between *F. graminearum* infecting live tissue vs. gene expression in *vitro.*

Table 3 Number of synonymous and non-synonymous mutations present within the FgSSP coding sequences in the *F. graminearum* pangenome.

Host[1]	Maize			Wheat			Wheat			Wheat			Wheat			Wheat		
Location[2]	USA[3]			RS[4]			RS			RS			RS			RS		
Disease level	+++			+++			+++			+++			+			++		
Year isolated	1996			2007			2009			2009			2010			2007		
Strain name	PH-1			CML3064			CML3065			CML3066			CML3067			CML3068		
SNP/INDEL	Syn[5]	Nonsyn[6]	Freq[7]	Syn	Nonsyn	Freq	Syn	Nonsyn	Freq	Syn	Nonsyn	Freq	Syn	Nonsyn	Freq	Syn	Nonsyn	Freq
FgSSP13	0	0	0	0	1	2.604	0	0	0	0	1	2.604	0	1	2.604	0	1	2.604
FgSSP14	0	0	0	0	0	0	0	0	0	0	0	0	0	0	0	0	0	0
FgSSP15	0	0	0	0	0	0	0	0	0	0	0	0	0	0	0	0	0	0
FgSSP16	0	0	0	1	0	3.367	1	0	3.367	1	0	3.367	1	0	3.367	1	0	3.367
FgSSP17	0	0	0	0	0	0	0	0	0	0	0	0	0	0	0	0	0	0
FgSSP18	0	0	0	1	1	4.505	1	0	2.252	1	1	4.505	1	1	4.505	1	0	2.252
FgSSP19	0	0	0	2	3	9.107	2	0	3.643	2	3	9.107	0	0	0	2	3	9.107
FgSSP20	0	0	0	1	0	1.812	1	0	1.812	1	0	1.812	0	0	0	1	0	1.812
FgSSP21	0	0	0	20	8	48.87	20	0	34.9	30	12	73.3	0	0	0	30	12	73.3
FgSSP22	0	0	0	1	1	7.168	3	0	10.75	3	1	14.34	2	0	7.168	1	1	7.168
FgSSP23	0	0	0	0	0	0	0	0	0	0	0	0	0	0	0	0	0	0
FgSSP24	0	0	0	0	0	0	0	0	0	0	0	0	0	0	0	0	0	0

FgSSP25	0	0	0	4	3	11.9	5	0	8.503	0	1	1.701	1	1	3.401	4	3	11.9
FgSSP26	0	0	0	0	0	0	0	0	0	0	0	0	1	0	2.778	0	0	0
FgSSP27	0	0	0	0	0	0	0	0	0	0	0	0	1	0	2.874	0	0	0
FgSSP28	0	0	0	1	2	6.135	1	0	2.045	0	1	2.045	0	0	0	1	2	6.135
FgSSP29	0	0	0	0	1	3.058	0	0	0	0	0	0	0	1	3.058	0	1	3.058
FgSSP30	0	0	0	1	3	11.7	1	0	2.924	1	3	11.7	1	2	8.772	1	3	11.7
FgSSP31	0	0	0	9	4	36.41	0	0	0	0	1	2.801	0	1	2.801	9	4	36.41
FgSSP32	0	0	0	0	0	0	0	0	0	0	0	0	0	0	0	0	0	0
FgSSP33	0	0	0	0	0	0	0	0	0	1	1	9.39	1	0	4.695	1	0	4.695
FgSSP34	0	0	0	11	9	73.26	11	0	40.29	1	2	10.99	11	9	73.26	1	2	10.99
FgSSP35	0	0	0	1	1	7.168	0	0	0	0	1	3.584	1	3	14.34	1	1	7.168
FgSSP6	0	0	0	1	1	4.762	1	0	2.381	0	1	2.381	0	1	2.381	1	1	4.762
FgSSP7	0	0	0	0	1	2.364	1	0	2.364	0	1	2.364	0	1	2.364	0	1	2.364
Tri4	0	0	0	1	0	0.64	1	0	0.64	2	0	1.28	0	0	0	1	0	0.64
Tri5	0	0	0	0	0	0	0	0	0	0	0	0	0	0	0	0	0	0
Host	**Wheat**			**Wheat**			**Wheat**			**Barley**			**Wheat**			**Wheat**		
Location	**RS**			**RS**			**RS**			**Australia**			**PR[8]**			**PR**		
Disease level	**+**			**++**			**++**			**+++**			**+++**			**+++**		
year	**2010**			**2011**			**2010**			**2001**			**2011**			**2011**		
Strain name	**CML3069**			**CML3070**			**CML3071**			**CS3005**			**CML3405**			**CML3403**		
SNP/INDEL	**Syn**	**Nonsyn**	**Freq**	**Syn**	**Nonsyn**	**Freq**	**Syn**	**Nonsyn**	**Freq**	**Syn**	**Nonsyn**	**Freq**	**Syn**	**Nonsyn**	**Freq**	**Syn**	**Nonsyn**	**Freq**

FgSSP13	0	1	2.604	0	1	2.604	0	0	0	0	0	0	0	1	2.604	0	1	2.604
FgSSP14	0	0	0	0	0	0	0	0	0	0	0	0	0	0	0	0	0	0
FgSSP15	0	0	0	0	0	0	0	0	0	0	0	0	0	0	0	0	0	0
FgSSP16	1	0	3.367	1	0	3.367	1	0	3.367	0	0	0	1	0	3.367	1	0	3.367
FgSSP17	0	0	0	0	0	0	0	0	0	0	0	0	0	0	0	0	0	0
FgSSP18	1	0	2.252	1	1	4.505	1	0	2.252	0	0	0	1	0	2.252	1	0	2.252
FgSSP19	2	3	9.107	2	3	9.107	2	0	3.643	2	0	3.643	2	2	7.286	0	0	0
FgSSP20	1	0	1.812	1	0	1.812	1	0	1.812	1	0	1.812	1	0	1.812	0	0	0
FgSSP21	20	8	48.87	30	12	73.3	23	0	40.14	0	0	0	20	8	48.87	31	12	75.04
FgSSP22	1	1	7.168	3	1	14.34	1	0	3.584	1	0	3.584	1	1	7.168	1	1	7.168
FgSSP23	0	0	0	0	0	0	0	0	0	0	0	0	0	0	0	0	0	0
FgSSP24	0	0	0	0	0	0	0	0	0	0	0	0	0	0	0	0	0	0
FgSSP25	4	4	13.61	1	1	3.401	1	0	1.701	4	0	6.803	4	3	11.9	4	4	13.61
FgSSP26	0	0	0	0	0	0	0	0	0	1	0	2.778	0	0	0	1	0	2.778
FgSSP27	0	0	0	0	0	0	0	0	0	0	0	0	0	0	0	0	0	0
FgSSP28	0	0	0	0	0	0	0	0	0	0	0	0	0	0	0	0	0	0
FgSSP29	0	0	0	0	1	3.058	0	0	0	0	0	0	0	1	3.058	0	0	0
FgSSP30	1	3	11.7	1	2	8.772	1	0	2.924	1	0	2.924	1	2	8.772	6	8	40.94
FgSSP31	0	1	2.801	2	1	8.403	2	0	5.602	10	0	28.01	0	2	5.602	2	1	8.403
FgSSP32	0	0	0	0	0	0	0	0	0	0	0	0	0	0	0	0	0	0

FgSSP33	0	0	0	1	1	9.39	1	0	4.695	0	0	0	1	0	4.695	0	0	0
FgSSP34	11	9	73.26	11	9	73.26	11	0	40.29	0	0	0	11	9	73.26	0	1	3.663
FgSSP35	0	1	3.584	1	1	7.168	1	0	3.584	0	0	0	1	1	7.168	0	1	3.584
FgSSP6	0	2	4.762	0	1	2.381	0	0	0	0	0	0	0	1	2.381	0	1	2.381
FgSSP7	0	1	2.364	0	1	2.364	0	0	0	0	0	0	0	1	2.364	0	1	2.364
Tri4	1	0	0.64	1	0	0.64	1	0	0.64	0	0	0	1	0	0.64	0	0	0
Tri5	0	0	0	0	0	0	0	0	0	0	0	0	0	0	0	0	0	0
Host	**Wheat**			**Wheat**			**Wheat**			**Wheat**			**Wheat**					
Location	**PR**			**PR**			**PR**			**PR**			**PR**					
Disease level	**+**			**+++**			**+++**			**++**			**+++**					
year	**2011**			**2011**			**2011**			**2011**			**2011**					
Strain name	**CML3404**			**CML3402**			**CML3406**			**CML3407**			**CML3409**					
SNP/INDEL	**Syn**	**Nonsyn**	**Freq**	**Syn**	**Nonsyn**	**Freq**	**Syn**	**Nonsyn**	**Freq**	**Syn**	**Nonsyn**	**Freq**	**Syn**	**Nonsyn**	**Freq**			
FgSSP13	0	1	2.604	0	1	2.604	0	0	0	0	1	2.604	0	1	2.604			
FgSSP14	0	0	0	0	1	5.128	0	0	0	0	0	0	0	0	0			
FgSSP15	0	0	0	0	0	0	0	0	0	0	0	0	0	0	0			
FgSSP16	1	0	3.367	1	0	3.367	1	0	3.367	1	0	3.367	1	0	3.367			
FgSSP17	0	0	0	0	0	0	0	0	0	0	0	0	0	0	0			
FgSSP18	1	1	4.505	1	0	2.252	1	0	2.252	1	1	4.505	1	0	2.252			
FgSSP19	2	3	9.107	2	2	7.286	2	0	3.643	2	3	9.107	2	3	9.107			

FgSSP20	0	0	0	0	0	0	0	0	0	1	0	1.812	0	0	0
FgSSP21	31	12	75.04	31	12	75.04	20	0	34.9	20	8	48.87	20	8	48.87
FgSSP22	1	1	7.168	1	1	7.168	1	0	3.584	1	1	7.168	1	1	7.168
FgSSP23	0	0	0	0	0	0	0	0	0	0	0	0	0	0	0
FgSSP24	0	0	0	0	0	0	0	0	0	0	0	0	0	0	0
FgSSP25	4	4	13.61	1	1	3.401	4	0	6.803	4	3	11.9	4	4	13.61
FgSSP26	1	0	2.778	1	0	2.778	1	0	2.778	0	0	0	0	0	0
FgSSP27	0	0	0	0	0	0	0	0	0	0	0	0	0	0	0
FgSSP28	1	2	6.135	0	0	0	0	0	0	0	0	0	0	0	0
FgSSP29	0	0	0	0	0	0	0	0	0	0	1	3.058	0	0	0
FgSSP30	1	2	8.772	1	2	8.772	1	0	2.924	1	3	11.7	1	3	11.7
FgSSP31	2	1	8.403	2	2	11.2	2	0	5.602	0	7	19.61	0	2	5.602
FgSSP32	0	0	0	0	0	0	0	0	0	0	0	0	0	0	0
FgSSP33	1	0	4.695	0	0	0	1	0	4.695	0	0	0	1	0	4.695
FgSSP34	11	9	73.26	11	9	73.26	11	0	40.29	11	9	73.26	11	9	73.26
FgSSP35	1	1	7.168	0	1	3.584	0	0	0	1	1	7.168	0	1	3.584
FgSSP6	1	1	4.762	0	1	2.381	0	0	0	0	1	2.381	0	1	2.381

FgSSP7	0	1	2.364	0	1	2.364	0	0	0	0	1	2.364	0	1	2.364
Tri4	0	0	0	1	0	0.64	0	0	0	1	0	0.64	1	0	0.64
Tri5	0	0	0	0	0	0	0	0	0	0	0	0	0	0	0

[1] Host from which *F. graminearum* strain was isolated.

[2] Location indicates which region where strain was isolated

[3] USA = United States of America

[4] RS = Rio Grande do Sul

[5] Syn = number of synonymous mutations present in the pangenome

[6] Nonsyn = number of non-synonymous mutations present in the pangenome

[7] Freq = frequency at which mutations occur within the pangenome

[8] PR = Parana

Table 4 Comparison of *FgSSP* expression on different hosts to identify host-specific genes (Harris et al. 2016b).

FgSSP	Wheat, barley & maize	Wheat & maize	Wheat & barley	Wheat only	Maize & barley	Barley only	Maize only
FgSSP13							
FgSSP14				x			
FgSSP15			x				
FgSSP16			x				
FgSSP17	x						
FgSSP18	x						
FgSSP19	x						
FgSSP20	x		x				
FgSSP21	x						
FgSSP22	x						
FgSSP23	x						
FgSSP24	x						
FgSSP25	x						
FgSSP26	x						
FgSSP27							x
FgSSP28	x						
FgSSP29			x				
FgSSP30			x				
FgSSP31			x				
FgSSP32			x				
FgSSP33			x				
FgSSP34	x						
FgSSP35				x			
FgSSP36			x				
FgSSP6							
FgSSP7	x						
TRI4	x						
TRI5	x						

Appendix 3: Statistical analysis outputs

Figure 4.2 Graph representing number of visibly diseased spikelets below the point of *F. graminearum* inoculation in wheat ears at 9 and 12dpi in a BSMV-VOX experiment. Numbers above bars represent the total number of wheat ears tested across seven experimental replicates. Asterix denotes treatments that are statistically different to the viral control (BSMV:MCS4D)(* = p<0.05; ** = p<0.01; GLMM analysis).

Generalized linear mixed model analysis

```
Method:             c.f. Schall (1991) Biometrika
Response variate:   %9
Binomial totals:    12
Distribution:       binomial
Link function:      logit
Random model:       Experiment_number + Experiment_number.Batch
Fixed model:        Constant + Treatment

Dispersion parameter estimated
```

Monitoring information

Iteration	Gammas		Dispersion	Max change
1	0.2445	0.1947	0.6337	5.6954E-01
2	0.2625	0.2550	0.6695	6.0275E-02
3	0.2618	0.2609	0.6798	1.0329E-02
4	0.2617	0.2608	0.6807	8.4127E-04
5	0.2616	0.2608	0.6807	7.5580E-05

Estimated variance components

Random term	component	s.e.
Experiment_number	0.1781	0.1255
Experiment_number.Batch	0.1775	0.0570

Residual variance model

Term	Model(order)	Parameter
	Estimate	s.e.
Dispersn	Identity	Sigma2
	0.681	0.0443

Estimated variance matrix for variance components

```
                Experiment_number   1     0.015748
 Experiment_number.Batch   2    -0.000341     0.003246
                Dispersn   3    -0.000034    -0.000158     0.001964
                                        1            2            3
```

Table of effects for Constant

```
  -0.1893    Standard error: 0.19609
```

Table of effects for Treatment

```
      Treatment
   BSMV:FgSSP22   0.0000
BSMV:FgSSP22-SP   0.2428
   BSMV:FgSSP23  -0.0159
   BSMV:FgSSP24  -0.0918
   BSMV:FgSSP26   0.2809
   BSMV:FgSSP30   0.2374
   BSMV:FgSSP32  -0.2166
BSMV:FgSSP32-SP   0.0209
   BSMV:FgSSP33  -0.1485
BSMV:FgSSP33-SP  -0.1616
     BSMV:MCS4D   0.1872
       No virus  -0.8455


Standard errors of differences

Average:                0.1393
Maximum:                0.1852
Minimum:               0.08258

Average variance of differences: 0.02005
```

Tables of means with standard errors

Table of predicted means for Treatment

```
      Treatment
   BSMV:FgSSP22  -0.1893
BSMV:FgSSP22-SP   0.0535
   BSMV:FgSSP23  -0.2052
   BSMV:FgSSP24  -0.2811
   BSMV:FgSSP26   0.0916
   BSMV:FgSSP30   0.0481
   BSMV:FgSSP32  -0.4059
BSMV:FgSSP32-SP  -0.1684
   BSMV:FgSSP33  -0.3379
BSMV:FgSSP33-SP  -0.3509
     BSMV:MCS4D  -0.0021
       No virus  -1.0348
```

Standard errors of differences

```
Average:               0.1393
Maximum:               0.1852
Minimum:              0.08258

Average variance of differences: 0.02005
```

Table of predicted means for Treatment

```
      Treatment
   BSMV:FgSSP22  -0.1893
BSMV:FgSSP22-SP   0.0535
   BSMV:FgSSP23  -0.2052
   BSMV:FgSSP24  -0.2811
   BSMV:FgSSP26   0.0916
   BSMV:FgSSP30   0.0481
   BSMV:FgSSP32  -0.4059
BSMV:FgSSP32-SP  -0.1684
   BSMV:FgSSP33  -0.3379
BSMV:FgSSP33-SP  -0.3509
     BSMV:MCS4D  -0.0021
       No virus  -1.0348
```

Standard errors

```
Average:               0.2010
Maximum:               0.2173
Minimum:               0.1827
```

Back-transformed Means (on the original scale)

```
      Treatment
   BSMV:FgSSP22      5.434
BSMV:FgSSP22-SP      6.160
   BSMV:FgSSP23      5.386
   BSMV:FgSSP24      5.162
   BSMV:FgSSP26      6.275
   BSMV:FgSSP30      6.144
   BSMV:FgSSP32      4.799
BSMV:FgSSP32-SP      5.496
   BSMV:FgSSP33      4.996
BSMV:FgSSP33-SP      4.958
     BSMV:MCS4D      5.994
       No virus      3.146
```

Approximate least significant differences (5% level) of REML means

Treatment

```
  Treatment BSMV:FgSSP22    1           *
Treatment BSMV:FgSSP22-SP   2      0.2958           *
```

```
  Treatment BSMV:FgSSP23    3      0.3145      0.3580           *
  Treatment BSMV:FgSSP24    4      0.3214      0.3639      0.3178   *
  Treatment BSMV:FgSSP26    5      0.2502      0.3380      0.3414
0.3479
  Treatment BSMV:FgSSP30    6      0.2514      0.3356      0.3383
0.3448
  Treatment BSMV:FgSSP32    7      0.2487      0.3001      0.2740
0.2791
Treatment BSMV:FgSSP32-SP   8      0.3024      0.3438      0.3405
0.3462
  Treatment BSMV:FgSSP33    9      0.2283      0.2773      0.2687
0.2761
Treatment BSMV:FgSSP33-SP  10      0.2557      0.2953      0.3117
0.3182
    Treatment BSMV:MCS4D             11      0.2012      0.2708
              0.2641 0.2723
      Treatment No virus             12      0.2147      0.2762
              0.2741 0.2825
                                      1           2           3   4


  Treatment BSMV:FgSSP26    5           *
  Treatment BSMV:FgSSP30    6      0.2571           *
  Treatment BSMV:FgSSP32    7      0.2832      0.2794           *
Treatment BSMV:FgSSP32-SP   8      0.3330      0.3300      0.2622   *
  Treatment BSMV:FgSSP33    9      0.2689      0.2651      0.1832
0.2541
Treatment BSMV:FgSSP33-SP  10      0.2968      0.2938      0.2325
0.2643
    Treatment BSMV:MCS4D             11      0.2375      0.2333
              0.1837 0.2522
      Treatment No virus             12      0.2497      0.2441
              0.1979 0.2704
                                      5           6           7   8


  Treatment BSMV:FgSSP33    9           *
Treatment BSMV:FgSSP33-SP  10      0.2141           *
    Treatment BSMV:MCS4D             11      0.1658      0.2083
                        *
      Treatment No virus             12      0.1767      0.2257
              0.1623    *
                                      9          10          11  12
```

Approximate least significant differences (1% level) of REML means

Treatment

```
  Treatment BSMV:FgSSP22    1           *
Treatment BSMV:FgSSP22-SP   2      0.3893           *
  Treatment BSMV:FgSSP23    3      0.4140      0.4711           *
  Treatment BSMV:FgSSP24    4      0.4230      0.4790      0.4183   *
  Treatment BSMV:FgSSP26    5      0.3293      0.4448      0.4494
0.4579
  Treatment BSMV:FgSSP30    6      0.3309      0.4416      0.4452
0.4538
  Treatment BSMV:FgSSP32    7      0.3274      0.3949      0.3606
0.3673
```

```
Treatment BSMV:FgSSP32-SP    8      0.3980      0.4524      0.4482
0.4556
  Treatment BSMV:FgSSP33     9      0.3005      0.3649      0.3537
0.3634
Treatment BSMV:FgSSP33-SP   10      0.3365      0.3886      0.4103
0.4188
    Treatment BSMV:MCS4D             11      0.2648      0.3563
                0.3476 0.3583
      Treatment No virus             12      0.2825      0.3635
                0.3608 0.3717
                                        1           2           3   4


  Treatment BSMV:FgSSP26     5           *
  Treatment BSMV:FgSSP30     6      0.3383           *
  Treatment BSMV:FgSSP32     7      0.3727      0.3678           *
Treatment BSMV:FgSSP32-SP    8      0.4382      0.4343      0.3451   *
  Treatment BSMV:FgSSP33     9      0.3539      0.3489      0.2411
0.3344
Treatment BSMV:FgSSP33-SP   10      0.3907      0.3867      0.3060
0.3478
    Treatment BSMV:MCS4D             11      0.3125      0.3071
                0.2418 0.3320
      Treatment No virus             12      0.3286      0.3213
                0.2605 0.3558
                                        5           6           7   8


  Treatment BSMV:FgSSP33     9           *
Treatment BSMV:FgSSP33-SP   10      0.2818           *
    Treatment BSMV:MCS4D             11      0.2182      0.2741
                      *
      Treatment No virus             12      0.2325      0.2970
                0.2136    *
                                        9          10          11  12
```

Table of predicted means for Treatment

Treatment	
BSMV:FgSSP22	-0.1893
BSMV:FgSSP22-SP	0.0535
BSMV:FgSSP23	-0.2052
BSMV:FgSSP24	-0.2811
BSMV:FgSSP26	0.0916
BSMV:FgSSP30	0.0481
BSMV:FgSSP32	-0.4059
BSMV:FgSSP32-SP	-0.1684
BSMV:FgSSP33	-0.3379
BSMV:FgSSP33-SP	-0.3509
BSMV:MCS4D	-0.0021
No virus	-1.0348

Standard errors

Treatment	
BSMV:FgSSP22	0.1961
BSMV:FgSSP22-SP	0.2167
BSMV:FgSSP23	0.2146
BSMV:FgSSP24	0.2173
BSMV:FgSSP26	0.2069
BSMV:FgSSP30	0.2056
BSMV:FgSSP32	0.1914
BSMV:FgSSP32-SP	0.2097
BSMV:FgSSP33	0.1870
BSMV:FgSSP33-SP	0.1971
BSMV:MCS4D	0.1827
No virus	0.1866

Standard errors

Average:	0.2010
Maximum:	0.2173
Minimum:	0.1827

Generalized linear mixed model analysis

Method:	c.f. Schall (1991) Biometrika
Response variate:	%12
Binomial totals:	12
Distribution:	binomial
Link function:	logit
Random model:	Experiment_number + Experiment_number.Batch
Fixed model:	Constant + Treatment

Dispersion parameter estimated

Monitoring information

Iteration	Gammas		Dispersion	Max change
1	0.3874	0.3315	1.489	7.4143E-01
2	0.5439	0.3193	1.564	1.5650E-01
3	0.6131	0.3400	1.643	7.8485E-02

4	0.6229	0.3454	1.669	2.5973E-02
5	0.6225	0.3454	1.673	4.6684E-03
6	0.6222	0.3454	1.673	2.6678E-04
7	0.6220	0.3454	1.673	1.6301E-04
8	0.6219	0.3454	1.673	9.9645E-05

Estimated variance components

Random term	component	s.e.
Experiment_number	1.041	0.694
Experiment_number.Batch	0.578	0.194

Residual variance model

Term	Model(order)	Parameter
	Estimate	s.e.
Dispersn	Identity	Sigma2
	1.673	0.115

Estimated variance matrix for variance components

Experiment_number	1	0.48201		
Experiment_number.Batch	2	-0.00410	0.03776	
Dispersn	3	-0.00063	-0.00115	0.01320
		1	2	3

Table of effects for Constant

1.168 Standard error: 0.4388

Table of effects for Treatment

Treatment	
BSMV:FgSSP22	0.0000
BSMV:FgSSP22-SP	0.4003
BSMV:FgSSP26	0.9036
BSMV:FgSSP30	0.5729
BSMV:FgSSP32	-0.1600
BSMV:FgSSP32-SP	0.2533
BSMV:FgSSP33	-0.1296
BSMV:FgSSP33-SP	-0.2427
BSMV:MCS4D	0.3582
No virus	-1.0541

Standard errors of differences

Average:	0.2514
Maximum:	0.3614
Minimum:	0.1554

Average variance of differences: 0.06584

Tables of means with standard errors

Table of predicted means for Treatment

Treatment	
BSMV:FgSSP22	1.168
BSMV:FgSSP22-SP	1.569
BSMV:FgSSP26	2.072
BSMV:FgSSP30	1.741
BSMV:FgSSP32	1.008
BSMV:FgSSP32-SP	1.422
BSMV:FgSSP33	1.039
BSMV:FgSSP33-SP	0.926
BSMV:MCS4D	1.526
No virus	0.114

Standard errors of differences

Average:	0.2514
Maximum:	0.3614
Minimum:	0.1554

Average variance of differences: 0.06584

Table of predicted means for Treatment

Treatment	
BSMV:FgSSP22	1.168
BSMV:FgSSP22-SP	1.569
BSMV:FgSSP26	2.072
BSMV:FgSSP30	1.741
BSMV:FgSSP32	1.008
BSMV:FgSSP32-SP	1.422
BSMV:FgSSP33	1.039
BSMV:FgSSP33-SP	0.926
BSMV:MCS4D	1.526
No virus	0.114

Standard errors

Average:	0.4490
Maximum:	0.4813
Minimum:	0.4245

Back-transformed Means (on the original scale)

Treatment	
BSMV:FgSSP22	9.154
BSMV:FgSSP22-SP	9.931
BSMV:FgSSP26	10.658

```
   BSMV:FgSSP30     10.210
   BSMV:FgSSP32      8.792
BSMV:FgSSP32-SP      9.667
   BSMV:FgSSP33      8.863
BSMV:FgSSP33-SP      8.594
     BSMV:MCS4D      9.858
       No virus      6.342
```

Approximate least significant differences (5% level) of REML means

Treatment

```
   Treatment BSMV:FgSSP22    1          *
Treatment BSMV:FgSSP22-SP    2     0.5205          *
   Treatment BSMV:FgSSP26    3     0.5132     0.6550          *
   Treatment BSMV:FgSSP30    4     0.4855     0.6252     0.5682   *
   Treatment BSMV:FgSSP32    5     0.4508     0.5453     0.5826
0.5471
Treatment BSMV:FgSSP32-SP    6     0.6039     0.6730     0.7104
0.6821
   Treatment BSMV:FgSSP33    7     0.3993     0.4941     0.5497
0.5123
Treatment BSMV:FgSSP33-SP    8     0.4443     0.5138     0.5915
0.5583
     Treatment BSMV:MCS4D               9     0.3597     0.4864
                0.5074 0.4682
       Treatment No virus              10     0.3590     0.4854
                0.5068 0.4614
                                        1          2          3   4


   Treatment BSMV:FgSSP32    5          *
Treatment BSMV:FgSSP32-SP    6     0.5455          *
   Treatment BSMV:FgSSP33    7     0.3535     0.5306          *
Treatment BSMV:FgSSP33-SP    8     0.4349     0.5643     0.3866   *
     Treatment BSMV:MCS4D               9     0.3650     0.5418
                0.3186 0.3841
       Treatment No virus              10     0.3690     0.5573
                0.3166 0.4010
                                        5          6          7   8


     Treatment BSMV:MCS4D               9          *
       Treatment No virus              10     0.3054   *
                                        9         10
```

Approximate least significant differences (5% level) of REML means

Treatment

```
   Treatment BSMV:FgSSP22    1          *
Treatment BSMV:FgSSP22-SP    2     0.5205          *
   Treatment BSMV:FgSSP26    3     0.5132     0.6550          *
```

```
  Treatment BSMV:FgSSP30    4      0.4855      0.6252      0.5682   *
  Treatment BSMV:FgSSP32    5      0.4508      0.5453      0.5826
0.5471
Treatment BSMV:FgSSP32-SP   6      0.6039      0.6730      0.7104
0.6821
  Treatment BSMV:FgSSP33    7      0.3993      0.4941      0.5497
0.5123
Treatment BSMV:FgSSP33-SP   8      0.4443      0.5138      0.5915
0.5583
    Treatment BSMV:MCS4D              9      0.3597      0.4864
                0.5074 0.4682
      Treatment No virus             10      0.3590      0.4854
                0.5068 0.4614
                                        1           2           3   4


  Treatment BSMV:FgSSP32    5           *
Treatment BSMV:FgSSP32-SP   6      0.5455           *
  Treatment BSMV:FgSSP33    7      0.3535      0.5306           *
Treatment BSMV:FgSSP33-SP   8      0.4349      0.5643      0.3866   *
    Treatment BSMV:MCS4D              9      0.3650      0.5418
                0.3186 0.3841
      Treatment No virus             10      0.3690      0.5573
                0.3166 0.4010
                                        5           6           7   8


    Treatment BSMV:MCS4D              9           *
      Treatment No virus             10      0.3054   *
                                        9          10
```

Table of predicted means for Treatment

Treatment	
BSMV:FgSSP22	1.168
BSMV:FgSSP22-SP	1.569
BSMV:FgSSP26	2.072
BSMV:FgSSP30	1.741
BSMV:FgSSP32	1.008
BSMV:FgSSP32-SP	1.422
BSMV:FgSSP33	1.039
BSMV:FgSSP33-SP	0.926
BSMV:MCS4D	1.526
No virus	0.114

Standard errors

BSMV:FgSSP220.439
BSMV:FgSSP22-SP0.470
BSMV:FgSSP260.476

BSMV:FgSSP30	0.465
BSMV:FgSSP32	0.437

BSMV:FgSSP32-SP0.481

BSMV:FgSSP33	0.429
BSMV:FgSSP33-SP	0.443
BSMV:MCS4D	0.426
No virus	0.425

Standard errors

Average:	0.4490
Maximum:	0.4813
Minimum:	0.4245

FIGURE 5.6 Graph showing the proportion of total leaf area exhibiting a 'necrotic' or 'pre-necrotic' response to FgSSPs. Data analysed using a one-way ANOVA on logit-transformed data. Comparisons made between treatments using LSDs on the logit scale (N=3). * denotes treatments that are significantly different from EV at P<0.05. ** denotes treatments that are significantly different from EV at P<0.01. Untransformed data is presented in this graph and error bars represent SEM.

Analysis of variance

Variate: logitnecrosis

Source of variation	d.f.	s.s.	m.s.	v.r.	F pr.
Treatment	3	50.7142	16.9047	36.69	<.001
Residual	8	3.6862	0.4608		
Total	11	54.4004			

Tables of means

Variate: logitnecrosis

Grand mean -1.62

Treatment	Buffer	EV	FgSSP32	FgSSP33
	-4.46	-2.63	-0.09	0.72

Standard errors of differences of means

Table	Treatment
rep.	3
d.f.	8
s.e.d.	0.554

Least significant differences of means (5% level)

Table	Treatment
rep.	3
d.f.	8
l.s.d.	1.278

Least significant differences of means (1% level)

Table	Treatment
rep.	3
d.f.	8
l.s.d.	1.860

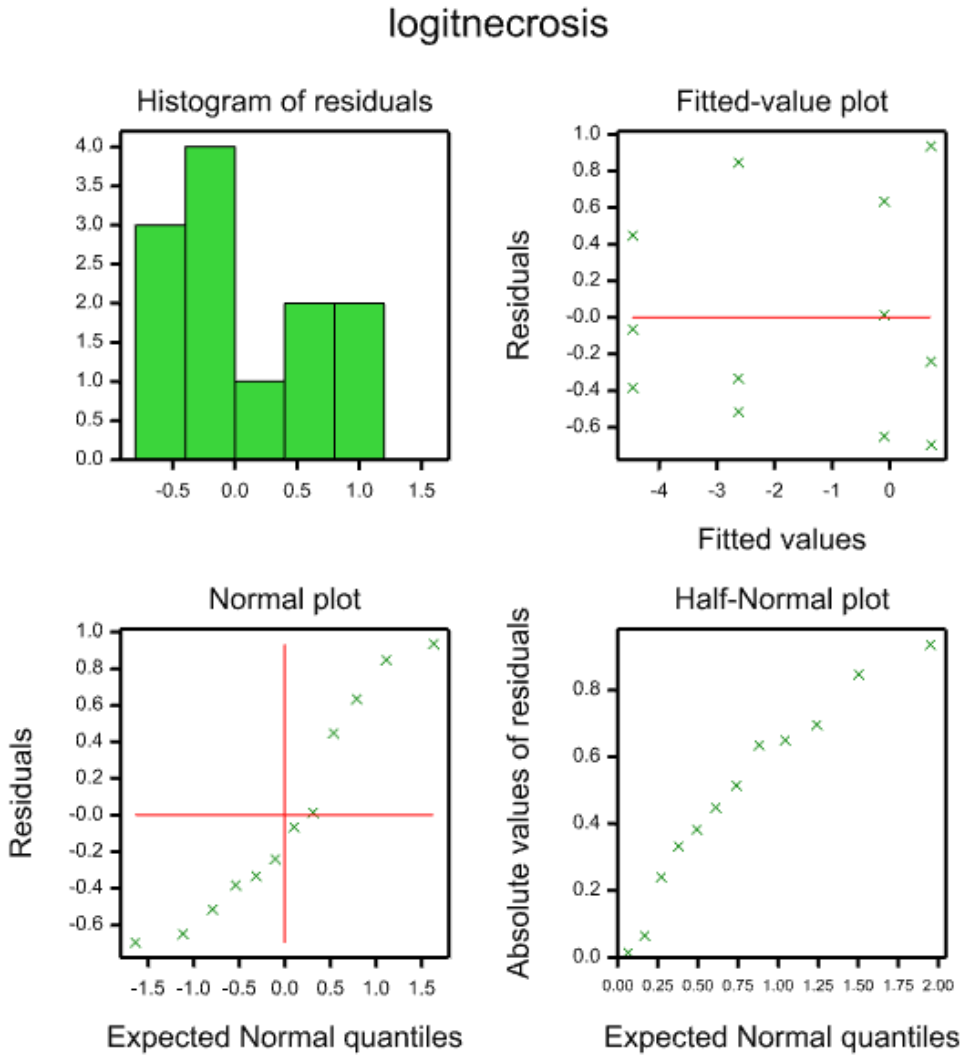
logitnecrosis
Histogram of residuals
Fitted-value plot
Residuals
Fitted values
Normal plot
Residuals
Expected Normal quantiles
Half-Normal plot
Absolute values of residuals
Expected Normal quantiles

FIGURE 5.7 Graph showing the proportion of total leaf area exhibiting a response to *Agrobacterium* infection / agroinfection. Data analysed using a one-way ANOVA on logit-transformed data. Comparisons made between treatments using LSDs on the logit scale. ** denotes treatments that are significantly different from the EV control (P<0.01, n=3). Untransformed data is presented in this graph and error bars represent SEM.

Analysis of variance

Variate: logitresponse (e.g. %agroresponse)

Source of variation	d.f.	s.s.	m.s.	v.r.	F pr.
Treatment (FgSSP)	3	112.3637	37.4546	97.00	<.001
Residual	8	3.0892	0.3861		
Total	11	115.4529			

Tables of means

Variate: logitresponse (e.g. %agroresponse)

Grand mean -4.69

Treatment	Buffer	EV	FgSSP32	FgSSP33
	-9.78	-1.61	-3.80	-3.56

Standard errors of differences of means

Table	Treatment (FgSSP)
rep.	3
d.f.	8
s.e.d.	0.507

Least significant differences of means (5% level)

Table	Treatment
rep.	3
d.f.	8
l.s.d.	1.170

Least significant differences of means (1% level)

Table	Treatment
rep.	3
d.f.	8
l.s.d.	1.702

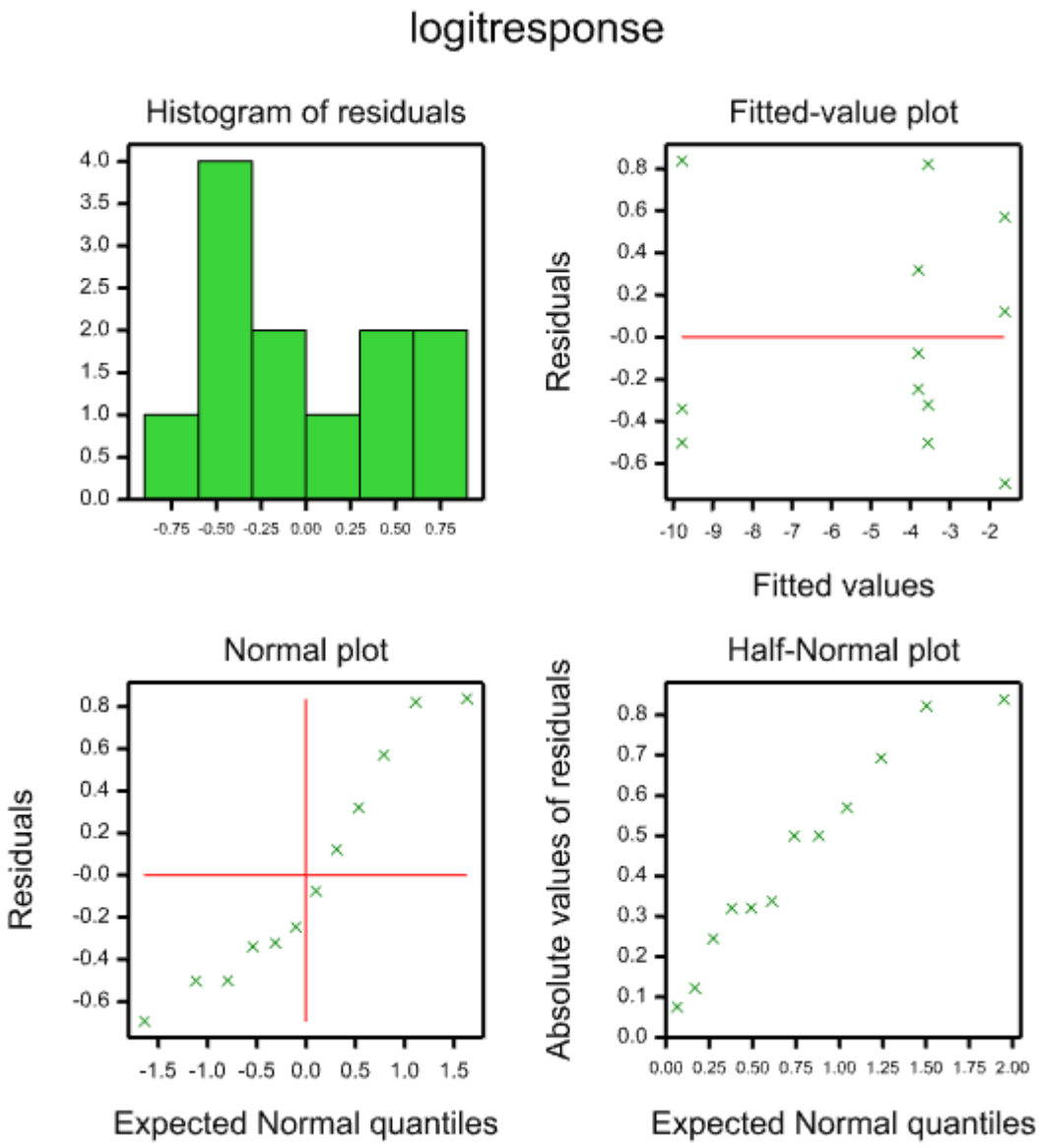
logitresponse
Histogram of residuals
Fitted-value plot
Residuals
Fitted values
Normal plot
Residuals
Expected Normal quantiles
Half-Normal plot
Absolute values of residuals
Expected Normal quantiles

FIGURE 5.8 Graph showing the percentage of the total leaf area exhibiting a response to FgSSP32 and FgSSP33 in VIGS plants. Silenced plants were statistically analysed independently of each other. Data was analysed using ANCOVA analysis whereby leaf area was fitted as a co-variate and logit-transformed % necrosis was fit as the main variate. The P values for the ANCOVA analysis for each group of silenced plants, GFP, BAK1, SOBIR1 and SGT1, are 0.073, 0.142, 0.508, 0.858 respectively.

Regression and ANCOVA analysis for GFP plants

Regression analysis

```
 Response variate: logitRMSITGFP
     Fitted terms: Constant + AreaGFP + FgSSPGFP + AreaGFP.FgSSPGFP
```

Summary of analysis

Source	d.f.	s.s.	m.s.	v.r.	F pr.
Regression	5	9.432	1.8864	10.59	<.001
Residual	11	1.959	0.1781		
Total	16	11.391	0.7120		

```
Percentage variance accounted for 75.0
Standard error of observations is estimated to be 0.422.

* MESSAGE: the following units have large standardized residuals.
         Unit     Response    Residual
            5       -7.709        2.40

* MESSAGE: the following units have high leverage.
         Unit     Response    Leverage
           10       -7.366        0.89
```

Estimates of parameters

Parameter	estimate	s.e.	t(11)	t pr.
Constant	-9.828	0.993	-9.90	<.001
AreaGFP	0.000350	0.000242	1.45	0.175
FgSSPGFP FgSSP32	5.02	1.10	4.56	<.001
FgSSPGFP FgSSP33	2.44	1.17	2.08	0.061
AreaGFP.FgSSPGFP FgSSP32	-0.001010	0.000266	-3.79	0.003
AreaGFP.FgSSPGFP FgSSP33	-0.000418	0.000284	-1.47	0.169

```
Parameters for factors are differences compared with the reference
level:
              Factor  Reference level
```

FgSSPGFP EV

Accumulated analysis of variance

Change	d.f.	s.s.	m.s.	v.r.	F pr.
+ AreaGFP	1	3.2230	3.2230	18.10	0.001
+ FgSSPGFP	2	2.7104	1.3552	7.61	0.008
+ AreaGFP.FgSSPGFP	2	3.4989	1.7495	9.82	0.004
Residual	11	1.9592	0.1781		
Total	16	11.3914	0.7120		

Analysis of variance (adjusted for covariate)

Variate: logitRMSITGFP
Covariate: AreaGFP

Source of variation	d.f.	s.s.	m.s.	v.r.	cov.ef.	F pr.
FgSSPGFP	2	2.7104	1.3552	3.23	1.00	0.073
Covariate	1	3.0993	3.0993	7.38		0.018
Residual	13	5.4581	0.4199		1.46	
Total	16	11.3914				

Covariate regressions

Variate: logitRMSITGFP

Covariate	coefficient	s.e.
AreaGFP	-0.00035	0.000129

Tables of means (adjusted for covariate)

Variate: logitRMSITGFP
Covariate: AreaGFP

Grand mean -7.80

FgSSPGFP	EV	FgSSP32	FgSSP33
	-8.40	-7.44	-7.67
rep.	5	6	6

Standard errors of differences of means

```
Table              FgSSPGFP
rep.                unequal
d.f.                     13
s.e.d.                0.410X min.rep
                      0.392  max-min
                      0.374  max.rep

(No comparisons in categories where s.e.d. marked with an X)
```

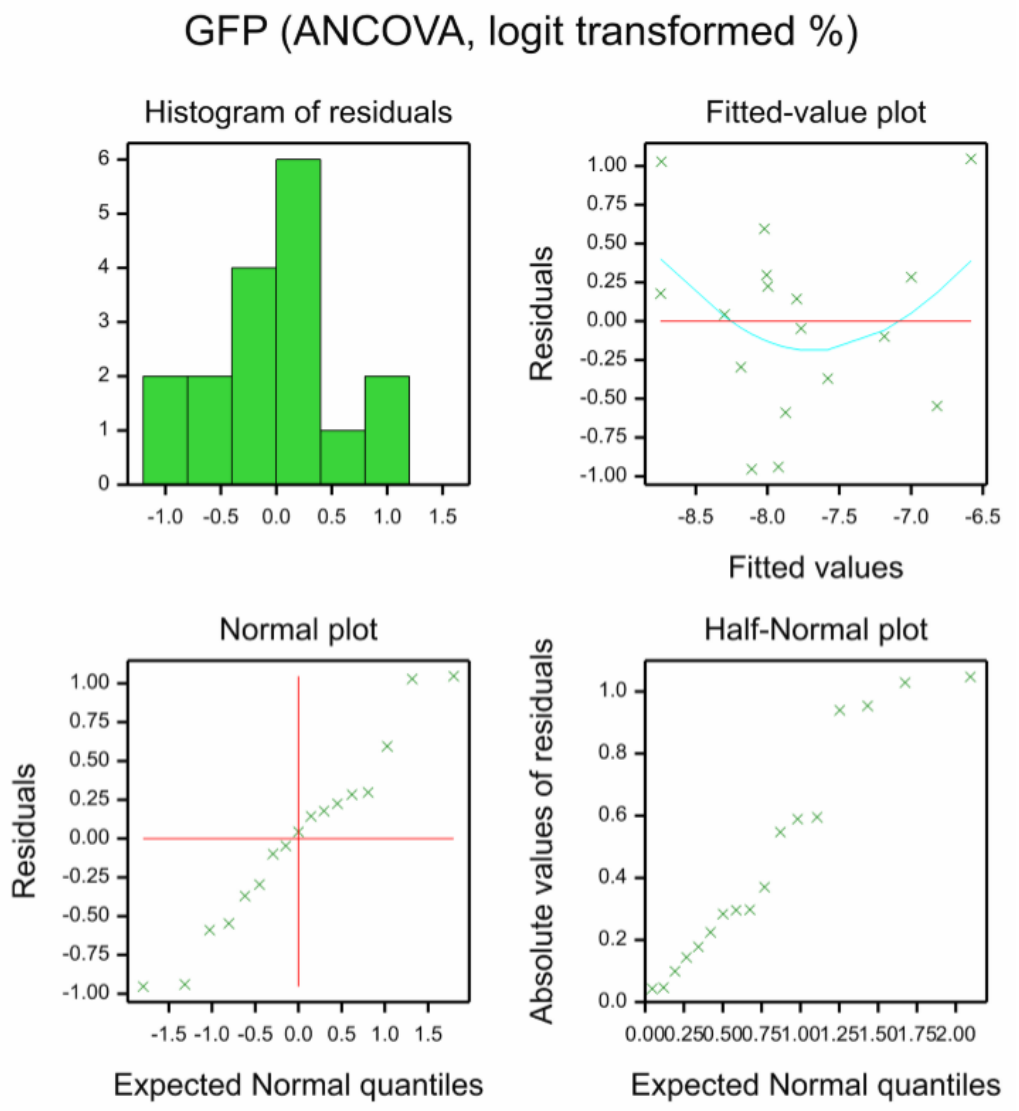

Regression and ANCOVA analysis for BAK1 plants

Regression analysis
==========

```
 Response variate: logitRMSITBAK1
     Fitted terms: Constant + AreaBAK1 + FgSSPBAK1 +
AreaBAK1.FgSSPBAK1
```

Summary of analysis

Source	d.f.	s.s.	m.s.	v.r.	F pr.
Regression	5	0.8891	0.17782	2.85	0.075
Residual	10	0.6236	0.06236		
Total	15	1.5127	0.10085		

Percentage variance accounted for 38.2
Standard error of observations is estimated to be 0.250.

* MESSAGE: the following units have large standardized residuals.

Unit	Response	Residual
1	-8.448	-2.09
2	-7.600	2.11

* MESSAGE: the following units have high leverage.

Unit	Response	Leverage
4	-7.131	0.80
15	-8.068	0.89

Estimates of parameters

Parameter	estimate	s.e.	t(10)	t pr.
Constant	-6.454	0.411	-15.70	<.001
AreaBAK1	-0.000462	0.000147	-3.14	0.010
FgSSPBAK1 FgSSP32	-1.051	0.474	-2.22	0.051
FgSSPBAK1 FgSSP33	-0.674	0.660	-1.02	0.332
AreaBAK1.FgSSPBAK1 FgSSP32	0.000301	0.000190	1.58	0.145
AreaBAK1.FgSSPBAK1 FgSSP33	0.000111	0.000295	0.38	0.715

Parameters for factors are differences compared with the reference level:

Factor	Reference level
FgSSPBAK1	EV

Accumulated analysis of variance

Change	d.f.	s.s.	m.s.	v.r.	F pr.
+ AreaBAK1	1	0.42834	0.42834	6.87	0.026
+ FgSSPBAK1	2	0.30071	0.15035	2.41	0.140

```
+ AreaBAK1.FgSSPBAK1              2      0.16006      0.08003
1.28  0.319
Residual                        10      0.62361      0.06236

Total                           15      1.51272      0.10085
```

Analysis of variance (adjusted for covariate)
==========

```
Variate: logitRMSITBAK1
Covariate: AreaBAK1

Source of variation     d.f.       s.s.       m.s.    v.r. cov.ef.
F pr.
FgSSPBAK1                  2    0.30071    0.15035    2.30    0.89
0.142
Covariate                  1    0.68364    0.68364   10.47
0.007
Residual                  12    0.78367    0.06531            1.73
Total                     15    1.51272


* MESSAGE: the following units have large residuals.

*units* 1          -0.514   approx. s.e. 0.221
*units* 8          -0.465   approx. s.e. 0.221
```

Covariate regressions
==========

```
Variate: logitRMSITBAK1

Covariate               coefficient        s.e.
AreaBAK1                  -0.000290   0.0000897
```

Tables of means (adjusted for covariate)
==========

```
Variate: logitRMSITBAK1
Covariate: AreaBAK1

Grand mean  -7.774

 FgSSPBAK1        EV  FgSSP32  FgSSP33
             -7.511   -7.873   -7.847
      rep.        4        7        5
```

Standard errors of differences of means

```
Table            FgSSPBAK1
rep.               unequal
d.f.                    12
s.e.d.             0.1915X min.rep
                   0.1698  max-min
                   0.1448X max.rep

(No comparisons in categories where s.e.d. marked with an X)
```

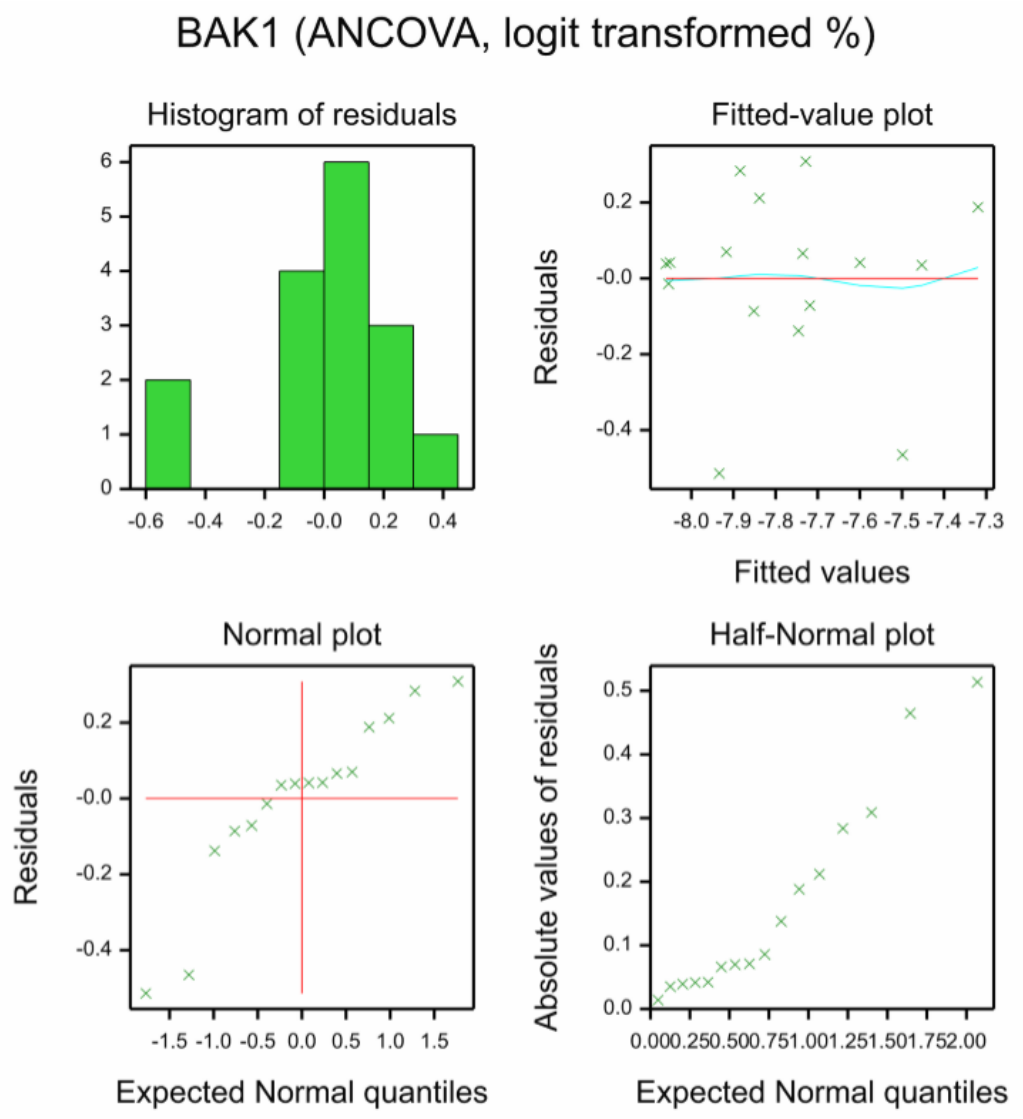
BAK1 (ANCOVA, logit transformed %)
Histogram of residuals
Fitted-value plot
Residuals
Fitted values
Normal plot
Half-Normal plot
Residuals
Absolute values of residuals
Expected Normal quantiles
Expected Normal quantiles

Regression and ANCOVA analysis for SGT1 plants

Regression analysis
==========

Response variate: logitRMSITSGT
Fitted terms: Constant + AreaSGT + FgSSPSGT + AreaSGT.FgSSPSGT

Summary of analysis

Source	d.f.	s.s.	m.s.	v.r.	F pr.
Regression	5	3.156	0.6312	1.34	0.314
Residual	12	5.665	0.4721		
Total	17	8.822	0.5189		

Percentage variance accounted for 9.0
Standard error of observations is estimated to be 0.687.

* MESSAGE: the following units have large standardized residuals.

Unit	Response	Residual
9	-6.043	2.99

* MESSAGE: the following units have high leverage.

Unit	Response	Leverage
16	-8.810	0.73

Estimates of parameters

Parameter	estimate	s.e.	t(12)	t pr.
Constant	-7.24	1.12	-6.49	<.001
AreaSGT	-0.000376	0.000287	-1.31	0.215
FgSSPSGT FgSSP32	0.67	2.68	0.25	0.807
FgSSPSGT FgSSP33	-1.86	2.54	-0.73	0.479
AreaSGT.FgSSPSGT FgSSP32	-0.000099	0.000887	-0.11	0.913
AreaSGT.FgSSPSGT FgSSP33	0.000477	0.000656	0.73	0.481

Parameters for factors are differences compared with the reference level:

Factor	Reference level
FgSSPSGT	EV

Accumulated analysis of variance

Change	d.f.	s.s.	m.s.	v.r.	F pr.
+ AreaSGT	1	2.2816	2.2816	4.83	0.048
+ FgSSPSGT	2	0.6029	0.3015	0.64	0.545
+ AreaSGT.FgSSPSGT	2	0.2717	0.1358	0.29	0.755
Residual	12	5.6654	0.4721		
Total	17	8.8216	0.5189		

Analysis of variance (adjusted for covariate)

Variate: logitRMSITSGT
Covariate: AreaSGT

Source of variation	d.f.	s.s.	m.s.	v.r.	cov.ef. F pr.
FgSSPSGT	2	0.6029	0.3015	0.71	0.82 0.508
Covariate	1	0.7013	0.7013	1.65	0.219
Residual	14	5.9371	0.4241		1.04
Total	17	8.8216			

* MESSAGE: the following units have large residuals.

units 9 1.84 s.e. 0.57

Covariate regressions

Variate: logitRMSITSGT

Covariate	coefficient	s.e.
AreaSGT	-0.00030	0.000234

Tables of means (adjusted for covariate)

Variate: logitRMSITSGT
Covariate: AreaSGT

Grand mean -8.43

FgSSPSGT	EV	FgSSP32	FgSSP33
	-8.57	-8.12	-8.60

Standard errors of differences of means

Table	FgSSPSGT
rep.	6
d.f.	14
s.e.d.	0.414

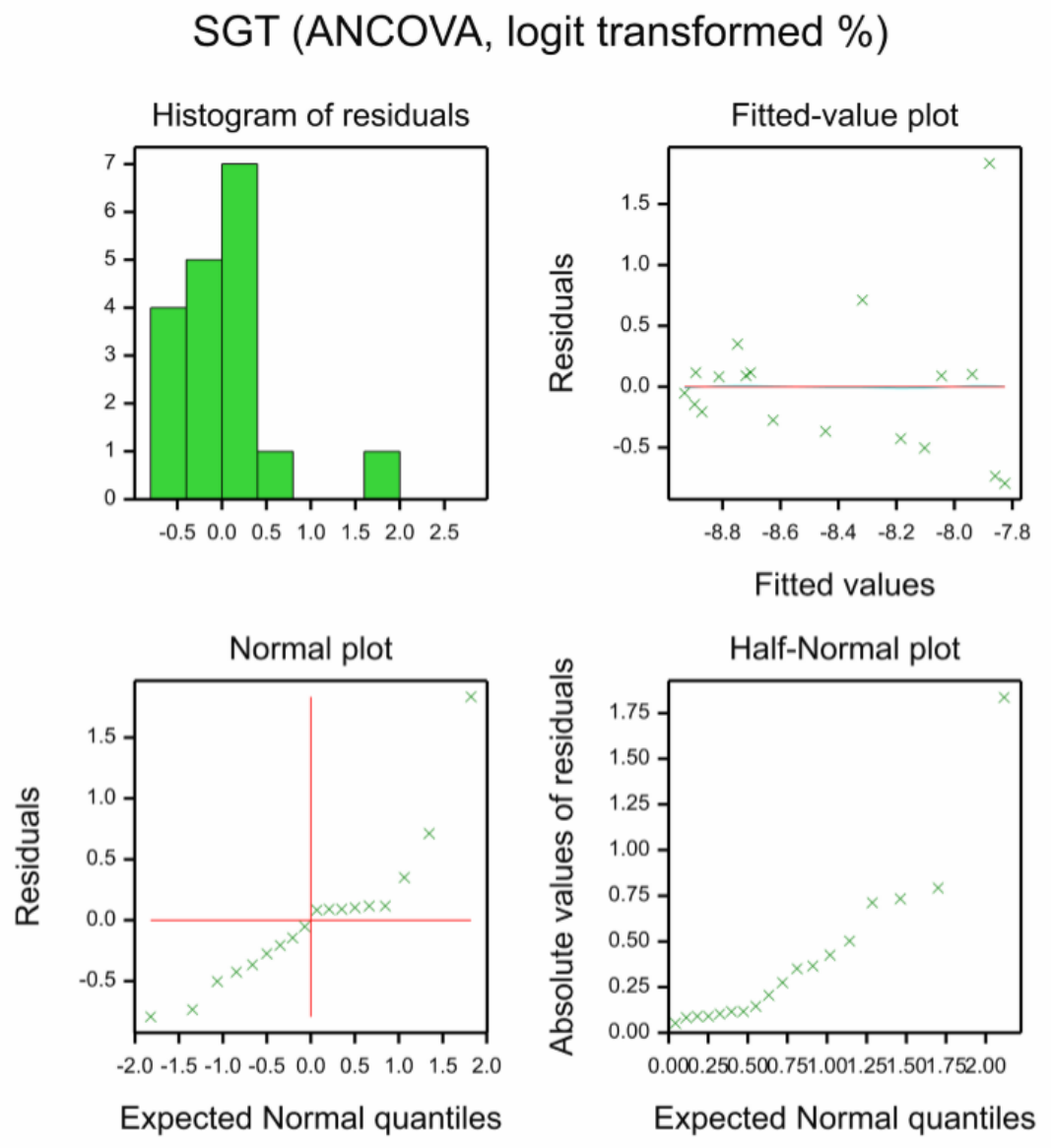
SGT (ANCOVA, logit transformed %)
Histogram of residuals
Fitted-value plot
Residuals
Fitted values
Normal plot
Residuals
Expected Normal quantiles
Half-Normal plot
Absolute values of residuals
Expected Normal quantiles

Regression and ANCOVA analysis for SOBIR1 plants

Regression analysis
==========

```
 Response variate: logitRMSITSOBIR1
     Fitted terms: Constant + AreaSOBIR1 + FgSSPSOBIR1 +
AreaSOBIR1.FgSSPSOBIR1
```

Summary of analysis

Source	d.f.	s.s.	m.s.	v.r.	F pr.
Regression	5	2.973	0.5946	1.75	0.205
Residual	11	3.744	0.3404		
Total	16	6.717	0.4198		

Percentage variance accounted for 18.9
Standard error of observations is estimated to be 0.583.

* MESSAGE: the following units have high leverage.

Unit	Response	Leverage
17	-8.932	0.81

Estimates of parameters

Parameter	estimate	s.e.	t(11)	t pr.
Constant	-10.76	1.23	-8.74	<.001
AreaSOBIR1	0.000468	0.000258	1.82	0.097
FgSSPSOBIR1 FgSSP32	4.31	1.54	2.80	0.017
FgSSPSOBIR1 FgSSP33	2.75	1.39	1.97	0.074
AreaSOBIR1.FgSSPSOBIR1 FgSSP32	-0.001047	0.000388	-2.70	0.021
AreaSOBIR1.FgSSPSOBIR1 FgSSP33	-0.000599	0.000318	-1.89	0.086

Parameters for factors are differences compared with the reference level:

Factor	Reference level
FgSSPSOBIR1	EV

Accumulated analysis of variance

Change	d.f.	s.s.	m.s.	v.r.	F pr.
+ AreaSOBIR1	1	0.2534	0.2534	0.74	0.407
+ FgSSPSOBIR1	2	0.1505	0.0752	0.22	0.805
+ AreaSOBIR1.FgSSPSOBIR1	2	2.5690	1.2845	3.77	0.056
Residual	11	3.7439	0.3404		
Total	16	6.7168	0.4198		

Analysis of variance (adjusted for covariate)
==========

Variate: logitRMSITSOBIR1
Covariate: AreaSOBIR1

Source of variation	d.f.	s.s.	m.s.	v.r.	cov.ef.	F pr.
FgSSPSOBIR1	2	0.1505	0.0752	0.15	0.83	0.858
Covariate	1	0.0821	0.0821	0.17		0.688
Residual	13	6.3129	0.4856		0.94	
Total	16	6.7168				

* MESSAGE: the following units have large residuals.

units 6 1.25 approx. s.e. 0.61

Covariate regressions
==========

Variate: logitRMSITSOBIR1

Covariate	coefficient	s.e.
AreaSOBIR1	-0.00007	0.000159

Tables of means (adjusted for covariate)
==========

Variate: logitRMSITSOBIR1
Covariate: AreaSOBIR1

Grand mean -8.41

FgSSPSOBIR1	EV	FgSSP32	FgSSP33
	-8.51	-8.27	-8.46
rep.	5	6	6

Standard errors of differences of means

Table	FgSSPSOBIR1
rep.	unequal
d.f.	13
s.e.d.	0.484X min.rep
	0.463 max-min
	0.442 max.rep

(No comparisons in categories where s.e.d. marked with an X)

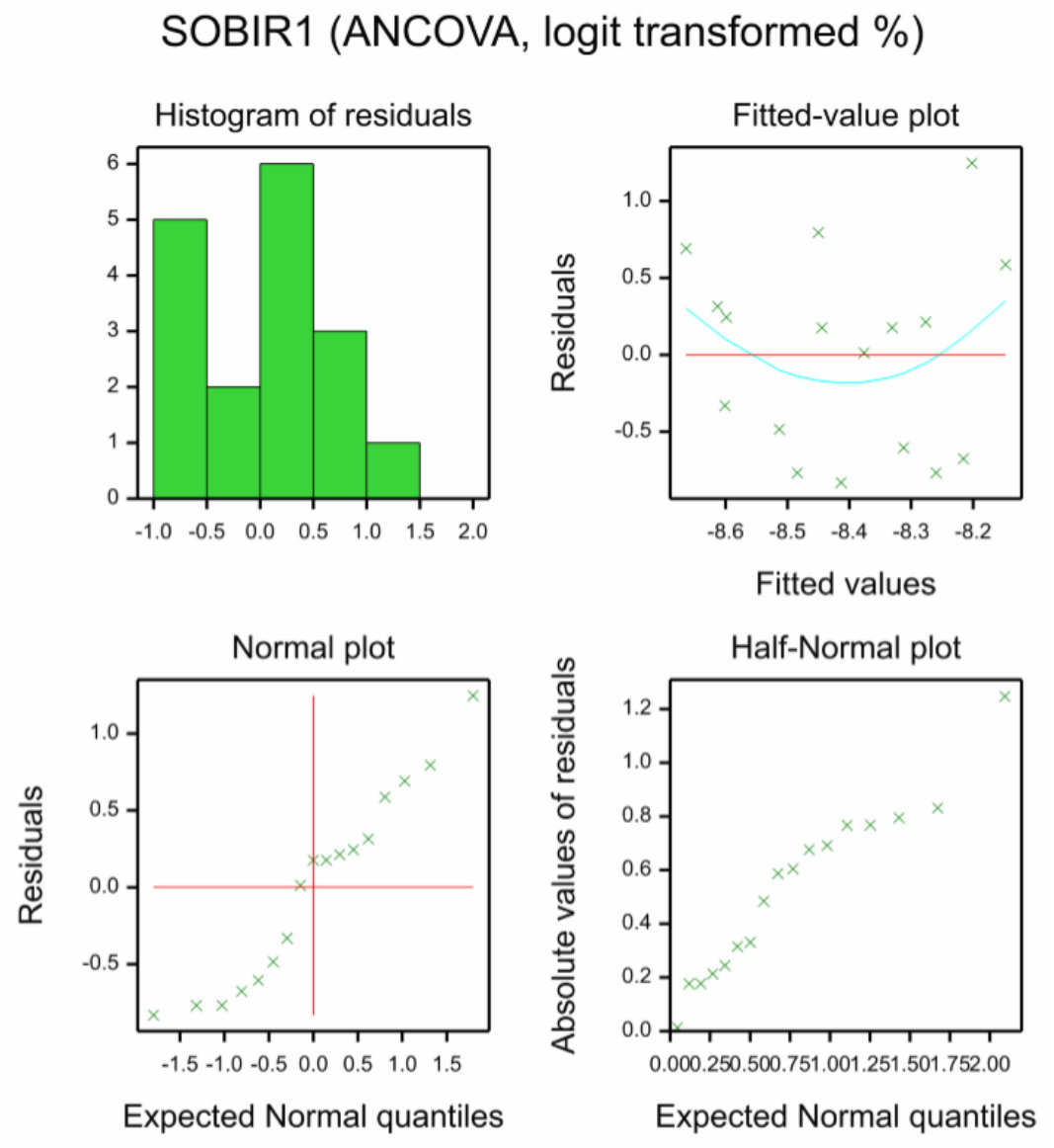
SOBIR1 (ANCOVA, logit transformed %)
Histogram of residuals
Fitted-value plot
Residuals
Fitted values
Normal plot
Residuals
Expected Normal quantiles
Half-Normal plot
Absolute values of residuals
Expected Normal quantiles

Figure 6.12 Graph showing the average lesion size of coleoptiles infected with *F. graminearum* FgSSP32 and FgSSP33 gene deletions seven dpi. Data analysed by one-way ANOVA and differences between treatments found to be non-significant (p=0.835, S.E.D= 3.77).

Analysis of variance

Variate: Lesion_size_mm

Source of variation	d.f.	s.s.	m.s.	v.r.	F pr.
Treatment	4	94.86	23.72	0.36	0.835
Residual	41	2699.88	65.85		
Total	45	2794.74			

Information summary

All terms orthogonal, none aliased.

Message: the following units have large residuals.

units 15 17.6 approx. s.e. 7.7

Tables of means

Grand mean 13.105

Treatment	FgSSP32.1	FgSSP32.5	FgSSP33.1	FgSSP33.2	PH-1
mean	15.024	12.552	14.639	11.097	12.514
rep.	9	9	8	9	11
s.e.	2.705	2.705	2.869	2.705	2.447

Minimum standard error of difference	3.647
Average standard error of difference	3.802
Maximum standard error of difference	3.943
Minimum least significant difference	7.366
Average least significant difference	7.678
Maximum least significant difference	7.963

Figure 6.13 Graph showing the number of infected spikelets below the point of inoculation in wheat ears infected with wild-type PH-1 and the gene deletion strains, FgSSP32.1, FgSSP32.5, FgSSP33.2 and FgSSP33.3. Data was analysed using a generalised linear model and differences between strains were not significant.

Regression analysis

```
   Response variate:  %6
    Binomial totals:  12
       Distribution:  Binomial
      Link function:  Logit
       Fitted terms:  Constant + Batch + Strain
```

Summary of analysis

Source	d.f.	deviance	mean deviance	deviance ratio	approx chi pr
Regression	7	22.28	3.1833	3.18	0.002
Residual	26	16.85	0.6481		
Total	33	39.13	1.1859		

Dispersion parameter is fixed at 1.00.

Message: deviance ratios are based on dispersion parameter with value 1.

Estimates of parameters

Parameter	estimate	s.e.	t(*)	t pr.	antilog of estimate
Constant	-3.39	1.10	-3.08	0.002	0.03380
Batch 2	1.77	1.09	1.63	0.103	5.896
Batch 3	-0.30	1.47	-0.20	0.841	0.7435
Batch 4	-0.66	1.26	-0.52	0.601	0.5178
Strain FgSSP32.5	-0.413	0.687	-0.60	0.548	0.6618
Strain FgSSP33.2	-0.615	0.719	-0.85	0.393	0.5406
Strain FgSSP33.3	-0.301	0.691	-0.44	0.663	0.7401
Strain PH-1	-0.263	0.697	-0.38	0.705	0.7684

Message: s.e.s are based on dispersion parameter with value 1.

Parameters for factors are differences compared with the reference level:

Factor	Reference level
Batch	1
Strain	FgSSP32.1

Response variate: %6

Strain	Prediction	s.e.
FgSSP32.1	-3.004	0.5400
FgSSP32.5	-3.417	0.5387
FgSSP33.2	-3.619	0.5921
FgSSP33.3	-3.305	0.5705
PH-1	-3.267	0.5468

Least significant differences of predictions (5% level)

Strain FgSSP32.1	1	*				
Strain FgSSP32.5	2	1.412	*			
Strain FgSSP33.2	3	1.479	1.449	*		
Strain FgSSP33.3	4	1.421	1.383	1.457	*	
Strain PH-1	5	1.432	1.446	1.519	1.461	
		1	2	3	4	

Strain PH-1	5	*
		5

Regression analysis

Response variate:	%9
Binomial totals:	12
Distribution:	Binomial
Link function:	Logit
Fitted terms:	Constant + Batch + Strain

Summary of analysis

Source	d.f.	deviance	mean deviance	deviance ratio	approx chi pr
Regression	7	25.01	3.572	3.57	<.001
Residual	26	28.85	1.110		
Total	33	53.86	1.632		

Dispersion parameter is fixed at 1.00.

Message: deviance ratios are based on dispersion parameter with value 1.

Message: the following units have large standardized residuals.

Unit	Response	Residual
4	0.00	-2.08
17	0.00	-2.84

Message: the following units have high leverage.

Unit	Response	Leverage
1	4.00	0.50

Estimates of parameters

Parameter	estimate	s.e.	t(*)	t pr.	antilog of estimate
Constant	-0.813	0.441	-1.84	0.065	0.4433
Batch 2	0.271	0.447	0.61	0.544	1.311
Batch 3	-0.795	0.575	-1.38	0.167	0.4518
Batch 4	-1.013	0.463	-2.19	0.029	0.3632
Strain FgSSP32.5	-0.357	0.413	-0.87	0.387	0.6996
Strain FgSSP33.2	-0.681	0.439	-1.55	0.121	0.5062
Strain FgSSP33.3	-0.367	0.448	-0.82	0.413	0.6928
Strain PH-1	-0.011	0.380	-0.03	0.976	0.9887

Message: s.e.s are based on dispersion parameter with value 1.

Parameters for factors are differences compared with the reference level:

Factor	Reference level
Batch	1
Strain	FgSSP32.1

Response variate: %9

Strain	Prediction	s.e.
FgSSP32.1	-1.214	0.2937
FgSSP32.5	-1.571	0.2819
FgSSP33.2	-1.895	0.3258
FgSSP33.3	-1.581	0.3376
PH-1	-1.225	0.2631

Least significant differences of predictions (5% level)

Strain FgSSP32.1	1	*				
Strain FgSSP32.5	2	0.8486	*			
Strain FgSSP33.2	3	0.9017	0.8673	*		
Strain FgSSP33.3	4	0.9212	0.8747	0.9324	*	
Strain PH-1	5	0.7817	0.8082	0.8725	0.8889	
		1	2	3	4	

Strain PH-1	5	*
		5

Message: s.e's, variances and lsd's are approximate, since the model is not linear.

Message: s.e's are based on dispersion parameter with value 1

Regression analysis

Response variate:	%12
Binomial totals:	12
Distribution:	Binomial
Link function:	Logit
Fitted terms:	Constant + Batch + Strain

Summary of analysis

Source	d.f.	deviance	mean deviance	deviance ratio	approx chi pr
Regression	7	55.71	7.959	7.96	<.001
Residual	26	95.76	3.683		
Total	33	151.47	4.590		

Dispersion parameter is fixed at 1.00.

Message: deviance ratios are based on dispersion parameter with value 1.

Message: the following units have large standardized residuals.

Unit	Response	Residual
3	4.50	-3.17
8	4.00	-2.49
16	12.00	4.19
17	2.00	-3.17
18	6.50	2.13
22	12.00	2.70
24	12.00	2.70
26	0.00	-4.58
30	5.00	-2.89
34	8.50	2.27

Message: the error variance does not appear to be constant; large responses are more variable than small responses.

Estimates of parameters

Parameter	estimate	s.e.	t(*)	t pr.	antilog of estimate
Constant	-0.259	0.403	-0.64	0.521	0.7722
Batch 2	1.404	0.420	3.34	<.001	4.072
Batch 3	0.294	0.470	0.63	0.531	1.342
Batch 4	-0.128	0.397	-0.32	0.747	0.8797
Strain FgSSP32.5	-0.518	0.350	-1.48	0.139	0.5957
Strain FgSSP33.2	-0.903	0.360	-2.50	0.012	0.4055
Strain FgSSP33.3	0.141	0.401	0.35	0.726	1.151
Strain PH-1	0.053	0.333	0.16	0.873	1.055

Message: s.e.s are based on dispersion parameter with value 1.

Parameters for factors are differences compared with the reference level:

Factor	Reference level
Batch	1
Strain	FgSSP32.1

Response variate: %12

Batch	Prediction	s.e.
1	-0.5331	0.3658
2	0.8710	0.1809
3	-0.2393	0.2737

```
            4    -0.6612     0.1745
```

Least significant differences of predictions (5% level)

Batch 1	1	*			
Batch 2	2	0.8641	*		
Batch 3	3	0.9652	0.6673	*	
Batch 4	4	0.8167	0.5233	0.6772	*
		1	2	3	4

Message: s.e's, variances and lsd's are approximate, since the model is not linear.

Message: s.e's are based on dispersion parameter with value 1

```
   Response variate:  %15
    Binomial totals:  12
       Distribution:  Binomial
      Link function:  Logit
       Fitted terms:  Constant + Batch + Strain
```

Summary of analysis

Source	d.f.	deviance	mean deviance	deviance ratio	approx chi pr
Regression	7	19.4	2.774	2.77	0.007
Residual	26	137.2	5.276		
Total	33	156.6	4.746		

Dispersion parameter is fixed at 1.00.

Message: deviance ratios are based on dispersion parameter with value 1.

Message: the following units have large standardized residuals.

Unit	Response	Residual
2	12.00	2.08
3	6.00	-3.34
5	5.00	-2.62
6	12.00	3.09
8	6.50	-3.04
13	12.00	2.98
15	12.00	2.52
16	12.00	2.52
17	6.00	-2.62
18	12.00	2.67
21	3.00	-3.14
22	12.00	2.47
23	12.00	2.47
24	12.00	2.47
26	2.00	-4.52
30	5.50	-4.01
33	12.00	2.73
34	12.00	2.73

Message: the following units have high leverage.

Unit	Response	Leverage
1	8.00	0.53

Estimates of parameters

Parameter	estimate	s.e.	t(*)	t pr.	antilog of estimate
Constant	0.283	0.426	0.66	0.507	1.326
Batch 2	1.567	0.466	3.36	<.001	4.790
Batch 3	1.690	0.569	2.97	0.003	5.419
Batch 4	0.732	0.425	1.72	0.085	2.079
Strain FgSSP32.5	0.067	0.410	0.16	0.871	1.069
Strain FgSSP33.2	-0.429	0.392	-1.09	0.274	0.6509
Strain FgSSP33.3	-0.337	0.453	-0.74	0.457	0.7140
Strain PH-1	0.256	0.386	0.66	0.506	1.292

Message: s.e.s are based on dispersion parameter with value 1.

Parameters for factors are differences compared with the reference level:

Factor	Reference level
Batch	1
Strain	FgSSP32.1

Response variate: %15

Strain	Prediction	s.e.
FgSSP32.1	1.410	0.2964
FgSSP32.5	1.477	0.2784
FgSSP33.2	0.981	0.2566
FgSSP33.3	1.073	0.3273
PH-1	1.666	0.2885

Least significant differences of predictions (5% level)

Strain FgSSP32.1	1	*			
Strain FgSSP32.5	2	0.8432	*		
Strain FgSSP33.2	3	0.8067	0.7695	*	
Strain FgSSP33.3	4	0.9308	0.8821	0.8531	*
Strain PH-1	5	0.7928	0.8403	0.8089	0.9287
		1	2	3	4

Strain PH-1	5	*
		5

Message: s.e's, variances and lsd's are approximate, since the model is not linear.

Message: s.e's are based on dispersion parameter with value 1

Appendix 4: Vectors used in this study

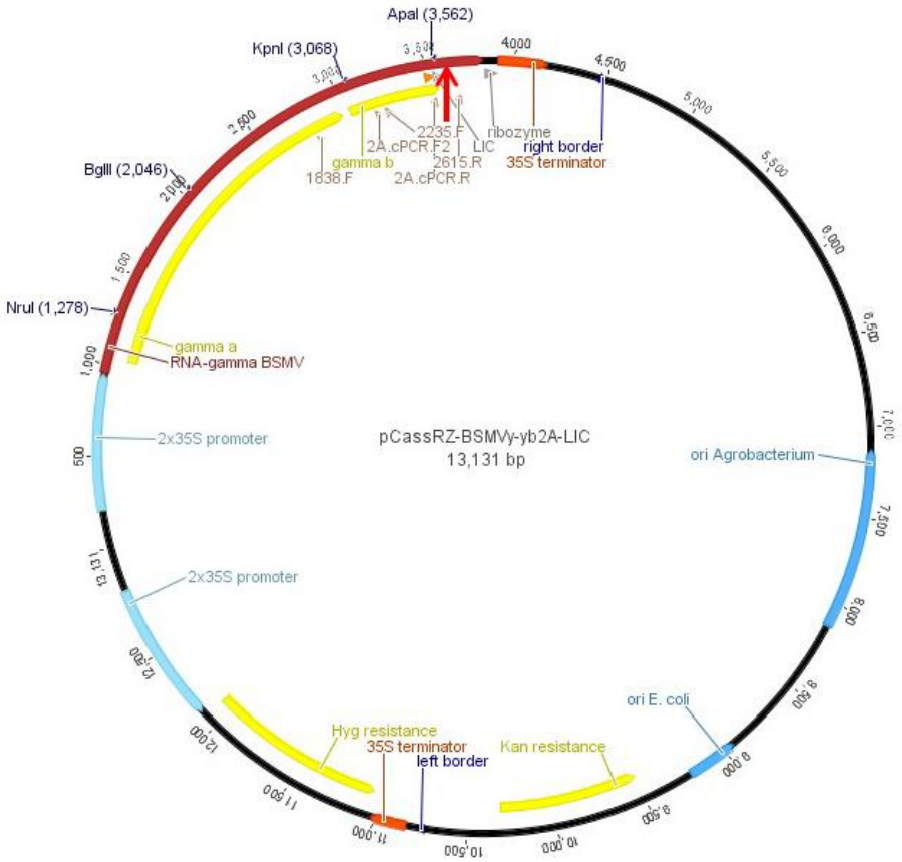

Figure S1 The T-DNA binary plasmid pCassRZ-BSMVγ-γb2A-LIC used for BSMV-mediated VOX study. The red arrow indicates the insertion site for the target gene sequence.

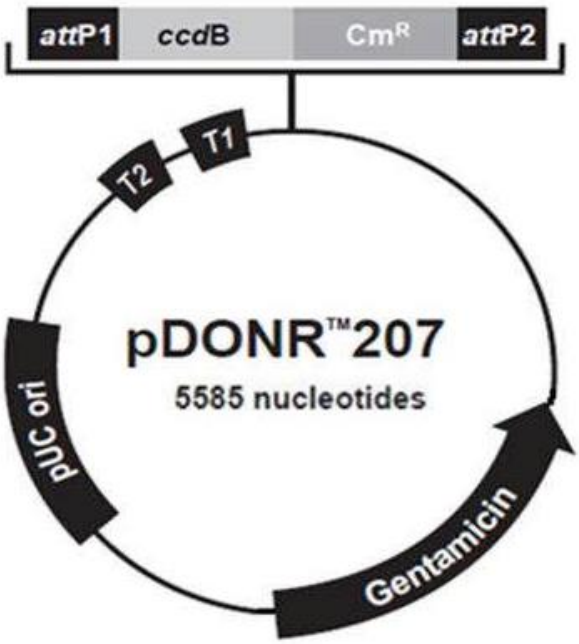

Figure S2. The pDONR207 vector map used for Gateway cloning of effectors in the pEA Q-HT-DEST3 vector.

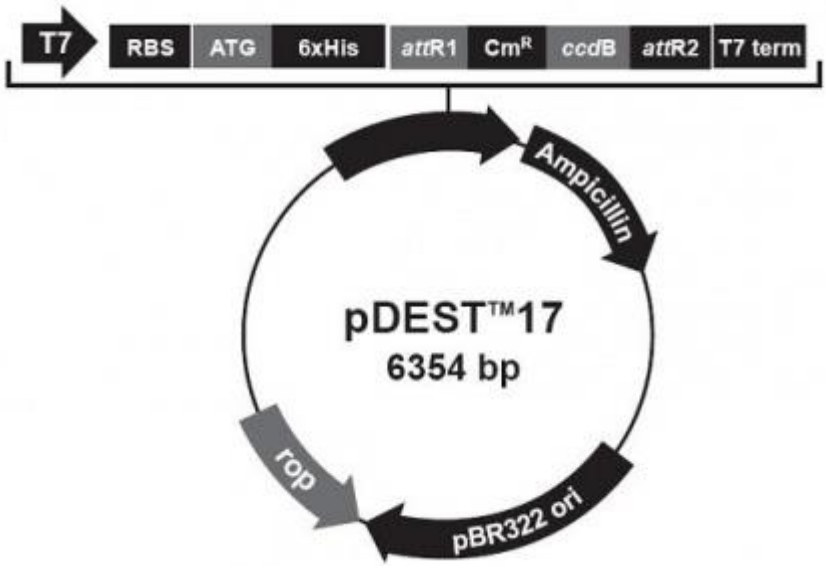

Figure S3. The pDEST17 vector map used for Gateway cloning of effectors into *E. coli*.

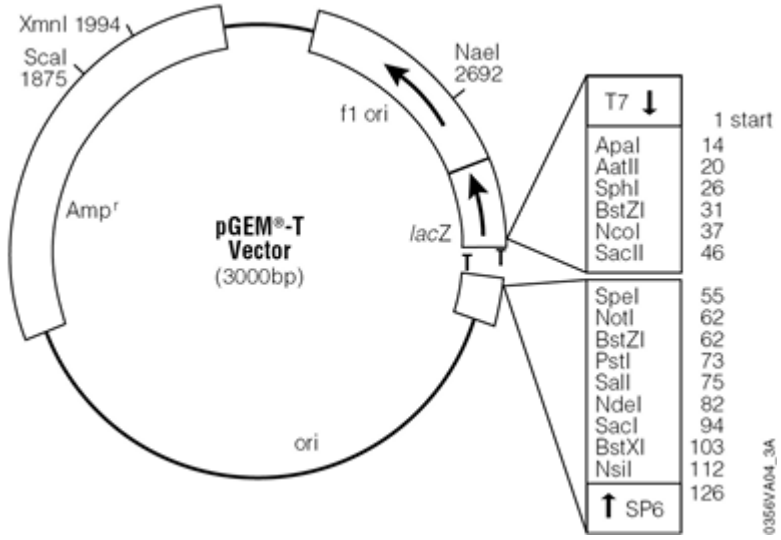

Figure S4. The pGEM®-T easy vector using for Gibson assembly cloning for the generation of *F. graminearum* gene deletion mutants.

Appendix 5: Protease cleavage sites present in FgSSP32 and FgSSP33

FgSSP32

Name of enzyme	No. of cleavages	Positions of cleavage sites
Arg-C proteinase	2	29 67
Asp-N endopeptidase + N-terminal Glu	3	29 32 60
BNPS-Skatole	1	45
CNBr	1	1
Chymotrypsin-high specificity (C-term to [FYW], not before P)	6	3 7 9 39 45 53
Chymotrypsin-low specificity (C-term to [FYWML], not before P)	13	1 3 7 8 9 12 14 25 39 45 49 52 53
Clostripain	2	29 67
Glutamyl endopeptidase	3	30 33 61
Hydroxylamine	1	23
Iodosobenzoic acid	1	45
LysC	3	32 38 41
LysN	3	31 37 40
NTCB (2-nitro-5-thiocyanobenzoic acid)	6	25 34 42 54 55 61
Pepsin (pH1.3)	17	2 3 6 7 8 9 11 12 13 14 24 25 38 39 48 49 57
Pepsin (pH>2)	21	2 3 6 7 8 9 11 12 13 14 24 25 38 39 44 45 48 49 52 53 57
Proline-endopeptidase [*]	1	42
Proteinase K	30	3 6 7 8 9 10 11 12 13 14 15 19 20 25 27 28 30 33 34 36 39 45 47 49 51 53 57 59 60 61
Staphylococcal peptidase I	3	30 33 61
Thermolysin	18	2 6 7 8 9 11 12 13 14 19 24 26 27 35 38 48 50 59
Trypsin	4	29 32 38 67

FgSSP33

Name of enzyme	No. of cleavages	Positions of cleavage sites
Asp-N endopeptidase	2	31 56
Asp-N endopeptidase + N-terminal Glu	4	31 36 41 56
CNBr	1	1
Chymotrypsin-high specificity (C-term to [FYW], not before P)	4	3 29 30 51
Chymotrypsin-low specificity (C-term to [FYWML], not before P)	12	1 3 9 28 29 30 36 50 51 62 63 65
Formic acid	2	32 57
Glutamyl endopeptidase	2	37 42
Hydroxylamine	1	25
LysC	4	20 34 40 67
LysN	4	19 33 39 66
NTCB (2-nitro-5-thiocyanobenzoic acid)	8	22 38 42 47 53 63 67 69
Pepsin (pH1.3)	14	2 3 8 9 27 28 35 49 50 51 61 63 64 65
Pepsin (pH>2)	16	2 3 8 9 27 28 29 30 35 49 50 51 61 63 64 65
Proteinase K	36	3 5 6 8 9 10 11 12 13 14 15 16 17 18 21 22 28 29 30 35 36 37 42 44 47 49 50 51 53 55 60 62 63 65 66 69
Staphylococcal peptidase I	2	37 42
Thermolysin	25	2 4 5 7 8 9 10 11 13 14 15 16 20 21 27 35 43 48 49 50 54 61 62 64 65
Trypsin	4	20 34 40 67

Appendix 6: High performance liquid chromatograms

Figure 6.1 A comparison of representative HPLC chromatograms observed between the healthy and EV controls and *N. benthamiana* plants expressing FgSSP32 and FgSSP33.

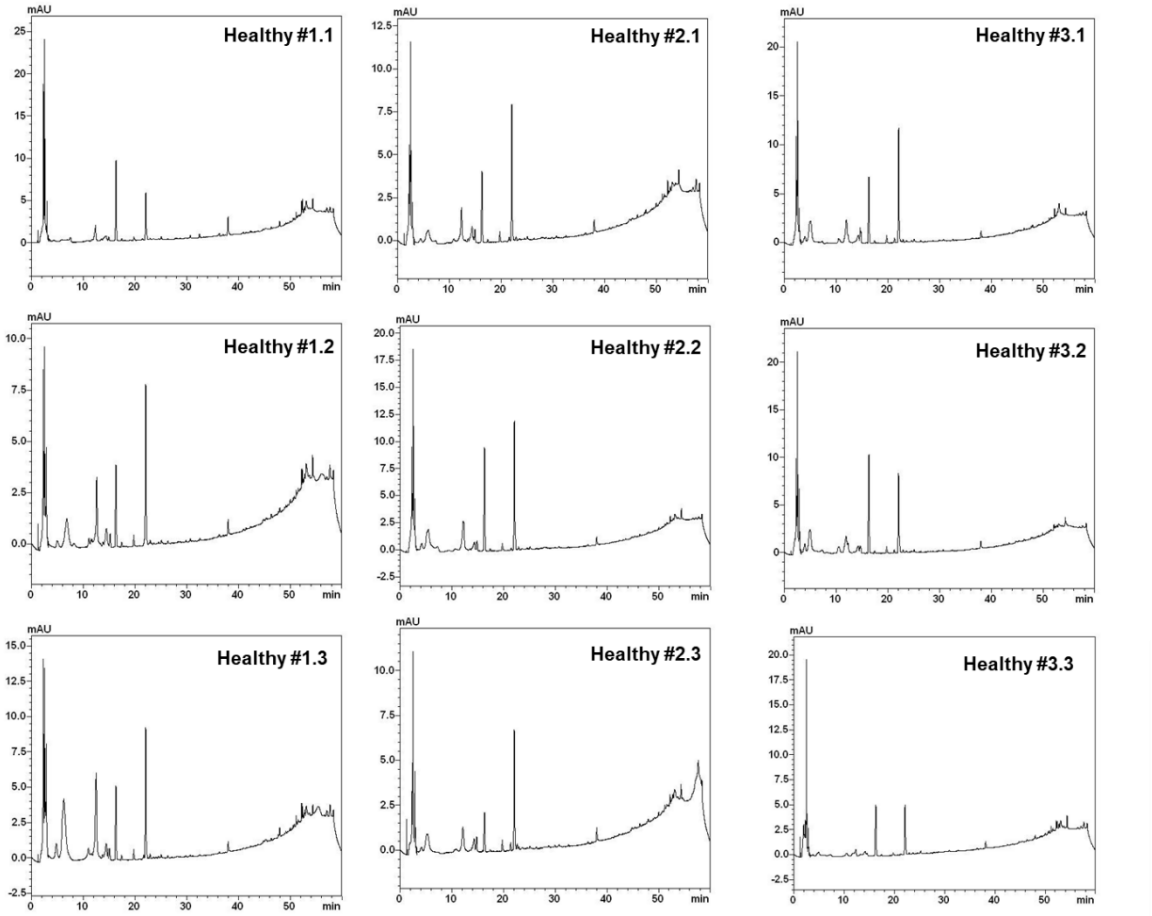

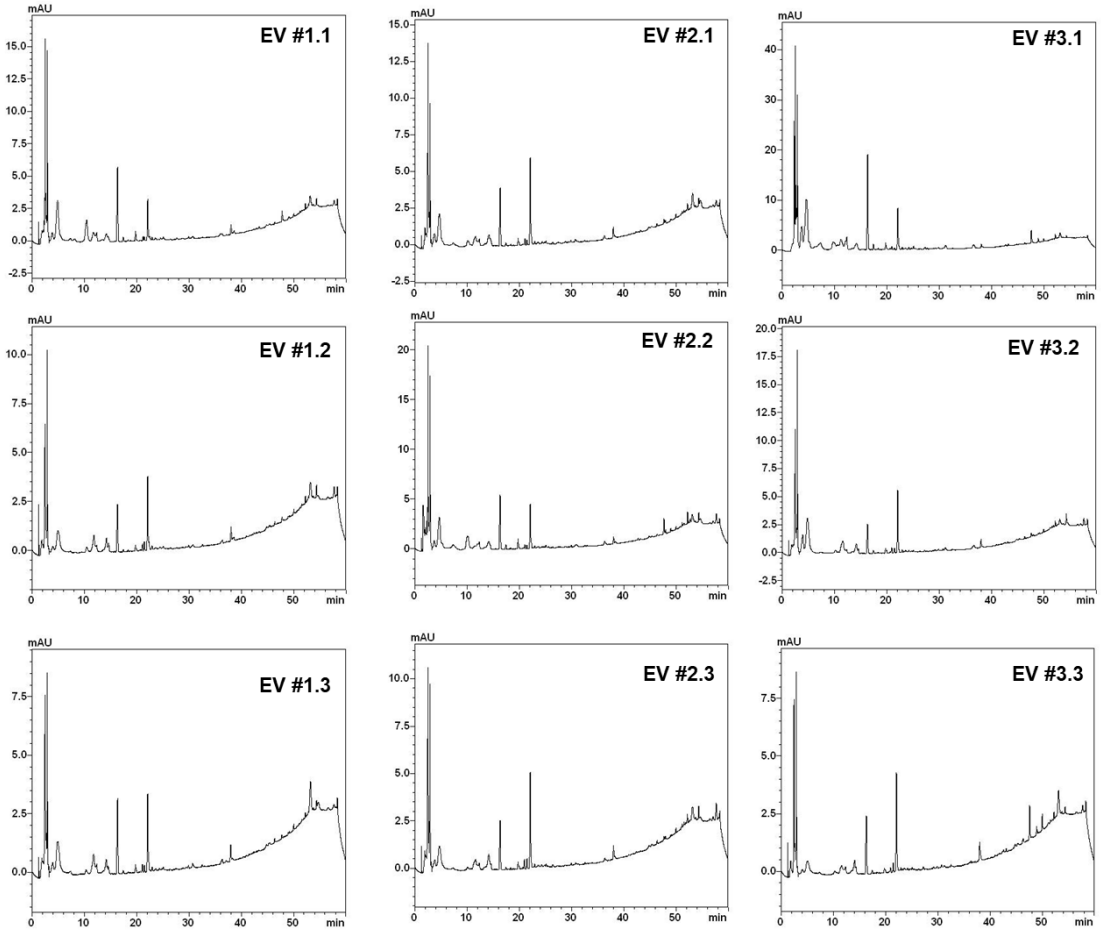
EV #1.1
EV #2.1
EV #3.1
EV #1.2
EV #2.2
EV #3.2
EV #1.3
EV #2.3
EV #3.3
mAU
min

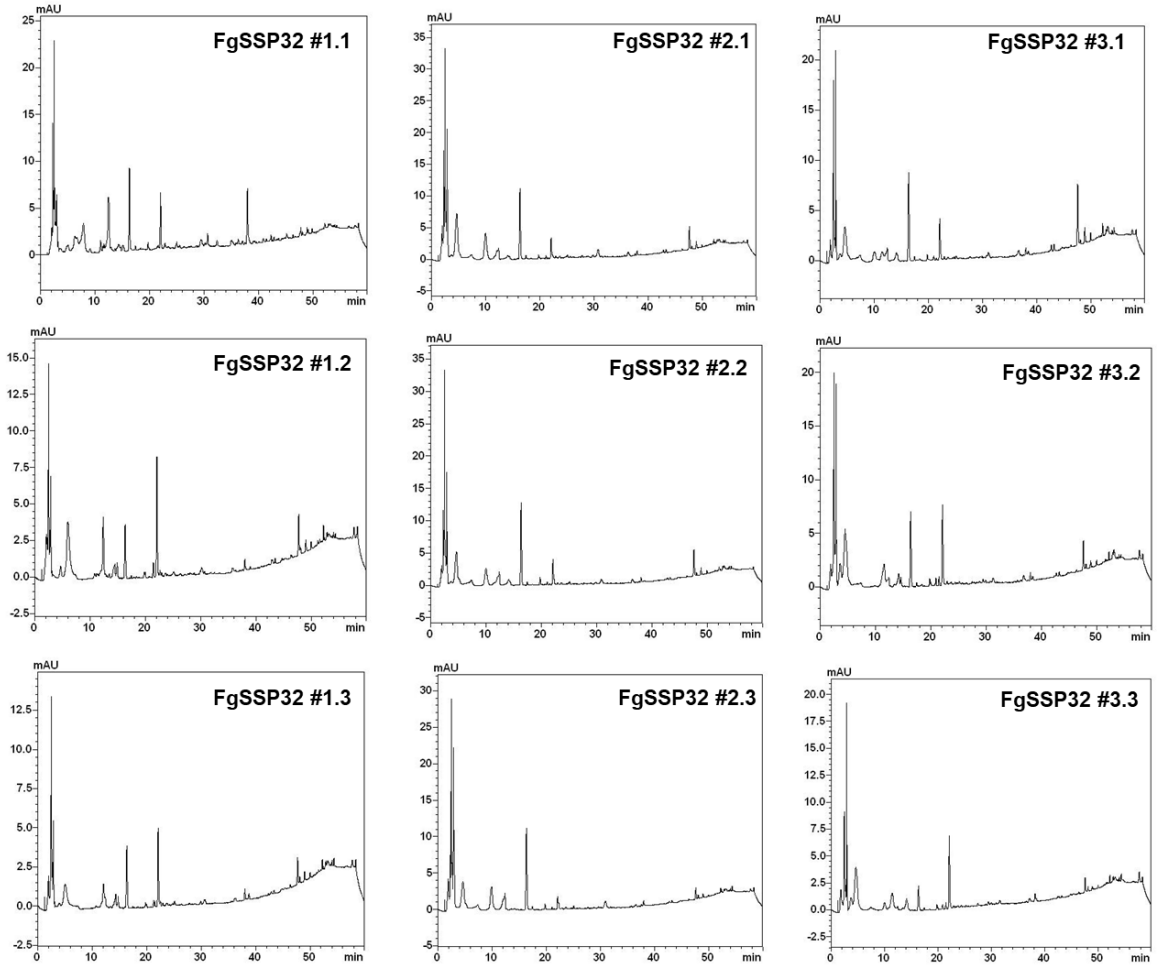
FgSSP32 #1.1
FgSSP32 #2.1
FgSSP32 #3.1
FgSSP32 #1.2
FgSSP32 #2.2
FgSSP32 #3.2
FgSSP32 #1.3
FgSSP32 #2.3
FgSSP32 #3.3
mAU
min

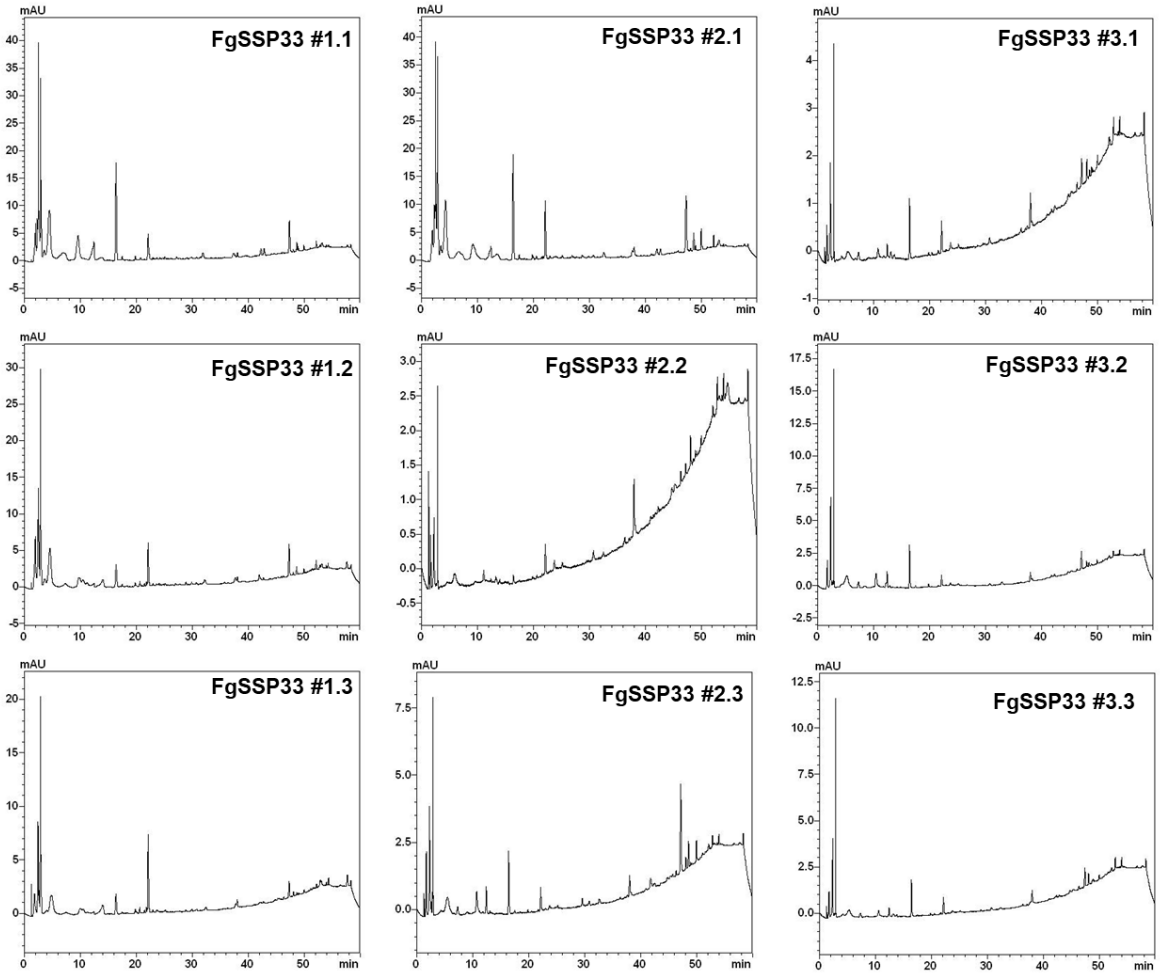
FgSSP33 #1.1
FgSSP33 #2.1
FgSSP33 #3.1
FgSSP33 #1.2
FgSSP33 #2.2
FgSSP33 #3.2
FgSSP33 #1.3
FgSSP33 #2.3
FgSSP33 #3.3
mAU
min

Appendix 7: Photodiode Array chromatograms

Figure 6.2 A comparison of representative PDA chromatograms observed between the healthy and EV controls and *N. benthamiana* plants expressing FgSSP32 and FgSSP33.

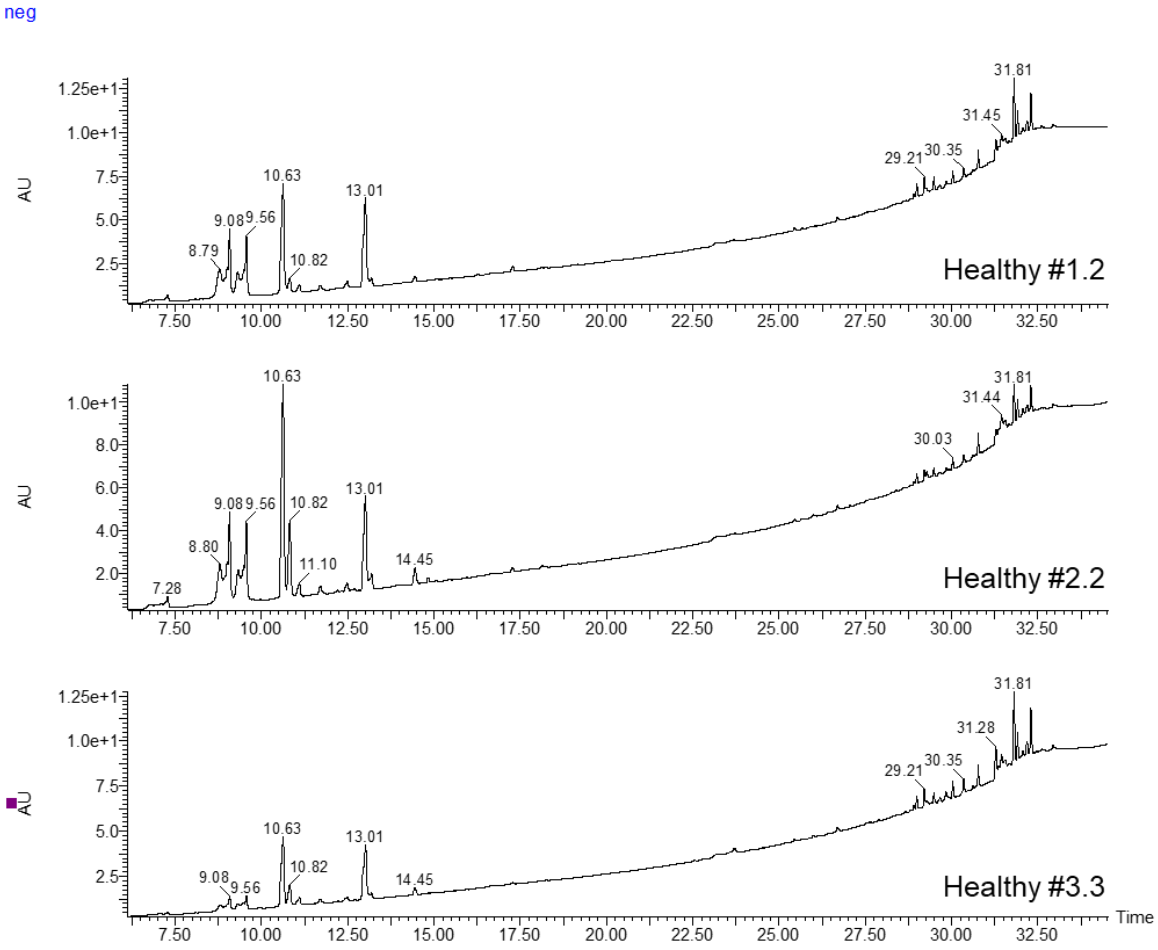

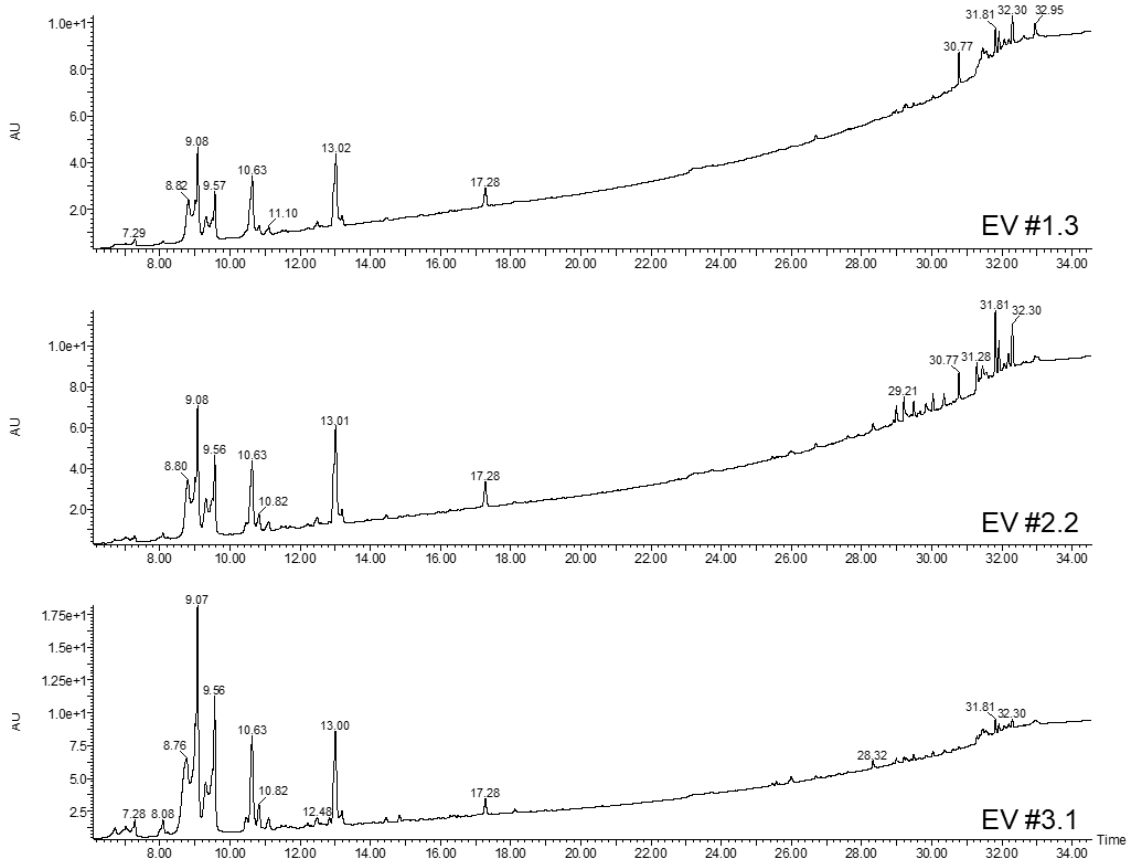
AU
Time
EV #1.3
EV #2.2
EV #3.1

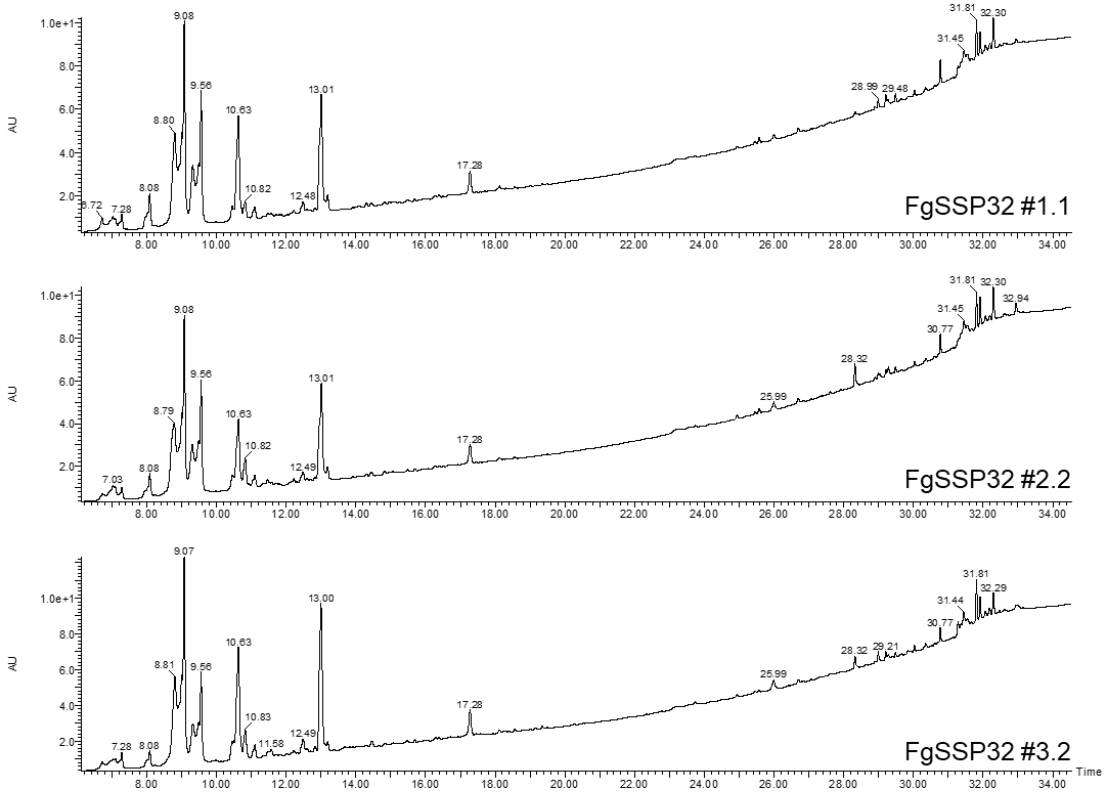
AU
Time
FgSSP32 #1.1
FgSSP32 #2.2
FgSSP32 #3.2

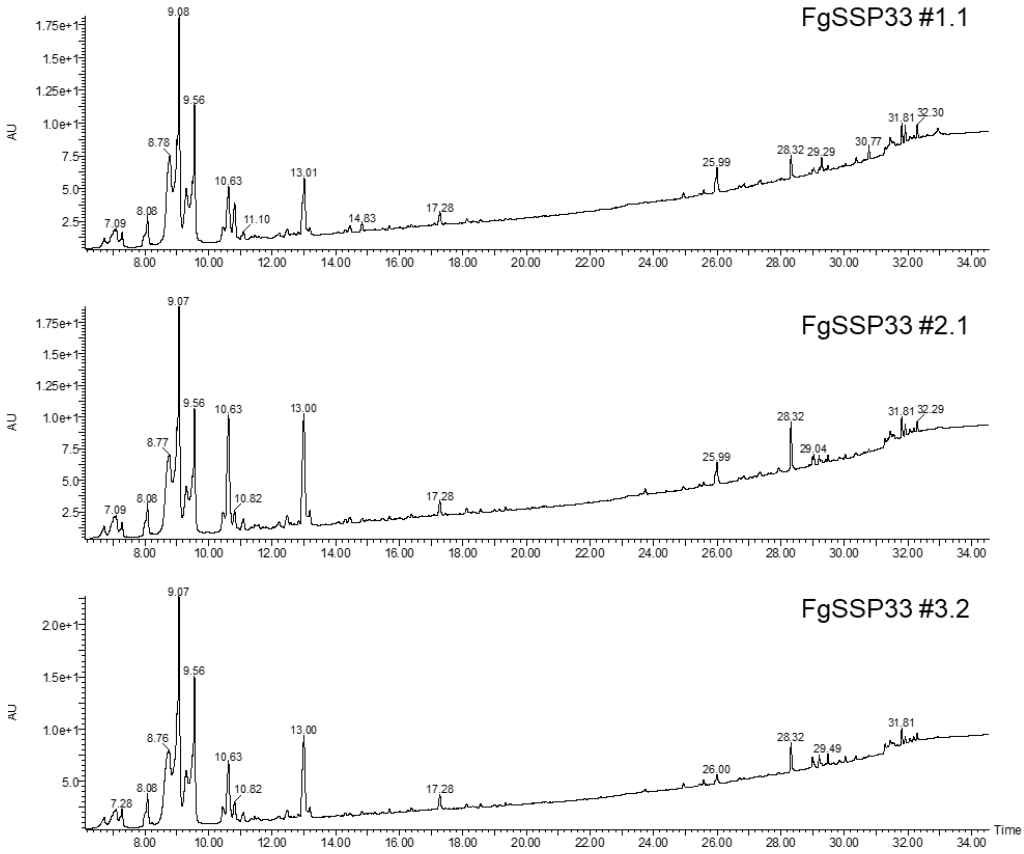
FgSSP33 #1.1
AU
9.08
9.56
8.78
10.63
13.01
7.09
8.08
11.10
14.83
17.28
25.99
28.32
29.29
30.77
31.81
32.30
FgSSP33 #2.1
AU
9.07
9.56
10.63
13.00
8.77
7.09
8.08
10.82
17.28
25.99
28.32
29.04
31.81
32.29
FgSSP33 #3.2
AU
9.07
9.56
13.00
8.76
10.63
7.28
8.08
10.82
17.28
26.00
28.32
29.49
31.81
Time

Appendix 8: Liquid-chromatography mass-spectrometry chromatograms from mass-spectrometry

Figure 6.3. A comparison of representative extracted LCMS chromatograms of healthy and EV controls and *N. benthamiana* plants expressing FgSSP32 and FgSSP33.

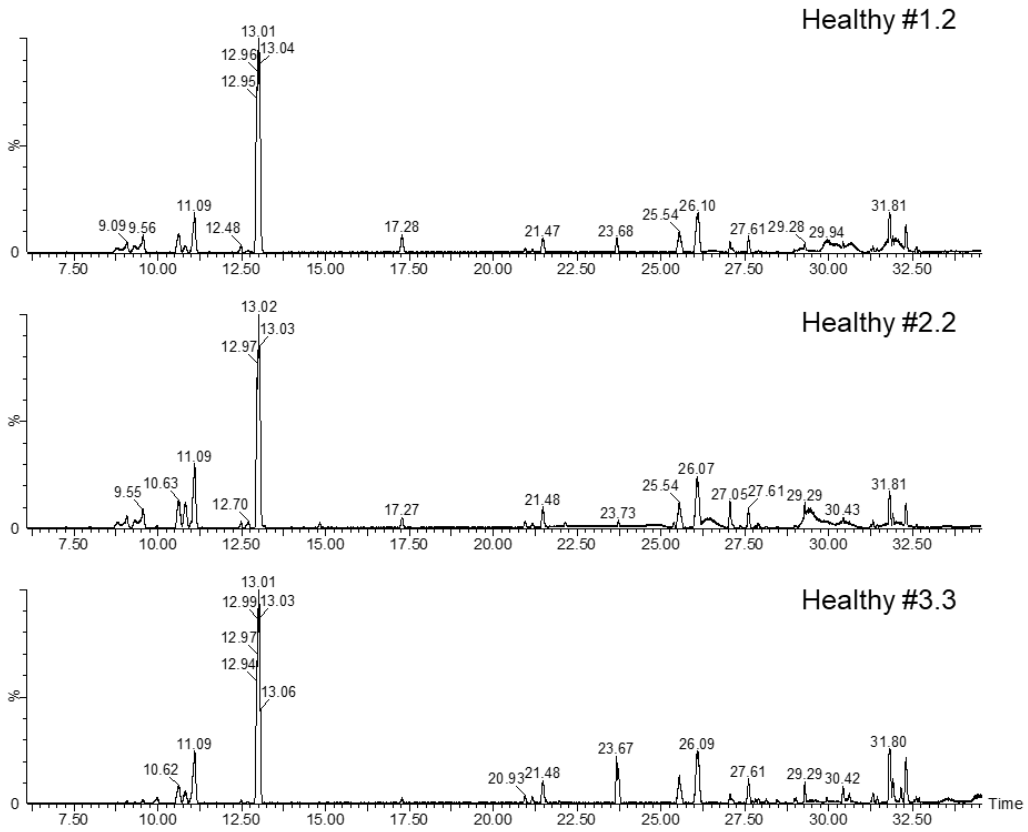

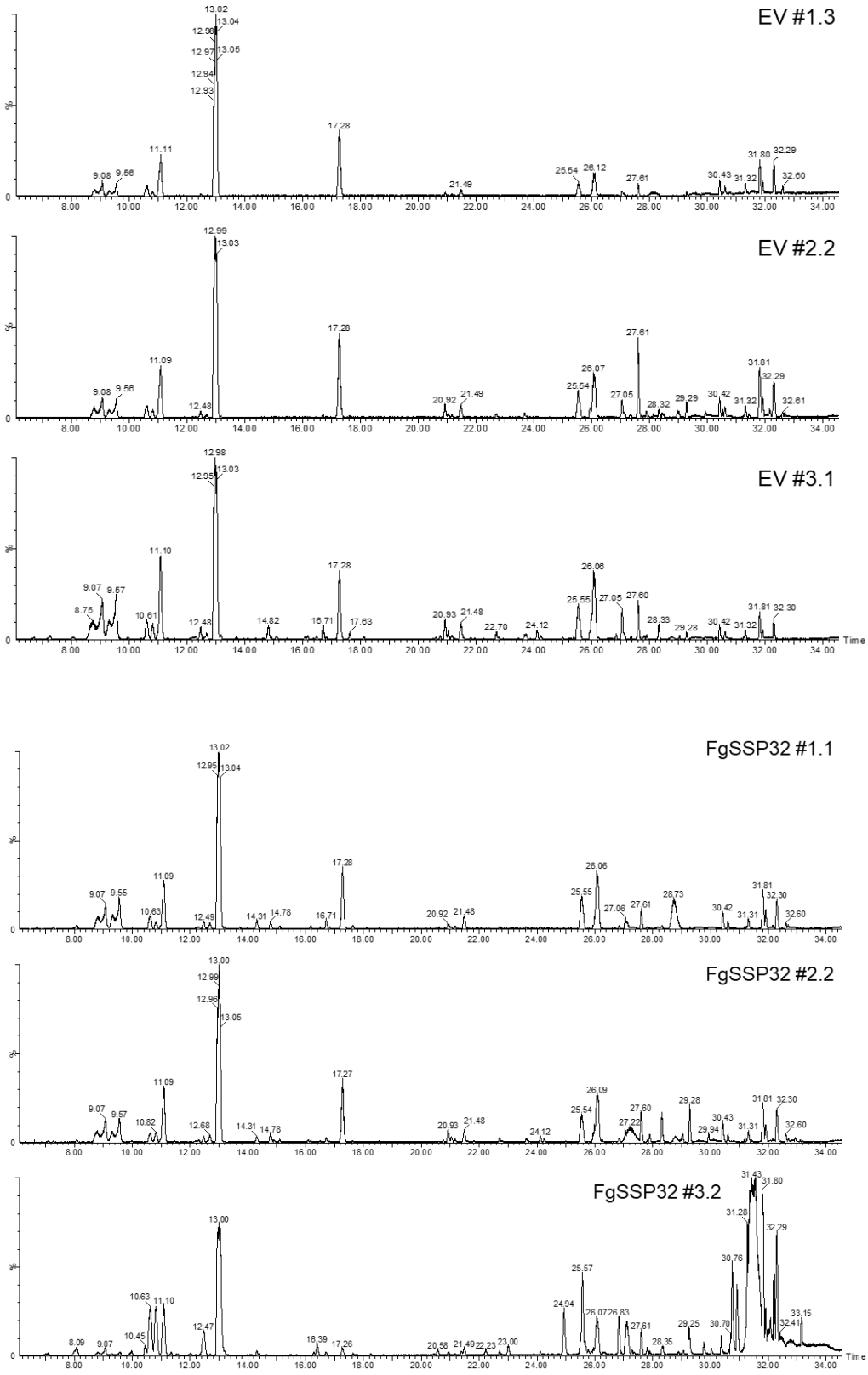
EV #1.3
EV #2.2
EV #3.1
FgSSP32 #1.1
FgSSP32 #2.2
FgSSP32 #3.2
Time

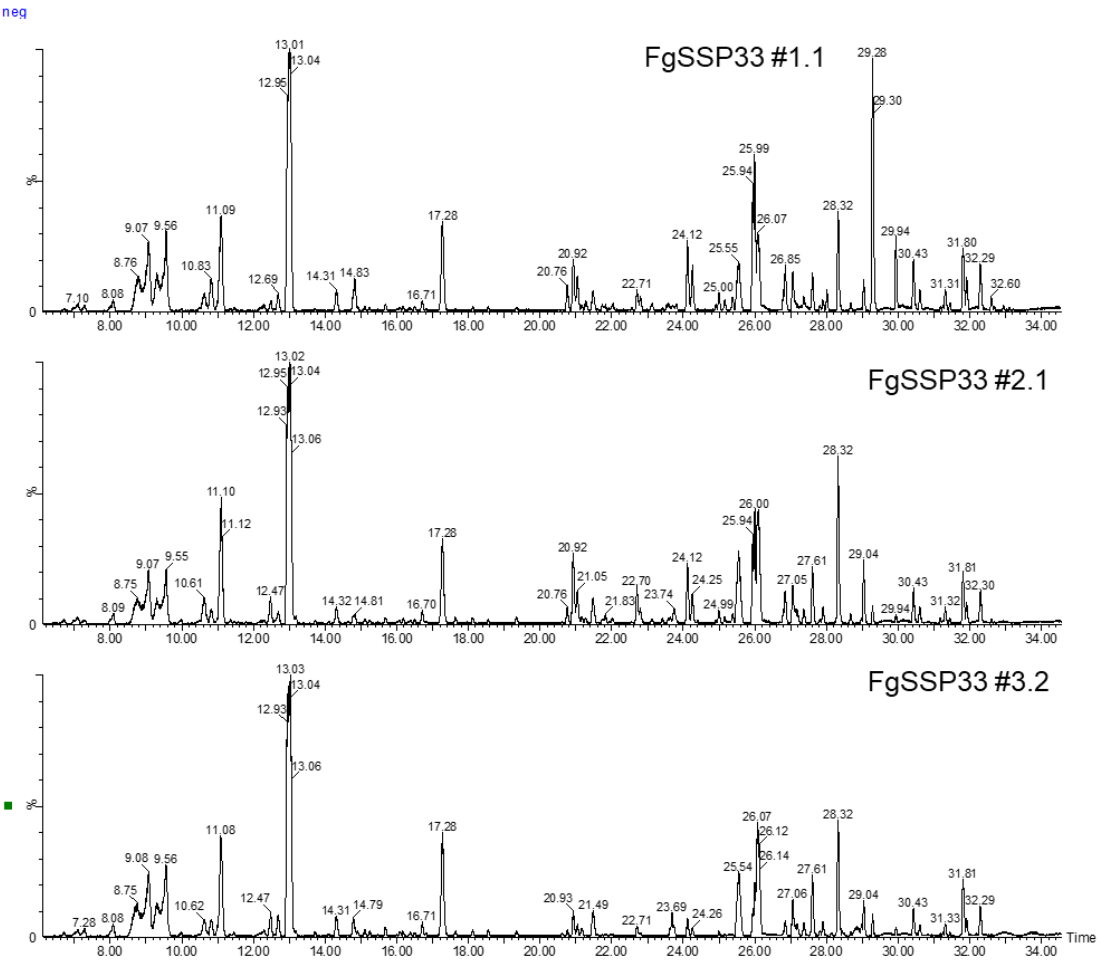
neg
FgSSP33 #1.1
FgSSP33 #2.1
FgSSP33 #3.2
%
Time

References

Abramovitch, R. B., Y. J. Kim, S. R. Chen, M. B. Dickman, and G. B. Martin. 2003. 'Pseudomonas type III effector AvrPtoB induces plant disease susceptibility by inhibition of host programmed cell death', *EMBO Journal*, 22: 60-69.

Adachi, H., S. Kamoun, and A. Maqbool. 2019. 'A resistosome-activated 'death switch'', *Nature Plants*, 5: 457-58.

Adelmant, G., B. K. Garg, M. Tavares, J. D. Card, and J. A. Marto. 2019. 'Tandem Affinity Purification and Mass Spectrometry (TAP-MS) for the Analysis of Protein Complexes', *Curr Protoc Protein Sci*, 96: e84.

Agovino, M., M. Casaccia, M. Ciommi, M. Ferrara, and K. Marchesano. 2019. 'Agriculture, climate change and sustainability: The case of eu-28', *Ecological Indicators*, 105: 525-43.

Ahmed, M. B., K. C. G. dos Santos, I. B. Sanchez, B. Petre, C. Lorrain, M. B. Plourde, S. Duplessis, I. Desgagne-Penix, and H. Germain. 2018. 'A rust fungal effector binds plant DNA and modulates transcription', *Scientific Reports*, 8.

Alabouvette, C., C. Olivain, and C. Steinberg. 2006. 'Biological control of plant diseases: the European situation', *European Journal of Plant Pathology*, 114: 329-41.

Albert, I., H. Bohm, M. Albert, C. E. Feiler, J. Imkampe, N. Wallmeroth, C. Brancato, T. M. Raaymakers, S. Oome, H. Q. Zhang, E. Krol, C. Grefen, A. A. Gust, J. J. Chai, R. Hedrich, G. Van den Ackerveken, and T. Nurnberger. 2015. 'An RLP23-SOBIR1-BAK1 complex mediates NLP-triggered immunity', *Nature Plants*, 1.

Alexander, N. J., R. H. Proctor, and S. P. McCormick. 2009. 'Genes, gene clusters, and biosynthesis of trichothecenes and fumonisins in Fusarium', *Toxin Reviews*, 28: 198-215.

Ali, Z., A. Eid, S. Ali, and M. M. Mahfouz. 2018. 'Pea early-browning virus-mediated genome editing via the CRISPR/Cas9 system in *Nicotiana benthamiana* and *Arabidopsis'*, *Virus Research*, 244: 333-37.

Amaro, T. M. M. M., G. J. A. Thilliez, G. B. Motion, and E. Huitema. 2017. 'A perspective on crn proteins in the genomics age: evolution, classification, delivery and function revisited', *Frontiers in Plant Science*, 8.

Amselem, J., C. A. Cuomo, J. A. L. van Kan, M. Viaud, E. P. Benito, A. Couloux, P. M. Coutinho, R. P. de Vries, P. S. Dyer, S. Fillinger, E. Fournier, L. Gout, M. Hahn, L. M. Kohn, N. Lapalu, K. M. Plummer, J. M. Pradier, E. Quevillon, A. Sharon, A. Simon, A. ten Have, B. Tudzynski, P. Tudzynski, P. Wincker, M. Andrew, V. Anthouard, R. E. Beever, R. Beffa, I. Benoit, O. Bouzid, B. Brault, Z. H. Chen, M. Choquer, J. Collemare, P. Cotton, E. G. Danchin, C. Da Silva, A. Gautier, C. Giraud, T. Giraud, C. Gonzalez, S. Grossetete, U. Guldener, B. Henrissat, B. J. Howlett, C. Kodira, M. Kretschmer, A. Lappartient, M. Leroch, C. Levis, E. Mauceli, C. Neuveglise, B. Oeser, M. Pearson, J. Poulain, N. Poussereau, H. Quesneville, C. Rascle, J. Schumacher, B. Segurens, A. Sexton, E. Silva, C. Sirven, D. M. Soanes, N. J. Talbot, M. Templeton, C. Yandava, O. Yarden, Q. D. Zeng, J. A. Rollins, M. H. Lebrun, and M. Dickman. 2011. 'Genomic Analysis of the Necrotrophic Fungal Pathogens *Sclerotinia sclerotiorum* and *Botrytis cinerea*', *PloS Genetics*, 7.

Antoniw, J., A. M. Beacham, T. K. Baldwin, M. Urban, J. J. Rudd, and K. E. Hammond-Kosack. 2011. 'OmniMapFree: A unified tool to visualise and explore sequenced genomes', *BMC Bioinformatics*, 12.

Arora, S., B. Steuernagel, K. Gaurav, S. Chandramohan, Y. M. Long, O. Matny, R. Johnson, J. Enk, S. Periyannan, N. Singh, M. A. M. Hatta, N. Athiyannan, J. Cheema, G. T. Yu, N. Kangara, S. Ghosh, L. J. Szabo, J. Poland, H. Bariana, J. D. G. Jones, A. R. Bentley, M. Ayliffe, E. Olson, S. S. Xu, B. J. Steffenson, E. Lagudah, and B. B. H. Wulff. 2019. 'Resistance gene cloning from a wild crop relative by sequence capture and association genetics', *Nature Biotechnology*, 37: 139.

Asai, S., O. J. Furzer, V. Cevik, D. S. Kim, N. Ishaque, S. Goritschnig, B. J. Staskawicz, K. Shirasu, and J. D. G. Jones. 2018. 'A downy mildew effector evades recognition by polymorphism of expression and subcellular localization', *Nature Communications*, 9.

Avesani, L., G. Marconi, F. Morandini, E. Albertini, M. Bruschetta, L. Bortesi, M. Pezzotti, and A. Porceddu. 2007. 'Stability of Potato virus X expression vectors is related to insert size: implications for replication models and risk assessment', *Transgenic Research*, 16: 587-97.

Awad, W. A., K. Ghareeb, J. Bohm, and J. Zentek. 2010. 'Decontamination and detoxification strategies for the *Fusarium* mycotoxin deoxynivalenol in animal feed and the effectiveness of microbial biodegradation', *Food Addit Contam Part A Chem Anal Control Expo Risk Assess*, 27: 510-20.

Azevedo, C., S. Betsuyaku, J. Peart, A. Takahashi, L. Noel, A. Sadanandom, C. Casais, J. Parker, and K. Shirasu. 2006. 'Role of SGT1 in resistance protein accumulation in plant immunity', *EMBO Journal*, 25: 2007-16.

Azmi, N. S. A., S. Singkaravanit-Ogawa, K. Ikeda, S. Kitakura, Y. Inoue, Y. Narusaka, K. Shirasu, M. Kaido, K. Mise, and Y. Takano. 2018. 'Inappropriate Expression of an NLP Effector in *Colletotrichum orbiculare* Impairs Infection on *Cucurbitaceae* Cultivars via Plant Recognition of the C-Terminal Region', *Molecular Plant-Microbe Interactions*, 31: 101-11.

Backhouse, D. 2014. 'Global distribution of *Fusarium graminearum, F. asiaticum* and *F. boothii f*rom wheat in relation to climate', *European Journal of Plant Pathology*, 139: 161-73.

Baebler, S., K. Witek, M. Petek, K. Stare, M. Tusek-Znidaric, M. Pompe-Novak, J. Renaut, K. Szajko, D. Strzelczyk-Zyta, W. Marczewski, K. Morgiewicz, K. Gruden, and J. Hennig. 2014. 'Salicylic acid is an indispensable component of the Ny-1 resistance-gene-mediated response against Potato virus Y infection in potato', *Journal of Experimental Botany*, 65: 1095-109.

Bai, G. H., R. Plattner, A. Desjardins, and F. Kolb. 2001. 'Resistance to Fusarium head blight and deoxynivalenol accumulation in wheat', *Plant Breeding*, 120: 1-6.

Bai, Y. L., S. Pavan, Z. Zheng, N. F. Zappel, A. Reinstadler, C. Lotti, C. De Giovanni, L. Ricciardi, P. Lindhout, R. Visser, K. Theres, and R. Panstruga. 2008. 'Naturally occurring broad-spectrum powdery mildew

resistance in a central American tomato accession is caused by loss of Mlo function', *Molecular Plant-Microbe Interactions*, 21: 30-39.

Bailey, B. A. 1995. 'Purification of a Protein from Culture Filtrates of *Fusarium oxysporum* That Induces Ethylene and Necrosis in Leaves of Erythroxylum-Coca', *Phytopathology*, 85: 1250-55.

Bally, J., H. Jung, C. Mortimer, F. Naim, J. G. Philips, R. Hellens, A. Bombarely, M. M. Goodin, and P. M. Waterhouse. 2018. 'The Rise and Rise of *Nicotiana benthamiana:* A Plant for All Reasons', *Annual Review of Phytopathology, Vol 56*, 56: 405-26.

Ban, T., and K. Suenaga. 2000. 'Genetic analysis of resistance to Fusarium head blight caused by *Fusarium graminearum* in Chinese wheat cultivar Sumai 3 and the Japanese cultivar Saikai 165', *Euphytica*, 113: 87-99.

Baum, J. A., T. Bogaert, W. Clinton, G. R. Heck, P. Feldmann, O. Ilagan, S. Johnson, G. Plaetinck, T. Munyikwa, M. Pleau, T. Vaughn, and J. Roberts. 2007. 'Control of coleopteran insect pests through RNA interference', *Nature Biotechnology*, 25: 1322-26.

Bebber, D. P., and S. J. Gurr. 2015. 'Crop-destroying fungal and oomycete pathogens challenge food security', *Fungal Genetics and Biology*, 74: 62-64.

Bennypaul, H. S., J. S. Mutti, S. Rustgi, N. Kumar, P. A. Okubara, and K. S. Gill. 2012. 'Virus-induced gene silencing (VIGS) of genes expressed in root, leaf, and meiotic tissues of wheat', *Functional & Integrative Genomics*, 12: 143-56.

Bidzinski, P., E. Ballini, A. Ducasse, C. Michel, P. Zuluaga, A. Genga, R. Chiozzotto, and J. B. Morel. 2016. 'Transcriptional Basis of Drought-Induced Susceptibility to the Rice Blast Fungus *Magnaporthe oryzae'*, *Frontiers in Plant Science*, 7.

Binder, U., M. L. Chu, N. D. Read, and F. Marx. 2010. 'The Antifungal Activity of the *Penicillium chrysogenum* Protein PAF Disrupts Calcium Homeostasis in Neurospora crassa', *Eukaryotic Cell*, 9: 1374-82.

Blumke, A., C. Falter, C. Herrfurth, B. Sode, R. Bode, W. Schafer, I. Feussner, and C. A. Voigt. 2014. 'Secreted Fungal Effector Lipase Releases Free Fatty Acids to Inhibit Innate Immunity-Related Callose

Formation during Wheat Head Infection', *Plant Physiology*, 165: 346-58.

Boedi, S., H. Berger, C. Sieber, M. Munsterkotter, I. Maloku, B. Warth, M. Sulyok, M. Lemmens, R. Schuhmacher, U. Guldener, and J. Strauss. 2016. 'Comparison of *Fusarium graminearum* Transcriptomes on Living or Dead Wheat Differentiates Substrate-Responsive and Defense-Responsive Genes', *Frontiers in Microbiolgy*, 7: 1113.

Boenisch, M. J., K. L. Broz, S. O. Purvine, W. B. Chrisler, C. D. Nicora, L. R. Connolly, M. Freitag, S. E. Baker, and H. C. Kistler. 2017. 'Structural reorganization of the fungal endoplasmic reticulum upon induction of mycotoxin biosynthesis', *Scientific Reports*, 7.

Boenisch, M. J., and W. Schafer. 2011. '*Fusarium graminearum* forms mycotoxin producing infection structures on wheat', *BMC Plant Biology*, 11.

Bohnert, H. U., I. Fudal, W. Dioh, D. Tharreau, J. L. Notteghem, and M. H. Lebrun. 2004. 'A putative polyketide synthase peptide synthetase from *Magnaporthe grisea* signals pathogen attack to resistant rice', *Plant Cell*, 16: 2499-513.

Boller, T., and G. Felix. 2009. 'A Renaissance of Elicitors: Perception of Microbe-Associated Molecular Patterns and Danger Signals by Pattern-Recognition Receptors', *Annual Review of Plant Biology*, 60: 379-406.

Bolton, M. D., H. P. van Esse, J. H. Vossen, R. de Jonge, I. Stergiopoulos, I. J. Stulemeijer, G. C. van den Berg, O. Borras-Hidalgo, H. L. Dekker, C. G. de Koster, P. J. de Wit, M. H. Joosten, and B. P. Thomma. 2008. 'The novel *Cladosporium fulvum* lysin motif effector Ecp6 is a virulence factor with orthologues in other fungal species', *Molecular Microbiology*, 69: 119-36.

Bombarely, A., H. G. Rosli, J. Vrebalov, P. Moffett, L. A. Mueller, and G. B. Martin. 2012. 'A Draft Genome Sequence of *Nicotiana benthamiana* to Enhance Molecular Plant-Microbe Biology Research', *Molecular Plant-Microbe Interactions*, 25: 1523-30.

Bonnighausen, J., N. Schauer, W. Schafer, and J. Bormann. 2019. 'Metabolic profiling of wheat rachis node infection by *Fusarium*

graminearum - decoding deoxynivalenol-dependent susceptibility', *New Phytologist*, 221: 459-69.

Bos, J. I., M. R. Armstrong, E. M. Gilroy, P. C. Boevink, I. Hein, R. M. Taylor, T. Zhendong, S. Engelhardt, R. R. Vetukuri, B. Harrower, C. Dixelius, G. Bryan, A. Sadanandom, S. C. Whisson, S. Kamoun, and P. R. Birch. 2010. '*Phytophthora infestans* effector AVR3a is essential for virulence and manipulates plant immunity by stabilizing host E3 ligase CMPG1', *Proceedings of the National Academy of Sciences,* 107: 9909-14.

Bos, J. I. B., T. D. Kanneganti, C. Young, C. Cakir, E. Huitema, J. Win, M. R. Armstrong, P. R. J. Birch, and S. Kamoun. 2006. 'The C-terminal half of *Phytophthora infestans* RXLR effector AVR3a is sufficient to trigger R3a-mediated hypersensitivity and suppress INF1-induced cell death in *Nicotiana benthamiana*', *Plant Journal*, 48: 165-76.

Boston, R. S., P. V. Viitanen, and E. Vierling. 1996. 'Molecular chaperones and protein folding in plants', *Plant Molecular Biology*, 32: 191-222.

Bottalico, A., and G. Perrone. 2002. 'Toxigenic Fusarium species and mycotoxins associated with head blight in small-grain cereals in Europe', *European Journal of Plant Pathology*, 108: 611-24.

Bouton, C., R. C. King, H. X. Chen, K. Azhakanandam, S. Bieri, K. E. Hammond-Kosack, and K. Kanyuka. 2018. 'Foxtail mosaic virus: A Viral Vector for Protein Expression in Cereals', *Plant Physiology*, 177: 1352-67.

Boyacioglu, D., and N. S. Hettiarachchy. 1995. 'Changes in Some Biochemical-Components of Wheat-Grain That Was Infected with *Fusarium graminearum*', *Journal of Cereal Science*, 21: 57-62.

Bozkurt, T. O., S. Schornack, J. Win, T. Shindo, M. Ilyas, R. Oliva, L. M. Cano, A. M. E. Jones, E. Huitema, R. A. L. van der Hoorn, and S. Kamoun. 2011. '*Phytophthora infestans* effector AVRblb2 prevents secretion of a plant immune protease at the haustorial interface', *Proceedings of the National Academy of Sciences,* 108: 20832-37.

Brar, G. S., A. L. Brule-Babel, Y. F. Ruan, M. A. Henriquez, C. J. Pozniak, H. R. Kutcher, and P. J. Hucl. 2019. 'Genetic factors affecting Fusarium head blight resistance improvement from introgression of exotic

Sumai 3 alleles (including Fhb1, Fhb2, and Fhb5) in hard red spring wheat', *BMC Plant Biology*, 19.

Brazma, A., H. Parkinson, U. Sarkans, M. Shojatalab, J. Vilo, N. Abeygunawardena, E. Holloway, M. Kapushesky, P. Kemmeren, G. G. Lara, A. Oezcimen, P. Rocca-Serra, and S. A. Sansone. 2003. 'ArrayExpress - a public repository for microarray gene expression data at the EBI', *Nucleic Acids Research*, 31: 68-71.

Brefort, T., S. Tanaka, N. Neidig, G. Doehlemann, V. Vincon, and R. Kahmann. 2014. 'Characterization of the Largest Effector Gene Cluster of *Ustilago maydis'*, *PloS Pathogens*, 10.

Brewer, H. C., and K. E. Hammond-Kosack. 2015. 'Host to a Stranger: Arabidopsis and Fusarium Ear Blight', *Trends in Plant Science*, 20: 651-63.

Bronnimann, S., J. Franke, S. U. Nussbaumer, H. J. Zumbuhl, D. Steiner, M. Trachsel, G. C. Hegerl, A. Schurer, M. Worni, A. Malik, J. Fluckiger, and C. C. Raible. 2019. 'Last phase of the Little Ice Age forced by volcanic eruptions', *Nature Geoscience*, 12: 650-+.

Brown, J. K. M. 2015. 'Durable Resistance of Crops to Disease: A Darwinian Perspective', *Annual Review of Phytopathology, Vol 53*, 53: 513-39.

Brown, N. A., J. Antoniw, and K. E. Hammond-Kosack. 2012. 'The Predicted Secretome of the Plant Pathogenic Fungus *Fusarium graminearum:* A Refined Comparative Analysis', *PloS One*, 7.

Brown, N. A., C. Bass, T. K. Baldwin, H. Chen, F. Massot, P. W. Carion, M. Urban, A. M. van de Meene, and K. E. Hammond-Kosack. 2011. 'Characterisation of the F*usarium graminearum*-Wheat Floral Interaction', *Journal of Pathogens*, 2011: 626345.

Brown, N. A., J. Evans, A. Mead, and K. E. Hammond-Kosack. 2017. 'A spatial temporal analysis of the *Fusarium graminearum* transcriptome during symptomless and symptomatic wheat infection', *Molecular Plant Pathology*, 18: 1295-312.

Brown, N. A., M. Urban, A. M. L. Van De Meene, and K. E. Hammond-Kosack. 2010. 'The infection biology of *Fusarium graminearum:* Defining the pathways of spikelet to spikelet colonisation in wheat ears', *Fungal Biology*, 114: 555-71.

Brown, Neil Andrew, and Kim E Hammond-Kosack. 2015. "Secreted biomolecules in fungal plant pathogenesis." In *Fungal biomolecules: sources, applications and recent developments*, 263-310

Bruun-Rasmussen, M., C. T. Madsen, S. Jessing, and M. Albrechtsen. 2007. 'Stability of Barley stripe mosaic virus - Induced gene silencing in barley', *Molecular Plant-Microbe Interactions*, 20: 1323-31.

Buerstmayr, H., T. Ban, and J. A. Anderson. 2009. 'QTL mapping and marker-assisted selection for Fusarium head blight resistance in wheat: a review', *Plant Breeding*, 128: 1-26.

Buerstmayr, H., M. Lemmens, L. Hartl, L. Doldi, B. Steiner, M. Stierschneider, and P. Ruckenbauer. 2002. 'Molecular mapping of QTLs for Fusarium head blight resistance in spring wheat. I. Resistance to fungal spread (type II resistance)', *Theoretical and Applied Genetics*, 104: 84-91.

Buhrow, L. M., S. M. Clark, and M. C. Loewen. 2016. 'Identification of an attenuated barley stripe mosaic virus for the virus-induced gene silencing of pathogenesis-related wheat genes', *Plant Methods*, 12.

Burgess, L. W., D. Backhouse, L. J. Swan, and R. J. Esdaile. 1996. 'Control of Fusarium crown rot of wheat by late stubble burning and rotation with sorghum', *Australasian Plant Pathology*, 25: 229-33.

Burlakoti, R. R., S. Ali, G. A. Secor, S. M. Neate, M. P. McMullen, and T. B. Adhikari. 2008. 'Comparative mycotoxin profiles of *Gibberella zeae* populations from barley, wheat, potatoes, and sugar beets', *Applied Environmental Microbioogyl*, 74: 6513-20.

Bushnell, W.R., B. E. Hazen, C. Pritsch, and K. Leonard. 2003. 'Histology and physiology of Fusarium head blight.' In, *Fusarium head blight of wheat and barley* (APS Press).

Caillaud, M. C., S. J. M. Piquerez, G. Fabro, J. Steinbrenner, N. Ishaque, J. Beynon, and J. D. G. Jones. 2012. 'Subcellular localization of the Hpa RxLR effector repertoire identifies a tonoplast-associated protein HaRxL17 that confers enhanced plant susceptibility', *Plant Journal*, 69: 252-65.

Cakir, C., M. E. Gillespie, and S. R. Scofield. 2010. 'Rapid Determination of Gene Function by Virus-induced Gene Silencing in Wheat and Barley', *Crop Science*, 50: S77-S84.

Cano-Delgado, A., Y. H. Yin, C. Yu, D. Vafeados, S. Mora-Garcia, J. C. Cheng, K. H. Nam, J. M. Li, and J. Chory. 2004. 'BRL1 and BRL3 are novel brassinosteroid receptors that function in vascular differentiation in Arabidopsis', *Development*, 131: 5341-51.

Cantarel, B. L., P. M. Coutinho, C. Rancurel, T. Bernard, V. Lombard, and B. Henrissat. 2009. 'The Carbohydrate-Active EnZymes database (CAZy): an expert resource for Glycogenomics', *Nucleic Acids Research*, 37: D233-D38.

Cao, L. X., M. C. Blekemolen, N. Tintor, B. J. C. Cornelissen, and F. L. W. Takken. 2018. 'The *Fusarium oxysporum* Avr2-Six5 Effector Pair Alters Plasmodesmatal Exclusion Selectivity to Facilitate Cell-to-Cell Movement of Avr2', *Molecular Plant*, 11: 691-705.

Catlett, N. L., B. Lee, O. C. Yoder, and B. G. Turgeon. 2003. 'Split-marker recombination for efficient targeted deletion of fungal genes', *Fungal Genetics Reports*, 50: 9-11.

Chaerle, L., S. Lenk, D. Hagenbeek, C. Buschmann, and D. Van Der Straeten. 2007. 'Multicolor fluorescence imaging for early detection of the hypersensitive reaction to tobacco mosaic virus', *Journal of Plant Physiology*, 164: 253-62.

Chakraborty, S., and A. C. Newton. 2011. 'Climate change, plant diseases and food security: an overview', *Plant Pathology*, 60: 2-14.

Chakravarthy, S., A. C. Velasquez, S. K. Ekengren, A. Collmer, and G. B. Martini. 2010. 'Identification of *Nicotiana benthamiana* Genes Involved in Pathogen-Associated Molecular Pattern-Triggered Immunity', *Molecular Plant-Microbe Interactions*, 23: 715-26.

Chapman, S., T. Kavanagh, and D. Baulcombe. 1992. 'Potato Virus-X as a Vector for Gene-Expression in Plants', *Plant Journal*, 2: 549-57.

Chen, K., Y. Wang, R. Zhang, H. Zhang, and C. Gao. 2019. 'CRISPR/Cas Genome Editing and Precision Plant Breeding in Agriculture', *Annual Review of Plant Biology*, 70: 667-97.

Chen, Q., H. Lai, J. Hurtado, J. Stahnke, K. Leuzinger, and M. Dent. 2013. 'Agroinfiltration as an Effective and Scalable Strategy of Gene Delivery for Production of Pharmaceutical Proteins', *Advanced Techniques in Biology and Medicine*, 1.

Chen, Yun, H Corby Kistler, and Zhonghua Ma. 2019. '*Fusarium graminearum* Trichothecene Mycotoxins: Biosynthesis, Regulation, and Management', *Annual Review of Phytopathology*, 57.

Cheng, C., X. Q. Gao, B. M. Feng, J. Sheen, L. B. Shan, and P. He. 2013. 'Plant immune response to pathogens differs with changing temperatures', *Nature Communications*, 4.

Cheuk, A., and M. Houde. 2018. 'A New Barley Stripe Mosaic Virus Allows Large Protein Overexpression for Rapid Function Analysis', *Plant Physiology*, 176: 1919-31.

Chinchilla, D., C. Zipfel, S. Robatzek, B. Kemmerling, T. Nurnberger, J. D. G. Jones, G. Felix, and T. Boller. 2007. 'A flagellin-induced complex of the receptor FLS2 and BAK1 initiates plant defence', *Nature*, 448: 497-U12.

Chiurugwi, T., S. Kemp, W. Powell, and L. T. Hickey. 2019. 'Speed breeding orphan crops', *Theoretical and Applied Genetics*, 132: 607-16.

Ciuffetti, L. M., V. A. Manning, I. Pandelova, M. F. Betts, and J. P. Martinez. 2010. 'Host-selective toxins, Ptr ToxA and Ptr ToxB, as necrotrophic effectors in the *Pyrenophora tritici-repentis*-wheat interaction', *New Phytologist*, 187: 911-9.

Cloutier, S., B. D. McCallum, C. Loutre, T. W. Banks, T. Wicker, C. Feuillet, B. Keller, and M. C. Jordan. 2007. 'Leaf rust resistance gene Lr1, isolated from bread wheat (Triticum aestivum L.) is a member of the large psr567 gene family', *Plant Molecular Biology*, 65: 93-106.

Cook, D. E., C. H. Mesarich, and B. P. H. J. Thomma. 2015. 'Understanding Plant Immunity as a Surveillance System to Detect Invasion', *Annual Review of Phytopathology, Vol 53*, 53: 541-63.

Cowger, C., J. Patton-Ozkurt, G. Brown-Guedira, and L. Perugini. 2009. 'Post-Anthesis Moisture Increased Fusarium Head Blight and Deoxynivalenol Levels in North Carolina Winter Wheat', *Phytopathology*, 99: 320-27.

Cui, Y., M. Y. Lee, N. X. Huo, J. Bragg, L. J. Yan, C. Yuan, C. Li, S. J. Holditch, J. Z. Xie, M. C. Luo, D. W. Li, J. L. Yu, J. Martin, W. Schackwitz, Y. Q. Gu, J. P. Vogel, A. O. Jackson, Z. Y. Liu, and D. F. Garvin. 2012. 'Fine Mapping of the Bsr1 Barley Stripe Mosaic Virus Resistance Gene in the Model Grass *Brachypodium distachyon*', *PloS One*, 7.

Cundliffe, E., M. Cannon, and J. Davies. 1974. 'Mechanism of inhibition of eukaryotic protein synthesis by trichothecene fungal toxins', *Proceedings of the National Academy of Sciences,* 71: 30-34.

Cuomo, C. A., U. Gueldener, J. R. Xu, F. Trail, B. G. Turgeon, A. Di Pietro, J. D. Walton, L. J. Ma, S. E. Baker, M. Rep, G. Adam, J. Antoniw, T. Baldwin, S. Calvo, Y. L. Chang, D. DeCaprio, L. R. Gale, S. Gnerre, R. S. Goswami, K. Hammond-Kosack, L. J. Harris, K. Hilburn, J. C. Kennell, S. Kroken, J. K. Magnuson, G. Mannhaupt, E. Mauceli, H. W. Mewes, R. Mitterbauer, G. Muehlbauer, M. Munsterkotter, D. Nelson, K. O'Donnell, T. Ouellet, W. H. Qi, H. Quesneville, M. I. G. Roncero, K. Y. Seong, I. V. Tetko, M. Urban, C. Waalwijk, T. J. Ward, J. Q. Yao, B. W. Birren, and H. C. Kistler. 2007. 'The *Fusarium graminearum* genome reveals a link between localized polymorphism and pathogen specialization', *Science*, 317: 1400-02.

Cuthbert, P. A., D. J. Somers, and A. Brule-Babel. 2007. 'Mapping of Fhb2 on chromosome 6BS: a gene controlling Fusarium head blight field resistance in bread wheat (*Triticum aestivum* L.)', *Theoretical and Applied Genetics*, 114: 429-37.

Cuthbert, P. A., D. J. Somers, J. Thomas, S. Cloutier, and A. Brule-Babel. 2006. 'Fine mapping Fhb1, a major gene controlling Fusarium head blight resistance in bread wheat (Triticum aestivum L.)', *Theoretical and Applied Genetics*, 112: 1465-72.

Cuzick, A., M. Urban, and K. Hammond-Kosack. 2008. '*Fusarium graminearum* gene deletion mutants map1 and tri5 reveal similarities and differences in the pathogenicity requirements to cause disease on Arabidopsis and wheat floral tissue', *New Phytologist*, 177: 990-1000.

Cuzick, A., M. Harris, B. Norman, K. Rutherford, J. Seager, M. Urban, V. Wood, and K. Hammond-Kosack. 2019. 'PHI-base: Capturing

phenotypes for inclusion in a multi-species interaction database', *F1000Research*, 8.

Dahal, K., J. Wang, G. D. Martyn, F. Rahimy, and G. C. Vanlerberghe. 2014. 'Mitochondrial Alternative Oxidase Maintains Respiration and Preserves Photosynthetic Capacity during Moderate Drought in *Nicotiana tabacum*', *Plant Physiology*, 166: 1560-74.

Dale, J., A. James, J. Y. Paul, H. Khanna, M. Smith, S. Peraza-Echeverria, F. Garcia-Bastidas, G. Kema, P. Waterhouse, K. Mengersen, and R. Harding. 2017. 'Transgenic Cavendish bananas with resistance to Fusarium wilt tropical race 4', *Nature Communications*, 8.

Dalio, R. J. D., J. Herlihy, T. S. Oliveira, J. M. McDowell, and M. Machado. 2018. 'Effector Biology in Focus: A Primer for Computational Prediction and Functional Characterization', *Molecular Plant-Microbe Interactions*, 31: 22-33.

Dangl, J. L., D. M. Horvath, and B. J. Staskawicz. 2013. 'Pivoting the Plant Immune System from Dissection to Deployment', *Science*, 341: 746-51.

Dangl, J. L., and J. D. Jones. 2001. 'Plant pathogens and integrated defence responses to infection', *Nature*, 411: 826-33.

Dangl, J. L., and J. D. G. Jones. 2019. 'A pentangular plant inflammasome', *Science*, 364: 31-32.

de Guillen, K., D. Ortiz-Vallejo, J. Gracy, E. Fournier, T. Kroj, and A. Padilla. 2015. 'Structure Analysis Uncovers a Highly Diverse but Structurally Conserved Effector Family in Phytopathogenic Fungi', *PloS Pathogens*, 11.

de Jonge, R., H. P. van Esse, A. Kombrink, T. Shinya, Y. Desaki, R. Bours, S. van der Krol, N. Shibuya, M. H. Joosten, and B. P. Thomma. 2010. 'Conserved fungal LysM effector Ecp6 prevents chitin-triggered immunity in plants', *Science*, 329: 953-5.

de Wit, P. J. G. M., R. Mehrabi, H. A. van den Burg, and I. Stergiopoulos. 2009. 'Fungal effector proteins: past, present and future', *Molecular Plant Pathology*, 10: 735-47.

De Wit, P. J. G. M., and Spikman, G. 1982a. 'Evidence for the occurrence of race and cultivar-specific elicitors of necrosis in intercellular fluids of

compatible interactions of *Cladosporium fulvum* and tomato', *Physiological Plant Pathology*, 21: 1IN19-8IN211.

De Wit, P.J.G.M, and G. J Spikman. 1982b. 'Evidence for the occurrence of race and cultivar-specific elicitors of necrosis in intercellular fluids of compatible interactions of Cladosporium fulvum and tomato', *Physiological Plant Pathology* 21: 1-11.

De Wolf, E. D., L. V. Madden, and P.E Lipps. 2003. 'Risk assessment models for wheat Fusarium head blight epidemics based on within-season weather data', *Phytopathology*, 93: 428-35.

Dean, J. D., P. H. Goodwin, and T. Hsiang. 2005. 'Induction of glutathione S-transferase genes of *Nicotiana benthamiana* following infection by *Colletotrichum destructivum* and *C. orbiculare* and involvement of one in resistance', *Journal of Experimental Botany*, 56: 1525-33.

Dean, R. A., N. J. Talbot, D. J. Ebbole, M. L. Farman, T. K. Mitchell, M. J. Orbach, M. Thon, R. Kulkarni, J. R. Xu, H. Q. Pan, N. D. Read, Y. H. Lee, I. Carbone, D. Brown, Y. Y. Oh, N. Donofrio, J. S. Jeong, D. M. Soanes, S. Djonovic, E. Kolomiets, C. Rehmeyer, W. X. Li, M. Harding, S. Kim, M. H. Lebrun, H. Bohnert, S. Coughlan, J. Butler, S. Calvo, L. J. Ma, R. Nicol, S. Purcell, C. Nusbaum, J. E. Galagan, and B. W. Birren. 2005. 'The genome sequence of the rice blast fungus *Magnaporthe grisea*', *Nature*, 434: 980-86.

Derbyshire, M., M. Denton-Giles, D. Hegedus, S. Seifbarghi, J. Rollins, J. van Kan, M. F. Seidl, L. Faino, M. Mbengue, O. Navaud, S. Raffaele, K. Hammond-Kosack, S. Heard, and R. Oliver. 2017. 'The Complete Genome Sequence of the Phytopathogenic Fungus *Sclerotinia sclerotiorum* Reveals Insights into the Genome Architecture of Broad Host Range Pathogens', *Genome Biology and Evolution*, 9: 593-618.

Desjardins, A. E., and R. H. Proctor. 2007. 'Molecular biology of Fusarium mycotoxins', *International Journal of Food Microbiology*, 119: 47-50.

Desmond, O. J., J. M. Manners, A. E. Stephens, D. J. MaClean, P. M. Schenk, D. M. Gardiner, A. L. Munn, and K. Kazan. 2008. 'The Fusarium mycotoxin deoxynivalenol elicits hydrogen peroxide production, programmed cell death and defence responses in wheat', *Molecular Plant Pathology*, 9: 435-45.

Dhokane, D., S. Karre, A. C. Kushalappa, and C. McCartney. 2016. 'Integrated Metabolo-Transcriptomics Reveals Fusarium Head Blight Candidate Resistance Genes in Wheat QTL-Fhb2', *PloS One*, 11.

Diamond, M., T. J. Reape, O. Rocha, S. M. Doyle, J. Kacprzyk, F. M. Doohan, and P. F. McCabe. 2013. 'The Fusarium Mycotoxin Deoxynivalenol Can Inhibit Plant Apoptosis-Like Programmed Cell Death', *PloS One*, 8.

Dickman, M., B. Williams, Y. R. Li, P. Figueiredo, and T. Wolpert. 2017. 'Reassessing apoptosis in plants', *Nature Plants*, 3: 773-79.

Dilks, T., K. Halsey, R. P. De Vos, K. E. Hammond-Kosack, and N. A. Brown. 2019. 'Non-canonical fungal G-protein coupled receptors promote Fusarium head blight on wheat', *PloS Pathogens*, 15.

Dill-Macky, R. 2008. 'Cultural control practices for Fusarium head blight: Problems and solutions', *Cereal Research Communications*, 36: 653-57.

Dill-Macky, R., and R. K. Jones. 2000. 'The effect of previous crop residues and tillage on Fusarium head blight of wheat', *Plant Disease*, 84: 71-76.

Dixon, R. A., and N. L. Paiva. 1995. 'Stress-Induced Phenylpropanoid Metabolism', *Plant Cell*, 7: 1085-97.

Djamei, A., K. Schipper, F. Rabe, A. Ghosh, V. Vincon, J. Kahnt, S. Osorio, T. Tohge, A. R. Fernie, I. Feussner, K. Feussner, P. Meinicke, Y. D. Stierhof, H. Schwarz, B. Macek, M. Mann, and R. Kahmann. 2011. 'Metabolic priming by a secreted fungal effector', *Nature*, 478: 395.

Doehlemann, G., S. Reissmann, D. Assmann, M. Fleckenstein, and R. Kahmann. 2011. 'Two linked genes encoding a secreted effector and a membrane protein are essential for *Ustilago maydis*-induced tumour formation', *Molecular Microbiology*, 81: 751-66.

Doehlemann, G., N. Requena, P. Schaefer, F. Brunner, R. O'Connell, and J. E. Parker. 2014. 'Reprogramming of plant cells by filamentous plant-colonizing microbes', *New Phytologist*, 204: 803-14.

Doehlemann, G., K. van der Linde, D. Amann, D. Schwammbach, A. Hof, A. Mohanty, D. Jackson, and R. Kahmann. 2009. 'Pep1, a Secreted

Effector Protein of *Ustilago maydis*, Is Required for Successful Invasion of Plant Cells', *PloS Pathogens*, 5.

Domazakis, E., X. Lin, C. Aguilera-Galvez, D. Wouters, G. Bijsterbosch, P. J. Wolters, and V. G. A. A. Vleeshouwers. 2017. 'Effectoromics-based identification of cell surface receptors in potato.' in, *Plant Pattern Recognition Receptors* (Springer).

Dong, S., G. Kong, D. Qutob, X. Yu, J. Tang, J. Kang, T. Dai, H. Wang, M. Gijzen, and Y. Wang. 2012. 'The NLP toxin family in *Phytophthora sojae* includes rapidly evolving groups that lack necrosis-inducing activity', *Molecular Plant-Microbe Interactions*, 25: 896-909.

Dong, Y., Y. Li, Z. Qi, X. Zheng, and Z. Zhang. 2016. 'Genome plasticity in filamentous plant pathogens contributes to the emergence of novel effectors and their cellular processes in the host', *Current Genetics*, 62: 47-51.

Du, J., E. Verzaux, A. Chaparro-Garcia, G. Bijsterbosch, L. C. P. Keizer, J. Zhou, T. W. H. Liebrand, C. H. Xie, F. Govers, S. Robatzek, E. A. G. van der Vossen, E. Jacobsen, R. G. F. Visser, S. Kamoun, and V. G. A. A. Vleeshouwers. 2015. 'Elicitin recognition confers enhanced resistance to *Phytophthora infestans* in potato', *Nature Plants*, 1.

Du, J., and V. G. Vleeshouwers. 2014. 'The do's and don'ts of effectoromics', *Plant Pathogen Interactions,* 1127: 257-68.

Du, J., and V. G Vleeshouwers. 2017. 'New strategies towards durable late blight resistance in potato.' in, *The Potato Genome* (Springer).

Du, L. Q., G. S. Ali, K. A. Simons, J. G. Hou, T. B. Yang, A. S. N. Reddy, and B. W. Poovaiah. 2009. 'Ca2+/calmodulin regulates salicylic-acid-mediated plant immunity', *Nature*, 457: 1154-U116.

Duveiller, E, RP Singh, PK Singh, AA Dababat, and M Mezzalama. 2012. 'Wheat diseases and pests: a guide for field identification'.

Ebbole, D. J. 2007. 'Magnaporthe as a model for understanding host-pathogen interactions', *Annual Review of Phytopathology*, 45: 437-56.

Edwards, M. C., and B. J. Steffenson. 1996. 'Genetics and mapping of barley stripe mosaic virus resistance in barley', *Phytopathology*, 86: 184-87.

Effertz, R. J., S. W. Meinhardt, J. A. Anderson, J. G. Jordahl, and L. J. Francl. 2002. 'Identification of a chlorosis-inducing toxin from

Pyrenophora tritici-repentis and the chromosomal location of an insensitivity locus in wheat', *Phytopathology*, 92: 527-33.

Fabregas, N., F. Lozano-Elena, D. Blasco-Escamez, T. Tohge, C. Martinez-Andujar, A. Albacete, S. Osorio, M. Bustamante, J. L. Riechmann, T. Nomura, T. Yokota, A. Conesa, F. P. Alfocea, A. R. Fernie, and A. I. Cano-Delgado. 2018. 'Overexpression of the vascular brassinosteroid receptor BRL3 confers drought resistance without penalizing plant growth', *Nature Communications*, 9.

Fan, J. R., M. Urban, J. E. Parker, H. C. Brewer, S. L. Kelly, K. E. Hammond-Kosack, B. A. Fraaije, X. L. Liu, and H. J. Cools. 2013. 'Characterization of the sterol 14 alpha-demethylases of *Fusarium graminearum* identifies a novel genus-specific CYP51 function', *New Phytologist*, 198: 821-35.

Fandohan, P., D. Zoumenou, D. J. Hounhouigan, W. F. Marasas, M. J. Wingfield, and K. Hell. 2005. 'Fate of aflatoxins and fumonisins during the processing of maize into food products in Benin', *International Journal of Food Microbiology*, 98: 249-59.

Fang, Y., and B. M. Tyler. 2016. 'Efficient disruption and replacement of an effector gene in the oomycete *Phytophthora sojae* using CRISPR/Cas9', *Molecular Plant Pathology*, 17: 127-39.

Faris, J. D., Z. C. Zhang, H. J. Lu, S. W. Lu, L. Reddy, S. Cloutier, J. P. Fellers, S. W. Meinhardt, J. B. Rasmussen, S. S. Xu, R. P. Oliver, K. J. Simons, and T. L. Friesen. 2010. 'A unique wheat disease resistance-like gene governs effector-triggered susceptibility to necrotrophic pathogens', *Proceedings of the National Academy of Sciences,*107: 13544-49.

Fellmann, T., P. Witzke, F. Weiss, B. Van Doorslaer, D. Drabik, I. Huck, G. Salputra, T. Jansson, and A. Leip. 2018. 'Major challenges of integrating agriculture into climate change mitigation policy frameworks', *Mitigation and Adaptation Strategies for Global Change*, 23: 451-68.

Feng, F., F. Yang, W. Rong, X. G. Wu, J. Zhang, S. Chen, C. Z. He, and J. M. Zhou. 2012. 'A *Xanthomonas uridine* 5 '-monophosphate transferase inhibits plant immune kinases', *Nature*, 485: 114-U49.

Fernandez-Acero, F. J., T. Colby, A. Harzen, M. Carbu, U. Wieneke, J. M. Cantoral, and J. Schmidt. 2010. '2-DE proteomic approach to the *Botrytis cinerea* secretome induced with different carbon sources and plant-based elicitors', *Proteomics*, 10: 2270-80.

Fernando, W. G. D., J. X. Zhang, M. Dusabenyagasani, X. W. Guo, H. Ahmed, and B. McCallum. 2006. 'Genetic Diversity of *Gibberella zeae* Isolates from Manitoba', *Plant Disease*, 90: 1337-42.

Ferre, F., and P. Clote. 2006. 'DiANNA 1.1: an extension of the DiANNA web server for ternary cysteine classification', *Nucleic Acids Research*, 34: W182-W85.

Fiehn, O., J. Kopka, P. Dormann, T. Altmann, R. N. Trethewey, and L. Willmitzer. 2000. 'Metabolite profiling for plant functional genomics', *Nature Biotechnology*, 18: 1157-61.

Fiorin, G. L., A. Sanchez-Vallet, D. P. D. Thomazella, P. F. V. do Prado, L. C. do Nascimento, A. V. D. Figueira, B. P. H. J. Thomma, G. A. G. Pereira, and P. J. P. L. Teixeira. 2018. 'Suppression of Plant Immunity by Fungal Chitinase-like Effectors', *Current Biology*, 28: 3023.

Fisher, K., and S. Turner. 2007. 'PXY, a receptor-like kinase essential for maintaining polarity during plant vascular-tissue development', *Current Biology*, 17: 1061-6.

Fisher, M. 2012. 'Emerging fungal threats to animal, plant and ecosystem health', *Mycoses*, 55: 79-80.

Fisher, M. C., N. J. Hawkins, D. Sanglard, and S. J. Gurr. 2018. 'Worldwide emergence of resistance to antifungal drugs challenges human health and food security', *Science*, 360: 739-42.

Forrer, H. R., T. Musa, F. Schwab, E. Jenny, T. D. Bucheli, F. E. Wettstein, and S. Vogelgsang. 2014. 'Fusarium Head Blight Control and Prevention of Mycotoxin Contamination in Wheat with Botanicals and Tannic Acid', *Toxins*, 6: 830-49.

Frias, M., C. Gonzalez, and N. Brito. 2011. 'BcSpl1, a cerato-platanin family protein, contributes to *Botrytis cinerea* virulence and elicits the hypersensitive response in the host', *New Phytologist*, 192: 483-95.

Friebe, B., L. L. Qi, D. L. Wilson, Z. J. Chang, D. L. Selfers, T. J. Martin, A. K. Fritz, and B. S. Gill. 2009. 'Wheat-Thinopyrum Intermedium

Recombinants Resistant to Wheat Streak Mosaic Virus and Triticum Mosaic Virus', *Crop Science*, 49: 1221-26.

Fu, Z. Q., M. Guo, B. R. Jeong, F. Tian, T. E. Elthon, R. L. Cerny, D. Staiger, and J. R. Alfano. 2007. 'A type III effector ADP-ribosylates RNA-binding proteins and quells plant immunity', *Nature*, 447: 284-U1.

Fudal, I., M. H. Balesdent, and T. Rouxel. 2018. 'Effector Biology in Fungal Pathogens of Nonmodel Crop Plants', *Trends in Plant Science*, 23: 753.

Fujisaki, K., Y. Abe, A. Ito, H. Saitoh, K. Yoshida, H. Kanzaki, E. Kanzaki, H. Utsushi, T. Yamashita, S. Kamoun, and R. Terauchi. 2015. 'Rice Exo70 interacts with a fungal effector, AVR-Pii, and is required for AVR-Pii-triggered immunity', *Plant Journal*, 83: 875-87.

Fukuda, H. 2000. 'Programmed cell death of tracheary elements as a paradigm in plants', *Plant Molecular Biology*, 44: 245-53.

Fukuoka, S., N. Saka, Y. Mizukami, H. Koga, U. Yamanouchi, Y. Yoshioka, N. Hayashi, K. Ebana, R. Mizobuchi, and M. Yano. 2015. 'Gene pyramiding enhances durable blast disease resistance in rice', *Scientific Reports*, 5.

Galagan, J. E., and E. U. Selker. 2004. 'RIP: the evolutionary cost of genome defense', *Trends in Genetics*, 20: 417-23.

Gale, L. R., L. F. Chen, C. A. Hernick, K. Takamura, and H. C. Kistler. 2002. 'Population Analysis of *Fusarium graminearum* from Wheat Fields in Eastern China', *Phytopathology*, 92: 1315-22.

Galgoczy, L., M. Viragh, L. Kovacs, B. Toth, T. Papp, and C. Vagvolgyi. 2013. 'Antifungal peptides homologous to the *Penicillium chrysogenum* antifungal protein (PAF) are widespread among Fusaria', *Peptides*, 39: 131-37.

Gan, P., K. Ikeda, H. Irieda, M. Narusaka, R. J. O'Connell, Y. Narusaka, Y. Takano, Y. Kubo, and K. Shirasu. 2013. 'Comparative genomic and transcriptomic analyses reveal the hemibiotrophic stage shift of Colletotrichum fungi', *New Phytologist*, 197: 1236-49.

Gao, X. Q., X. S. Ruan, Y. L. Sun, X. E. Wang, and B. M. Feng. 2019. 'BAKing up to Survive a Battle: Functional Dynamics of BAK1 in Plant Programmed Cell Death', *Frontiers in Plant Science*, 9.

Garcia-Bastidas, F., N. Ordonez, J. Konkol, M. Al-Qasim, Z. Naser, M. Abdelwali, N. Salem, C. Waalwijk, R. C. Ploetz, and G. H. J. Kema. 2014. 'First Report of *Fusarium oxysporum f. sp cubense* Tropical Race 4 Associated with Panama Disease of Banana outside Southeast Asia', *Plant Disease*, 98: 694-94.

Garrett, K. A., S. P. Dendy, E. E. Frank, M. N. Rouse, and S. E. Travers. 2006. 'Climate change effects on plant disease: Genomes to ecosystems', *Annual Review of Phytopathology*, 44: 489-509.

Gawehns, F., L. S. Ma, O. Bruning, P. M. Houterman, S. Boeren, B. J. C. Cornelissen, M. Rep, and F. L. W. Takken. 2015. 'The effector repertoire of *Fusarium oxysporum* determines the tomato xylem proteome composition following infection', *Frontiers in Plant Science*, 6.

Gibriel, H. A., B. P. Thomma, and M. F. Seidl. 2016. 'The age of effectors: genome-based discovery and applications', *Phytopathology*.

Gibson, CM. 1904. 'Notes on infection experiments with various Uredineae', *New Phytologist*, 3: 184-91.

Gijzen, M., and T. Nurnberger. 2006. 'Nep1-like proteins from plant pathogens: recruitment and diversification of the NPP1 domain across taxa', *Phytochemistry*, 67: 1800-7.

Giraldo, M. C., Y. F. Dagdas, Y. K. Gupta, T. A. Mentlak, M. Yi, A. L. Martinez-Rocha, H. Saitoh, R. Terauchi, N. J. Talbot, and B. Valent. 2013. 'Two distinct secretion systems facilitate tissue invasion by the rice blast fungus *Magnaporthe oryzae*', *Nature Communications*, 4.

Glazebrook, J. 2005. 'Contrasting mechanisms of defense against biotrophic and necrotrophic pathogens', *Annual Review of Phytopathology*, 43: 205-27.

Godfray, H. C., and T. Garnett. 2014. 'Food security and sustainable intensification', *Philosophical Transactions of the Royal Society London B: Biological Scencesi*, 369: 20120273.

Goffeau, A., B. G. Barrell, H. Bussey, R. W. Davis, B. Dujon, H. Feldmann, F. Galibert, J. D. Hoheisel, C. Jacq, M. Johnston, E. J. Louis, H. W. Mewes, Y. Murakami, P. Philippsen, H. Tettelin, and S. G. Oliver. 1996. 'Life with 6000 genes', *Science*, 274: 546-&.

Golkari, S., J. Gilbert, T. Ban, and J. D. Procunier. 2009. 'QTL-specific microarray gene expression analysis of wheat resistance to Fusarium head blight in Sumai-3 and two susceptible NILs', *Genome*, 52: 409-18.

Goodin, M. M., D. Zaitlin, R. A. Naidu, and S. A. Lommel. 2008. '*Nicotiana benthamiana:* Its history and future as a model for plant-pathogen interactions', *Molecular Plant-Microbe Interactions*, 21: 1015-26.

Gorczyca, A., A. Oleksy, D. Gala-Czekaj, M. Urbaniak, M. Laskowska, A. Waskiewicz, and L. Stepien. 2018. 'Fusarium head blight incidence and mycotoxin accumulation in three durum wheat cultivars in relation to sowing date and density', *Science of Nature*, 105.

Goswami, R. S. 2012. 'Targeted gene replacement in fungi using a split-marker approach', *Methods in Molecular Biology*, 835: 255-69.

Goswami, R. S., and H. C. Kistler. 2004. 'Heading for disaster: *Fusarium graminearum* on cereal crops', *Molecular Plant Pathology*, 5: 515-25.

———. 2005. 'Pathogenicity and in planta mycotoxin accumulation among members of the *Fusarium graminearum* species complex on wheat and rice', *Phytopathology*, 95: 1397-404.

Goswami, R. S., J. R. Xu, and H. C. Kistler. 2004. 'Genomic analysis of host-pathogen interactions between *Fusarium graminearum* and its gramineous hosts', *Phytopathology*, 94: S35-S36.

Gout, L., I. Fudal, M. L. Kuhn, F. Blaise, M. Eckert, L. Cattolico, M. H. Balesdent, and T. Rouxel. 2006. 'Lost in the middle of nowhere: the AvrLm1 avirulence gene of the Dothideomycete *Leptosphaeria maculans*', *Molecular Microbiology*, 60: 67-80.

Grant, M. R., and J. D. G. Jones. 2009. 'Hormone (Dis)harmony Moulds Plant Health and Disease', *Science*, 324: 750-52.

Grimsley, N., B. Hohn, T. Hohn, and R. Walden. 1986. 'Agroinfection, an Alternative Route for Viral-Infection of Plants by Using the Ti Plasmid', *Proceedings of the National Academy of Sciences,* 83: 3282-86.

Gu, Q., Y. Chen, Y. Liu, C. Q. Zhang, and Z. H. Ma. 2015. 'The transmembrane protein FgSho1 regulates fungal development and pathogenicity via the MAPK module Ste50-Ste11-Ste7 in *Fusarium graminearum*', *New Phytologist*, 206: 315-28.

Guenther, J. C., H. E. Hallen-Adams, H. Bucking, Y. Shachar-Hill, and F. Trail. 2009. 'Triacylglyceride Metabolism by *Fusarium graminearum* During Colonization and Sexual Development on Wheat', *Molecular Plant-Microbe Interactions*, 22: 1492-503.

Guenther, J. C., and F. Trail. 2005. 'The development and differentiation of *Gibberella zeae* (anamorph : *Fusarium graminearum*) during colonization of wheat', *Mycologia*, 97: 229-37.

Guijas, C., J. R. Montenegro-Burke, X. Domingo-Almenara, A. Palermo, B. Warth, G. Hermann, G. Koellensperger, T. Huan, W. Uritboonthai, A. E. Aisporna, D. W. Wolan, M. E. Spilker, H. P. Benton, and G. Siuzdak. 2018. 'METLIN: A Technology Platform for Identifying Knowns and Unknowns', *Analytical Chemistry*, 90: 3156-64.

Guldener, U., G. Mannhaupt, M. Munsterkotter, D. Haase, M. Oesterheld, V. Stumpflen, H. W. Mewes, and G. Adam. 2006. 'FGDB: a comprehensive fungal genome resource on the plant pathogen *Fusarium graminearum*', *Nucleic Acids Research*, 34: D456-D58.

Guldener, U., K. Y. Seong, J. Boddu, S. H. Cho, F. Trail, J. R. Xu, G. Adam, H. W. Mewes, G. J. Muehlbauer, and H. C. Kistler. 2006a. 'Development of a *Fusarium graminearum* Affymetrix GeneChip for profiling fungal gene expression in vitro and in planta', *Fungal Genetics and Biology*, 43: 316-25.

Guldener, U., K. Y. Seong, J. Boddu, S. Cho, F. Trail, J. R. Xu, G. Adam, H. W. Mewes, G. J. Muehlbauer, and H. C. Kistler. 2006b. 'Development of a *Fusarium graminearum* Affymetrix GeneChip for profiling fungal gene expression in vitro and in planta', *Fungal Genetics and Biology*, 43: 316-25.

Gunupuru, L. R., A. Perochon, and F. M. Doohan. 2017. 'Deoxynivalenol resistance as a component of FHB resistance', *Tropical Plant Pathology*, 42: 175-83.

Guo, B. D., H. N. Wang, B. Yang, W. J. Jiang, M. F. Jing, H. Y. Li, Y. A. Xia, Y. P. Xu, Q. L. Hu, F. F. Wang, F. Yu, Y. Wang, W. W. Ye, S. M. Dong, W. M. Xing, and Y. C. Wang. 2019. *'Phytophthora sojae* Effector PsAvh240 Inhibits Host Aspartic Protease Secretion to Promote Infection', *Molecular Plant*, 12: 552-64.

Guy, E., M. Lautier, M. Chabannes, B. Roux, E. Lauber, M. Arlat, and L. D. Noel. 2013. 'xopAC-triggered Immunity against Xanthomonas Depends on Arabidopsis Receptor-Like Cytoplasmic Kinase Genes PBL2 and RIPK', *PloS One*, 8.

Hahn, M. 2014. 'The rising threat of fungicide resistance in plant pathogenic fungi: Botrytis as a case study', *Journal of Chemical Biology*, 7: 133-41.

Haley, S.D., T.J. Martin, J.S. Quick, D.L. Seifers, J.A. Stromberger, S.R. Clayshulte, B.L. Clifford, F.B. Peairs, J.B. Rudolph, and J.J. Johnson. 2002. 'Registration of CO960293-2 wheat germplasm resistant to Wheat streak mosaic virus and Russian wheat aphid. (Registrations Of Germplasm)', *Crop Science* , 42: 1381-83.

Hallen, H. E., M. Huebner, S. H. Shiu, U. Giildener, and F. Trail. 2007. 'Gene expression shifts during perithecium development in *Gibberella zeae* (anamorph *Fusarium graminearum*), with particular emphasis on ion transport proteins', *Fungal Genetics and Biology*, 44: 1146-56.

Hammond-Kosack, K.E., B.J. Staskawicz, J.D.G. Jones, and D.C. Baulcombe. 1995. 'Functional expression of a fungal avirulence gene from a modified potato virus X genome', *Molecular plant-microbe interactions: MPMI (USA)*.

Hammond-Kosack, K. E., K. Harrison, and J. D. G. Jones. 1994. 'Developmentally regulated cell death on expression of the fungal avirulence gene Avr9 in tomato seedlings carrying the disease-resistance gene Cf-9', *Proceedings of the National Academy of Sciences*, 91: 10445-49.

Hammond-Kosack, K. E., P. Silverman, I. Raskin, and J. D. G. Jones. 1996. 'Race-specific elicitors of *Cladosporium fulvum* induce changes in cell morphology and the synthesis of ethylene and salicylic acid in tomato plants carrying the corresponding Cf disease resistance gene', *Plant Physiology*, 110: 1381-94.

Han, X. W., F. Altegoer, W. Steinchen, L. Binnebesel, J. Schuhmacher, T. Glatter, P. I. Giammarinaro, A. Djamei, S. A. Rensing, S. Reissmann, R. Kahmann, and G. Bange. 2019. 'A kiwellin disarms the metabolic activity of a secreted fungal virulence factor', *Nature*, 565: 650.

Harris, L. J., M. Balcerzak, A. Johnston, D. Schneiderman, and T. Ouellet. 2016a. 'Host-preferential *Fusarium graminearum* gene expression during infection of wheat, barley, and maize', *Fungal Biology*, 120: 111-23.

———. 2016b. 'Host-preferential *Fusarium graminearum* gene expression during infection of wheat, barley, and maize', *Fungal Biology*, 120: 111-23.

Harris, L. J., A. E. Desjardins, R. D. Plattner, P. Nicholson, G. Butler, J. C. Young, G. Weston, R. H. Proctor, and T. M. Hohn. 1999. 'Possible role of trichothecene mycotoxins in virulence of *Fusarium graminearum* on maize', *Plant Disease*, 83: 954-60.

Hauck, P., R. Thilmony, and S. Y. He. 2003. 'A *Pseudomonas syringae* type III effector suppresses cell wall-based extracellular defense in susceptible Arabidopsis plants', *Proceedings of the National Academy of Sciences*,, 100: 8577-82.

Haupt, S., G. H. Duncan, S. Holzberg, and K. J. Oparka. 2001. 'Evidence for symplastic phloem unloading in sink leaves of barley', *Plant Physiology*, 125: 209-18.

Heese, A., D. R. Hann, S. Gimenez-Ibanez, A. M. E. Jones, K. He, J. Li, J. I. Schroeder, S. C. Peck, and J. P. Rathjen. 2007. 'The receptor-like kinase SERK3/BAK1 is a central regulator of innate immunity in plants', *Proceedings of the National Academy of Sciences*, 104: 12217-22.

Heier, T., S. K. Jain, K. H. Kogel, and J. Pons-Kuhnemann. 2005. 'Influence of N-fertilization and fungicide strategies on Fusarium head blight severity and mycotoxin content in winter wheat', *Journal of Phytopathology*, 153: 551-57.

Hemetsberger, C., C. Herrberger, B. Zechmann, M. Hillmer, and G. Doehlemann. 2012. 'The *Ustilago maydis* Effector Pep1 Suppresses Plant Immunity by Inhibition of Host Peroxidase Activity', *PloS Pathogens*, 8.

Herker, E., H. Jungwirth, K. A. Lehmann, C. Maldener, K. U. Frohlich, S. Wissing, S. Buttner, M. Fehr, S. Sigrist, and F. Madeo. 2004.

'Chronological aging leads to apoptosis in yeast', *Journal of Cell Biology*, 164: 501-7.

Hickman, R., M. C. Van Verk, A. J. H. Van Dijken, M. P. Mendes, I. A. Vroegop-Vos, L. Caarls, M. Steenbergen, I. Van der Nagel, G. J. Wesselink, A. Jironkin, A. Talbot, J. Rhodes, M. De Vries, R. C. Schuurink, K. Denby, C. M. J. Pieterse, and S. C. M. Wees. 2017. 'Architecture and Dynamics of the Jasmonic Acid Gene Regulatory Network', *Plant Cell*, 29: 2086-105.

Hogenhout, S. A., R. A. L. Van der Hoorn, R. Terauchi, and S. Kamoun. 2009. 'Emerging Concepts in Effector Biology of Plant-Associated Organisms', *Molecular Plant-Microbe Interactions*, 22: 115-22.

Holton, N., V. Nekrasov, P. C. Ronald, and C. Zipfel. 2015. 'The Phylogenetically-Related Pattern Recognition Receptors EFR and XA21 Recruit Similar Immune Signaling Components in Monocots and Dicots', *PloS Pathogens*, 11.

Hood, M. E., and H. D. Shew. 1996. 'Applications of KOH-aniline blue fluorescence in the study of plant-fungal interactions', *Phytopathology*, 86: 704-08.

Hou, R., C. Jiang, Q. Zheng, C. Wang, and J. R. Xu. 2015. 'The AreA transcription factor mediates the regulation of deoxynivalenol (DON) synthesis by ammonium and cyclic adenosine monophosphate (cAMP) signalling in *Fusarium graminearum*', *Molecular Plant Pathology*, 16: 987-99.

House, J. D., C. M. Nyachoti, and D. Abramson. 2003. 'Deoxynivalenol removal from barley intended as swine feed through the use of an abrasive pearling procedure', *Journal of Agricultural and Food Chemistry*, 51: 5172-5.

Houterman, P. M., L. Ma, G. van Ooijen, M. J. de Vroomen, B. J. C. Cornelissen, F. L. W. Takken, and M. Rep. 2009. 'The effector protein Avr2 of the xylem-colonizing fungus *Fusarium oxysporum* activates the tomato resistance protein I-2 intracellularly', *Plant Journal*, 58: 970-78.

Hu, S., X. Y. Zhou, X. Y. Gu, S. L. Cao, C. F. Wang, and J. R. Xu. 2014. 'The cAMP-PKA Pathway Regulates Growth, Sexual and Asexual

Differentiation, and Pathogenesis in *Fusarium graminearum*', *Molecular Plant-Microbe Interactions*, 27: 557-66.

Huang, G. H., H. F. Wang, S. Chou, X. Y. Nie, J. Y. Chen, and H. P. Liu. 2006. 'Bistable expression of WOR1, a master regulator of white-opaque switching in *Candida albicans*', *Proceedings of the National Academy of Sciences,* 103: 12813-18.

Hurgobin, B., and D. Edwards. 2017. 'SNP Discovery Using a Pangenome: Has the Single Reference Approach Become Obsolete?', *Biology (Basel)*, 6.

Irieda, H., S. Ogawa, and Y. Takano. 2016. 'Focal effector accumulation in a biotrophic interface at the primary invasion sites of *Colletotrichum orbiculare* in multiple susceptible plants', *Plant Signaling & Behavior*, 11.

Jansen, C., D. von Wettstein, W. Schafer, K. H. Kogel, A. Felk, and F. J. Maier. 2005. 'Infection patterns in barley and wheat spikes inoculated with wild-type and trichodiene synthase gene disrupted *Fusarium graminearum*', *Proceedings of the National Academy of Sciences*, 102: 16892-97.

Jarosch, B., K. H. Kogel, and U. Schaffrath. 1999. 'The ambivalence of the barley Mlo locus: Mutations conferring resistance against powdery mildew (*Blumeria graminis f. sp, hordei)* enhance susceptibility to the rice blast fungus *Magnaporthe grisea*', *Molecular Plant-Microbe Interactions*, 12: 508-14.

Jeong, J. S., T. K. Mitchell, and R. A. Dean. 2007. 'The *Magnaporthe grisea* snodprot1 homolog, MSPI, is required for virulence', *Fems Microbiology Letters*, 273: 157-65.

Jia, H. Y., J. Y. Zhou, S. L. Xue, G. Q. Li, H. S. Yan, C. F. Ran, Y. D. Zhang, J. X. Shi, L. Jia, X. Wang, J. Luo, and Z. Q. Ma. 2018. 'A journey to understand wheat Fusarium head blight resistance in the Chinese wheat landrace Wangshuibai', *Crop Journal*, 6: 48-59.

Jia, L. J., H. Y. Tang, W. Q. Wang, T. L. Yuan, W. Q. Wei, B. Pang, X. M. Gong, S. F. Wang, Y. J. Li, D. Zhang, W. Liu, and W. H. Tang. 2019. 'A linear nonribosomal octapeptide from *Fusarium graminearum* facilitates cell-to-cell invasion of wheat', *Nature Communications*, 10.

Jia, L. J., W. Q. Wang, and W. H. Tang. 2017. 'Wheat Coleoptile Inoculation by *Fusarium graminearum* for Large-scale Phenotypic Analysis', *Bio-Protocol*, 7.

Jia, Y., S. A. McAdams, G. T. Bryan, H. P. Hershey, and B. Valent. 2000. 'Direct interaction of resistance gene and avirulence gene products confers rice blast resistance', *EMBO Journal*, 19: 4004-14.

Jiang, R. H. Y., S. Tripathy, F. Govers, and B. M. Tyler. 2008. 'RXLR effector reservoir in two Phytophthora species is dominated by a single rapidly evolving superfamily with more than 700 members', *Proceedings of the National Academy of Sciences*, 105: 4874-79.

Jiang, S. S., J. Yao, K. W. Ma, H. B. Zhou, J. K. Song, S. Y. He, and W. B. Ma. 2013. 'Bacterial Effector Activates Jasmonate Signaling by Directly Targeting JAZ Transcriptional Repressors', *PloS Pathogens*, 9.

Jiang, W. Z., H. B. Zhou, H. H. Bi, M. Fromm, B. Yang, and D. P. Weeks. 2013. 'Demonstration of CRISPR/Cas9/sgRNA-mediated targeted gene modification in Arabidopsis, tobacco, sorghum and rice', *Nucleic Acids Research*, 41.

Johansen, L. K., and J. C. Carrington. 2001. 'Silencing on the spot. Induction and suppression of RNA silencing in the Agrobacterium-mediated transient expression system', *Plant Physiology*, 126: 930-38.

Jones, D. A. B., S. Bertazzoni, C. J. Turo, R. A. Syme, and J. K. Hane. 2018. 'Bioinformatic prediction of plant-pathogenicity effector proteins of fungi', *Current Opinion in Microbiology*, 46: 43-49.

Jones, J. D. G., and J. L. Dangl. 2006. 'The plant immune system', *Nature*, 444: 323-29.

Jonkers, W., Y. H. Dong, K. Broz, and H. C. Kistler. 2012. 'The Wor1-like Protein Fgp1 Regulates Pathogenicity, Toxin Synthesis and Reproduction in the Phytopathogenic Fungus *Fusarium graminearum*', *PloS Pathogens*, 8.

Joosten, M. H. A. J., and P. J. G. M. de Wit. 1999. 'The tomato - C*ladosporium fulvum interaction:* A versatile experimental system to study plant-pathogen interactions', *Annual Review of Phytopathology*, 37: 335-67.

Joshi, R. L., V. Joshi, and D. W. Ow. 1990. 'BSMV genome mediated expression of a foreign gene in dicot and monocot plant cells', *EMBO Journal*, 9: 2663-9.

Jupe, F., L. Pritchard, G. J. Etherington, K. MacKenzie, P. J. A. Cock, F. Wright, S. K. Sharma, D. Bolser, G. J. Bryan, J. D. G. Jones, and I. Hein. 2012. 'Identification and localisation of the NB-LRR gene family within the potato genome', *BMC Genomics*, 13.

Kale, S. D., B. A. Gu, D. G. S. Capelluto, D. L. Dou, E. Feldman, A. Rumore, F. D. Arredondo, R. Hanlon, I. Fudal, T. Rouxel, C. B. Lawrence, W. X. Shan, and B. M. Tyler. 2010. 'External Lipid PI3P Mediates Entry of Eukaryotic Pathogen Effectors into Plant and Animal Host Cells', *Cell*, 142: 284-95.

Kamoun, S., P. van West, V. G. A. A. Vleeshouwers, K. E. de Groot, and F. Govers. 1998. 'Resistance of *Nicotiana benthamiana* to *Phytophthora infestans* is mediated by the recognition of the elicitor protein INF1', *Plant Cell*, 10: 1413-25.

Kamper, J., R. Kahmann, M. Bolker, L. J. Ma, T. Brefort, B. J. Saville, F. Banuett, J. W. Kronstad, S. E. Gold, O. Muller, M. H. Perlin, H. A. B. Wosten, R. de Vries, J. Ruiz-Herrera, C. G. Reynaga-Pena, K. Snetselaar, M. McCann, J. Perez-Martin, M. Feldbrugge, C. W. Basse, G. Steinberg, J. I. Ibeas, W. Holloman, P. Guzman, M. Farman, J. E. Stajich, R. Sentandreu, J. M. Gonzalez-Prieto, J. C. Kennell, L. Molina, J. Schirawski, A. Mendoza-Mendoza, D. Greilinger, K. Munch, N. Rossel, M. Scherer, M. Vranes, O. Ladendorf, V. Vincon, U. Fuchs, B. Sandrock, S. Meng, E. C. H. Ho, M. J. Cahill, K. J. Boyce, J. Klose, S. J. Klosterman, H. J. Deelstra, L. Ortiz-Castellanos, W. X. Li, P. Sanchez-Alonso, P. H. Schreier, I. Hauser-Hahn, M. Vaupel, E. Koopmann, G. Friedrich, H. Voss, T. Schluter, J. Margolis, D. Platt, C. Swimmer, A. Gnirke, F. Chen, V. Vysotskaia, G. Mannhaupt, U. Guldener, M. Munsterkotter, D. Haase, M. Oesterheld, H. W. Mewes, E. W. Mauceli, D. DeCaprio, C. M. Wade, J. Butler, S. Young, D. B. Jaffe, S. Calvo, C. Nusbaum, J. Galagan, and B. W. Birren. 2006. 'Insights from the genome of the biotrophic fungal plant pathogen *Ustilago maydis*', *Nature*, 444: 97-101.

Kankanala, P., K. Czymmek, and B. Valent. 2007. 'Roles for rice membrane dynamics and plasmodesmata during biotrophic invasion by the blast fungus', *Plant Cell*, 19: 706-24.

Kanneganti, T. D., M. Lamkanfi, and G. Nunez. 2007. 'Intracellular NOD-like receptors in host Defense and disease', *Immunity*, 27: 549-59.

Kanzaki, H., K. Yoshida, H. Saitoh, K. Fujisaki, A. Hirabuchi, L. Alaux, E. Fournier, D. Tharreau, and R. Terauchi. 2012. 'Arms race co-evolution of *Magnaporthe oryzae* AVR-Pik and rice Pik genes driven by their physical interactions', *Plant Journal*, 72: 894-907.

Kazan, K., and D. M. Gardiner. 2018. 'Transcriptomics of cereal-*Fusarium graminearum* interactions: what we have learned so far', *Molecular Plant Pathology*, 19: 764-78.

Kelly, A. C., and T. J. Ward. 2018. 'Population genomics of *Fusarium graminearum* reveals signatures of divergent evolution within a major cereal pathogen', *PloS One*, 13.

Kenny, G. J., and P. A. Harrison. 1992. 'Thermal and moisture limits of grain maize in Europe: model testing and sensitivity to climate change', *Climate research*, 2: 113-29.

Kenton, P., L. A. J. Mur, R. Atzorn, C. Wasternack, and J. Draper. 1999. '(-)-jasmonic acid accumulation in tobacco hypersensitive response lesions', *Molecular Plant-Microbe Interactions*, 12: 74-78.

Kerppola, T. K. 2006. 'Design and implementation of bimolecular fluorescence complementation (BiFC) assays for the visualization of protein interactions in living cells', *Nature Protocols*, 1: 1278-86.

Kettles, G. J., C. Bayon, G. Canning, J. J. Rudd, and K. Kanyuka. 2017. 'Apoplastic recognition of multiple candidate effectors from the wheat pathogen *Zymoseptoria tritici* in the nonhost plant *Nicotiana benthamiana*', *New Phytologist*, 213: 338-50.

Khang, C. H., R. Berruyer, M. C. Giraldo, P. Kankanala, S. Y. Park, K. Czymmek, S. Kang, and B. Valent. 2010. 'Translocation of *Magnaporthe oryzae* Effectors into Rice Cells and Their Subsequent Cell-to-Cell Movement', *Plant Cell*, 22: 1388-403.

Khang, C. H., S. Y. Park, H. S. Rho, Y. H. Lee, and S. Kang. 2006. 'Filamentous Fungi (*Magnaporthe grisea* and *Fusarium oxysporum*)', *Methods in Molecular Biology*, 344: 403-20.

Kim, H. J., H. R. Lee, K. R. Jo, S. M. Mortazavian, D. J. Huigen, B. Evenhuis, G. Kessel, R. G. Visser, E. Jacobsen, and J. H. Vossen. 2012. 'Broad spectrum late blight resistance in potato differential set plants MaR8 and MaR9 is conferred by multiple stacked R genes', *Theoretical and Applied Genetics*, 124: 923-35.

Kim, H. K., Y. H. Choi, and R. Verpoorte. 2011. 'NMR-based plant metabolomics: where do we stand, where do we go?', *Trends in Biotechnology*, 29: 267-75.

Kim, K. S., J. Y. Min, and M. B. Dickman. 2008. 'Oxalic acid is an elicitor of plant programmed cell death during *Sclerotinia sclerotiorum* disease development', *Molecular Plant-Microbe Interactions*, 21: 605-12.

Kim, S., I. P. Ahn, H. S. Rho, and Y. H. Lee. 2005. 'MHP1, a *Magnaporthe grisea* hydrophobin gene, is required for fungal development and plant colonization', *Molecular Microbiology*, 57: 1224-37.

King, R., M. Urban, M. C. Hammond-Kosack, K. Hassani-Pak, and K. E. Hammond-Kosack. 2015a. 'The completed genome sequence of the pathogenic ascomycete fungus *Fusarium graminearum*', *BMC Genomics*, 16: 544.

King, R., M. Urban, R. P. Lauder, N. Hawkins, M. Evans, A. Plummer, K. Halsey, A. Lovegrove, K. Hammond-Kosack, and J. J. Rudd. 2017. 'A conserved fungal glycosyltransferase facilitates pathogenesis of plants by enabling hyphal growth on solid surfaces', *PloS Pathogens*, 13.

Kleemann, J., L. J. Rincon-Rivera, H. Takahara, U. Neumann, E. V. L. van Themaat, H. C. van der Does, S. Hacquard, K. Stuber, I. Will, W. Schmalenbach, E. Schmelzer, and R. J. O'Connell. 2012. 'Sequential Delivery of Host-Induced Virulence Effectors by Appressoria and Intracellular Hyphae of the Phytopathogen C*olletotrichum higginsianum*', *PloS Pathogens*, 8.

Koch, A., D. Biedenkopf, A. Furch, L. Weber, O. Rossbach, E. Abdellatef, L. Linicus, J. Johannsmeier, L. Jelonek, A. Goesmann, V. Cardoza, J.

McMillan, T. Mentzel, and K. H. Kogel. 2016. 'An RNAi-Based Control of *Fusarium graminearum* Infections Through Spraying of Long dsRNAs Involves a Plant Passage and Is Controlled by the Fungal Silencing Machinery', *PloS Pathogens*, 12.

Koch, A., N. Kumar, L. Weber, H. Keller, J. Imani, and K. H. Kogel. 2013. 'Host-induced gene silencing of cytochrome P450 lanosterol C14 alpha-demethylase-encoding genes confers strong resistance to Fusarium species', *Proceedings of the National Academy of Sciences,* 110: 19324-29.

Kohler, G. A., A. Brenot, E. Haas-Stapleton, N. Agabian, R. Deva, and S. Nigam. 2006. 'Phospholipase A(2) and phospholipase B activities in fungi', *Biochimica Et Biophysica Acta-Molecular and Cell Biology of Lipids*, 1761: 1391-99.

Koonin, E. V. 2005. 'Orthologs, paralogs, and evolutionary genomics', *Annual Review of Genetics*, 39: 309-38.

Kourelis, J., F. Kaschani, F. M. Grosse-Holz, F. Homma, M. Kaiser, and R. A. L. Van Der Hoorn. 2018. 'Re-annotated *Nicotiana benthamiana* gene models for enhanced proteomics and reverse genetics', *BioRxiv*: 373506.

Kruger, J., C. M. Thomas, C. Golstein, M. S. Dixon, M. Smoker, S. Tang, L. Mulder, and J. D. Jones. 2002. 'A tomato cysteine protease required for Cf-2-dependent disease resistance and suppression of autonecrosis', *Science*, 296: 744-7.

Kushalappa, A. C., and R. Gunnaiah. 2013. 'Metabolo-proteomics to discover plant biotic stress resistance genes', *Trends in Plant Science*, 18: 522-31.

Lacombe, S., A. Rougon-Cardoso, E. Sherwood, N. Peeters, D. Dahlbeck, H. P. van Esse, M. Smoker, G. Rallapalli, B. P. H. J. Thomma, B. Staskawicz, J. D. G. Jones, and C. Zipfel. 2010. 'Interfamily transfer of a plant pattern-recognition receptor confers broad-spectrum bacterial resistance', *Nature Biotechnology*, 28: 365-U94.

Lahrmann, U., Y. Ding, A. Banhara, M. Rath, M. R. Hajirezaei, S. Dohlemann, N. von Wiren, M. Parniske, and A. Zuccaro. 2013. 'Host-related metabolic cues affect colonization strategies of a root

endophyte', *Proceedings of the National Academy of Sciences* 110: 13965-70.

Lanver, D., M. Tollot, G. Schweizer, L. Lo Presti, S. Reissmann, L. S. Ma, M. Schuster, S. Tanaka, L. Liang, N. Ludwig, and R. Kahmann. 2017. '*Ustilago maydis* effectors and their impact on virulence', *Nature Reviews Microbiology*, 15: 409-21.

Lapin, D., V. Kovacova, X. Sun, J. A. Dongus, D. D. Bhandari, P. von Born, J. Bautor, N. Guarneri, J. Rzemieniewski, J. Stuttmann, A. Beyer, and J. E. Parker. 2019. 'A coevolved EDS1-SAG101-NRG1 module mediates cell death signaling by TIR-domain immune receptors', *The Plant Cell*: tpc.00118.2019.

Larionov, A., A. Krause, and W. Miller. 2005. 'A standard curve based method for relative real time PCR data processing', *BMC Bioinformatics*, 6: 62.

Lawrence, D. M., and A. O. Jackson. 2001. 'Requirements for cell-to-cell movement of Barley stripe mosaic virus in monocot and dicot hosts', *Molecular Plant Pathology*, 2: 65-75.

Lee, H. J., and D. Ryu. 2017. 'Worldwide Occurrence of Mycotoxins in Cereals and Cereal-Derived Food Products: Public Health Perspectives of Their Co-occurrence', *Journal of Agricultural and Food Chemistry*, 65: 7034-51.

Lee, J., B. Orosa, L. Millyard, M. Edwards, K. Kanyuka, A. Gatehouse, J. Rudd, K. Hammond-Kosack, N. Pain, and A. Sadanandom. 2015. 'Functional analysis of a Wheat Homeodomain protein, TaR1, reveals that host chromatin remodelling influences the dynamics of the switch to necrotrophic growth in the phytopathogenic fungus *Zymoseptoria tritici*', *New Phytologist*, 206: 598-605.

Lee, L. Y., and S. B. Gelvin. 2014. 'Bimolecular fluorescence complementation for imaging protein interactions in plant hosts of microbial pathogens', *Methods in Molecular Biology*, 1197: 185-208.

Lee, W. S., K. E. Hammond-Kosack, and K. Kanyuka. 2012. 'Barley Stripe Mosaic Virus-Mediated Tools for Investigating Gene Function in Cereal Plants and Their Pathogens: Virus-Induced Gene Silencing,

Host-Mediated Gene Silencing, and Virus-Mediated Overexpression of Heterologous Protein', *Plant Physiology*, 160: 582-90.

Lee, W. S., J. J. Rudd, K. E. Hammond-Kosack, and K. Kanyuka. 2014. '*Mycosphaerella graminicola* LysM effector-mediated stealth pathogenesis subverts recognition through both CERK1 and CEBiP homologues in wheat', *Molecular Plant-Microbe Interactions*, 27: 236-43.

Lemmens, M., U. Scholz, F. Berthiller, C. Dall'Asta, A. Koutnik, R. Schuhmacher, G. Adam, H. Buerstmayr, A. Mesterhazy, R. Krska, and P. Ruckenbauer. 2005. 'The ability to detoxify the mycotoxin deoxynivalenol colocalizes with a major quantitative trait locus for Fusarium head blight resistance in wheat', *Molecular Plant-Microbe Interactions*, 18: 1318-24.

Lepesheva, G. I., and M. R. Waterman. 2007. 'Sterol 14 alpha-demethylase cytochrome P450 (CYP51), a P450 in all biological kingdoms', *Biochimica Et Biophysica Acta-General Subjects*, 1770: 467-77.

Levdansky, E., J. Romano, Y. Shadkchan, H. Sharon, K. J. Verstrepen, G. R. Fink, and N. Osherov. 2007. 'Coding tandem repeats generate diversity in *Aspergillus fumigatus* genes', *Eukaryotic Cell*, 6: 1380-91.

Lewis, S. L., and M. A. Maslin. 2015. 'Defining the Anthropocene', *Nature*, 519: 171-80.

Li, G. L., and Y. Yen. 2008. 'Jasmonate and ethylene signaling pathway may mediate Fusarium head blight resistance in wheat', *Crop Science*, 48: 1888-96.

Li, Y. Z., H. G. Cui, X. Y. Cui, and A. M. Wang. 2016. 'The altered photosynthetic machinery during compatible virus infection', *Current Opinion in Virology*, 17: 19-24.

Liu, C., C. Pedersen, T. Schultz-Larsen, G. B. Aguilar, K. Madriz-Ordenana, M. S. Hovmoller, and H. Thordal-Christensen. 2016. 'The stripe rust fungal effector PEC6 suppresses pattern-triggered immunity in a host species-independent manner and interacts with adenosine kinases', *New Phytologist*.

Liu, H. Q., S. J. Zhang, J. W. Ma, Y. F. Dai, C. H. Li, X. L. Lyu, C. F. Wang, and J. R. Xu. 2015. 'Two Cdc2 Kinase Genes with Distinct Functions

in Vegetative and Infectious Hyphae in *Fusarium graminearum*', *PloS Pathogens*, 11.

Liu, N., K. Xie, Q. Jia, J. P. Zhao, T. Y. Chen, H. G. Li, X. Wei, X. M. Diao, Y. G. Hong, and Y. L. Liu. 2016. 'Foxtail Mosaic Virus-Induced Gene Silencing in Monocot Plants', *Plant Physiology*, 171: 1801-07.

Liu, Z. H., Y. Y. Gao, Y. M. Kim, J. D. Faris, W. L. Shelver, P. J. G. M. de Wit, S. S. Xu, and T. L. Friesen. 2016. 'SnTox1, a *Parastagonospora nodorum* necrotrophic effector, is a dual-function protein that facilitates infection while protecting from wheat-produced chitinases', *New Phytologist*, 211: 1052-64.

Liu, Z. H., Z. C. Zhang, J. D. Faris, R. P. Oliver, R. Syme, M. C. McDonald, B. A. McDonald, P. S. Solomon, S. W. Lu, W. L. Shelver, S. Xu, and T. L. Friesen. 2012. 'The Cysteine Rich Necrotrophic Effector SnTox1 Produced by *Stagonospora nodorum* Triggers Susceptibility of Wheat Lines Harboring Snn1', *PloS Pathogens*, 8.

Lo Presti, L., D. Lanver, G. Schweizer, S. Tanaka, L. Liang, M. Tollot, A. Zuccaro, S. Reissmann, and R. Kahmann. 2015. 'Fungal effectors and plant susceptibility', *Annual Review of Plant Biology*, 66: 513-45.

Lo Presti, L., B. Zechmann, J. Kumlehn, L. Liang, D. Lanver, S. Tanaka, R. Bock, and R. Kahmann. 2017. 'An assay for entry of secreted fungal effectors into plant cells', *New Phytologist*, 213: 956-64.

Locato, Vittoria, and Laura De Gara. 2018. 'Programmed Cell Death in Plants: An Overview.' in Laura De Gara and Vittoria Locato (eds.), *Plant Programmed Cell Death: Methods and Protocols* (Springer New York: New York, NY).

Lorang, J. 2019. 'Necrotrophic Exploitation and Subversion of Plant Defense: A Lifestyle or Just a Phase, and Implications in Breeding Resistance', *Phytopathology*, 109: 332-46.

Lorrain, C., B. Petre, and S. Duplessis. 2018. 'Show me the way: rust effector targets in heterologous plant systems', *Current Opinion in Microbiology*, 46: 19-25.

Lu, D. P., S. J. Wu, X. Q. Gao, Y. L. Zhang, L. B. Shan, and P. He. 2010. 'A receptor-like cytoplasmic kinase, BIK1, associates with a flagellin

receptor complex to initiate plant innate immunity', *Proceedings of the National Academy of Sciences*, 107: 496-501.

Lu, Q. X., M. Lillemo, H. Skinnes, X. Y. He, J. R. Shi, F. Ji, Y. H. Dong, and A. Bjornstad. 2013. 'Anther extrusion and plant height are associated with Type I resistance to Fusarium head blight in bread wheat line 'Shanghai-3/Catbird'', *Theoretical and Applied Genetics*, 126: 317-34.

Lu, S. W., and M. C. Edwards. 2016. 'Genome-Wide Analysis of Small Secreted Cysteine-Rich Proteins Identifies Candidate Effector Proteins Potentially Involved in F*usarium graminearum*-Wheat Interactions', *Phytopathology*, 106: 166-76.

Lysoe, E., K. Y. Seong, and H. C. Kistler. 2011. 'The Transcriptome of *Fusarium graminearum* During the Infection of Wheat', *Molecular Plant-Microbe Interactions*, 24: 995-1000.

Lyu, X., C. Shen, Y. Fu, J. Xie, D. Jiang, G. Li, and J. Cheng. 2016. 'A Small Secreted Virulence-Related Protein Is Essential for the Necrotrophic Interactions of *Sclerotinia sclerotiorum* with Its Host Plants', *PloS Pathogens*, 12: e1005435.

Ma, L. J., H. C. van der Does, K. A. Borkovich, J. J. Coleman, M. J. Daboussi, A. Di Pietro, M. Dufresne, M. Freitag, M. Grabherr, B. Henrissat, P. M. Houterman, S. Kang, W. B. Shim, C. Woloshuk, X. H. Xie, J. R. Xu, J. Antoniw, S. E. Baker, B. H. Bluhm, A. Breakspear, D. W. Brown, R. A. E. Butchko, S. Chapman, R. Coulson, P. M. Coutinho, E. G. J. Danchin, A. Diener, L. R. Gale, D. M. Gardiner, S. Goff, K. E. Hammond-Kosack, K. Hilburn, A. Hua-Van, W. Jonkers, K. Kazan, C. D. Kodira, M. Koehrsen, L. Kumar, Y. H. Lee, L. D. Li, J. M. Manners, D. Miranda-Saavedra, M. Mukherjee, G. Park, J. Park, S. Y. Park, R. H. Proctor, A. Regev, M. C. Ruiz-Roldan, D. Sain, S. Sakthikumar, S. Sykes, D. C. Schwartz, B. G. Turgeon, I. Wapinski, O. Yoder, S. Young, Q. D. Zeng, S. G. Zhou, J. Galagan, C. A. Cuomo, H. C. Kistler, and M. Rep. 2010. 'Comparative genomics reveals mobile pathogenicity chromosomes in Fusarium', *Nature*, 464: 367-73.

Ma, L., E. Lukasik, F. Gawehns, and F. L. Takken. 2012. 'The use of agroinfiltration for transient expression of plant resistance and fungal

effector proteins in *Nicotiana benthamiana* leaves', *Methods in Molecular Biology*, 835: 61-74.

Ma, L. S., P. M. Houterman, F. Gawehns, L. X. Cao, F. Sillo, H. Richter, M. J. Clavijo-Ortiz, S. M. Schmidt, S. Boeren, J. Vervoort, B. J. C. Cornelissen, M. Rep, and F. L. W. Takken. 2015. 'The AVR2-SIX5 gene pair is required to activate I-2-mediated immunity in tomato', *New Phytologist*, 208: 507-18.

Ma, W., and D. S. Guttman. 2008. 'Evolution of prokaryotic and eukaryotic virulence effectors', *Current Opinion in Plant Biology*, 11: 412-9.

Machado, A. K., N. A. Brown, M. Urban, K. Kanyuka, and K. E. Hammond-Kosack. 2018. 'RNAi as an emerging approach to control Fusarium head blight disease and mycotoxin contamination in cereals', *Pest Management Science*, 74: 790-99.

Madgwick, J. W., J. S. West, R. P. White, M. A. Semenov, J. A. Townsend, J. A. Turner, and B. D. L. Fitt. 2011. 'Impacts of climate change on wheat anthesis and Fusarium ear blight in the UK', *European Journal of Plant Pathology*, 130: 117-31.

Maekawa, T., T. A. Kufer, and P. Schulze-Lefert. 2011. 'NLR functions in plant and animal immune systems: so far and yet so close', *Nature Immunology*, 12: 818-26.

Maier, F. J., S. Malz, A. P. Losch, T. Lacour, and W. Schafer. 2005. 'Development of a highly efficient gene targeting system for *Fusarium graminearum* using the disruption of a polyketide synthase gene as a visible marker', *FEMS Yeast Res*, 5: 653-62.

Makandar, R., V. Nalam, R. Chaturvedi, R. Jeannotte, A. A. Sparks, and J. Shah. 2010. 'Involvement of Salicylate and Jasmonate Signaling Pathways in Arabidopsis Interaction with *Fusarium graminearum*', *Molecular Plant-Microbe Interactions*, 23: 861-70.

Manning, V. A., A. L. Chu, S. R. Scofield, and L. M. Ciuffetti. 2010. 'Intracellular expression of a host-selective toxin, ToxA, in diverse plants phenocopies silencing of a ToxA-interacting protein, ToxABP1', *New Phytologist*, 187: 1034-47.

Manning, V. A., and L. M. Ciuffetti. 2005. 'Localization of Ptr ToxA produced by *Pyrenophora tritici-repentis* reveals protein import into wheat mesophyll cells', *Plant Cell*, 17: 3203-12.

Manning, V. A., S. M. Hamilton, P. A. Karplus, and L. M. Ciuffetti. 2008. 'The Arg-Gly-Asp-containing, solvent-exposed loop of Ptr ToxA is required for internalization', *Molecular Plant-Microbe Interactions*, 21: 315-25.

Manteau, S., S. Abouna, B. Lambert, and L. Legendre. 2003. 'Differential regulation by ambient pH of putative virulence factor secretion by the phytopathogenic fungus *Botrytis cinerea'*, *Fems Microbiology Ecology*, 43: 359-66.

Marchler-Bauer, A., M. K. Derbyshire, N. R. Gonzales, S. N. Lu, F. Chitsaz, L. Y. Geer, R. C. Geer, J. He, M. Gwadz, D. I. Hurwitz, C. J. Lanczycki, F. Lu, G. H. Marchler, J. S. Song, N. Thanki, Z. X. Wang, R. A. Yamashita, D. C. Zhang, C. J. Zheng, and S. H. Bryant. 2015. 'CDD: NCBI's conserved domain database', *Nucleic Acids Research*, 43: D222-D26.

Maresca, M. 2013. 'From the Gut to the Brain: Journey and Pathophysiological Effects of the Food-Associated Trichothecene Mycotoxin Deoxynivalenol', *Toxins*, 5: 784-820.

Marsian, J., and G. P. Lomonossoff. 2016. 'Molecular pharming - VLPs made in plants', *Current Opinion in Biotechnology*, 37: 201-06.

Marx, F. 2004. 'Small, basic antifungal proteins secreted from filamentous ascomycetes: a comparative study regarding expression, structure, function and potential application', *Applied Microbiology and Biotechnology*, 65: 133-42.

McCann, H. C., H. Nahal, S. Thakur, and D. S. Guttman. 2012. 'Identification of innate immunity elicitors using molecular signatures of natural selection', *Proceedings of the Nationall Academy of Sciences*, 109: 4215-20.

McMullen, M., G. Bergstrom, E. De Wolf, R. Dill-Macky, D. Hershman, G. Shaner, and D. Van Sanford. 2012. 'A Unified Effort to Fight an Enemy of Wheat and Barley: Fusarium Head Blight', *Plant Disease*, 96: 1712-28.

McMullen, M. D., M. W. Jones, K. D. Simcox, and R. Louie. 1994. '3 Genetic-Loci Control Resistance to Wheat Streak Mosaic-Virus in the Maize Inbred Pa405', *Molecular Plant-Microbe Interactions*, 7: 708-12.

Mehlmer, N., N. Parvin, C. H. Hurst, M. R. Knight, M. Teige, and U. C. Vothknecht. 2012. 'A toolset of aequorin expression vectors for in planta studies of subcellular calcium concentrations in *Arabidopsis thaliana*', *Journal of Experimental Botany*, 63: 1751-61.

Meister, U., and M. Springer. 2004. 'Mycotoxins in cereals and cereal products - occurrence and changes during processing', *Journal of Applied Botany and Food Quality-Angewandte Botanik*, 78: 168-73.

Melin, P., J. Schnurer, and E. G. Wagner. 2003. 'Characterization of phiA, a gene essential for phialide development in *Aspergillus nidulans'*, *Fungal Genetics and Biology*, 40: 234-41.

Meng, Y., M. J. Moscou, and R. P. Wise. 2009. 'Blufensin1 Negatively Impacts Basal Defense in Response to Barley Powdery Mildew', *Plant Physiology*, 149: 271-85.

Menke, J., J. Weber, K. Broz, and H. C. Kistler. 2013. 'Cellular Development Associated with Induced Mycotoxin Synthesis in the Filamentous Fungus *Fusarium graminearum*', *PloS One*, 8.

Mentlak, T. A., A. Kombrink, T. Shinya, L. S. Ryder, I. Otomo, H. Saitoh, R. Terauchi, Y. Nishizawa, N. Shibuya, B. P. Thomma, and N. J. Talbot. 2012. 'Effector-mediated suppression of chitin-triggered immunity by *Magnaporthe oryzae* is necessary for rice blast disease', *Plant Cell*, 24: 322-35.

Merhej, J., F. Richard-Forget, and C. Barreau. 2011. 'The pH regulatory factor Pac1 regulates Tri gene expression and trichothecene production in *Fusarium graminearum*', *Fungal Genetics and Biology*, 48: 275-84.

Mes, J. J., A. A. van Doorn, J. Wijbrandi, G. Simons, B. J. C. Cornelissen, and M. A. Haring. 2000. 'Expression of the Fusarium resistance gene I-2 colocalizes with the site of fungal containment', *Plant Journal*, 23: 183-93.

Mesterhazy, A. 2002. 'Role of deoxynivalenol in aggressiveness of *Fusarium graminearum* and *F. culmorum* and in resistance to Fusarium head blight', *European Journal of Plant Pathology*, 108: 675-84.

Meszka, B., and A. Bielenin. 2010. 'Polyversum WP a new biological product against strawberry grey mould', *Phytopathology*, 58: 13-19.

Michelmore, R. W. 2003. 'The impact zone: genomics and breeding for durable disease resistance', *Current Opinion in Plant Biology*, 6: 397-404.

Moco, S., R. J. Bino, O. Vorst, H. A. Verhoeven, J. de Groot, T. A. van Beek, J. Vervoort, and C.H. Ric de Vos. 2006. 'A Liquid Chromatography-Mass Spectrometry-Based Metabolome Database for Tomato', *Plant Physiology*, 141: 1205-18.

Motteram, J., I. Kufner, S. Deller, F. Brunner, K. E. Hammond-Kosack, T. Nurnberger, and J. J. Rudd. 2009. 'Molecular characterization and functional analysis of MgNLP, the sole NPP1 domain-containing protein, from the fungal wheat leaf pathogen *Mycosphaerella graminicola'*, *Molecular Plant-Microbe Interactions*, 22: 790-9.

Mueller, A. N., S. Ziemann, S. Treitschke, D. Assmann, and G. Doehlemann. 2013. 'Compatibility in the *Ustilago maydis*-Maize Interaction Requires Inhibition of Host Cysteine Proteases by the Fungal Effector Pit2', *PloS Pathogens*, 9.

Mukhtar, M. S., M. E. McCormack, C. T. Argueso, and K. M. Pajerowska-Mukhtar. 2016. 'Pathogen Tactics to Manipulate Plant Cell Death', *Current Biology*, 26: R608-R19.

Mur, L. A. J., P. Kenton, R. Atzorn, O. Miersch, and C. Wasternack. 2006. 'The outcomes of concentration-specific interactions between salicylate and jasmonate signaling include synergy, antagonism, and oxidative stress leading to cell death', *Plant Physiology*, 140: 249-62.

Myers, S. S., M. R. Smith, S. Guth, C. D. Golden, B. Vaitla, N. D. Mueller, A. D. Dangour, and P. Huybers. 2017. 'Climate Change and Global Food Systems: Potential Impacts on Food Security and Undernutrition', *Annual Review of Public Health, Vol 38*, 38: 259-77.

Naim, F., K. Nakasugi, R. N. Crowhurst, E. Hilario, A. B. Zwart, R. P. Hellens, J. M. Taylor, P. M. Waterhouse, and C. C. Wood. 2012.

'Advanced Engineering of Lipid Metabolism in *Nicotiana benthamiana* Using a Draft Genome and the V2 Viral Silencing-Suppressor Protein', *PloS One*, 7.

Nakasugi, K., R. Crowhurst, J. Bally, and P. Waterhouse. 2014. 'Combining Transcriptome Assemblies from Multiple De Novo Assemblers in the Allo-Tetraploid Plant *Nicotiana benthamiana*', *PloS One*, 9.

Nalam, V. J., S. Alam, J. Keereetaweep, B. Venables, D. Burdan, H. Lee, H. N. Trick, S. Sarowar, R. Makandar, and J. Shah. 2015. 'Facilitation of *Fusarium graminearum* Infection by 9-Lipoxygenases in Arabidopsis and Wheat', *Molecular Plant-Microbe Interactions*, 28: 1142-52.

Navarre, D. A., and T. J. Wolpert. 1995. 'Inhibition of the Glycine Decarboxylase Multienzyme Complex by the Host-Selective Toxin Victorin', *Plant Cell*, 7: 463-71.

Nekrasov, V. 2019. 'Sequence-specific nucleases as tools for enhancing disease resistance in crops', *Transgenic Research*, 28: 75-80.

Nekrasov, V., B. Staskawicz, D. Weigel, J. D. G. Jones, and S. Kamoun. 2013. 'Targeted mutagenesis in the model plant *Nicotiana benthamiana* using Cas9 RNA-guided endonuclease', *Nature Biotechnology*, 31: 691-93.

Neukom, R., L. A. Barboza, M. P. Erb, F. Shi, J. Emile-Geay, M. N. Evans, J. Franke, D. S. Kaufman, L. Lucke, K. Rehfeld, A. Schurer, F. Zhu, S. Bronnimann, G. J. Hakim, B. J. Henley, F. C. Ljungqvist, N. McKay, V. Valler, L. von Gunten, and Pages 2k Consortium. 2019. 'Consistent multidecadal variability in global temperature reconstructions and simulations over the Common Era', *Nature Geoscience*, 12: 643.

Neukom, R., N. Steiger, J. J. Gomez-Navarro, J. H. Wang, and J. P. Werner. 2019. 'No evidence for globally coherent warm and cold periods over the preindustrial Common Era', *Nature*, 571: 550.

Nganje, W. E., D. A. Bangsund, F. L. Leistritz, W. W. Wilson, and N. M. Tiapo. 2004. 'Regional economic impacts of Fusarium Head Blight in wheat and barley', *Review of Agricultural Economics*, 26: 332-47.

Nirmaladevi, D., M. Venkataramana, R. K. Srivastava, S. R. Uppalapati, V. K. Gupta, T. Yli-Mattila, K. M. Clement Tsui, C. Srinivas, S. R. Niranjana, and N. S. Chandra. 2016. 'Molecular phylogeny, pathogenicity and

toxigenicity of F*usarium oxysporum f. sp. lycopersici*', *Scientific Reports*, 6: 21367.

Niwa, S., K. Kubo, J. Lewis, R. Kikuchi, M. Alagu, and T. Ban. 2014. 'Variations for Fusarium head blight resistance associated with genomic diversity in different sources of the resistant wheat cultivar 'Sumai 3'', *Breeding Science*, 64: 90-96.

Nodvig, C. S., J. B. Nielsen, M. E. Kogle, and U. H. Mortensen. 2015. 'A CRISPR-Cas9 System for Genetic Engineering of Filamentous Fungi', *PloS One*, 10.

Nomura, H., T. Komori, S. Uemura, Y. Kanda, K. Shimotani, K. Nakai, T. Furuichi, K. Takebayashi, T. Sugimoto, S. Sano, I. N. Suwastika, E. Fukusaki, H. Yoshioka, Y. Nakahira, and T. Shiina. 2012. 'Chloroplast-mediated activation of plant immune signalling in Arabidopsis', *Nature Communications*, 3.

Nowara, D., A. Gay, C. Lacomme, J. Shaw, C. Ridout, D. Douchkov, G. Hensel, J. Kumlehn, and P. Schweizer. 2010. 'HIGS: Host-Induced Gene Silencing in the Obligate Biotrophic Fungal Pathogen *Blumeria graminis*', *Plant Cell*, 22: 3130-41.

O'Connell, R. J., M. R. Thon, S. Hacquard, S. G. Amyotte, J. Kleemann, M. F. Torres, U. Damm, E. A. Buiate, L. Epstein, N. Alkan, J. Altmuller, L. Alvarado-Balderrama, C. A. Bauser, C. Becker, B. W. Birren, Z. Chen, J. Choi, J. A. Crouch, J. P. Duvick, M. A. Farman, P. Gan, D. Heiman, B. Henrissat, R. J. Howard, M. Kabbage, C. Koch, B. Kracher, Y. Kubo, A. D. Law, M. H. Lebrun, Y. H. Lee, I. Miyara, N. Moore, U. Neumann, K. Nordstrom, D. G. Panaccione, R. Panstruga, M. Place, R. H. Proctor, D. Prusky, G. Rech, R. Reinhardt, J. A. Rollins, S. Rounsley, C. L. Schardl, D. C. Schwartz, N. Shenoy, K. Shirasu, U. R. Sikhakolli, K. Stuber, S. A. Sukno, J. A. Sweigard, Y. Takano, H. Takahara, F. Trail, H. C. van der Does, L. M. Voll, I. Will, S. Young, Q. Zeng, J. Zhang, S. Zhou, M. B. Dickman, P. Schulze-Lefert, E. Ver Loren van Themaat, L. J. Ma, and L. J. Vaillancourt. 2012. 'Lifestyle transitions in plant pathogenic Colletotrichum fungi deciphered by genome and transcriptome analyses', *Nature Genetics*, 44: 1060-5.

O'Donnell, K., H. C. Kistler, B. K. Tacke, and H. H. Casper. 2000. 'Gene genealogies reveal global phylogeographic structure and reproductive isolation among lineages of *Fusarium graminearum*, the fungus causing wheat scab', *Proceedings of the National Academy of Sciences*, 97: 7905-10.

O'Leary, B. M., A. Rico, S. McCraw, H. N. Fones, and G. M. Preston. 2014. 'The Infiltration-centrifugation Technique for Extraction of Apoplastic Fluid from Plant Leaves Using *Phaseolus vulgaris* as an Example', *Jove-Journal of Visualized Experiments*.

O'Neill, J. R. 2010. *Irish Potato Famine* (ABDO).

Oerke, E. C. 2006. 'Crop losses to pests', *Journal of Agricultural Science*, 144: 31-43.

Oide, S., F. Berthiller, G. Wiesenberger, G. Adam, and B. G. Turgeon. 2014. 'Individual and combined roles of malonichrome, ferricrocin, and TAFC siderophores in *Fusarium graminearum* pathogenic and sexual development', *Frontiers in Microbiology*, 5: 759.

Oide, S., W. Moeder, S. Krasnoff, D. Gibson, H. Haas, K. Yoshioka, and B. G. Turgeon. 2006. 'NPS6, encoding a nonribosomal peptide synthetase involved in siderophore-mediated iron metabolism, is a conserved virulence determinant of plant pathogenic ascomycetes', *Plant Cell*, 18: 2836-53.

Ordon, J., J. Gantner, J. Kemna, L. Schwalgun, M. Reschke, J. Streubel, J. Boch, and J. Stuttmann. 2017. 'Generation of chromosomal deletions in dicotyledonous plants employing a user-friendly genome editing toolkit', *Plant Journal*, 89: 155-68.

Ori, N., Y. Eshed, I. Paran, G. Presting, D. Aviv, S. Tanksley, D. Zamir, and R. Fluhr. 1997. 'The I2C family from the wilt disease resistance locus I2 belongs to the nucleotide binding, leucine-rich repeat superfamily of plant resistance genes', *Plant Cell*, 9: 521-32.

Osborne, L. E., and J. M. Stein. 2007. 'Epidemiology of Fusarium head blight on small-grain cereals', *International Journal of Food Microbiology*, 119: 103-08.

Palazzini, J., V. Fumero, N. Yerkovich, G. Barros, M. Cuniberti, and S. Chulze. 2015. 'Correlation between *Fusarium graminearum* and

Deoxynivalenol during the 2012/13 Wheat Fusarium Head Blight Outbreak in Argentina', *Cereal Research Communications*, 43: 627-37.

Palazzini, J. M., M. L. Ramirez, A. M. Torres, and S. N. Chulze. 2007. 'Potential biocontrol agents for Fusarium head blight and deoxynivalenol production in wheat', *Crop Protection*, 26: 1702-10.

Panavas, T., and B. Rubinstein. 1998. 'Oxidative events during programmed cell death of daylily (Hemerocallis hybrid) petals', *Plant Science*, 133: 125-38.

Pandelova, I., M. F. Betts, V. A. Manning, L. J. Wilhelm, T. C. Mockler, and L. M. Ciuffetti. 2009. 'Analysis of Transcriptome Changes Induced by Ptr ToxA in Wheat Provides Insights into the Mechanisms of Plant Susceptibility', *Molecular Plant*, 2: 1067-83.

Panwar, V., B. McCallum, and G. Bakkeren. 2013. 'Host-induced gene silencing of wheat leaf rust fungus *Puccinia triticina* pathogenicity genes mediated by the Barley stripe mosaic virus', *Plant Molecular Biology*, 81: 595-608.

Park, C. H., S. B. Chen, G. Shirsekar, B. Zhou, C. H. Khang, P. Songkumarn, A. J. Afzal, Y. S. Ning, R. Y. Wang, M. Bellizzi, B. Valent, and G. L. Wang. 2012. 'The *Magnaporthe oryzae* Effector AvrPiz-t Targets the RING E3 Ubiquitin Ligase APIP6 to Suppress Pathogen-Associated Molecular Pattern-Triggered Immunity in Rice', *Plant Cell*, 24: 4748-62.

Park, D. L., R. Lopez-Garcia, S. Trujillo-Preciado, and R. L. Price. 1996. 'Reduction of risks associated with fumonisin contamination in corn', *Advanced Technologies for Protein Complex Production and Characterization*, 392: 335-44.

Parry, D. W., P. Jenkinson, and L. Mcleod. 1995. 'Fusarium Ear Blight (Scab) in Small-Grain Cereals - a Review', *Plant Pathology*, 44: 207-38.

Pazzagli, L., G. Cappugi, G. Manao, G. Camici, A. Santini, and A. Scala. 1999. 'Purification, characterization, and amino acid sequence of cerato-platanin, a new phytotoxic protein from *Ceratocystis fimbriata f. sp platani*', *Journal of Biological Chemistry*, 274: 24959-64.

Pearce, R. B., R. N. Strange, and H. Smith. 1976. 'Glycinebetaine and Choline in Wheat - Distribution and Relation to Infection by *Fusarium graminearum*', *Phytochemistry*, 15: 953-54.

Peart, J. R., R. Lu, A. Sadanandom, I. Malcuit, P. Moffett, D. C. Brice, L. Schauser, D. A. W. Jaggard, S. Y. Xiao, M. J. Coleman, M. Dow, J. D. G. Jones, K. Shirasu, and D. C. Baulcombe. 2002. 'Ubiquitin ligase-associated protein SGT1 is required for host and nonhost disease resistance in plants', *Proceedings of the National Academy of Sciences*, 99: 10865-69.

Pereyra, S. A., R. Dill-Macky, and A. L. Sims. 2004. 'Survival and inoculum production of *Gibberella zeae* in wheat residue', *Plant Disease*, 88: 724-30.

Pestka, J. J., and A. T. Smolinski. 2005. 'Deoxynivalenol: Toxicology and potential effects on humans', *Journal of Toxicology and Environmental Health-Part B-Critical Reviews*, 8: 39-69.

Petersen, T. N., S. Brunak, G. von Heijne, and H. Nielsen. 2011. 'SignalP 4.0: discriminating signal peptides from transmembrane regions', *Nature Methods*, 8: 785-86.

Petre, B., C. Lorrain, D. G. Saunders, J. Win, J. Sklenar, S. Duplessis, and S. Kamoun. 2016. 'Rust fungal effectors mimic host transit peptides to translocate into chloroplasts', *Cellular Microbiology*, 18: 453-65.

Petre, B., D. G. O. Saunders, J. Sklenar, C. Lorrain, K. V. Krasileva, J. Win, S. Duplessis, and S. Kamoun. 2016. 'Heterologous Expression Screens in *Nicotiana benthamiana* Identify a Candidate Effector of the Wheat Yellow Rust Pathogen that Associates with Processing Bodies', *PloS One*, 11.

Petre, B., D. G. O. Saunders, J. Sklenar, C. Lorrain, J. Win, S. Duplessis, and S. Kamoun. 2015. 'Candidate Effector Proteins of the Rust Pathogen *Melampsora larici-populina* Target Diverse Plant Cell Compartments', *Molecular Plant-Microbe Interactions*, 28: 689-700.

Petty, I. T. D., B. G. Hunter, N. Wei, and A. O. Jackson. 1989. 'Infectious Barley Stripe Mosaic-Virus Rna Transcribed Invitro from Full-Length Genomic cDNA Clones', *Virology*, 171: 342-49.

Peyret, H., and G. P. Lomonossoff. 2013. 'The pEAQ vector series: the easy and quick way to produce recombinant proteins in plants', *Plant Molecular Biology*, 83: 51-58.

Phalip, V., F. Delalande, C. Carapito, F. Goubet, D. Hatsch, E. Leize-Wagner, P. Dupree, A. Van Dorsselaer, and J. M. Jeltsch. 2005. 'Diversity of the exoproteome of *Fusarium graminearum* grown on plant cell wall', *Current Genetics*, 48: 366-79.

Pi, J., and L. Sael. 2013. 'Mass Spectrometry Coupled Experiments and Protein Structure Modeling Methods', *International Journal of Molecular Sciences*, 14: 20635-57.

Ploetz, R. C. 2006. 'Fusarium wilt of banana is caused by several pathogens referred to as *Fusarium oxysporum f. sp. cubense*', *Phytopathology*, 96: 653-56.

Proctor, R. H., T. M. Hohn, and S. P. Mccormick. 1995. 'Reduced Virulence of *Gibberella-Zeae* Caused by Disruption of a Trichothecene Toxin Biosynthetic Gene', *Molecular Plant-Microbe Interactions*, 8: 593-601.

Proestos, C., D. Sereli, and M. Komaitis. 2006. 'Determination of phenolic compounds in aromatic plants by RP-HPLC and GC-MS', *Food Chemistry*, 95: 44-52.

Pugh, G. W., H. Johann, and J. G. Dickson. 1933. 'Factors affecting infection of Wheat heads by *Gibberella saubiuetii'*, *Journal of Agricultural Research*, 46: 771-97.

Qi, P. F., M. Balcerzak, H. Rocheleau, W. Leung, Y. M. Wei, Y. L. Zheng, and T. Ouellet. 2016. 'Jasmonic acid and abscisic acid play important roles in host-pathogen interaction between *Fusarium graminearum* and wheat during the early stages of fusarium head blight', *Physiological and Molecular Plant Pathology*, 93: 39-48.

Qiao, Y. L., L. Liu, Q. Xiong, C. Flores, J. Wong, J. X. Shi, X. B. Wang, X. G. Liu, Q. J. Xiang, S. S. Jiang, F. C. Zhang, Y. C. Wang, H. S. Judelson, X. M. Chen, and W. B. Ma. 2013. 'Oomycete pathogens encode RNA silencing suppressors', *Nature Genetics*, 45: 330-33.

Qin, J., G. H. Wang, C. Jiang, J. R. Xu, and C. F. Wang. 2015. 'Fgk3 glycogen synthase kinase is important for development, pathogenesis, and stress responses in *Fusarium graminearum*', *Scientific Reports*, 5.

Qiu, J. B., F. Dong, M. Z. Yu, J. H. Xu, and J. R. Shi. 2016. 'Effect of preceding crop on Fusarium species and mycotoxin contamination of wheat grains', *Journal of the Science of Food and Agriculture*, 96: 4536-41.

Qutob, D., B. Kemmerling, F. Brunner, I. Kufner, S. Engelhardt, A. A. Gust, B. Luberacki, H. U. Seitz, D. Stahl, T. Rauhut, E. Glawischnig, G. Schween, B. Lacombe, N. Watanabe, E. Lam, R. Schlichting, D. Scheel, K. Nau, G. Dodt, D. Hubert, M. Gijzen, and T. Nurnberger. 2006. 'Phytotoxicity and innate immune responses induced by Nep1-like proteins', *Plant Cell*, 18: 3721-44.

Rafiqi, M., J. G. Ellis, V. A. Ludowici, A. R. Hardham, and P. N. Dodds. 2012. 'Challenges and progress towards understanding the role of effectors in plant-fungal interactions', *Current Opinion in Plant Biology*, 15: 477-82.

Ramamoorthy, V., X. H. Zhao, A. K. Snyder, J. R. Xu, and D. M. Shah. 2007. 'Two mitogen-activated protein kinase signalling cascades mediate basal resistance to antifungal plant defensins in *Fusarium graminearum*', *Cellular Microbiology*, 9: 1491-506.

Rampitsch, C., J. Day, R. Subramaniam, and S. Walkowiak. 2013. 'Comparative secretome analysis of *Fusarium graminearum* and two of its non-pathogenic mutants upon deoxynivalenol induction in vitro', *Proteomics*, 13: 1913-21.

Ratcliff, F., A. M. Martin-Hernandez, and D. C. Baulcombe. 2001. 'Tobacco rattle virus as a vector for analysis of gene function by silencing', *Plant Journal*, 25: 237-45.

Rawat, N., M. O. Pumphrey, S. X. Liu, X. F. Zhang, V. K. Tiwari, K. Ando, H. N. Trick, W. W. Bockus, E. Akhunov, J. A. Anderson, and B. S. Gill. 2016. 'Wheat Fhb1 encodes a chimeric lectin with agglutinin domains and a pore-forming toxin-like domain conferring resistance to Fusarium head blight', *Nature Genetics*, 48: 1576-80.

Rep, M. 2005. 'Small proteins of plant-pathogenic fungi secreted during host colonization', *Fems Microbiology Letters*, 253: 19-27.

Rep, M., and H. C. Kistler. 2010. 'The genomic organization of plant pathogenicity in Fusarium species', *Current Opinion in Plant Biology*, 13: 420-26.

Rittenour, W. R., and S. D. Harris. 2010. 'An in vitro method for the analysis of infection-related morphogenesis in *Fusarium graminearum*', *Molecular Plant Pathology*, 11: 361-69.

Robinson, D., Y. Ding, and L. W. Jiang. 2016. 'Unconventional protein secretion in plants: a critical assessment', *Protoplasma*, 253: 31-43.

Rogelj, J., M. den Elzen, N. Hohne, T. Fransen, H. Fekete, H. Winkler, R. S. Chaeffer, F. Ha, K. Riahi, and M. Meinshausen. 2016. 'Paris Agreement climate proposals need a boost to keep warming well below 2 degrees C', *Nature*, 534: 631-39.

Rojas, E. C., H. J. L. Jørgensen, B. Jensen, and D. B. Collinge. 2018. 'Fusarium diseases: biology and management perspectives'.

Rolland, S., C. Jobic, M. Fevre, and C. Bruel. 2003. 'Agrobacterium-mediated transformation of *Botrytis cinerea*, simple purification of monokaryotic transformants and rapid conidia-based identification of the transfer-DNA host genomic DNA flanking sequences', *Current Genetics*, 44: 164-71.

Rooney, H. C. E. 2005. 'Cladosporium Avr2 inhibits tomato Rcr3 protease required for Cf-2-dependent disease resistance (vol 308, pg 1783, 2005)', *Science*, 310: 54-54.

Routledge, A. P. M., G. Shelley, J. V. Smith, N. J. Talbot, J. Draper, and L. A. J. Mur. 2004. '*Magnaporthe grisea* interactions with the model grass Brachypodium distachyon closely resemble those with rice (Oryza sativa)', *Molecular Plant Pathology*, 5: 253-65.

Rouxel, T., J. Grandaubert, J. K. Hane, C. Hoede, A. P. van de Wouw, A. Couloux, V. Dominguez, V. Anthouard, P. Bally, S. Bourras, A. J. Cozijnsen, L. M. Ciuffetti, A. Degrave, A. Dilmaghani, L. Duret, I. Fudal, S. B. Goodwin, L. Gout, N. Glaser, J. Linglin, G. H. J. Kema, N. Lapalu, C. B. Lawrence, K. May, M. Meyer, B. Ollivier, J. Poulain, C. L. Schoch, A. Simon, J. W. Spatafora, A. Stachowiak, B. G. Turgeon, B. M. Tyler, D. Vincent, J. Weissenbach, J. Amselem, H. Quesneville, R. P. Oliver, P. Wincker, M. H. Balesdent, and B. J. Howlett. 2011.

'Effector diversification within compartments of the *Leptosphaeria maculans* genome affected by Repeat-Induced Point mutations', *Nature Communications*, 2.

Rudd, J. J., K. Kanyuka, K. Hassani-Pak, M. Derbyshire, A. Andongabo, J. Devonshire, A. Lysenko, M. Saqi, N. M. Desai, S. J. Powers, J. Hooper, L. Ambroso, A. Bharti, A. Farmer, K. E. Hammond-Kosack, R. A. Dietrich, and M. Courbot. 2015. 'Transcriptome and Metabolite Profiling of the Infection Cycle of *Zymoseptoria tritici* on Wheat Reveals a Biphasic Interaction with Plant Immunity Involving Differential Pathogen Chromosomal Contributions and a Variation on the Hemibiotrophic Lifestyle Definition', *Plant Physiology*, 167: 1158.

Sainsbury, F., E. C. Thuenemann, and G. P. Lomonossoff. 2009. 'pEAQ: versatile expression vectors for easy and quick transient expression of heterologous proteins in plants', *Plant Biotechnology Journal*, 7: 682-93.

Saintenac, C., W. S. Lee, F. Cambon, J. J. Rudd, R. C. King, W. Marande, S. J. Powers, H. Berges, A. L. Phillips, C. Uauy, K. E. Hammond-Kosack, T. Langin, and K. Kanyuka. 2018. 'Wheat receptor-kinase-like protein Stb6 controls gene-for-gene resistance to fungal pathogen *Zymoseptoria tritici*', *Nature Genetics*, 50: 368.

Sanchez-Martin, J., and B. Keller. 2019. 'Contribution of recent technological advances to future resistance breeding', *Theoretical and Applied Genetics*, 132: 713-32.

Sanchez-Vallet, A., F. E. Hartmann, T. C. Marcel, and D. Croll. 2018. 'Nature's genetic screens: using genome-wide association studies for effector discovery', *Molecular Plant Pathology*, 19: 3-6.

Sarlin, T., T. Kivioja, N. Kalkkinen, M. B. Linder, and T. Nakari-Setala. 2012. 'Identification and characterization of gushing-active hydrophobins from *Fusarium graminearum* and related species', *Journal of Basic Microbiology*, 52: 184-94.

Sarma, G. N., V. A. Manning, L. M. Ciuffetti, and P. A. Karplus. 2005. 'Structure of Ptr ToxA: An RGD-containing host-selective toxin from *Pyrenophora tritici-repentis*', *Plant Cell*, 17: 3190-202.

Sarowar, S., S. T. Alam, R. Makandar, H. Lee, H. N. Trick, Y. H. Dong, and J. Shah. 2019. 'Targeting the pattern-triggered immunity pathway to enhance resistance to *Fusarium graminearum*', *Molecular Plant Pathology*, 20: 626-40.

Sarris, P. F., Z. Duxbury, S. U. Huh, Y. Ma, C. Segonzac, J. Sklenar, P. Derbyshire, V. Cevik, G. Rallapalli, S. B. Saucet, L. Wirthmueller, F. L. H. Menke, K. H. Sohn, and J. D. G. Jones. 2015. 'A Plant Immune Receptor Detects Pathogen Effectors that Target WRKY Transcription Factors', *Cell*, 161: 1089-100.

Savary, S., A. Ficke, J. N. Aubertot, and C. Hollier. 2012. 'Crop losses due to diseases and their implications for global food production losses and food security', *Food Security*, 4: 519-37.

Schaafsma, A. W., L. Tamburic-Ilincic, and D. C. Hooker. 2005. 'Effect of previous crop, tillage, field size, adjacent crop, and sampling direction on airborne propagules of *Gibberella zeae/Fusarium graminearum*, Fusarium head blight severity, and deoxynivalenol accumulation in winter wheat', *Canadian Journal of Plant Pathology*, 27: 217-24.

Schaller, A., and A. Stintzi. 2009. 'Enzymes in jasmonate biosynthesis - Structure, function, regulation', *Phytochemistry*, 70: 1532-38.

Scherr, S. J., and J. A. McNeely. 2008. 'Biodiversity conservation and agricultural sustainability: towards a new paradigm of 'ecoagriculture' landscapes', *Philosophical Transactions of the Royal Society B-Biological Sciences*, 363: 477-94.

Schisler, D. A., N. I. Khan, and M. J. Boehm. 2002. 'Biological control of Fusarium head blight of wheat and deoxynivalenol levels in grain via use of microbial antagonists', *Mycotoxins and Food Safety*, 504: 53-69.

Schisler, D. A., N. I. Khan, M. J. Boehm, P. E. Lipps, P. J. Slininger, and S. Zhang. 2006. 'Selection and evaluation of the potential of choline-metabolizing microbial strains to reduce Fusarium head blight', *Biological Control*, 39: 497-506.

Schmidt, S. M., P. M. Houterman, I. Schreiver, L. S. Ma, S. Amyotte, B. Chellappan, S. Boeren, F. L. W. Takken, and M. Rep. 2013. 'MITEs in

the promoters of effector genes allow prediction of novel virulence genes in *Fusarium oxysporum*', *BMC Genomics*, 14.

Schneider, C. A., W. S. Rasband, and K. W. Eliceiri. 2012. 'NIH Image to ImageJ: 25 years of image analysis', *Nature Methods*, 9: 671-75.

Schoonbeek, H. J., H. H. Wang, F. L. Stefanato, M. Craze, S. Bowden, E. Wallington, C. Zipfel, and C. J. Ridout. 2015. 'Arabidopsis EF-Tu receptor enhances bacterial disease resistance in transgenic wheat', *New Phytologist*, 206: 606-13.

Schottens-Toma, Ingrid MJ, P. J. G. M. de Wit, and molecular plant pathology. 1988. 'Purification and primary structure of a necrosis-inducing peptide from the apoplastic fluids of tomato infected with *Cladosporium fulvum* (syn. Fulvia fulva)', *Journal of Physiological and Molecular Plant Pathology*33: 59-67.

Schouten, A., P. van Baarlen, and J. A. L. van Kan. 2008. 'Phytotoxic Nep1-like proteins from the necrotrophic fungus *Botrytis cinerea* associate with membranes and the nucleus of plant cells', *New Phytologist*, 177: 493-505.

Schultink, A., T. C. Qi, J. Bally, and B. Staskawicz. 2019. 'Using forward genetics in *Nicotiana benthamiana* to uncover the immune signaling pathway mediating recognition of the *Xanthomonas perforans* effector XopJ4', *New Phytologist*, 221: 1001-09.

Schuster, M., G. Schweizer, and R. Kahmann. 2018. 'Comparative analyses of secreted proteins in plant pathogenic smut fungi and related basidiomycetes', *Fungal Genetics and Biology*, 112: 21-30.

Schweiger, W., B. Steiner, C. Ametz, G. Siegwart, G. Wiesenberger, F. Berthiller, M. Lemmens, H. Y. Jia, G. Adam, G. J. Muehlbauer, D. P. Kreil, and H. Buerstmayr. 2013. 'Transcriptomic characterization of two major Fusarium resistance quantitative trait loci (QTLs), Fhb1 and Qfhs.ifa-5A, identifies novel candidate genes', *Molecular Plant Pathology*, 14: 772-85.

Schwessinger, B., O. Bahar, N. Thomas, N. Holton, V. Nekrasov, D. L. Ruan, P. E. Canlas, A. Daudi, C. J. Petzold, V. R. Singan, R. Kuo, M. Chovatia, C. Daum, J. L. Heazlewood, C. Zipfel, and P. C. Ronald. 2015. 'Transgenic Expression of the Dicotyledonous Pattern

Recognition Receptor EFR in Rice Leads to Ligand-Dependent Activation of Defense Responses', *PloS Pathogens*, 11.

Scofield, S. R., L. Huang, A. S. Brandt, and B. S. Gill. 2005. 'Development of a virus-induced gene-silencing system for hexaploid wheat and its use in functional analysis of the Lr21-mediated leaf rust resistance pathway', *Plant Physiology*, 138: 2165-73.

See, P. T., E. M. Iagallo, R. P. Oliver, and C. S. Moffat. 2019. 'Heterologous Expression of the *Pyrenophora tritici-repentis* Effector Proteins ToxA and ToxB, and the Prevalence of Effector Sensitivity in Australian Cereal Crops', *Frontiers in Microbiology*, 10: 182.

Seeholzer, S., T. Tsuchimatsu, T. Jordan, S. Bieri, S. Pajonk, W. Yang, A. Jahoor, K. K. Shimizu, B. Keller, and P. Schulze-Lefert. 2010. 'Diversity at the Mla powdery mildew resistance locus from cultivated barley reveals sites of positive selection', *Molecular Plant-Microbe Interactions*, 23: 497-509.

Seong, K. Y., M. Pasquali, X. Zhou, J. Song, K. Hilburn, S. McCormick, Y. Dong, J. R. Xu, and H. C. Kistler. 2009a. 'Global gene regulation by Fusarium transcription factors Tri6 and Tri10 reveals adaptations for toxin biosynthesis', *Molecular Microbiology*, 72: 354-67.

Seong, K. Y., M. Pasquali, X. Y. Zhou, J. Song, K. Hilburn, S. McCormick, Y. H. Dong, J. R. Xu, and H. C. Kistler. 2009b. 'Global gene regulation by Fusarium transcription factors Tri6 and Tri10 reveals adaptations for toxin biosynthesis', *Molecular Microbiology*, 72: 354-67.

Seong, K. Y., X. Zhao, J. R. Xu, U. Guldener, and H. C. Kistler. 2008. 'Conidial germination in the filamentous fungus *Fusarium graminearum*', *Fungal Genetics and Biology*, 45: 389-99.

Shah, D. A., P. A. Paul, E. D. De Wolf, and L. V. Madden. 2019. 'Predicting plant disease epidemics from functionally represented weather series', *Philosophical Transactions of the Royal Society B-Biological Sciences*, 374.

Shaner, G. 2003. 'Epidemiology of Fusarium head blight of small grain cereals in North America', *Fusarium head blight of wheat and barley*.

Shi, G. J., Z. C. Zhang, T. L. Friesen, D. Raats, T. Fahima, R. S. Brueggeman, S. W. Lu, H. N. Trick, Z. H. Liu, W. Chao, Z. Frenkel, S.

S. Xu, J. B. Rasmussen, and J. D. Faris. 2016. 'The hijacking of a receptor kinase-driven pathway by a wheat fungal pathogen leads to disease', *Science Advances*, 2.

Shirasu, K. 2009. 'The HSP90-SGT1 Chaperone Complex for NLR Immune Sensors', *Annual Review of Plant Biology*, 60: 139-64.

Shirasu, K., and P. Schulze-Lefert. 2003. 'Complex formation, promiscuity and multi-functionality: protein interactions in disease-resistance pathways', *Trends in Plant Science*, 8: 252-58.

Sikhakolli, U. R., F. Lopez-Giraldez, N. Li, R. Common, J. P. Townsend, and F. Trail. 2012. 'Transcriptome analyses during fruiting body formation in *Fusarium graminearum* and *Fusarium verticillioides* reflect species life history and ecology', *Fungal Genetics and Biology*, 49: 663-73.

Singh, R. P., P. K. Singh, J. Rutkoski, D. P. Hodson, X. Y. He, L. N. Jorgensen, M. S. Hovmoller, and J. Huerta-Espino. 2016. 'Disease Impact on Wheat Yield Potential and Prospects of Genetic Control', *Annual Review of Phytopathology, Vol 54*, 54: 303-22.

Sisler, WW, and RG %J Plant Dis Rep Timian. 1956. 'Inheritance of the barley stripe mosaic virus resistance of Modjo (CI 3212) and CI 3212-1', 40: 1106-07.

Skibbe, D. S., G. Doehlemann, J. Fernandes, and V. Walbot. 2010. 'Maize Tumors Caused by *Ustilago maydis* Require Organ-Specific Genes in Host and Pathogen', *Science*, 328: 89-92.

Smith, P., M. Bustamante, H. Ahammad, H. Clark, H. Dong, E. A. Elsiddig, H. Haberl, R. Harper, J. House, and M. Jafari. 2014. 'Agriculture, forestry and other land use (AFOLU).' in, *Climate change 2014: mitigation of climate change. Contribution of Working Group III to the Fifth Assessment Report of the Intergovernmental Panel on Climate Change* (Cambridge University Press).

Soding, J., A. Biegert, and A. N. Lupas. 2005. 'The HHpred interactive server for protein homology detection and structure prediction', *Nucleic Acids Research*, 33: W244-W48.

Solomon, P. S., R. G. Lowe, K. C. Tan, O. D. Waters, and R. P. Oliver. 2006. '*Stagonospora nodorum*: cause of stagonospora nodorum blotch of wheat', *Molecular Plant Pathology*, 7: 147-56.

Spanu, P. D., H. G. Pennington, R. Jones, S. Kwon, G. Bonciani, H. Thieron, T. Chandler, P. Luong, S. Morgan, and Mi. Przydacz. 2018. 'A fungal ribonuclease-like effector protein inhibits plant host ribosomal RNA degradation', *BioRxiv*: 291427.

Sperschneider, J., P. N. Dodds, D. M. Gardiner, J. M. Manners, K. B. Singh, and J. M. Taylor. 2015. 'Advances and challenges in computational prediction of effectors from plant pathogenic fungi', *PloS Pathogens*, 11: e1004806.

Sperschneider, J., P. N. Dodds, D. M. Gardiner, K. B. Singh, and J. M. Taylor. 2018. 'Improved prediction of fungal effector proteins from secretomes with EffectorP 2.0', *Molecular Plant Pathology*, 19: 2094-110.

Sprague, S. J., S. J. Marcroft, H. L. Hayden, and B. J. Howlett. 2006. 'Major gene resistance to blackleg in *Brassica napus* overcome within three years of commercial production in southeastern Australia', *Plant Disease*, 90: 190-98.

Steiner, Barbara, Maria Buerstmayr, Christian Wagner, Andrea Danler, Babur Eshonkulov, Magdalena Ehn, and Hermann Buerstmayr. 2019. 'Fine-mapping of the Fusarium head blight resistance QTL Qfhs.ifa-5A identifies two resistance QTL associated with anther extrusion', *Theoretical and Applied Genetics*.

Stephens, A. E., D. M. Gardiner, R. G. White, A. L. Munn, and J. M. Manners. 2008. 'Phases of Infection and Gene Expression of *Fusarium graminearum* During Crown Rot Disease of Wheat', *Molecular Plant-Microbe Interactions*, 21: 1571-81.

Stergiopoulos, I., H. A. van den Burg, B. Okmen, H. G. Beenen, S. van Liere, G. H. Kema, and P. J. de Wit. 2010. 'Tomato Cf resistance proteins mediate recognition of cognate homologous effectors from fungi pathogenic on dicots and monocots', *Proceddings of the Nationall Academy of Sciences*, 107: 7610-5.

Stover, R. H. 1962. 'Fusarial wilt (Panama Disease) of bananas and other Musa species', *Fusarial wilt (Panama disease) of bananas and other Musa species.*

Strelkov, S. E., L. Lamar, R. Sayoud, and R. B. Smith. 2002. 'Comparative virulence of chlorosis-inducing races of *Pyrenophora tritici-repentis*', *Canadian Journal of Plant Pathology-Revue Canadienne De Phytopathologie*, 24: 29-35.

Stubner, M., G. Lutterschmid, R. F. Vogel, and L. Niessen. 2010. 'Heterologous expression of the hydrophobin FcHyd5p from *Fusarium culmorum* in *Pichia pastoris* and evaluation of its surface activity and contribution to gushing of carbonated beverages', *International Journal of Food Microbiology*, 141: 110-15.

Su, Z. Q., A. Bernardo, B. Tian, H. Chen, S. Wang, H. X. Ma, S. B. Cai, D. T. Liu, D. D. Zhang, T. Li, H. Trick, P. St Amand, J. M. Yu, Z. Y. Zhang, and G. H. Bai. 2019. 'A deletion mutation in TaHRC confers Fhb1 resistance to Fusarium head blight in wheat', *Nature Genetics*, 51: 1099.

Su, Z. Q., S. J. Jin, D. D. Zhang, and G. H. Bai. 2018. 'Development and validation of diagnostic markers for Fhb1 region, a major QTL for Fusarium head blight resistance in wheat', *Theoretical and Applied Genetics*, 131: 2371-80.

Sunde, M., A. H. Kwan, M. D. Templeton, R. E. Beever, and J. P. Mackay. 2008. 'Structural analysis of hydrophobins', *Micron*, 39: 773-84.

Szurek, B., O. Rossier, G. Hause, and U. Bonas. 2002. 'Type III-dependent translocation of the Xanthomonas AvrBs3 protein into the plant cell', *Molecular Microbiology*, 46: 13-23.

Takahashi, A., C. Casais, K. Ichimura, and K. Shirasu. 2003. 'HSP90 interacts with RAR1 and SGT1 and is essential for RPS2-mediated disease resistance in Arabidopsis', *Proceedings of the National Academy of Sciences*, 100: 11777-82.

Takahashi, H., Y. Kanayama, M. S. Zheng, T. Kusano, S. Hase, M. Ikegami, and J. Shah. 2004. 'Antagonistic interactions between the SA and JA signaling pathways in Arabidopsis modulate expression of defense genes and gene-for-gene resistance to cucumber mosaic virus', *Plant and Cell Physiology*, 45: 803-09.

Taki, N., Y. Sasaki-Sekimoto, T. Obayashi, A. Kikuta, K. Kobayashi, T. Ainai, K. Yagi, N. Sakurai, H. Suzuki, T. Masuda, K. Takamiya, D. Shibata,

Y. Kobayashi, and H. Ohta. 2005. '12-oxo-phytodienoic acid triggers expression of a distinct set of genes and plays a role in wound-induced gene expression in Arabidopsis', *Plant Physiology*, 139: 1268-83.

Tan, K. C., and R. P. Oliver. 2017. 'Regulation of proteinaceous effector expression in phytopathogenic fungi', *PloS Pathogens*, 13.

Tanaka, S., T. Brefort, N. Neidig, A. Djamei, J. Kahnt, W. Vermerris, S. Koenig, K. Feussner, I. Feussner, and R. Kahmann. 2014. 'A secreted *Ustilago maydis* effector promotes virulence by targeting anthocyanin biosynthesis in maize', *Elife*, 3.

Tatineni, S., F. Kovacs, and R. French. 2014. 'Wheat Streak Mosaic Virus Infects Systemically despite Extensive Coat Protein Deletions: Identification of Virion Assembly and Cell-to-Cell Movement Determinants', *Journal of Virology*, 88: 1366-80.

Tatineni, S., A. J. McMechan, M. Bartels, G. L. Hein, and R. A. Graybosch. 2015. 'In Vitro Transcripts of Wild-Type and Fluorescent Protein-Tagged Triticum mosaic virus (Family Potyviridae) are Biologically Active in Wheat', *Phytopathology*, 105: 1496-505.

Taylor, R. D., A. Saparno, B. Blackwell, V. Anoop, S. Gleddie, N. A. Tinker, and L. J. Harris. 2008. 'Proteomic analyses of *Fusarium graminearum* grown under mycotoxin-inducing conditions', *Proteomics*, 8: 2256-65.

Thatcher, L. F., D. M. Gardiner, K. Kazan, and J. M. Manners. 2012. 'A Highly Conserved Effector in *Fusarium oxysporum* Is Required for Full Virulence on Arabidopsis', *Molecular Plant-Microbe Interactions*, 25: 180-90.

Thomma, B. P., V. A. N. Esse HP, P. W. Crous, and D. E. Wit PJ. 2005. 'C*ladosporium fulvum (syn. Passalora fulva*), a highly specialized plant pathogen as a model for functional studies on plant pathogenic Mycosphaerellaceae', *Molecular Plant Pathology*, 6: 379-93.

Tillmann, M., A. von Tiedemann, and M. Winter. 2017. 'Crop rotation effects on incidence and diversity of Fusarium species colonizing stem bases and grains of winter wheat', *Journal of Plant Diseases and Protection*, 124: 121-30.

Timian, RG, and JD %J Barley Genetics Newsletter Franckowiak. 1987. 'Location of a factor for barley stripe mosaic virus reaction on chromosome 1', 17: 79-82.

Torrance, L., G. H. Cowan, T. Gillespie, A. Ziegler, and C. Lacomme. 2006. 'Barley stripe mosaic virus-encoded proteins triple-gene block 2 and gamma b localize to chloroplasts in virus-infected monocot and dicot plants, revealing hitherto-unknown roles in virus replication', *Journal of General Virology*, 87: 2403-11.

Trail, F. 2009. 'For Blighted Waves of Grain: *Fusarium graminearum* in the Postgenomics Era', *Plant Physiology*, 149: 103-10.

Trail, F., and R. Common. 2000. 'Perithecial development by *Gibberella zeae*: a light microscopy study', *Mycologia*, 92: 130-38.

Tufan, H. A., F. L. Stefanato, G. R. D. McGrann, R. MacCormack, and L. A. Boyd. 2011. 'The Barley stripe mosaic virus system used for virus-induced gene silencing in cereals differentially affects susceptibility to fungal pathogens in wheat', *Journal of Plant Physiology*, 168: 990-94.

Tuori, R. P., T. J. Wolpert, and L. M. Ciuffetti. 2000. 'Heterologous expression of functional Ptr ToxA', *Molecular Plant-Microbe Interactions*, 13: 456-64.

Uhse, S., and A. Djamei. 2018. 'Effectors of plant-colonizing fungi and beyond', *PloS Pathogens*, 14.

Ujvari, A., S. Chamnongpol, O. Kourennaia, K. Myers, V. Bressler, J. Hubbard, A. Schweitzer, and C. Kubu. 2014. 'Concordance of Affymetrix GeneChip (R) Human Transcriptome Array 2.0 and USB (R) VeriQuest (TM) real-time PCR data', *Faseb Journal*, 28.

Union, European Commission %J Off J Eur. 2007. 'Commission Regulation (EC) No 1126/2007 of 28 September 2007 amending Regulation (EC) No 1881/2006 setting maximum levels for certain contaminants in foodstuffs as regards Fusarium toxins in maize and maize products', 255: 14-17.

Upadhyaya, N. M., R. Mago, B. J. Staskawicz, M. A. Ayliffe, J. G. Ellis, and P. N. Dodds. 2014. 'A bacterial type III secretion assay for delivery of fungal effector proteins into wheat', *Molecular Plant-Microbe Interactions*, 27: 255-64.

Urban, M., S. Daniels, E. Mott, and K. Hammond-Kosack. 2002. 'Arabidopsis is susceptible to the cereal ear blight fungal pathogens *Fusarium graminearum* and *Fusarium culmorum*', *Plant Journal*, 32: 961-73.

Urban, M., A. G. Irvine, A. Cuzick, and K. E. Hammond-Kosack. 2015. 'Using the pathogen-host interactions database (PHI-base) to investigate plant pathogen genomes and genes implicated in virulence', *Frontiers in Plant Science*, 6.

Urban, M., E. Mott, T. Farley, and K. Hammond-Kosack. 2003. 'The *Fusarium graminearum* MAP1 gene is essential for pathogenicity and development of perithecia', *Molecular Plant Pathology*, 4: 347-59.

Urban, M., and K. E. Hammond-Kosack. 2013. 'Molecular genetics and genomic approaches to explore Fusarium infection of wheat floral tissue', *Fusarium Genomics and Molecular and Cellular Biology (Proctor, RH and Brown, D., eds)*: 43-79.

Van den Ackerveken, G. F. J. M., A. L. Van Kan, M. H. A. J. Joosten, J. M. Muisers, H. M. Verbakel and P. J. G. M. De Wit. 1993. 'Characterization of two putative pathogenicity genes of the fungal tomato pathogen *Cladosporium fulvum*', *Molecular Plant-Microbe Interactions*, 6: 210-15.

Van den Ackerveken, G. 2017. 'Seeing is believing: imaging the delivery of pathogen effectors during plant infection', *New Phytologist*, 216: 8-10.

van den Burg, H. A., S. J. Harrison, M. H. Joosten, J. Vervoort, and P. J. de Wit. 2006. '*Cladosporium fulvum* Avr4 protects fungal cell walls against hydrolysis by plant chitinases accumulating during infection', *Molecular Plant-Microbe Interactions*, 19: 1420-30.

Van der Hoorn, Renier AL, Franck Laurent, Ronelle Roth, and Pierre JGM %J Molecular Plant-Microbe Interactions De Wit. 2000. 'Agroinfiltration is a versatile tool that facilitates comparative analyses of Avr 9/Cf-9-induced and Avr 4/Cf-4-induced necrosis', 13: 439-46.

van Esse, H. P., M. D. Bolton, I. Stergiopoulos, P. J. de Wit, and B. P. Thomma. 2007. 'The chitin-binding *Cladosporium fulvum* effector protein Avr4 is a virulence factor', *Molecular Plant-Microbe Interactions*,20: 1092-101.

van Esse, H. P., J. W. Van't Klooster, M. D. Bolton, K. A. Yadeta, P. van Baarlen, S. Boeren, J. Vervoort, P. J. de Wit, and B. P. Thomma. 2008. 'The *Cladosporium fulvum* virulence protein Avr2 inhibits host proteases required for basal defense', *Plant Cell*, 20: 1948-63.

van Kan, J. A. L., G. F. J. M. Van den Ackerveken, and P. J. G. M. De Wit. 1991. 'Cloning and characterization of cDNA of avirulence gene avr9 of the fungal pathogen *Cladosporium fulvum*, causal agent of tomato leaf mold', *Molecular Plant-Microbe Interactions*, 4: 52-59.

Varden, F. A., H. Saitoh, K. Yoshino, M. Franceschetti, S. Kamoun, R. Terauchi, and M. J. Banfield. 2019. 'Cross-reactivity of a rice NLR immune receptor to distinct effectors from the rice blast pathogen *Magnaporthe oryzae* provides partial disease resistance', *Journal of Biological Chemistry*, 294: 13006-16.

Vaughan, M., D. Backhouse, and E. M. Del Ponte. 2016. 'Climate change impacts on the ecology of *Fusarium graminearum* species complex and susceptibility of wheat to Fusarium head blight: a review', *World Mycotoxin Journal*, 9: 685-700.

Velasquez, A. C., C. D. M. Castroverde, and S. Y. He. 2018. 'Plant-Pathogen Warfare under Changing Climate Conditions', *Current Biology*, 28: R619-R34.

Veloso, J., and J. A. L. van Kan. 2018. 'Many Shades of Grey in Botrytis-Host Plant Interactions', *Trends in Plant Science*, 23: 613-22.

Vleeshouwers, V. G. A. A., and R. P. Oliver. 2014. 'Effectors as Tools in Disease Resistance Breeding Against Biotrophic, Hemibiotrophic, and Necrotrophic Plant Pathogens', *Molecular Plant-Microbe Interactions*, 27: 196-206.

Voigt, C. A., W. Schafer, and S. Salomon. 2005. 'A secreted lipase of *Fusarium graminearum* is a virulence factor required for infection of cereals', *Plant Journal*, 42: 364-75.

von der Ohe, C., V. Gauthier, L. Tamburic-Ilincic, A. Brule-Babel, W. G. D. Fernando, R. Clear, T. J. Ward, and T. Miedaner. 2010. 'A comparison of aggressiveness and deoxynivalenol production between Canadian *Fusarium graminearum* isolates with 3-acetyl and 15-

acetyldeoxynivalenol chemotypes in field-grown spring wheat', *European Journal of Plant Pathology*, 127: 407-17.

Walkowiak, S., O. Rowland, N. Rodrigue, and R. Subramaniam. 2016. 'Whole genome sequencing and comparative genomics of closely related Fusarium Head Blight fungi: *Fusarium graminearum*, *F. meridionale* and *F. asiaticum*', *BMC Genomics*, 17.

Walter, S., P. Nicholson, and F. M. Doohan. 2010. 'Action and reaction of host and pathogen during Fusarium head blight disease', *New Phytologist*, 185: 54-66.

Wang, G. X., L. Wang, Y. Cui, M. H. Yu, C. Dang, H. Wang, X. J. Jin, L. J. Yan, Q. H. Wu, D. W. Li, and Z. Y. Liu. 2017. 'RNA-seq analysis of *Brachypodium distachyon* responses to Barley stripe mosaic virus infection', *Crop Journal*, 5: 1-10.

Wang, J. Z., M. J. Hu, J. Wang, J. F. Qi, Z. F. Han, G. X. Wang, Y. J. Qi, H. W. Wang, J. M. Zhou, and J. J. Chai. 2019. 'Reconstitution and structure of a plant NLR resistosome conferring immunity', *Science*, 364: 44.

Wang, J. Z., J. Wang, M. J. Hu, S. Wu, J. F. Qi, G. X. Wang, Z. F. Han, Y. J. Qi, N. Gao, H. W. Wang, J. M. Zhou, and J. J. Chai. 2019. 'Ligand-triggered allosteric ADP release primes a plant NLR complex', *Science*, 364: 43.

Wang, M., and H. L. Jin. 2017. 'Spray-Induced Gene Silencing: a Powerful Innovative Strategy for Crop Protection', *Trends in Microbiology*, 25: 4-6.

Wang, M., A. Weiberg, E. Dellota, D. Yamane, and H. L. Jin. 2017. 'Botrytis small RNA Bc-siR37 suppresses plant defense genes by cross-kingdom RNAi', *RNA Biology*, 14: 421-28.

Wang, S. M., P. C. Boevink, L. Welsh, R. F. Zhang, S. C. Whisson, and P. R. J. Birch. 2017. 'Delivery of cytoplasmic and apoplastic effectors from *Phytophthora infestans* haustoria by distinct secretion pathways', *New Phytologist*, 216: 205-15.

Wang, Y., Z. L. Bao, Y. Zhu, and J. Hua. 2009. 'Analysis of Temperature Modulation of Plant Defense Against Biotrophic Microbes', *Molecular Plant-Microbe Interactions*, 22: 498-506.

Wang, Z., M. Gerstein, and M. Snyder. 2009. 'RNA-Seq: a revolutionary tool for transcriptomics', *Nature Reviews Genetics*, 10: 57-63.

Ward, H. M.. 1902. 'On the relations between host and parasite in the bromes and their brown rust, *Puccinia dispersa* (Erikss)', *Annals of Botany*, 16: 233-315.

Ward, T. J., R. M. Clear, A. P. Rooney, K. O'Donnell, D. Gaba, S. Patrick, D. E. Starkey, J. Gilbert, D. M. Geiser, and T. W. Nowicki. 2008. 'An adaptive evolutionary shift in Fusarium head blight pathogen populations is driving the rapid spread of more toxigenic Fusarium graminearum in North America', *Fungal Genetics and Biology*, 45: 473-84.

Wawra, S., A. Djamei, I. Albert, T. Nurnberger, R. Kahmann, and P. van West. 2013. 'In Vitro Trans location Experiments with RxLR-Reporter Fusion Proteins of Avr1b from *Phytophthora sojae* and AVR3a from *Phytophthora infestans* Fail to Demonstrate Specific Autonomous Uptake in Plant and Animal Cells', *Molecular Plant-Microbe Interactions*, 26: 528-36.

Wegulo, S. N., P. S. Baenziger, J. H. Nopsa, W. W. Bockus, and H. Hallen-Adams. 2015. 'Management of Fusarium head blight of wheat and barley', *Crop Protection*, 73: 100-07.

Wei, C. F., B. H. Kvitko, R. Shimizu, E. Crabill, J. R. Alfano, N. C. Lin, G. B. Martin, H. C. Huang, and A. Collmer. 2007. 'A *Pseudomonas syringae* pv. tomato DC3000 mutant lacking the type III effector HopQ1-1 is able to cause disease in the model plant *Nicotiana benthamiana*', *Plant Journal*, 51: 32-46.

Weiberg, A., M. Wang, F. M. Lin, H. W. Zhao, Z. H. Zhang, I. Kaloshian, H. D. Huang, and H. L. Jin. 2013. 'Fungal Small RNAs Suppress Plant Immunity by Hijacking Host RNA Interference Pathways', *Science*, 342: 118-23.

West, J. S., G. G. M. Canning, S. A. Perryman, and K. King. 2017. 'Novel Technologies for the detection of Fusarium head blight disease and airborne inoculum', *Tropical Plant Pathology*, 42: 203-09.

Wheeler, T., and J. von Braun. 2013. 'Climate Change Impacts on Global Food Security', *Science*, 341: 508-13.

Whisson, S. C., P. C. Boevink, L. Moleleki, A. O. Avrova, J. G. Morales, E. M. Gilroy, M. R. Armstrong, S. Grouffaud, P. van West, S. Chapman, I. Hein, I. K. Toth, L. Pritchard, and P. R. J. Birch. 2007. 'A translocation signal for delivery of oomycete effector proteins into host plant cells', *Nature*, 450: 115.

Williams, B., M. Kabbage, H. J. Kim, R. Britt, and M. B. Dickman. 2011. 'Tipping the Balance: *Sclerotinia sclerotiorum* Secreted Oxalic Acid Suppresses Host Defenses by Manipulating the Host Redox Environment', *PloS Pathogens*, 7.

Williamson, B., B. Tudzynski, P. Tudzynski, and J. A. van Kan. 2007. '*Botrytis cinerea*: the cause of grey mould disease', *Molecular Plant Pathology*, 8: 561-80.

Winnenburg, R., T. K. Baldwin, M. Urban, C. Rawlings, J. Kohler, and K. E. Hammond-Kosack. 2006. 'PHI-base: a new database for pathogen host interactions', *Nucleic Acids Research*, 34: D459-D64.

Wong, P., M. Walter, W. Lee, G. Mannhaupt, M. Munsterkotter, H. W. Mewes, G. Adam, and U. Guldener. 2011. 'FGDB: revisiting the genome annotation of the plant pathogen *Fusarium graminearum*', *Nucleic Acids Research*, 39: D637-D39.

Wright, P. C., J. Noirel, S. Y. Ow, and A. Fazeli. 2012. 'A review of current proteomics technologies with a survey on their widespread use in reproductive biology investigations', *Theriogenology*, 77: 738-65.

Xin, X. F., K. Nomura, K. Aung, A. C. Velasquez, J. Yao, F. Boutrot, J. H. Chang, C. Zipfel, and S. Y. He. 2016. 'Bacteria establish an aqueous living space in plants crucial for virulence', *Nature*, 539: 524.

Xu, J. R., M. Urban, J. A. Sweigard, and J. E. Hamer. 1997. 'The CPKA gene of Magnaporthe grisea is essential for appressorial penetration', *Molecular Plant-Microbe Interactions*, 10: 187-94.

Xu, R. Q., S. Blanvillain, J. X. Feng, B. L. Jiang, X. Z. Li, H. Y. Wei, T. Kroj, E. Lauber, D. Roby, B. Chen, Y. Q. He, G. T. Lu, D. J. Tang, J. Vasse, M. Arlat, and J. L. Tang. 2008. 'AvrAC(Xcc8004), a type III effector with a leucine-rich repeat domain from *Xanthomonas campestris* pathovar campestris confers avirulence in vascular tissues of

Arabidopsis thaliana ecotype col-0', *Journal of Bacteriology*, 190: 343-55.

Yang, F., S. Jacobsen, H. J. L. Jorgensen, D. B. Collinge, B. Svensson, and C. Finnie. 2013. '*Fusarium graminearum* and its interactions with cereal heads: studies in the proteomics era', *Frontiers in Plant Science*, 4.

Yang, F., J. D. Jensen, B. Svensson, H. J. L. Jorgensen, D. B. Collinge, and C. Finnie. 2012. 'Secretomics identifies *Fusarium graminearum* proteins involved in the interaction with barley and wheat', *Molecular Plant Pathology*, 13: 445-53.

Yang, G. G., L. G. Tang, Y. D. Gong, J. T. Xie, Y. P. Fu, D. H. Jiang, G. Q. Li, D. B. Collinge, W. D. Chen, and J. S. Cheng. 2018. 'A cerato-platanin protein SsCP1 targets plant PR1 and contributes to virulence of *Sclerotinia sclerotiorum'*, *New Phytologist*, 217: 739-55.

Yi, X., J. Y. Cheng, Z. N. Jiang, W. J. Hu, T. D. Bie, D. R. Gao, D. S. Li, R. L. Wu, Y. L. Li, S. L. Chen, X. M. Cheng, J. Liu, Y. Zhang, and S. H. Cheng. 2018. 'Genetic Analysis of Fusarium Head Blight Resistance in CIMMYT Bread Wheat Line C615 Using Traditional and Conditional QTL Mapping', *Frontiers in Plant Science*, 9.

Yoshino, K., H. Irieda, F. Sugimoto, H. Yoshioka, T. Okuno, and Y. Takano. 2012. 'Cell Death of *Nicotiana benthamiana* Is Induced by Secreted Protein NIS1 of C*olletotrichum orbiculare* and Is Suppressed by a Homologue of CgDN3', *Molecular Plant-Microbe Interactions*, 25: 625-36.

Yun, Y. Z., Z. Y. Liu, Y. N. Yin, J. H. Jiang, Y. Chen, J. R. Xu, and Z. H. Ma. 2015. 'Functional analysis of the *Fusarium graminearum* phosphatome', *New Phytologist*, 207: 119-34.

Zaidi, S. S., M. S. Mukhtar, and S. Mansoor. 2018. 'Genome Editing: Targeting Susceptibility Genes for Plant Disease Resistance', *Trends in Biotechnology*, 36: 898-906.

Zeller, K. A., R. L. Bowden, and J. F. Leslie. 2004. 'Population differentiation and recombination in wheat scab populations of *Gibberella zeae* from the United States', *Molecular Ecology*, 13: 563-71.

Zerbino, D. R., P. Achuthan, W. Akanni, M. R. Amode, D. Barrell, J. Bhai, K. Billis, C. Cummins, A. Gall, C. G. Giron, L. Gil, L. Gordon, L. Haggerty, E. Haskell, T. Hourlier, O. G. Izuogu, S. H. Janacek, T. Juettemann, J. K. To, M. R. Laird, I. Lavidas, Z. C. Liu, J. E. Loveland, T. Maurel, W. McLaren, B. Moore, J. Mudge, D. N. Murphy, V. Newman, M. Nuhn, D. Ogeh, C. K. Ong, A. Parker, M. Patricio, H. S. Riat, H. Schuilenburg, D. Sheppard, H. Sparrow, K. Taylor, A. Thormann, A. Vullo, B. Walts, A. Zadissa, A. Frankish, S. E. Hunt, M. Kostadima, N. Langridge, F. J. Martin, M. Muffato, E. Perry, M. Ruffier, D. M. Staines, S. J. Trevanion, B. L. Aken, F. Cunningham, A. Yates, and P. Flicek. 2018. 'Ensembl 2018', *Nucleic Acids Research*, 46: D754-D61.

Zhang, C. K., Y. Wang, J. Q. Wang, Z. Z. Zhai, L. H. Zhang, W. H. Zheng, W. Zheng, W. Y. Yu, J. Zhou, G. D. Lu, W. B. Shim, and Z. H. Wang. 2013. 'Functional characterization of Rho family small GTPases in *Fusarium graminearum*', *Fungal Genetics and Biology*, 61: 90-99.

Zhang, H. F., B. Li, Q. Fang, Y. Li, X. B. Zheng, and Z. G. Zhang. 2016. 'SNARE protein FgVam7 controls growth, asexual and sexual development, and plant infection in *Fusarium graminearum*', *Molecular Plant Pathology*, 17: 108-19.

Zhang, S. J., and J. R. Xu. 2014. 'Effectors and Effector Delivery in *Magnaporthe oryzae*', *PloS Pathogens*, 10.

Zhang, X. W., L. J. Jia, Y. Zhang, G. Jiang, X. Li, D. Zhang, and W. H. Tang. 2012a. 'In Planta Stage-Specific Fungal Gene Profiling Elucidates the Molecular Strategies of *Fusarium graminearum* Growing inside Wheat Coleoptiles', *Plant Cell*, 24: 5159-76.

———. 2012b. 'In planta stage-specific fungal gene profiling elucidates the molecular strategies of *Fusarium graminearum* growing inside wheat coleoptiles', *Plant Cell*, 24: 5159-76.

Zheng, H. W., W. H. Zheng, C. X. Wu, J. Yang, Y. Xi, Q. R. Xie, X. Zhao, X. L. Deng, G. D. Lu, G. P. Li, D. Ebbole, J. Zhou, and Z. H. Wang. 2015. 'Rab GTPases are essential for membrane trafficking-dependent growth and pathogenicity in F*usarium graminearum*', *Environmental Microbiology*, 17: 4580-99.

Zhong, Z., T. C. Marcel, F. E. Hartmann, X. Ma, C. Plissonneau, M. Zala, A. Ducasse, J. Confais, J. Compain, N. Lapalu, J. Amselem, B. A. McDonald, D. Croll, and J. Palma-Guerrero. 2017. 'A small secreted protein in *Zymoseptoria tritici* is responsible for avirulence on wheat cultivars carrying the Stb6 resistance gene', *New Phytologist*, 214: 619-31.

Zhou, H. B., S. F. Li, Z. Y. Deng, X. P. Wang, T. Chen, J. S. Zhang, S. Y. Chen, H. Q. Ling, A. M. Zhang, D. W. Wang, and X. Q. Zhang. 2007. 'Molecular analysis of three new receptor-like kinase genes from hexaploid wheat and evidence for their participation in the wheat hypersensitive response to stripe rust fungus infection', *Plant Journal*, 52: 420-34.

Zhu, Q. L., L. Sun, J. J. Lian, X. L. Gao, L. Zhao, M. Y. Ding, J. Li, and Y. C. Liang. 2016. 'The phospholipase C (FgPLC1) is involved in regulation of development, pathogenicity, and stress responses in *Fusarium graminearum*', *Fungal Genetics and Biology*, 97: 1-9.

Zhu, W. J., M. Ronen, Y. Gur, A. Minz-Dub, G. Masrati, N. Ben-Tal, A. Savidor, I. Sharon, E. Eizner, O. Valerius, G. H. Braus, K. Bowler, M. Bar-Peled, and A. Sharon. 2017. 'BcXYG1, a Secreted Xyloglucanase from *Botrytis cinerea*, Triggers Both Cell Death and Plant Immune Responses', *Plant Physiology*, 175: 438-56.

Zhu, W., W. Wei, Y. Fu, J. Cheng, J. Xie, G. Li, X. Yi, Z. Kang, M. B. Dickman, and D. Jiang. 2013. 'A secretory protein of necrotrophic fungus *Sclerotinia sclerotiorum* that suppresses host resistance', *PloS One*, 8: e53901.

Zipfel, C., and G. Felix. 2005. 'Plants and animals: a different taste for microbes?', *Current Opinion in Plant Biology*, 8: 353-60.